

# Exploring the resistance against root parasitic plants in *Arabidopsis* and tomato



**Xi Cheng**



# **Exploring the resistance against root parasitic plants in *Arabidopsis* and tomato**

**Xi Cheng**

## **Thesis committee**

### **Promotor**

Prof. Dr H.J. Bouwmeester  
Professor of Plant Hormone Biology  
Swammerdam Institute for Life Sciences, University of Amsterdam

### **Co-promotor**

Dr C.P. Ruyter-Spira  
Researcher, Laboratory of Plant Physiology  
Wageningen University & Research

### **Other members**

Prof. Dr M. Dicke, Wageningen University & Research  
Dr ing. J.J.B. Keurentjes, Wageningen University & Research  
Prof. Dr P. Delavault, University of Nantes, France  
Dr P.M. Bleeker, Enza Zaden, Enkhuizen

This research was conducted under the auspices of the Graduate  
School of Experimental Plant Sciences (EPS)



# **Exploring the resistance against root parasitic plants in *Arabidopsis* and tomato**

**Xi Cheng**

## **Thesis**

submitted in fulfilment of the requirements for the degree of doctor  
at Wageningen University

by the authority of the Rector Magnificus,

Prof. Dr A.P.J. Mol,

in the presence of the

Thesis Committee appointed by the Academic Board

to be defended in public

on Thursday 19 October 2017

at 11 a.m. in the Aula.

Xi Cheng

Exploring the resistance against root parasitic plants in *Arabidopsis*  
and tomato  
306 pages

PhD thesis, Wageningen University, Wageningen, the Netherlands  
(2017)  
With references, with summary in English

ISBN: 978-94-6343-700-4

DOI: <https://doi.org/10.18174/423176>

# Contents

## Chapter 1

General introduction

[7](#)

## Chapter 2

Genome-wide association analysis of natural variation in susceptibility to the parasitic plant *Phelipanche ramosa* in *Arabidopsis thaliana*

[41](#)

## Chapter 3

The role of endogenous strigolactones and their interaction with ABA during the infection process of the parasitic weed *Phelipanche ramosa* in tomato plants

[99](#)

## Chapter 4

The interaction between strigolactones and other plant hormones in the regulation of plant development

[127](#)

## Chapter 5

The tomato *MAX1* homolog- *SIMAX1* - is involved in the conversion of carlactone to orobanchol

[167](#)

## Chapter 6

Dissection of hypocotyl and root response to strigolactone in darkness in a genome-wide association study

[203](#)

## Chapter 7

General discussion

[257](#)

## Summary

[295](#)

## Acknowledgements

[299](#)

## Curriculum Vitae

[302](#)

## Publications

[303](#)

## Education Statement

[305](#)



# CHAPTER 1

---

## General introduction

---



### Root parasitic plants

Parasitic plants are plants that have the capacity to absorb water and nutrients from their host plants by establishing a vascular connection with them. Some parasitic plants attach to the host stem or branches, while others invade the vascular system of the host root. Another way to distinguish between different types of parasitic plants is their level of host plant dependency. Holoparasites, such as *Orobanche* spp. and *Phelipanche* spp., do not have chlorophyll and therefore are not able to photosynthesize, resulting in complete host dependency to sustain their growth and development (obligate). In contrast, the hemiparasites, such as *Striga* spp., which do have chlorophyll and only partially rely on their host. Only a few of the hemiparasites are facultative, being able to complete life cycle without a host, such as *Rhinanthus* spp.

The family of the Orobanchaceae is the largest family of parasitic plants. Among them, the aggressive witchweeds, *Striga* spp., and broomrapes, *Orobanche* and *Phelipanche* spp., are the most notorious agricultural weeds (Schneeweiss, 2007; Joel, 2009). Most weedy broomrapes, such as *Orobanche crenata* and *Phelipanche ramosa* (previously named *Orobanche ramosa*) (Joel, 2009), have a wide host range, while other species only parasitize a limited number of host species, such as *Orobanche cumana* that only parasitizes sunflower.

These weedy parasitic plants adapt well to diverse geographical locations, environments and agricultural practices used to grow their hosts and can pose a great threat to crop yield. The tiny seeds of the parasitic plants are spread easily by the use of machines and with crop seeds and their occurrence can quickly expand by intensive farming using monoculture. Furthermore, the broad host range of some of the parasitic plant species makes them difficult to control by crop rotation. The *P. ramosa*, for example, invades a wide range of crops especially common on Brassicaceae (eg. oilseed rape) and the Solanaceae (eg. tomato, tobacco, eggplant and potato) in the Mediterranean region, Europe, Asia, Africa and United States (Parker, 1991; Mohamed *et al.*, 2006) (**Figure 1**). The *P. ramosa* is known as a serious pest of tomato in Europe, especially a problem in France and Morocco, also expanding into Western Europe (Parker, 1991; Mohamed *et al.*, 2006). Several reports have estimated yield losses of at least 30-50% for tomato, tobacco and rapeseed upon infection with this parasite (Cagán and Tóth, 2003; Buschmann *et al.*, 2005a; Buschmann *et al.*, 2005b; Timus and Croitoru, 2007; Gibot-Leclerc *et al.*, 2012). For tomato, not only is crop yield heavily reduced, the quality of crop products can also be significantly

affected by parasitic plant infestation (Mauromicale *et al.*, 2008; Longo *et al.*, 2010). The *P. ramosa* remarkably reduces aerial biomass of the parasitized tomato plants by acting as a competing sink for assimilates and by influencing the efficiency of carbon assimilation (Mauromicale *et al.*, 2008). In addition, in the presence of *P. ramosa*, there is also a strong reduction in tomato fruit biomass, mesocarp thickness, fruit colour as well as in the contents of sugars and soluble solids in the fruits of parasitized tomato plants (Longo *et al.*, 2010). These mentioned influence of *P. ramosa* infection pose a great threat to tomato production and devalues the commercial tomato fruits.

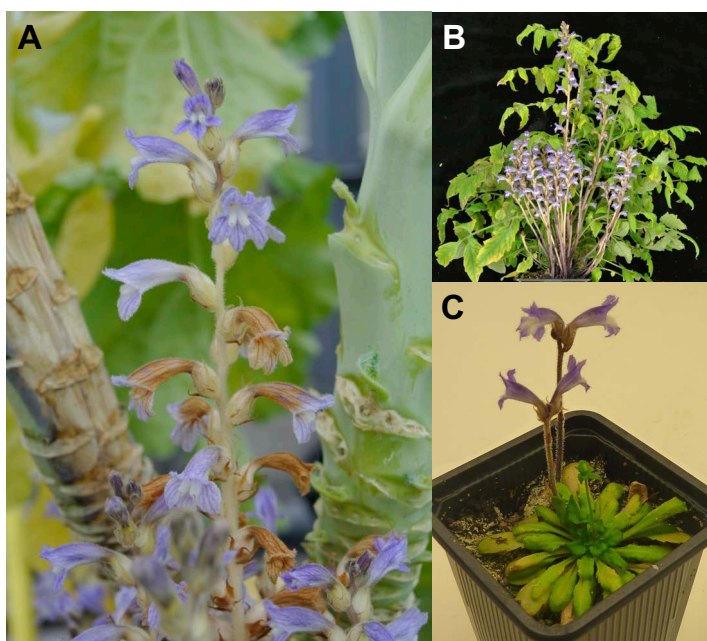


**Figure 1.** *Phelipanche ramosa* growing on various plant species such as oilseed rape (A), tomato (B) and *Arabidopsis* (C). Photographs were taken by Xi Cheng.

### The interaction between parasitic plants and their hosts

The life cycle of the holoparasitic Orobanchaceae includes several developmental stages, during which the parasitic plant has an intimate interaction with the host plant (**Figure 2**).



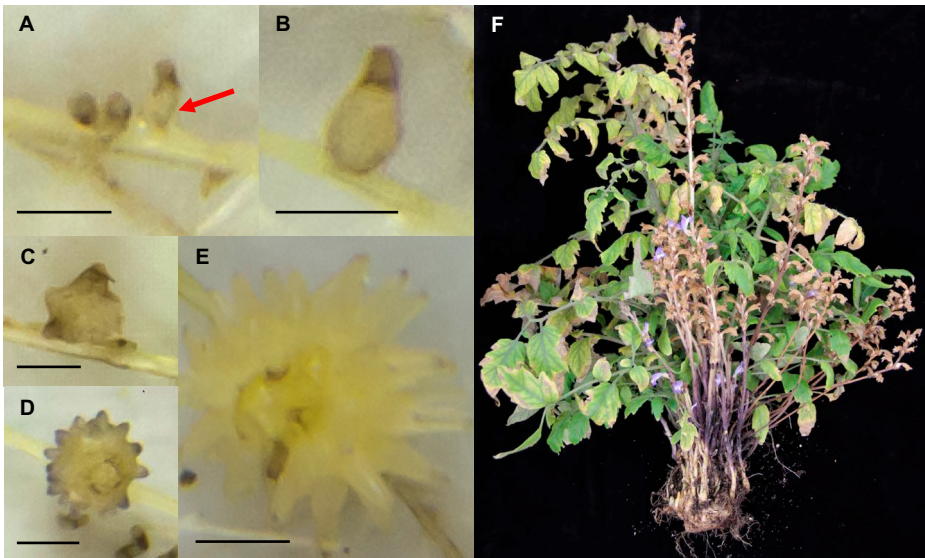


**Figure 2. Different developmental stages of *Phelipanche ramosa* on the roots of host tomato.** A germinated *P. ramosa* seed develops a haustorium (red arrow) and subsequently attaches to tomato roots (A). As the parasite attaches to the host root, a swollen tubercle is formed to store assimilates that the parasite obtains from the host (B-C). The tubercle further differentiates, and multiple adventitious roots will occur at the base of the tubercle, forming a spider-like structure (D-E). Mature *P. ramosa* shoots and flowers emerge aboveground (F). The *P. ramosa* flowers have started to produce seeds. The growth of the tomato host plant is clearly compromised (F). Bars = 1mm. Photographs were taken by Xi Cheng.

Before having any physical contact with the host roots, the seeds of parasitic plants that are present in the soil await signals from their host, ensuring that they will only germinate when they are located within the host's rhizosphere. This feature is very important since they will not survive long after germination if they cannot reach the host roots that should support them with nutrients and water. Host-derived germination stimulants are required to induce germination; the strigolactones have been recognized as the major group of compounds responsible for inducing seed germination of parasitic Orobanchaceae species (Bouwmeester *et al.*, 2003).

Strigolactones have also been shown to act as host recognition

signals for arbuscular mycorrhizal fungi (AMF) and to stimulate the establishment of a symbiotic relationship (Akiyama *et al.*, 2005). However, also non-mycorrhizal plants produce strigolactones in their roots and strigolactones were recently shown to be an important plant hormone that is involved in several biological processes, such as shoot branching, root growth, seed germination and secondary growth (Gomez-Roldan *et al.*, 2008; Agusti *et al.*, 2011; Koltai, 2011; Toh *et al.*, 2012a). Apart from strigolactones, also other compounds serve as seed germination stimulants for parasitic plants. In *Arabidopsis*, the germination percentage of *P. ramosa* seeds exposed to roots of strigolactone-deficient mutants did not differ from that of wild-type ecotype Col-0 (Auger *et al.*, 2012). In a recent study using rapeseed (*Brassica napus*), the glucosinolate-derived compound isothiocyanate has been identified as the main germination stimulant. It specifically induces the germination of *P. ramosa* seeds rather than *O. minor*, *O. cumana*, *O. crenata* and *P. aegyptiaca*, in the rapeseed rhizosphere (Auger *et al.*, 2012). This is consistent with the hypothesis that a selective pressure was posed on some *P. ramosa* populations (coined pathovar A by (Benharrat *et al.*, 2005), which originally parasitized on wild host species, with the expansion of rapeseed production. This resulted in the emergence of virulence of *P. ramosa* specifically on rapeseed (Benharrat *et al.*, 2005; Brault *et al.*, 2007). Indeed, it has been proposed that a host-driven selection pressure plays a critical role in the evolutionary divergence of parasitic plants (Thorogood *et al.*, 2008; Thorogood *et al.*, 2009). Similarly, dihydrocostuslactone, a sesquiterpene lactone, specifically induced *O. cumana* seed germination in the sunflower rhizosphere (Joel *et al.*, 2011), giving another example of evolutionary diversification of parasitic plant seed response to particular host germination stimulants. The response towards novel and structurally different germination stimulants has demonstrated the high adaptation potential of Orobanchaceae species. Further research on the host germination stimulants and their compatibility with the parasites should help us further understand the evolution of host recognition mechanisms.

After seed germination, the parasite's radicle tip, upon contact with the host root and/or its exudates, develops into a haustorium which is the key organ in plant parasitism. The haustorium attaches to and subsequently invades the host root, and establishes a connection between the vasculature of host and parasite. Our knowledge of early initiation and development of the haustorium is still quite limited. The initiation of *Orobanche* haustoria does not seem to be induced by host-derived signals, whereas some other parasitic plant species, such as *Striga*, need host-derived chemical stimulants to initiate haustorium development (Joel and Losner-Goshen, 1994).

These host-derived chemicals are called haustorium-inducing factors or xenognosins. The only known haustorium-inducing factor for *Striga* is a quinone, 2,6-dimethoxy-*p*-benzoquinone (2,6-DMBQ), which has been isolated from sorghum root extracts (Chang and Lynn, 1986). Quinones and phenols have been found to act as signal molecules between plant roots and other organisms such as microbes and insects, and their activity was found to be associated with their redox state (Siqueira *et al.*, 1991; Kessler and Baldwin, 2002; Hirsch *et al.*, 2003). The haustorium-inducing factors can activate haustorium development via a signal transduction pathway initiated by redox cycling between quinone and hydroquinone states (Chang and Lynn, 1986; Keyes *et al.*, 2001; Keyes *et al.*, 2007; Bandaranayake *et al.*, 2010; Yoshida and Shirasu, 2012; Joel and Gressel, 2013).

After the establishment of the initial vascular connection with the host, a tubercle is formed. A tubercle, is a local swelling in the parasitic seedling just outside the host root. This structure will further develop into a mature tubercle from which adventitious roots and an apical shoot will emerge, which will result in a spider-like shape. The adventitious roots may develop functional lateral haustoria, depending on the presence of adjacent host roots (Joel and Gressel, 2013). Finally, the shoots of mature parasitic plants emerge above the soil.

The vascular connection (through xylem and/or phloem) between parasitic plants and their host is vital for the acquisition of nutrients and bioactive solute from hosts to parasites (Smith *et al.*, 2013). It has been demonstrated that the vascular continuity is directed by the polar flow of auxin (Bar-Nun *et al.*, 2008). A chemical disruption of the local auxin flow reduced the severity of an infection (percentage of host roots infected) with *P. aegyptiaca* in *Arabidopsis* (Bar-Nun *et al.*, 2008). After the establishment of the vascular connection, *Orobanche* spp. have been found to be able to selectively accumulate certain mineral ions (eg. potassium) and sugar/ sugar alcohols (eg. mannitol) (Hibberd *et al.*, 1999; Brotherson *et al.*, 2005; Abbes *et al.*, 2009b; Labrousse *et al.*, 2010). A few studies on the facultative hemiparasite *Rhinanthus minor* and *Melampyrum arvense* have also shown that levels of plant hormones such as cytokinin and abscisic acid (ABA) can be increased in the parasite after attachment to a host (Lechowski, 1996; Lechowski and Bialczyk, 1996; Jiang *et al.*, 2004; Jiang *et al.*, 2005). For holoparasitic plants, all carbon and nitrogen resources are derived from their host. Parasites convert host-derived sugars into favoured sugars and also turn nitrogenous compounds into their favoured amino acids (Abbes *et al.*, 2009a; Joel and Gressel, 2013). These products are assimilated and stored

in the tubercle, which then acts as a source for the subsequent growth of the shoot and flowers (Abbes *et al.*, 2009a; Joel and Gressel, 2013). In addition to these small molecules, macromolecules such as proteins and nucleic acids (eg. RNA, DNA), are also transferred between host and parasite (Smith *et al.*, 2013). In recent studies, this knowledge was used to develop RNAi silencing strategies to target genes in the parasite that are essential in plant root parasitism (Aly *et al.*, 2009; Bandaranayake and Yoder, 2013; Aly *et al.*, 2014; Kirigia *et al.*, 2014).

### **Agronomic control of parasitic plants**

A lot of research has been done to improve control of weedy parasitic plants with agricultural practices.

The most common weed control method is hand weeding. Early weeding could prevent yield loss of crops and dispersal of parasite seeds. However, the weeding of root parasitic weeds like *Orobanche*, *Phelipanche* and *Striga* can only be conducted once they emerge aboveground, when the host has already suffered much from the weeds. Nevertheless, hand weeding is still recommended to be carried out prior to weed seed production in order to effectively reduce future infestations, if work labour is sufficient (Rodenburg *et al.*, 2006).

Improving soil fertility also helps to reduce the occurrence of parasitic weeds. A shortage of phosphate and sometimes nitrogen have been shown to induce the biosynthesis of the germination stimulants, the strigolactones, and thus promote weed infestation (Rodenburg *et al.*, 2005; Yoneyama *et al.*, 2007; Jamil *et al.*, 2011a). In addition, nitrogen has also been shown to inhibit radicle elongation and development of *Orobanche* seedlings (Westwood and Foy, 1999). Therefore, supplying phosphate and nitrogen fertilizers could reduce parasitic weed infestation. However, although there are several successful examples of reducing weeds by fertilizer treatments (Adagba *et al.*, 2002a; Adagba *et al.*, 2002b; Jamil *et al.*, 2012a; Jamil *et al.*, 2012b), this method is not always shown to be effective, probably due to varying soil conditions (Westwood and Foy, 1999; Jamil *et al.*, 2012a). For instance, sandy soils may suffer less from acidic pH which can influence the phosphate availability after fertilizer application (Jamil *et al.*, 2012a).

Another traditional approach to combat parasitic plants is the application of herbicides. The main purpose is to kill or restrict root parasitic plants before they emerge aboveground. For the use of chemical control

methods, the cost of the chemical, time and location of application, effectiveness, safety for the host plants as well as environmental issues need to be considered. The main obstacle for successful application of herbicides is that many crops are also sensitive to the herbicide. Generally, there are two approaches to solve this problem. One approach is to develop herbicide-resistant or -tolerant crops that can degrade the herbicide to non-toxic compounds or are no longer sensitive to the herbicide (Joel *et al.*, 1995; Tan *et al.*, 2005). In the latter approach the herbicide-target in the host, usually an enzyme from primary metabolism, is modified to prevent herbicide binding without changing the normal function of the enzyme, allowing the herbicide to be translocated from the treated host to the parasite (Joel *et al.*, 1995). Besides, soil fumigants that release toxic compounds have also been used to fight *Orobanche* and *Phelipanche* spp. But the effect of this method is, to some extent, dependent on the soil conditions and precise application procedures (Joel and Gressel, 2013).

An interesting alternative approach is the application of germination stimulants to the soil with the aim to induce suicidal germination of parasitic plant seeds and thus reduce the weed seed bank before planting of the host crops (Mwakaboko and Zwanenburg 2011). The most successful example of this approach is the use of ethane (ethylene) which is injected into the soil provoking *Striga* seeds to germinate without a suitable host (Robert, 1975). However, the equipment for applying the gas to soil is expensive and this approach only applies to *Striga* because other parasite such as *Orobanche* and *Phelipanche* species are not responsive to ethylene (Parker, 1991; Rodenburg *et al.*, 2005; Zwanenburg *et al.*, 2016). Recently, researchers put their interests on strigolactone analogs. Some researchers have claimed that strigolactone analogs are not very stable in the soil, especially in alkaline soil (Rubiales *et al.*, 2009). However, a number of experiments have successfully applied strigolactone analogs to induce suicidal weed seed germination in pots and in field trials (Kgosi *et al.*, 2012). Intriguingly, one novel idea to prevent parasitic plant seed germination, is to directly decompose strigolactones in the soil. This allows manipulation of host plant derived strigolactones without interfering with host plant growth and architecture, which would be the case if strigolactone production would have been targeted in the host plant itself (Kannan and Zwanenburg, 2014; Kannan *et al.*, 2015). Using this concept, simple chemicals such as borax and thiourea are applied to quickly and effectively deactivate exuded host strigolactones without affecting host growth (Kannan and Zwanenburg, 2014; Kannan *et al.*, 2015).



Intentional introduction of exotic biotic agents, such as insects and microorganisms, is potentially a more ecological approach to minimize damage caused by parasitic weeds (Klein and Kroschel, 2002; Sands and Pilgeram, 2009). However, this is also a complex issue. Application of natural enemies of parasitic weeds like insects, such as *Phytomyza* for *Orobanch*e and *Smicronyx* for *Striga*, could help to reduce the soil seed bank and seed dispersal of the weeds (Smith *et al.*, 1993; Klein and Kroschel, 2002). Another approach is to utilize microorganisms that can infect parasitic weeds. Isolates of soil-borne *Fusarium* spp., for example, that inhibit seed germination or infect parasitic attachment organs, have been considered as potential biocontrol agents for *Orobanch*e and *Striga* (Abbasher and Sauerborn, 1992; Thomas, 1999; Zonno and Vurro, 1999; Cohen *et al.*, 2002; Zonno and Vurro, 2002; Elzein and Kroschel, 2004; Saremi and Okhovvat, 2008; Kohlschmid *et al.*, 2009). This approach can indeed reduce the viability of parasitic plants and is already in the development and commercialization phase (Joel and Gressel, 2013). However, so far it has not been shown to significantly improve crop yield (Kohlschmid *et al.*, 2009). Moreover, parasitic plants may evolve resistance to the pathogens. Therefore, it is necessary to carefully evaluate against multiple weed populations across different environments to determine the efficacy of the microorganism isolates before biocontrol agents are made commercially available. Additionally, one mostly recent study demonstrates that a few beneficial fungi (*Trichoderma harzianum* and *Fusarium oxysporum*) are capable of degrading germination stimulants, the strigolactones (Boari *et al.*, 2016). This finding provides another promising biocontrol for parasitic plants.

### Resistance against parasitic plants

Host plants, as well as non-host plants, have developed multiple strategies to combat or at least delay the attachment and invasion of parasitic plants. Physical barriers are often formed within the host root cortex. Hosts attempts to prevent parasite entry consist for example of reinforcing the cell wall, or blocking the access to the host's vascular system, either by lignification or necrosis (Botanga and Timko, 2005; Letousey *et al.*, 2007; Irving and Cameron, 2009). Studies on resistant genotypes have reported a rapid accumulation of polyphenolics, (other) phytoalexins and lignin at the host-parasite interface. In some cases of parasitic plant resistance, a rapid browning and necrosis of localized host cells at the site of the host-parasite interface was observed, which appears to be similar to the hypersensitive response (HR) that is often observed in plant-pathogen

interactions (Goldwasser *et al.*, 2000a; Mohamed *et al.*, 2003; Gurney *et al.*, 2006). Other resistance responses occur after the successful establishment of the vascular connection between host and parasite. For instance, sealing the host vessels with gum-like substances or mucilage will disturb water and nutrient transport from the host, leading to delayed development or even necrosis of the developing tubercles (Labrousse, 2001; Pérez-de-Luque *et al.*, 2006).

The challenge in studying parasitic plant resistance lies in the identification of the genes that contribute to resistance mechanisms against parasitic plants. The comparison of differential gene expression during compatible (susceptible) and incompatible (resistant) host-parasite interaction has been widely used, and several plant defence-related genes/proteins have been suggested to play a role in resistance against parasitic weeds, such as genes/proteins that are involved in isoprenoid and phenylpropanoid biosynthesis, cell wall modification, detoxification of reaction oxygen species (ROS), wounding response, pleiotropic drug-resistance ABC transporters, regulation of transcription, protein synthesis, jasmonic acid (JA) signalling, salicylic acid (SA) signalling, ethylene signalling and ABA response (Joel, 1998; Dos Santos *et al.*, 2003a; Dos Santos *et al.*, 2003b; Angeles Castillejo *et al.*, 2004; Griffiths *et al.*, 2004; Lejeune *et al.*, 2006; De Zélicourt *et al.*, 2007; Kusumoto *et al.*, 2007; Letousey *et al.*, 2007; Swarbrick *et al.*, 2008; Hiraoka *et al.*, 2009; Li *et al.*, 2009; Runyon *et al.*, 2010; Huang *et al.*, 2012; Torres-Vera *et al.*, 2016). For instance, expression of one of JA-responsive lipoxygenases (LOX1), which play a role in the response to wounding, pathogen and insect feeding (Moran and Thompson, 2001; Porta and Rocha-Sosa, 2002), have been shown to be up-regulated in *P. ramosa*-infested *Arabidopsis* (Dos Santos *et al.*, 2003b). A few genes/proteins have been found to be specific for the host-parasite interaction, such as the sunflower *HaDEF1*, encoding a defensin, which is responsible for inducing cell death (necrosis) at the radicle apex of attached *Orobanch*e seedlings (De Zélicourt *et al.*, 2007).

Currently, the safest approach to combat parasitic plant infestation is to generate parasitic plant-resistant cultivars through breeding strategies, which are based on understanding of the genetic basis of host resistance against parasitic plants. In many crops, susceptible and resistant host resources have been identified, such as in legumes against *Orobanch*e (Rubiales *et al.*, 2003; Rubiales *et al.*, 2014), and in maize, sorghum and rice against *Striga* (Gurney *et al.*, 2002; Haussmann *et al.*, 2004; Cissoko *et al.*, 2011; Jamil *et al.*, 2011b; Cardoso *et al.*, 2014). By using these susceptible

and resistant parental lines, mapping populations such as recombinant inbred lines (RILs) and backcrossing inbred lines (BILs) have been constructed to identify genomic regions that influence resistance against parasitic weeds (Hausmann *et al.*, 2004; Gurney *et al.*, 2006). These identified QTLs (Quantitative Trait Locus) are then candidates for marker-assisted selection (MAS) in crop breeding. So far, some major QTLs have been identified for resistance against *Orobanch*e in legumes and *Striga* in rice and sorghum (Pérez-Vich *et al.*, 2004; Valderrama *et al.*, 2004; Gurney *et al.*, 2006; Molinero-Ruiz *et al.*, 2006; Satish *et al.*, 2012). These QTLs could only explain low to moderate levels of variation for resistance, especially for resistance against *Orobanch*e (Gurney *et al.*, 2002; Rubiales *et al.*, 2003; Rubiales *et al.*, 2014), making the future breeding programs more difficult and time-consuming.

Only in a few cases, single dominant/recessive genes have been identified that are causal for the resistance against parasitic plants. In sunflower, five single dominant genes *Or1* to *Or5* were identified as resistance genes against five pathogenic races of *O. cumana* (Pérez-Vich *et al.*, 2004; Molinero-Ruiz *et al.*, 2006). Among these genes, *Or5*, conferring resistance to *O. cumana* race E, was mapped to a region that is enriched with NBS-LRR type R-gene homologs (Radwan *et al.*, 2008). Recessive alleles at two loci were found to confer resistance to *O. cumana* race F in germplasm derived from cultivated sunflower (line P-96 and KI-534) (Akhtouch *et al.*, 2002). It was later found that the resistance conferred by the line P-96 was determined by six QTLs with small or moderate effect on reducing the number of parasites per host plant (Pérez-Vich *et al.*, 2004). Some of these QTLs are race-specific while others are not. In legumes, resistance to *Orobanch*e and *Phelipanche* spp. is reported to be polygenic with a low heritability and high environment-dependency (Valderrama *et al.*, 2004; Rubiales *et al.*, 2006). For example, several QTLs such as *Oc1* to *Oc5* that are linked to resistance against *O. crenata*, were identified in faba bean (Díaz-Ruiz *et al.*, 2010). However, only *Oc2* and *Oc3* were stable QTLs that could be detected across different environments, while the other QTLs only appeared in a single environment (Díaz-Ruiz *et al.*, 2010). Considering the environment-dependent and race-specific nature of parasitic plant resistance, caution should be taken in interpretation and subsequent use of QTLs identified in single experiments. Therefore, prior to the application of MAS programs, it is essential to validate QTLs across different environments or in different genetic backgrounds, to ensure development of robust molecular markers (Swarbrick *et al.*, 2009; Rubiales *et al.*, 2014).



In addition to QTL mapping, omics technologies, such as transcriptomics and proteomics, could also provide resistance candidate genes. Many defense-related genes and/or proteins have been identified by dissecting differential gene expression before and after *Orobanche* infection or in susceptible and resistant cultivars (Dos Santos *et al.*, 2003a; Dos Santos *et al.*, 2003b; Castillejo *et al.*, 2009; Die *et al.*, 2009).

Biotechnology could potentially help in the development of new, transgenic based, resistances in host plants to help eradicate parasitic weeds. However, successful examples of genetic engineering, using resistance genes against Orobanchaceae, are still limited. Due to the fact that there is RNA exchange between host and parasite, it is also possible to target specific transcripts in parasitic plants using gene silencing strategies (Aly *et al.*, 2009). One successful example comes from a tomato line transformed with an inverted-repeat fragment designed to silence the gene *Mannose 6-Phosphate Reductase (M6PR)* in *P. aegyptiaca* (Aly *et al.*, 2009). The level of *M6PR* mRNA in the parasite was indeed suppressed. Since M6PR is a key enzyme in mannitol biosynthesis, which is important for tubercle development, this approach resulted in a significant decrease in healthy *P. aegyptiaca* tubercles (Aly *et al.*, 2009). More and more studies reveal that there is translocation of viruses and macromolecules between host plant and parasitic weeds, suggesting that there is a great potential for this transgenic approach to control weeds (Gal-On *et al.*, 2009; Aly *et al.*, 2011; Aly, 2012; 2013; Aly *et al.*, 2014; Ibdah *et al.*, 2014; Zhang *et al.*, 2014a).

In conclusion, it is clear that single control measures or resistance genes will not bring a durable solution for parasitic weed control. Rather, various approaches should be integrated to achieve this. Resources of resistance and resistance/tolerance mechanisms should be further explored, not only within hosts but also within non-host species. A better understanding of the genes that underlie resistance may also help to optimize the protection of crops against parasitic weeds.

### ***Arabidopsis* as a model to explore host-parasite interaction**

As a model plant, *Arabidopsis* has not only been used to study general plant development but also to explore plant interactions with other organisms and with its environment. *Arabidopsis* offers many advantages in plant research such as its compact size, its short life cycle, the available information of a fully sequenced genome, sufficient genetic markers, various

mutants and all the established databases and molecular technologies.

1 Although *Arabidopsis* is not a natural host for parasitic plants, its potential to serve as a model to investigate the interaction between host and parasitic plants has been explored. Goldwasser and Yoder (2001) tested the ability of *Arabidopsis* to induce germination of *P. ramosa* seeds. Although all of the ecotypes and fast-neutron mutated M2 plants in these tests were susceptible, variation in the *P. ramosa* germination-inducing capacity of these lines was observed, and therefore low germination stimulating lines could be selected (Goldwasser and Yoder, 2001). In a few other studies, the susceptibility of *Arabidopsis* to different *Orobanch*e and *Phelipanche* species (*P. aegyptiaca*, *O. minor*, *P. ramosa*, *O. crenata*, *O. cernua*) was tested (Goldwasser *et al.*, 2000b; Westwood, 2000). Although *Arabidopsis* could not induce seed germination of some of the *Orobanch*e species (such as *O. minor*, *O. crenata* and *O. cernua*), *O. minor* and *O. crenata* could successfully establish tubercles along *Arabidopsis* roots when their seeds were pre-germinated with the strigolactone analog GR24 (Goldwasser *et al.*, 2000b; Westwood, 2000). This implies that *Arabidopsis* may be a good model to investigate especially the process of post-germination parasitism (Westwood, 2000; Dos Santos *et al.*, 2003a; Dos Santos *et al.*, 2003b; Birschwilks *et al.*, 2007; Mor *et al.*, 2008). The availability of large collections of *Arabidopsis* mutants would then facilitate studies on the importance of certain genes in the host-parasite interaction. For instance, *Arabidopsis* mutants that are compromised in the production of reaction oxygen species (ROS) have been used to validate the ROS production at the site of host-*P. aegyptiaca* interaction, helping to decipher the role of ROS in promoting adventitious root elongation of the parasite tubercles and the loosening of the host cell wall during parasite attachment (Mor *et al.*, 2008).

Note that although strigolactones are the main germination stimulants for parasitic plants in many crops (Goldwasser *et al.*, 2008) and also have been detected in *Arabidopsis* root exudate (Kohlen *et al.*, 2011), strigolactones could hardly be detected in *Arabidopsis* in other experiments (Abe *et al.*, 2014). Other compounds in *Arabidopsis* such as isothiocyanates or other non-strigolactone compounds may also act as germination stimulants for broomrape (Kohlen *et al.*, 2011; Auger *et al.*, 2012). Recently, methyl carlactonoate (MeCLA), a strigolactone-like molecule (SL-LIKE1), has been detected in *Arabidopsis* wildtype root extracts. This compound was shown to stimulate germination of both *Orobanch*e and *Striga* seeds (Abe *et al.*, 2014; Seto *et al.*, 2014). It is still not clear whether crop plants that produce real and larger amounts of strigolactones share the same

mechanisms as *Arabidopsis* in stimulating parasite seed germination. Therefore, whether the knowledge of germination stimulants from *Arabidopsis* can be directly utilized in crops remains a question.

### Applications of genome-wide association mapping

As described above, QTL mapping has been used to identify genomic regions involved in parasitic plant resistance. However, QTL mapping populations only harbour limited allelic diversity, *viz.* the genetic diversity that resides in the two parents used to create the mapping population. In addition to this, the overall low recombination frequency in mapping populations results in a relatively low mapping resolution. These disadvantages could be compensated by intercrossing diverse accessions before constructing the RIL population (Cavanagh *et al.*, 2008). Nevertheless, the allelic diversity and recombination frequencies of these artificial/lab populations is still not comparable to that observed in natural populations, and therefore limits our understanding of functional diversity.

Genome-wide association mapping (GWA mapping, also known as linkage disequilibrium mapping) can overcome these disadvantages of QTL mapping. Rather than analysing the association of phenotypic traits and genotypic marker information in a population containing the genetic variation derived from two parents, GWA mapping evaluates the marker-trait association in a collection of genetically diverse individuals (Nordborg and Tavaré, 2002). Because the allelic diversity in such a population results from recombination events that have accumulated during many generations, GWA mapping can achieve a much higher resolution than conventional QTL mapping approaches. Besides this, because readily available collections of ecotypes can be directly exploited, time and efforts to make crosses, which is needed to make QTL mapping populations, becomes superfluous. The drawbacks of GWA mapping mainly lie in the fact that its power and false positive rate is unpredictable. This partly results from the unknown population structure, and the high number of markers needed, which increase the likelihood of false-positive associations due to multiple testing (Lander and Schork, 1994; Nordborg and Tavaré, 2002; Zondervan and Cardon, 2004; Korte and Farlow, 2013). Therefore, it is highly recommended to integrate GWA mapping with other QTL mapping approaches and/or 'omics' technologies to gain more power to obtain a better prediction of causal genes underlying the trait of interest (Adamski, 2012).

*Arabidopsis*, as a model plant, is the first being used in GWA map-

ping to explore natural variation in plant development and plant response to different environments and stresses. With the advance of genome sequencing and high-density single nucleotide polymorphism (SNP) panels, GWA studies are also becoming more and more popular in other plant species, including agricultural crops. This applies not only to phenotypes of plant growth such as flowering time (Aranzana *et al.*, 2005; Atwell *et al.*, 2010; Brachi *et al.*, 2010) and root architectural traits (Courtois *et al.*, 2013; Zurek *et al.*, 2015), but also for plant responses to abiotic and biotic stresses (Chan *et al.*, 2010; Setter *et al.*, 2010; Kloth *et al.*, 2012; Wang *et al.*, 2012; Verslues *et al.*, 2014; Bac-Molenaar *et al.*, 2015a; Bac-Molenaar *et al.*, 2015b; Kumar *et al.*, 2015; Samayoa *et al.*, 2015; Bac-Molenaar *et al.*, 2016; Davila Olivas *et al.*, 2016; Kloth *et al.*, 2016; Thoen *et al.*, 2017).

### The biology of strigolactones

As already mentioned in the first part of this chapter, strigolactones, a group of carotenoid-derived compounds, have been recognized as host-derived germination stimulants for root parasitic plants such as broomrapes (*Orobanche* and *Phelipanche* spp.) and witchweeds (*Striga* spp.) (Bouwmeester *et al.*, 2003). They were also found to function as allelochemicals in symbiosis with arbuscular mycorrhizal fungi (AMF) (Akiyama *et al.*, 2005). Recently, biological functions of strigolactones have been further exploited and it has become apparent that besides their function as rhizosphere signalling molecules, they also play an important role as endogenous plant hormones. As such, they regulate shoot branching (Gomez-Roldan *et al.*, 2008), seed germination (Toh *et al.*, 2012a; Toh *et al.*, 2012b), root development (Koltai *et al.*, 2009; Kapulnik *et al.*, 2011a; Kapulnik *et al.*, 2011b; Koltai, 2011; Ruyter-Spira *et al.*, 2011; De Cuyper *et al.*, 2015; Jiang *et al.*, 2016), hypocotyl / mesocotyl growth (Hu *et al.*, 2010; Shen *et al.*, 2012; Hu *et al.*, 2014; Jia *et al.*, 2014) and secondary growth (Agusti *et al.*, 2011). Many of these strigolactone-mediated processes are not only important during plant development, but also during the response to various biotic and abiotic stresses (Bu *et al.*, 2014; Kapulnik and Koltai, 2014; Torres-Vera *et al.*, 2014; Liu *et al.*, 2015; Piisila *et al.*, 2015). It would be interesting to explore whether strigolactones are also involved in the plant defence mechanism against parasitic plants during post-germination parasitism, apart from their germination stimulatory role for the parasitic weeds.

In recent years, there is a growing interest in exploring the biosynthesis and signalling pathways of this plant hormone. We now know

that strigolactones are derived from the carotenoid pathway and that their formation is catalysed by key enzymes including DWARF27 (D27), CAROTENOID CLEAVAGE DIOXYGENASE 7 and 8 (CCD7 and CCD8), and MAX1 (Booker *et al.*, 2004; Lin *et al.*, 2009; Vogel *et al.*, 2010; Alder *et al.*, 2012; Kohlen *et al.*, 2012; Liu *et al.*, 2013; Abe *et al.*, 2014; Zhang *et al.*, 2014b; Bruno and Al-Babili, 2016). The MORE AXILARY GROWTH2 (MAX2) in *Arabidopsis* or DWARF3 (D3) in rice, an F-box component of the Skp-Cullin-F-box (SCF) E3 ubiquitin ligase complex, has been recognized as a key enzyme in the strigolactone signalling pathway (Mashiguchi *et al.*, 2009; Nelson *et al.*, 2011). Another key enzyme in the strigolactone signalling pathway is an  $\alpha/\beta$  hydrolase, DWARF14 (D14), which serves as a receptor of strigolactones and will then bind to MAX2 (Arite *et al.* 2009; Hamiaux *et al.* 2012; Chevalier *et al.* 2014). DWARF 53 (D53), that also binds to D14, acts as a repressor of strigolactone signalling. Strigolactones inhibit axillary bud outgrowth through the degradation of D53, which is mediated by the D14 and SCF<sup>D3</sup> ubiquitin ligase complex (Zhou *et al.* 2013; Jiang *et al.* 2013; Kong *et al.* 2014). In addition, a few other proteins are known to act downstream of the strigolactones or interact with strigolactone signalling, such as SHY2 (SHORT HYPOCOTYL 2), OsMADS57 and BES1 (*bri1*-EMS-suppressor 1) (Guo *et al.*, 2013; Koren *et al.*, 2013; Wang *et al.*, 2013). However, our understanding of strigolactone biosynthesis and signalling remains limited. More efforts should be made to explore the missing parts in the strigolactone biosynthesis pathway, resolving the enzymatic steps in diversification, and in the strigolactone downstream signalling pathways that are involved in various strigolactone mediated responses.

## Scope of the thesis

A joint effort has been made to explore resistance mechanisms against multiple biotic and abiotic stresses in an STW-funded project “Learning from Nature (LFN)” (Thoen *et al.*, 2017). This project consists of several research projects which investigate natural variation in tolerance to specific biotic/abiotic stresses in the same *Arabidopsis* population. GWA mapping is used to search for candidate QTLs for tolerance to these stresses. The similar research approach of all the research projects also allows the comparisons between results from each project and to identify stress-specific QTLs. The results obtained from *Arabidopsis* are then translated to crops of interest, with the contributions from industrial partners. As part of the LFN project, this thesis explored natural variation in resistance against the parasitic plant *P. ramosa* in *Arabidopsis* and tomato by using genetic and physiological approaches.

In **Chapter 1**, I first introduce parasitic plants, their problems, their interaction with host plants, as well as current strategies to control them. *Arabidopsis* is used as a model to better understand the interaction between host and parasite. Another important genetic tool, GWA mapping, can be utilized to explore host resistance mechanisms. In addition, the biology of strigolactones, the parasitic plant seed germination stimulant, is highlighted.

In **Chapter 2**, I performed GWA analysis on parasitic plant resistance during post-germination process of infection in a natural *Arabidopsis* population. Quantification of tubercle growth during time, results in the characterization of different mechanisms underlying *Arabidopsis* susceptibility to *P. ramosa*. Significant SNPs have been identified, and candidate genes selected and prioritized. Several top candidate genes are characterized in T-DNA mutants. Gene expression of these candidates is verified in Col-0 with and without *P. ramosa* infection.

As strigolactones, the predominant germination stimulants for parasitic plants, have been suggested to play a role in plant defence in several reports, this thesis also explores if strigolactones may also exert their effects on post-germination parasitism. For this purpose, I compare the response of a strigolactone-deficient tomato line (*SlCCD8* RNAi lines) with its wildtype upon infection with *P. ramosa* in **Chapter 3**. In this study, specific attention is paid to the absolute parasite infection level and the effect of the parasite on host biomass, plant architecture, the level of ABA and its metabolites, leaf water loss and stomatal characteristics. The potential roles of strigolactones and other hormones in host defence against parasitic plants are discussed.

In **Chapter 4**, I further discuss the interaction of the strigolactones with other plant hormones in a published review. This review introduces how strigolactones interact with other hormones during plant development, such as shoot branching, root growth and secondary growth and in response to environmental stimuli.

In addition, I try to further increase our understanding of strigolactone biosynthesis in tomato by characterizing a strigolactone-deficient tomato mutant *Slmax1* (**Chapter 5**). Compared to wild type tomato, the *Slmax1* mutant displays obvious phenotypes as a strigolactone-deficient mutant. The role of MAX1 in the strigolactone biosynthetic pathway is discussed.

With the aim to further explore the underlying mechanisms of strigolactone signalling in hypocotyl and root growth, another GWA mapping approach is performed on the response in hypocotyl length, root length and

root length/hypocotyl length ratio, to strigolactone treatment in the dark (**Chapter 6**). Based on the association of phenotypic variation with genetic markers, significant SNPs are identified, after which de novo candidate genes are selected. Several candidate genes are characterized by using Arabidopsis T-DNA lines. This study is a first attempt to use association mapping to explore genetic mechanisms involved in strigolactone signalling.

Finally, in **Chapter 7**, I give an update and perspectives on the strigolactone biosynthesis and signalling pathways. Additionally, I discuss the phenotyping tools used for studying host-parasite interaction. I also discuss the current efforts on studying resistance mechanisms against parasitic plants. Finally, I give suggestions and recommendations on future study on the strigolactone pathway and plant defence against parasitic plants.



## References

- Abbasher, A.A., and Sauerborn, J.** (1992). *Fusarium nygamai*, a potential bioherbicide for *Striga hermonthica* control in sorghum. *Biol Control* 2(4), 291-296.
- Abbes, Z., Kharrat, M., Delavault, P., Chaïbi, W., and Simier, P.** (2009a). Osmoregulation and nutritional relationships between *Orobanche foetida* and faba bean. *Plant Signal Behav* 4(4), 336-338.
- Abbes, Z., Kharrat, M., Delavault, P., Chaïbi, W., and Simier, P.** (2009b). Nitrogen and carbon relationships between the parasitic weed *Orobanche foetida* and susceptible and tolerant faba bean lines. *Plant Physiol Biochem* 47(2), 153-159.
- Abe, S., Sado, A., Tanaka, K., Kisugi, T., Asami, K., et al.** (2014). Carlactone is converted to carlactonoic acid by MAX1 in *Arabidopsis* and its methyl ester can directly interact with AtD14 in vitro. *Proc Natl Acad Sci U S A* 111(50), 18084-18089.
- Adagba, M.A., Lagoke, S.T.O., and Imolehin, E.D.** (2002a). Nitrogen effect on the incidence of *Striga hermonthica* (Del.) Benth in upland rice. *Acta Agronomica Hungarica* 50(2), 145-150.
- Adagba, M.A., Lagoke, T.O., and Usman, A.** (2002b). Management of *Striga hermonthica* (Del.) Benth in upland rice: influence of upland rice varieties and rates of nitrogen fertilizer. *Niger Agric J* 33, 119-127.
- Adamski, J.** (2012). Genome-wide association studies with metabolomics. *Genome Med* 4(4), 34.
- Agusti, J., Herold, S., Schwarz, M., Sanchez, P., Ljung, K., et al.** (2011). Strigolactone signaling is required for auxin-dependent stimulation of secondary growth in plants. *Proc Natl Acad Sci U S A* 108(50), 20242-20247.
- Akhtouch, B., Munoz-Ruz, J., Melero-Vara, J., Fernandez-Martinez, J., and Dominguez, J.** (2002). Inheritance of resistance to race F of broomrape in sunflower lines of different origins. *Plant Breeding* 121(3), 266-268.
- Akiyama, K., Matsuzaki, K., and Hayashi, H.** (2005). Plant sesquiterpenes induce hyphal branching in arbuscular mycorrhizal fungi. *Nature* 435(7043), 824-827.
- Alder, A., Jamil, M., Marzorati, M., Bruno, M., Vermathen, M., et al.** (2012). The path from beta-carotene to carlactone, a strigolactone-like plant hormone. *Science* 335(6074), 1348-1351.
- Aly, R.** (2012). Advanced technologies for parasitic weed control. *Weed Sci* 60(2), 290-294.
- Aly, R.** (2013). Trafficking of molecules between parasitic plants and their hosts. *Weed Res* 53(4), 231-241.
- Aly, R., Cholak, H., Joel, D.M., Leibman, D., Steinitz, B., et al.** (2009). Gene silencing of mannose 6-phosphate reductase in the parasitic weed *Orobanche aegyptiaca* through the production of homologous dsRNA sequences in the host plant. *Plant Biotechnol J* 7(6), 487-498.
- Aly, R., Dubey, N.K., Yahyaa, M., Abu-Nassar, J., and Ibdah, M.** (2014). Gene silencing of *CCD7* and *CCD8* in *Phelipanche aegyptiaca* by tobacco rattle virus system retarded



- p>the parasite development on the host.
- Plant Signal Behav*
- 9(8), e29376.
- Aly, R., Hamamouch, N., Abu-Nassar, J., Wolf, S., Joel, D.M., et al.** (2011). Movement of protein and macromolecules between host plants and the parasitic weed *Phelipanche aegyptiaca* Pers. *Plant Cell Rep* 30(12), 2233-2241.
- Angeles Castillejo, M., Amiour, N., Dumas-Gaudot, E., Rubiales, D., and Jorrín, J.V.** (2004). A proteomic approach to studying plant response to crenate broomrape (*Orobanche crenata*) in pea (*Pisum sativum*). *Phytochemistry* 65(12), 1817-1828.
- Aranzana, M.J., Kim, S., Zhao, K., Bakker, E., Horton, M., et al.** (2005). Genome-wide association mapping in *Arabidopsis* identifies previously known flowering time and pathogen resistance genes. *PLoS Genet* 1(5), e60.
- Atwell, S., Huang, Y.S., Vilhjálmsson, B.J., Willems, G., Horton, M., et al.** (2010). Genome-wide association study of 107 phenotypes in *Arabidopsis thaliana* inbred lines. *Nature* 465(7298), 627-631.
- Auger, B., Pouvreau, J.B., Pouponneau, K., Yoneyama, K., Montiel, G., et al.** (2012). Germination stimulants of *Phelipanche ramosa* in the rhizosphere of *Brassica napus* are derived from the glucosinolate pathway. *Mol Plant Microbe Interact* 25(7), 993-1004.
- Bac-Molenaar, J.A., Fradin, E.F., Becker, F.F.M., Rienstra, J.A., van der Schoot, J., et al.** (2015a). Genome-wide association mapping of fertility reduction upon heat stress reveals developmental stage-specific QTLs in *Arabidopsis thaliana*. *Plant Cell* 27(7), 1857-1874.
- Bac-Molenaar, J.A., Granier, C., Keurentjes, J.J., and Vreugdenhil, D.** (2016). Genome-wide association mapping of time-dependent growth responses to moderate drought stress in *Arabidopsis*. *Plant Cell Environ* 39(1), 88-102.
- Bac-Molenaar, J.A., Vreugdenhil, D., Granier, C., and Keurentjes, J.J.B.** (2015b). Genome-wide association mapping of growth dynamics detects time-specific and general quantitative trait loci. *J Exp Bot* 66(18), 5567-5580.
- Bandaranayake, P.C.G., Filappova, T., Tomilov, A., Tomilova, N.B., Jamison-McClung, D., et al.** (2010). A single-electron reducing quinone oxidoreductase is necessary to induce haustorium development in the root parasitic plant *Triphysaria*. *Plant Cell* 22(4), 1404-1419.
- Bandaranayake, P.C.G., and Yoder, J.I.** (2013). Trans-specific gene silencing of acetyl-CoA carboxylase in a root-parasitic plant. *Mol Plant Microbe Interact* 26(5), 575-584.
- Bar-Nun, N., Sachs, T., and Mayer, A.M.** (2008). A role for IAA in the infection of *Arabidopsis thaliana* by *Orobanche aegyptiaca*. *Ann Bot* 101(2), 261-265.
- Benharrat, H., Boulet, C., Theodet, C., and Thalouarn, P.** (2005). Virulence diversity among branched broomrape (*O. ramosa* L.) populations in France. *Agron Sustain Dev* 25(1), 123-128.
- Birschwilks, M., Sauer, N., Scheel, D., and Neumann, S.** (2007). *Arabidopsis thaliana* is a susceptible host plant for the holoparasite *Cuscuta spec.* *Planta* 226(5), 1231-1241.
- Boari, A., Ciasca, B., Pineda-Martos, R., Lattanzio, V.M., Yoneyama, K., et al.** (2016).

Parasitic weed management by using strigolactone-degrading fungi. *Pest Manag Sci* 72(11), 2043-2047.

**Booker, J., Auldridge, M., Wills, S., McCarty, D., Klee, H., et al.** (2004). MAX3/CCD7 is a carotenoid cleavage dioxygenase required for the synthesis of a novel plant signaling molecule. *Curr Biol* 14(14), 1232-1238.

**Botanga, C.J., and Timko, M.P.** (2005). Genetic structure and analysis of host and nonhost interactions of *Striga gesnerioides* (witchweed) from central Florida. *Phytopathology* 95(10), 1166-1173.

**Bouwmeester, H.J., Matusova, R., Zhongkui, S., and Beale, M.H.** (2003). Secondary metabolite signalling in host–parasitic plant interactions. *Curr Opin Plant Biol* 6(4), 358-364.

**Brachi, B., Faure, N., Horton, M., Flahauw, E., Vazquez, A., et al.** (2010). Linkage and association mapping of *Arabidopsis thaliana* flowering time in nature. *PLoS Genet* 6(5), e1000940.

**Brault, M., Betsou, F., Jeune, B., Tuquet, C., and SALLE, G.** (2007). Variability of *Orobancha ramosa* populations in France as revealed by cross infestations and molecular markers. *Environ Exp Bot* 61(3), 272-280.

**Brotherson, J.D., Simmons, B.T., and Ball, T.** (2005). Nutrient relationships between *Orobancha fasciculata* Nutt. and its host *Artemisia pygmaea* Gray in the Uinta basin of Utah, USA. *Western North American Naturalist* 65(2), 242-247

**Bruno, M., and Al-Babili, S.** (2016). On the substrate specificity of the rice strigolactone biosynthesis enzyme DWARF27. *Planta* 243(6), 1429-1440.

**Bu, Q., Lv, T., Shen, H., Luong, P., Wang, J., et al.** (2014). Regulation of drought tolerance by the F-box protein MAX2 in *Arabidopsis*. *Plant Physiol* 164(1), 424-439.

**Buschmann, H., Gonsior, G., and Sauerborn, J.** (2005a). Pathogenicity of branched broomrape (*Orobancha ramosa*) populations on tobacco cultivars. *Plant Pathol* 54(5), 650-656.

**Buschmann, H., Kömle, S., Gonsior, G., and Sauerborn, J.** (2005b). Susceptibility of oil-seed rape (*Brassica napus* ssp. *napus*) to branched broomrape (*Orobancha ramosa* L.). *Zeitschrift für Pflanzenkrankheiten und Pflanzenschutz* 112(1), 65-70.

**Cagán, L., and Tóth, P.** (2003). A decrease in tomato yield caused by branched broomrape (*Orobancha ramosa*) parasitization. *Acta Fytotechnica et Zootechnica*, 65-68.

**Cardoso, C., Zhang, Y., Jamil, M., Hepworth, J., Charnikhova, T., et al.** (2014). Natural variation of rice strigolactone biosynthesis is associated with the deletion of two MAX1 orthologs. *Proc Natl Acad Sci U S A* 111(6), 2379-2384.

**Castillejo, M.A., Maldonado, A.M., Dumas-Gaudot, E., Fernandez-Aparicio, M., Susin, R., et al.** (2009). Differential expression proteomics to investigate responses and resistance to *Orobancha crenata* in *Medicago truncatula*. *BMC Genomics* 10(1), 294.

**Cavanagh, C., Morell, M., Mackay, I., and Powell, W.** (2008). From mutations to MAG-IC: resources for gene discovery, validation and delivery in crop plants. *Curr Opin Plant Biol* 11(2), 215-221.

- Chan, E.K.F., Rowe, H.C., and Kliebenstein, D.J.** (2010). Understanding the evolution of defense metabolites in *Arabidopsis thaliana* using genome-wide association mapping. *Genetics* 185(3), 991-1007.
- Chang, M., and Lynn, D.G.** (1986). The haustorium and the chemistry of host recognition in parasitic angiosperms. *J Chem Ecol* 12(2), 561-579.
- Cissoko, M., Boissard, A., Rodenburg, J., Press, M.C., and Scholes, J.D.** (2011). New Rice for Africa (NERICA) cultivars exhibit different levels of post attachment resistance against the parasitic weeds *Striga hermonthica* and *Striga asiatica*. *New Phytol* 192(4), 952-963.
- Cohen, B.A., Amsellem, Z., Lev-Yadun, S., and Gressel, J.** (2002). Infection of tubercles of the parasitic weed *Orobanchae aegyptiaca* by mycoherbicidal *Fusarium* species. *Ann Bot* 90(5), 567-578.
- Courtois, B., Audebert, A., Dardou, A., Roques, S., Ghneim-Herrera, T., et al.** (2013). Genome-wide association mapping of root traits in a japonica rice panel. *PLoS One* 8(11), e78037.
- Davila Olivas, N.H., Kruijer, W., Gort, G., Wijnen, C.L., van Loon, J.J.A., et al.** (2016). Genome-wide association analysis reveals distinct genetic architectures for single and combined stress responses in *Arabidopsis thaliana*. *New Phytol* 213(2), 835-851.
- De Cuyper, C., Fromentin, J., Yocgo, R.E., De Keyser, A., Guillotin, B., et al.** (2015). From lateral root density to nodule number, the strigolactone analogue GR24 shapes the root architecture of *Medicago truncatula*. *J Exp Bot* 66(13), 4091.
- De Zélicourt, A., Letousey, P., Thoiron, S., Campion, C., Simoneau, P., et al.** (2007). Ha-DEF1, a sunflower defensin, induces cell death in *Orobanchae* parasitic plants. *Planta* 226(3), 591-600.
- Díaz-Ruiz, R., Torres, A.M., Satovic, Z., Gutierrez, M.V., Cubero, J.I., et al.** (2010). Validation of QTLs for *Orobanchae crenata* resistance in faba bean (*Vicia faba* L.) across environments and generations. *Theor Appl Genet* 120(5), 909-919.
- Die, J.V., González Verdejo, C.I., Dita, M.A., Nadal, S., and Román, B.** (2009). Gene expression analysis of molecular mechanisms of defense induced in *Medicago truncatula* parasitized by *Orobanchae crenata*. *Plant Physiol Biochem* 47(7), 635-641.
- Dos Santos, C.V., Delavault, P., and Letousey, P.** (2003a). Identification by suppression subtractive hybridization and expression analysis of *Arabidopsis thaliana* putative defence genes during *Orobanchae ramosa* infection. *Physiol Mol Plant Pathol* 62(5), 297-303.
- Dos Santos, C.V., Letousey, P., Delavault, P., and Thalouarn, P.** (2003b). Defense gene expression analysis of *Arabidopsis thaliana* parasitized by *Orobanchae ramosa*. *Phytopathology* 93(4), 451-457.
- Elzein, A., and Kroschel, J.** (2004). *Fusarium oxysporum* Foxy 2 shows potential to control both *Striga hermonthica* and *S. asiatica*. *Weed Res* 44(6), 433-438.
- Gal-On, A., Naglis, A., Leibman, D., Ziadna, H., Kathiravan, K., et al.** (2009). Broomrape can acquire viruses from its hosts. *Phytopathology* 99(11), 1321-1329.

- Gibot-Leclerc, S., Sallé, G., Reboud, X., and Moreau, D.** (2012). What are the traits of *Phelipanche ramosa* (L.) Pomel that contribute to the success of its biological cycle on its host *Brassica napus* L.? *Flora* 207(7), 512-521.
- Goldwasser, Y., Plakhine, D., Kleifeld, Y., and Zamski, E.** (2000a). The differential susceptibility of vetch (*Vicia* spp.) to *Orobanche aegyptiaca*: anatomical studies. *Ann Bot* 85(2), 257-262.
- Goldwasser, Y., Plakhine, D., and Yoder, J.I.** (2000b). *Arabidopsis thaliana* susceptibility to *Orobanche* spp. *Weed Sci* 48(3), 342-346.
- Goldwasser, Y., and Yoder, J.I.** (2001). Differential induction of *Orobanche* seed germination by *Arabidopsis thaliana*. *Plant Sci* 160(5), 951-959.
- Goldwasser, Y., Yoneyama, K., Xie, X., and Yoneyama, K.** (2008). Production of strigolactones by *Arabidopsis thaliana* responsible for *Orobanche aegyptiaca* seed germination. *Plant Growth Regul* 55(1), 21-28.
- Gomez-Roldan, V., Fermas, S., Brewer, P.B., Puech-Pagès, V., Dun, E.A., et al.** (2008). Strigolactone inhibition of shoot branching. *Nature* 455(7210), 189-194.
- Griffitts, A.A., Cramer, C.L., and Westwood, J.H.** (2004). Host gene expression in response to Egyptian broomrape (*Orobanche aegyptiaca*). *Weed Sci* 52(5), 697-703.
- Guo, S., Xu, Y., Liu, H., Mao, Z., Zhang, C., et al.** (2013). The interaction between OsMADS57 and OsTB1 modulates rice tillering via DWARF14. *Nat Commun* 4, 1566.
- Gurney, A.L., Slate, J., Press, M.C., and Scholes, J.D.** (2006). A novel form of resistance in rice to the angiosperm parasite *Striga hermonthica*. *New Phytol* 169(1), 199-208.
- Gurney, A.L., Taylor, A., Mbwaga, A., Scholes, J.D., and Press, M.C.** (2002). Do maize cultivars demonstrate tolerance to the parasitic weed *Striga asiatica*? *Weed Res* 42(4), 299-306.
- Hausmann, B.I.G., Hess, D.E., Omany, G.O., Folkertsma, R.T., Reddy, B.V.S., et al.** (2004). Genomic regions influencing resistance to the parasitic weed *Striga hermonthica* in two recombinant inbred populations of sorghum. *Theor Appl Genet* 109(5), 1005-1016.
- Hibberd, J.M., Quick, W.P., Press, M.C., Scholes, J.D., and Jeschke, W.D.** (1999). Solute fluxes from tobacco to the parasitic angiosperm *Orobanche cernua* and the influence of infection on host carbon and nitrogen relations. *Plant Cell Environ* 22(8), 937-947.
- Hiraoka, Y., Ueda, H., and Sugimoto, Y.** (2009). Molecular responses of *Lotus japonicus* to parasitism by the compatible species *Orobanche aegyptiaca* and the incompatible species *Striga hermonthica*. *J Exp Bot* 60(2), 641-650.
- Hirsch, A.M., Bauer, W.D., Bird, D.M., Cullimore, J., Tyler, B., et al.** (2003). Molecular signals and receptors: controlling rhizosphere interactions between plants and other organisms. *Ecology* 84(4), 858-868.
- Hu, Z., Yamauchi, T., Yang, J., Jikumar, Y., Tsuchida-Mayama, T., et al.** (2014). Strigolactone and cytokinin act antagonistically in regulating rice mesocotyl elongation in darkness. *Plant Cell Physiol* 55(1), 30-41.
- Hu, Z., Yan, H., Yang, J., Yamaguchi, S., Mackawa, M., et al.** (2010). Strigolactones nega-

tively regulate mesocotyl elongation in rice during germination and growth in darkness. *Plant Cell Physiol* 51(7), 1136-1142.

- Huang, K., Mellor, K.E., Paul, S.N., Lawson, M.J., Mackey, A.J., et al.** (2012). Global changes in gene expression during compatible and incompatible interactions of cowpea (*Vigna unguiculata* L.) with the root parasitic angiosperm *Striga gesnerioides*. *BMC Genomics* 13(1), 402.
- Ibdah, M., Dubey, N.K., Eizenberg, H., Dabour, Z., Abu-Nassar, J., et al.** (2014). *Cucumber Mosaic Virus* as a carotenoid inhibitor reducing *Phelipanche aegyptiaca* infection in tobacco plants. *Plant Signal Behav* 9(10), e972146.
- Irving, L.J., and Cameron, D.D.** (2009). You are what you eat: interactions between root parasitic plants and their hosts. *Adv Bot Res* 50, 87-138.
- Jamil, M., Charnikhova, T., Cardoso, C., JAMIL, T., UENO, K., et al.** (2011a). Quantification of the relationship between strigolactones and *Striga hermonthica* infection in rice under varying levels of nitrogen and phosphorus. *Weed Res* 51(4), 373-385.
- Jamil, M., Kanampiu, F.K., Karaya, H., Charnikhova, T., and Bouwmeester, H.J.** (2012a). *Striga hermonthica* parasitism in maize in response to N and P fertilisers. *Field Crops Res* 134, 1-10.
- Jamil, M., Rodenburg, J., Charnikhova, T., and Bouwmeester, H.J.** (2011b). Pre-attachment *Striga hermonthica* resistance of New Rice for Africa (NERICA) cultivars based on low strigolactone production. *New Phytol* 192(4), 964-975.
- Jamil, M., van MOURIK, T.A., Charnikhova, T., and Bouwmeester, H.J.** (2012b). Effect of diammonium phosphate application on strigolactone production and *Striga hermonthica* infection in three sorghum cultivars. *Weed Res* 53(2), 121-130.
- Jia, K.P., Luo, Q., He, S.B., Lu, X.D., and Yang, H.Q.** (2014). Strigolactone-regulated hypocotyl elongation is dependent on cryptochrome and phytochrome signaling pathways in *Arabidopsis*. *Mol Plant* 7(3), 528-540.
- Jiang, F., Jeschke, W.D., and Hartung, W.** (2004). Absciscic acid (ABA) flows from *Hordeum vulgare* to the hemiparasite *Rhinanthus minor* and the influence of infection on host and parasite absciscic acid relations. *J Exp Bot* 55(406), 2323-2329.
- Jiang, F., Veselova, S., Veselov, D., Kudoyarova, G., Jeschke, W.D., et al.** (2005). Cytokinin flows from *Hordeum vulgare* to the hemiparasite *Rhinanthus minor* and the influence of infection on host and parasite cytokinins relations. *Functional Plant Biol* 32(7), 619.
- Jiang, L., Matthys, C., Marquez-Garcia, B., De Cuyper, C., Smet, L., et al.** (2016). Strigolactones spatially influence lateral root development through the cytokinin signaling network. *J Exp Bot* 67(1), 379-389.
- Joel, D.** (1998). The angiospermous root parasite *Orobancha* L. (*Orobanchaceae*) induces expression of a pathogenesis related (PR) gene in susceptible tobacco roots. *Ann Bot* 81(6), 779-781.
- Joel, D.M.** (2009). The new nomenclature of *Orobancha* and *Phelipanche*. *Weed Res* 49, 6-7.
- Joel, D.M., Chaudhuri, S.K., Plakhine, D., Ziadna, H., and Steffens, J.C.** (2011). Dehy-

drocostus lactone is exuded from sunflower roots and stimulates germination of the root parasite *Phytochemistry* 72(7), 624-634.

Joel, D.M., and Gressel, J. (2013). *Parasitic Orobanchaceae*. Springer Science; Business Media.

Joel, D.M., Kleifeld, Y., Losner-Goshen, D., Herzlinger, G., and Gressel, J. (1995). Transgenic crops against parasites. *Nature* 374(6519), 220-221.

Joel, D.M., and Losner-Goshen, D. (1994). The attachment organ of the parasitic angiosperms *Orobanche cumana* and *O. aegyptiaca* and its development. *Can J Bot.* 72(5), 564-574.

Kannan, C., Aditi, P., and Zwanenburg, B. (2015). Quenching the action of germination stimulants using borax and thiourea, a new method for controlling parasitic weeds: A proof of concept. *Crop Prot* 70, 92-98.

Kannan, C., and Zwanenburg, B. (2014). A novel concept for the control of parasitic weeds by decomposing germination stimulants prior to action. *Crop Prot* 61, 11-15.

Kapulnik, Y., Delaux, P.M., Resnick, N., Mayzlish-Gati, E., Wininger, S., *et al.* (2011a). Strigolactones affect lateral root formation and root-hair elongation in *Arabidopsis*. *Planta* 233(1), 209-216.

Kapulnik, Y., and Koltai, H. (2014). Strigolactone involvement in root development, response to abiotic stress, and interactions with the biotic soil environment. *Plant Physiol* 166(2), 560-569.

Kapulnik, Y., Resnick, N., Mayzlish-Gati, E., Kaplan, Y., Wininger, S., *et al.* (2011b). Strigolactones interact with ethylene and auxin in regulating root-hair elongation in *Arabidopsis*. *J Exp Bot* 62(8), 2915-2924.

Kessler, A., and Baldwin, I.T. (2002). Plant responses to insect herbivory: the emerging molecular analysis. *Annu Rev Plant Biol* 53, 299-328.

Keyes, W.J., Palmer, A.G., Erbil, W.K., Taylor, J.V., Apkarian, R.P., *et al.* (2007). Sema-genesis and the parasitic angiosperm *Striga asiatica*. *Plant J* 51(4), 707-716.

Keyes, W.J., Taylor, J.V., Apkarian, R.P., and Lynn, D.G. (2001). Dancing together. Social controls in parasitic plant development. *Plant Physiol* 127(4), 1508-1512.

Kgosi, R.L., Zwanenburg, B., Mwakaboko, A.S., and Murdoch, A.J. (2012). Strigolactone analogues induce suicidal seed germination of *Striga* spp. in soil. *Weed Res* 52(3), 197-203.

Kirigia, D., Runo, S., and Alakonya, A. (2014). A virus-induced gene silencing (VIGS) system for functional genomics in the parasitic plant *Striga hermonthica*. *Plant Methods* 10(1), 16.

Klein, O., and Kroschel, J. (2002). Biological control of *Orobanche* spp. with *Phytomyza orobanchia*, a review. *BioControl* 47(3), 245-277.

Kloth, K.J., Thoen, M.P.M., Bouwmeester, H.J., Jongsma, M.A., and Dicke, M. (2012). Association mapping of plant resistance to insects. *Trends Plant Sci* 17(5), 311-319.

Kloth, K.J., Wiegiers, G.L., Busscher-Lange, J., van Haarst, J.C., Kruijer, W., *et al.* (2016). *AtWRKY22* promotes susceptibility to aphids and modulates salicylic acid and



jasmonic acid signalling. *J Exp Bot* 67(11), 3383-3396.

- Kohlen, W., Charnikhova, T., Lammers, M., Pollina, T., Toth, P., et al.** (2012). The tomato *CAROTENOID CLEAVAGE DIOXYGENASE 8* (*SICCD8*) regulates rhizosphere signaling, plant architecture and affects reproductive development through strigolactone biosynthesis. *New Phytol* 196(2), 535-547.
- Kohlen, W., Charnikhova, T., Liu, Q., Bours, R., Domagalska, M.A., et al.** (2011). Strigolactones are transported through the xylem and play a key role in shoot architectural response to phosphate deficiency in nonarbuscular mycorrhizal host *Arabidopsis*. *Plant Physiol* 155(2), 974-987.
- Kohlschmid, E., Sauerborn, J., and Müller-Stöver, D.** (2009). Impact of *Fusarium oxysporum* on the holoparasitic weed *Phelipanche ramosa*: biocontrol efficacy under field-grown conditions. *Weed Res* 49, 56-65.
- Koltai, H.** (2011). Strigolactones are regulators of root development. *New Phytol* 190(3), 545-549.
- Koltai, H., Dor, E., Hershenhorn, J., Joel, D.M., Weininger, S., et al.** (2009). Strigolactones' effect on root growth and root-hair elongation may be mediated by auxin-efflux carriers. *J Plant Growth Regul* 29(2), 129-136.
- Koren, D., Resnick, N., Mayzlish Gati, E., Belausov, E., Weininger, S., et al.** (2013). Strigolactone signaling in the endodermis is sufficient to restore root responses and involves *SHORT HYPOCOTYL 2* (*SHY2*) activity. *New Phytol* 198(3), 866-874.
- Korte, A., and Farlow, A.** (2013). The advantages and limitations of trait analysis with GWAS: a review. *Plant Methods* 9(1), 1-1.
- Kumar, V., Singh, A., Mithra, S.V.A., Krishnamurthy, S.L., Parida, S.K., et al.** (2015). Genome-wide association mapping of salinity tolerance in rice (*Oryza sativa*). *DNA Res* 22(2), 133-145.
- Kusumoto, D., Goldwasser, Y., Xie, X., Yoneyama, K., Takeuchi, Y., et al.** (2007). Resistance of red clover (*Trifolium pratense*) to the root parasitic plant *Orobancha minor* is activated by salicylate but not by jasmonate. *Ann Bot* 100(3), 537-544.
- Labrousse, P.** (2001). Several mechanisms are involved in resistance of *Helianthus* to *Orobancha cumana* Wallr. *Ann Bot* 88(5), 859-868.
- Labrousse, P.L., Delmail, D.D., Arnaud, M.C.A., and Thalouarn, P.T.** (2010). Mineral nutrient concentration influences sunflower infection by broomrape (*Orobancha cumana*). *Botany* 88(9), 839-849.
- Lander, E.S., and Schork, N.J.** (1994). Genetic dissection of complex traits. *Science*.
- Lechowski, Z.** (1996). Abscissic acid content in the root hemiparasite *Melampyrum arvense* L. before and after attachment to the host plant. *Biol Plant* 38(4), 489-494.
- Lechowski, Z., and Bialczyk, J.** (1996). Cytokinins in the hemiparasite *Melampyrum arvense* L. before and after attachment to the host. *Biol Plant* 38(4), 481-488.
- Lejeune, A., Constant, S., Delavault, P., Simier, P., Thalouarn, P., et al.** (2006). Involvement of a putative *Lycopersicon esculentum* wall-associated kinase in the early steps of tomato-*Orobancha ramosa* interaction. *Physiol Mol Plant Pathol* 69(1-3), 3-12.

- Letousey, P., De Zélicourt, A., Vieira Dos Santos, C., Thoiron, S., Monteau, F., et al.** (2007). Molecular analysis of resistance mechanisms to *Orobancha cumana* in sunflower. *Plant Pathol* 56(3), 536-546.
- Li, J., Lis, K.E., and Timko, M.P.** (2009). Molecular genetics of race-specific resistance of cowpea to *Striga gesnerioides* (Willd.). *Pest Manag Sci* 65(5), 520-527.
- Lin, H., Wang, R., Qian, Q., Yan, M., Meng, X., et al.** (2009). DWARF27, an iron-containing protein required for the biosynthesis of strigolactones, regulates rice tiller bud outgrowth. *Plant Cell* 21(5), 1512-1525.
- Liu, J., He, H., Vitali, M., Visentin, I., Charnikhova, T., et al.** (2015). Osmotic stress represses strigolactone biosynthesis in *Lotus japonicus* roots: exploring the interaction between strigolactones and ABA under abiotic stress. *Planta* 241(6), 1435-1451.
- Liu, J., Novero, M., Charnikhova, T., Ferrandino, A., Schubert, A., et al.** (2013). *CAROTENOID CLEAVAGE DIOXYGENASE 7* modulates plant growth, reproduction, senescence, and determinate nodulation in the model legume *Lotus japonicus*. *J Exp Bot* 64(7), 1967-1981.
- Longo, A.M.G., Lo Monaco, A., and Mauromicale, G.** (2010). The effect of *Phelipanche ramosa* infection on the quality of tomato fruit. *Weed Res* 50(1), 58-66.
- Mashiguchi, K., Sasaki, E., Shimada, Y., Nagae, M., Ueno, K., et al.** (2009). Feed-back-regulation of strigolactone biosynthetic genes and strigolactone-regulated genes in *Arabidopsis*. *Biosci Biotechnol Biochem* 73(11), 2460-2465.
- Mauromicale, G., Monaco, A.L., and Longo, A.M.G.** (2008). Effect of branched broomrape (*Orobancha ramosa*) infection on the growth and photosynthesis of tomato. *Weed Sci* 56(4), 574-581.
- Mohamed, A., Ellicott, A., Housley, T.L., and Ejeta, G.** (2003). Hypersensitive response to *Striga* infection in sorghum. *Crop Sci* 43(4), 1320.
- Mohamed, K.I., Papes, M., Williams, R., Benz, B.W., and Peterson, A.T.** (2006). Global invasive potential of 10 parasitic witchweeds and related *Orobanchaceae*. *AMBIO* 35(6), 281-288.
- Molinero-Ruiz, M.L., Melero-Vara, J.M., García-Ruiz, R., and Domínguez, J.** (2006). Pathogenic diversity within field populations of *Orobancha cumana* and different reactions on sunflower genotypes. *Weed Res* 46(6), 462-469.
- Mor, A., Mayer, A.M., and Levine, A.** (2008). Possible peroxidase functions in the interaction between the parasitic plant, *Orobancha aegyptiaca*, and its host, *Arabidopsis thaliana*. *Weed Biol Manage* 8(1), 1-10.
- Moran, P.J., and Thompson, G.A.** (2001). Molecular responses to aphid feeding in *Arabidopsis* in relation to plant defense pathways. *Plant Physiol* 125(2), 1074-1085.
- Nelson, D.C., Scaffidi, A., Dun, E.A., Waters, M.T., Flematti, G.R., et al.** (2011). F-box protein MAX2 has dual roles in karrikin and strigolactone signaling in *Arabidopsis thaliana*. *Proc Natl Acad Sci U S A* 108(21), 8897-8902.
- Nordborg, M., and Tavaré, S.** (2002). Linkage disequilibrium: what history has to tell us. *Trends Genet* 18(2), 83-90.



- Parker, C.** (1991). Protection of crops against parasitic weeds. *Crop Prot* 10(1), 6-22.
- Pérez-de-Luque, A., Lozano, M.D., Cubero, J.I., González-Melendi, P., Risueño, M.C., et al.** (2006). Mucilage production during the incompatible interaction between *Orobanche crenata* and *Vicia sativa*. *J Exp Bot* 57(4), 931-942.
- Pérez-Vich, B., Akhtouch, B., Knapp, S.J., Leon, A.J., Velasco, L., et al.** (2004). Quantitative trait loci for broomrape (*Orobanche cumana* Wallr.) resistance in sunflower. *Theor Appl Genet* 109(1), 92-102.
- Piisila, M., Keceli, M.A., Brader, G., Jakobson, L., Joesaar, I., et al.** (2015). The F-box protein MAX2 contributes to resistance to bacterial phytopathogens in *Arabidopsis thaliana*. *BMC Plant Biol* 15(1), 53.
- Porta, H., and Rocha-Sosa, M.** (2002). Plant lipoxygenases. Physiological and molecular features. *Plant Physiol* 130(1), 15-21.
- Radwan, O., Gandhi, S., Heesacker, A., Whitaker, B., Taylor, C., et al.** (2008). Genetic diversity and genomic distribution of homologs encoding NBS-LRR disease resistance proteins in sunflower. *Mol Genet Genomics* 280(2), 111-125.
- Robert, E.E.** (1975). Ethylene: a witchweed seed germination stimulant. *Weed Sci* 23(5), 433-436.
- Rodenburg, J., Bastiaans, L., Kropff, M.J., and Van Ast, A.** (2006). Effects of host plant genotype and seedbank density on *Striga* reproduction. *Weed Res* 46(3), 251-263.
- Rodenburg, J., Bastiaans, L., Weltzien, E., and Hess, D.E.** (2005). How can field selection for *Striga* resistance and tolerance in sorghum be improved? *Field Crops Res* 93(1), 34-50.
- Rubiales, D., Fernández-Aparicio, M., WEGMANN, K., and Joel, D.M.** (2009). Revisiting strategies for reducing the seedbank of *Orobanche* and *Phelipanche* spp. *Weed Res* 49(s1), 23-33.
- Rubiales, D., Flores, F., Emeran, A.A., Kharrat, M., Amri, M., et al.** (2014). Identification and multi-environment validation of resistance against broomrapes (*Orobanche crenata* and *Orobanche foetida*) in faba bean (*Vicia faba*). *Field Crops Res* 166, 58-65.
- Rubiales, D., Pérez-de-Luque, A., Fernández-Aparicio, M., Sillero, J.C., Román, B., et al.** (2006). Screening techniques and sources of resistance against parasitic weeds in grain legumes. *Euphytica* 147(1-2), 187-199.
- Rubiales, D., Pérez-de-Luque, A., Joel, D.M., Alcántara, C., and Sillero, J.C.** (2003). Characterization of resistance in chickpea to crenate broomrape (*Orobanche crenata*). *Weed Sci* 51(5), 702-707.
- Runyon, J.B., Mescher, M.C., Felton, G.W., and De Moraes, C.M.** (2010). Parasitism by *Cuscuta pentagona* sequentially induces JA and SA defence pathways in tomato. *Plant Cell Environ* 33(2), 290-303.
- Ruyter-Spira, C., Kohlen, W., Charnikhova, T., van Zeijl, A., van Bezouwen, L., et al.** (2011). Physiological effects of the synthetic strigolactone analog GR24 on root system architecture in *Arabidopsis*: another belowground role for strigolactones? *Plant Physiol* 155(2), 721-734.

- Samayoa, L.F., Malvar, R.A., Olukolu, B.A., Holland, J.B., and Butrón, A.** (2015). Genome-wide association study reveals a set of genes associated with resistance to the Mediterranean corn borer (*Sesamia nonagrioides* L.) in a maize diversity panel. *BMC Plant Biol* 15(1), 35.
- Sands, D.C., and Pilgeram, A.L.** (2009). Methods for selecting hypervirulent biocontrol agents of weeds: why and how. *Pest Manag Sci* 65(5), 581-587.
- Saremi, H., and Okhovvat, S.M.** (2008). Biological control of *Orobanche aegyptiaca* by *Fusarium oxysporum* F. sp. *Orobanche* in northwest Iran. *Commun Agric Appl Biol Sci* 73(4), 931-938.
- Satish, K., Gutema, Z., Grenier, C., Rich, P.J., and Ejeta, G.** (2012). Molecular tagging and validation of microsatellite markers linked to the low germination stimulant gene (*lgs*) for *Striga* resistance in sorghum [*Sorghum bicolor* (L.) Moench]. *Theor Appl Genet* 124(6), 989-1003.
- Schneeweiss, G.M.** (2007). Correlated evolution of life history and host range in the non-photosynthetic parasitic flowering plants *Orobanche* and *Phelipanche* (Orobanchaceae). *J Evol Biol* 20(2), 471-478.
- Seto, Y., Sado, A., Asami, K., Hanada, A., Umehara, M., et al.** (2014). Carlactone is an endogenous biosynthetic precursor for strigolactones. *Proc Natl Acad Sci U S A* 111(4), 1640-1645.
- Setter, T.L., Yan, J., Warburton, M., Ribaut, J.M., Xu, Y., et al.** (2010). Genetic association mapping identifies single nucleotide polymorphisms in genes that affect abscisic acid levels in maize floral tissues during drought. *J Exp Bot* 62(2), 701-716.
- Shen, H., Zhu, L., Bu, Q.-Y., and Huq, E.** (2012). *MAX2* affects multiple hormones to promote photomorphogenesis. *Mol Plant* 5(3), 750-762.
- Siqueira, J.O., Nair, M.G., Hammerschmidt, R., Safir, G.R., and Putnam, A.R.** (1991). Significance of phenolic compounds in plant soil microbial systems. *Critical Rev Plant Sci* 10(1), 63-121.
- Smith, J.D., Mescher, M.C., and De Moraes, C.M.** (2013). Implications of bioactive solute transfer from hosts to parasitic plants. *Curr Opin Plant Biol* 16(4), 464-472.
- Smith, M.C., Holt, J., and Webb, M.** (1993). Population model of the parasitic weed *Striga hermonthica* (Scrophulariaceae) to investigate the potential of *Smicronyx umbrinus* (Coleoptera: Curculionidae) for biological control in Mali. *Crop Prot* 12(6), 470-476.
- Swarbrick, P.J., Huang, K., Liu, G., Slate, J., Press, M.C., et al.** (2008). Global patterns of gene expression in rice cultivars undergoing a susceptible or resistant interaction with the parasitic plant *Striga hermonthica*. *New Phytol* 179(2), 515-529.
- Swarbrick, P.J., Scholes, J.D., Press, M.C., and Slate, J.** (2009). A major QTL for resistance of rice to the parasitic plant *Striga hermonthica* is not dependent on genetic background. *Pest Manag Sci* 65(5), 528-532.
- Tan, S., Evans, R.R., Dahmer, M.L., Singh, B.K., and Shaner, D.L.** (2005). Imidazolinone tolerant crops: history, current status and future. *Pest Manag Sci* 61(3), 246-257.
- Thoen, M.P., Davila Olivas, N.H., Kloth, K.J., Coolen, S., Huang, P.P., et al.** (2017).

Genetic architecture of plant stress resistance: multi-trait genome-wide association mapping. *New Phytol* 213(3), 1346-1362.

- Thomas, H.** (1999). *Fusarium oxysporum* f. sp. *orthoceras*, a potential mycoherbicide, parasitizes seeds of *Orobancha cumana* (sunflower broomrape): a cytological study. *Ann Bot* 83(4), 453-458.
- Thorogood, C.J., Rumsey, F.J., Harris, S.A., and Hiscock, S.J.** (2008). Host-driven divergence in the parasitic plant *Orobancha minor* Sm. (*Orobanchaceae*). *Mol Ecol* 17(19), 4289-4303.
- Thorogood, C.J., Rumsey, F.J., and Hiscock, S.J.** (2009). Host-specific races in the holoparasitic angiosperm *Orobancha minor*: implications for speciation in parasitic plants. *Ann Bot* 103(7), 1005-1014.
- Timus, A., and Croitoru, N.** (2007). The state of tobacco culture in Republic Moldova and phytosanitary problems of tobacco production. *Rasteniev'dni Nauki* 44(3), 209-212.
- Toh, S., Kamiya, Y., Kawakami, N., Nambara, E., McCourt, P., et al.** (2012a). Thermoinhibition uncovers a role for strigolactones in *Arabidopsis* seed germination. *Plant Cell Physiol* 53(1), 107-117.
- Toh, S., McCourt, P., and Tsuchiya, Y.** (2012b). HY5 is involved in strigolactone-dependent seed germination in *Arabidopsis*. *Plant Signal Behav* 7(5), 556-558.
- Torres-Vera, R., García, J.M., Pozo, M.J., and López-Ráez, J.A.** (2014). Do strigolactones contribute to plant defence? *Mol Plant Pathol* 15(2), 211-216.
- Torres-Vera, R., García, J.M., Pozo, M.J., and López-Ráez, J.A.** (2016). Expression of molecular markers associated to defense signaling pathways and strigolactone biosynthesis during the early interaction tomato-*Phelipanche ramosa*. *Physiol Mol Plant Pathol* 94, 100-107.
- Valderrama, M.R., Román, B., Satovic, Z., Rubiales, D., Cubero, J.I., et al.** (2004). Locating quantitative trait loci associated with *Orobancha crenata* resistance in pea. *Weed Res* 44(4), 323-328.
- Verslues, P.E., Lasky, J.R., Juenger, T.E., Liu, T.-W., and Kumar, M.N.** (2014). Genome-wide association mapping combined with reverse genetics identifies new effectors of low water potential-induced proline accumulation in *Arabidopsis*. *Plant Physiol* 164(1), 144-159.
- Vogel, J.T., Walter, M.H., Giavalisco, P., Lytovchenko, A., Kohlen, W., et al.** (2010). *SICCD7* controls strigolactone biosynthesis, shoot branching and mycorrhiza-induced apocarotenoid formation in tomato. *Plant J* 61(2), 300-311.
- Wang, M., Yan, J., Zhao, J., Song, W., Zhang, X., et al.** (2012). Genome-wide association study (GWAS) of resistance to head smut in maize. *Plant Sci* 196, 125-131.
- Wang, Y., Sun, S., Zhu, W., Jia, K., Yang, H., et al.** (2013). Strigolactone/MAX2-induced degradation of brassinosteroid transcriptional effector BES1 regulates shoot branching. *Dev Cell* 27(6), 681-688.
- Westwood, J.H.** (2000). Characterization of the *Orobancha*-*Arabidopsis* system for studying parasite-host interactions. *Weed Sci* 48(6), 742-748.

- Westwood, J.H., and Foy, C.L.** (1999). Influence of nitrogen on germination and early development of broomrape (*Orobanch*e spp.). *Weed Sci* 47, 2-7.
- Yoneyama, K., Xie, X., Kusumoto, D., Sekimoto, H., Sugimoto, Y., et al.** (2007). Nitrogen deficiency as well as phosphorus deficiency in sorghum promotes the production and exudation of 5-deoxystrigol, the host recognition signal for arbuscular mycorrhizal fungi and root parasites. *Planta* 227(1), 125-132.
- Yoshida, S., and Shirasu, K.** (2012). Plants that attack plants: molecular elucidation of plant parasitism. *Curr Opin Plant Biol* 15(6), 708-713.
- Zhang, D., Qi, J., Yue, J., Huang, J., Sun, T., et al.** (2014a). Root parasitic plant *Orobanch*e *aegyptiaca* and shoot parasitic plant *Cuscuta australis* obtained *Brassicaceae*-specific strictosidine synthase-like genes by horizontal gene transfer. *BMC Plant Biol* 14(1), 19.
- Zhang, Y., van Dijk, A.D., Scaffidi, A., Flematti, G.R., Hofmann, M., et al.** (2014b). Rice cytochrome P450 MAX1 homologs catalyze distinct steps in strigolactone biosynthesis. *Nat Chem Biol* 10(12), 1028-1033.
- Zondervan, K.T., and Cardon, L.R.** (2004). The complex interplay among factors that influence allelic association. *Nat Rev Genet* 5(2), 89-100.
- Zonno, and Vurro** (1999). Effect of fungal toxins on germination of *Striga hermonthica* seeds. *Weed Res* 39(1), 15-20.
- Zonno, M.C., and Vurro, M.** (2002). Inhibition of germination of *Orobanch*e *ramosa* seeds by *Fusarium* toxins. *Phytoparasitica* 30(5), 519-524.
- Zurek, P.R., Topp, C.N., and Benfey, P.N.** (2015). Quantitative trait locus mapping reveals regions of the maize genome controlling root system architecture. *Plant Physiol* 167(4), 1487-1496.
- Zwanenburg, B., Mwakaboko, A.S., and Kannan, C.** (2016). Suicidal germination for parasitic weed control. *Pest Manag Sci* 72(11), 2016-2025.





# Genome-wide association analysis of natural variation in susceptibility to the parasitic plant *Phelipanche ramosa* in *Arabidopsis thaliana*

---

**Running title:**

GWA analysis of broomrape parasitism in *Arabidopsis*

**Authors:**

Xi Cheng, Carolien Ruyter-Spira, Harro Bouwmeester<sup>\*,\*</sup>

**Affiliations:**

Laboratory of Plant Physiology, Wageningen University,  
Droevendaalsesteeg 1, 6708 PB Wageningen, the Netherlands

<sup>+</sup>Present address: Plant Hormone Biology lab, Swammerdam Institute  
for Life Sciences, University of Amsterdam, Science Park 904, 1098 XH  
Amsterdam, the Netherlands

<sup>\*</sup>Correspondence: h.j.bouwmeester@uva.nl, tel. +31 620387674

### Abstract

2 Broomrapes *Orobanche* and *Phelipanche* spp. are destructive agricultural weeds that pose a great threat to both crop production and quality. Broomrape infection of a host is a complex process, encompassing seed germination, host root penetration and attachment, development of a storage organ (called tubercle), and finally the emergence of a shoot and flowers aboveground. Quantitative genetics has been widely used to explore resistance mechanisms against parasitic weeds. However, traditional quantitative trait loci (QTL) mapping has limited mapping resolution and does therefore not allow the identification of the underlying genes. Here, we utilized a collection of *Arabidopsis thaliana* ecotypes to identify genomic associations and the underlying genes involved in (resistance to) parasitism, especially focusing on the number of tubercles and their growth during the post-attachment stage. By performing genome-wide association (GWA) mapping, we were able to pinpoint multiple significant SNPs that are associated with tubercle development. GWA mapping allowed us to compose a list of candidate genes. A T-DNA mutant of one of the top candidate genes, *RHB1A* (*RING-H2 FINGER B1A*), displayed significantly reduced total tubercle area compared to the corresponding wildtype. The expression of *RHB1A* showed a trend of increase after three weeks' parasite infection although at the border of statistical significance. Further investigations are needed to characterize other candidate genes.

### Keywords

linkage disequilibrium, broomrape, parasitic plant, post-attachment, defense response



## Introduction

The Orobanchaceae are the largest family of parasitic plants. Witchweeds *Striga* spp. and broomrapes *Orobanche* spp. and *Phelipanche* spp. are the most notorious agricultural weeds from this family that also contains wild, non-weedy parasitic plants. *Phelipanche ramosa*, formerly called *Orobanche ramosa*, has a wide host range, and especially poses a threat to Solanaceae (eg. tomato, tobacco and eggplant). Several reports have estimated at least 30 - 50% yield loss for tomato, tobacco and rapeseed when parasitized by *P. ramosa* (Cagán and Tóth, 2003; Buschmann *et al.*, 2005a; Buschmann *et al.*, 2005b; Timus and Croitoru, 2007; Gibot-Leclerc *et al.*, 2012). Not only is crop yield heavily reduced, but the quality of crop products can also be negatively affected by an infestation with this parasite (Longo *et al.*, 2010).

Tremendous efforts have been made to combat the weedy parasitic plants, however, broomrapes are difficult to control due to several reasons. First of all, parasitism is difficult to monitor as the life cycle of these parasites occurs partially underground. Their life cycle involves seed germination in close vicinity of a host root, the initiation and development of an absorptive organ (haustorium) which establishes a vascular connection with the host root, the development of a swollen nutrient storage organ (called a tubercle) on the root surface of the host-parasite connection, and finally, the subsequent shoot and flower development aboveground. Resistance against root parasitic plants can consist of different layers of incompatibility between host and parasite and different resistance mechanisms underlying the parasitism process (Die *et al.*, 2009; Yoshida and Shirasu, 2009; Thorogood and Hiscock, 2010; Louarn *et al.*, 2016). In most cases resistance is of polygenic nature complicating the identification of the genes that are involved (Pérez-Vich *et al.*, 2004; Rubiales *et al.*, 2009; Díaz-Ruiz *et al.*, 2010; Louarn *et al.*, 2016). Only in a few cases resistance was shown to be controlled by single broomrape race-specific dominant alleles (Pérez-Vich *et al.*, 2004; Velasco *et al.*, 2011; Rodríguez-Ojeda *et al.*, 2013). Another complication is that resistance against these parasites is highly influenced by the environment and the heritability is often low (Rubiales *et al.*, 2009; Díaz-Ruiz *et al.*, 2010). Finally, new virulent races of parasitic plants can emerge due to selective pressure exerted by cultivars with monogenic-resistance (Pérez-de-Luque *et al.*, 2009; Martín-Sanz *et al.*, 2016).

Quantitative genetics has been widely used to explore resistance

mechanisms against parasitic weeds. In many crops, *Orobanch* / *Striga*-susceptible and resistant host resources have been identified, enabling the establishment of mapping populations (Hausmann *et al.*, 2004; Fondevilla *et al.*, 2009). The development of genetic maps and quantitative trait locus (QTL) analysis have enabled the identification of genomic regions associated with quantitative traits. In addition, the identification of resistance-linked molecular markers could help with breeding programs by replacing screening tests. In this way, several QTLs for resistance against parasitic plants have been identified, such as in the interaction between *Orobancha cumana* and sunflower (Velasco *et al.*, 2011; Louarn *et al.*, 2016), *Orobancha crenata* and faba bean (Díaz-Ruiz *et al.*, 2010), *Striga hermonthica* and sorghum (Hausmann *et al.*, 2004), *S. hermonthica* and rice (Gurney *et al.*, 2006; Swarbrick *et al.*, 2009) and *Striga gesnerioides* and cowpea (Li *et al.*, 2009). For example, QTL mapping of sunflower resistance to *O. cumana* across different infection stages identified a few QTLs that explained a low to moderate proportion of the phenotypic variance (Louarn *et al.*, 2016). However, due to limited genome information available for many of these crops, only a few candidate resistance genes have been identified (Louarn *et al.*, 2016). Compared to conventional QTL mapping, genome-wide association (GWA) mapping evaluates the marker-trait association in a population of different genotypes, achieving much higher resolution (Nordborg and Tavaré, 2002).

Several groups showed that *Arabidopsis thaliana* is a suitable model to investigate the interaction between a host and the parasitic plant *P. ramosa* (Goldwasser *et al.*, 2000; Westwood, 2000; Goldwasser and Yoder, 2001; Dos Santos *et al.*, 2003; Bar-Nun and Mayer, 2008; Denev *et al.*, 2014). Goldwasser and Yoder (2001) designed a high-throughput assay to quantify the germination stimulant production of *Arabidopsis* using *P. ramosa* and *P. aegyptiaca* seeds. Although in this screen none of the *Arabidopsis* ecotypes exhibited complete resistance (induced no germination), there was variation among ecotypes and mutants in the capacity to induce seed germination and low germination stimulating genotypes could be selected (Goldwasser and Yoder, 2001). In another study the response of *Arabidopsis* to different *Orobanch* species was investigated (Goldwasser *et al.*, 2000; Westwood, 2000). Although *Arabidopsis* did not induce seed germination in all *Orobanch* species tested, it was highly susceptible to parasite invasion once the parasitic seeds had been induced to germinate with the synthetic germination stimulant GR24 (Goldwasser *et al.*, 2000; Westwood, 2000). This implies that *Arabidopsis* can serve as a model to study the process of post-germination

parasitism. In addition, mutant analysis, gene expression analysis and transgenic technology have been proven to be mature research approaches for this model plant and these methods have already facilitated investigators to characterize genes of interest for plant defense against parasitic plants in *Arabidopsis* (Westwood, 2000; Dos Santos *et al.*, 2003; Birschwilks *et al.*, 2007; Mor *et al.*, 2008). In the present study, we used a large collection of *Arabidopsis* ecotypes to explore the natural variation in parasitism by the broomrape *P. ramosa*, especially focusing on the development of the parasite storage organ, the tubercle, during the so-called post-attachment (or post-haustorial) process. Quantification of tubercle growth during a time series enabled identification of different patterns of tubercle growth between the various *Arabidopsis* ecotypes. GWA analysis was performed to identify genomic associations for *Arabidopsis* susceptibility to *P. ramosa*.

## Materials & Methods

### Plant materials

A core set of 359 *Arabidopsis* accessions, which was developed from a global collection to minimize redundancy and relatedness, was used (Baxter *et al.*, 2010; Li *et al.*, 2010; Horton *et al.*, 2012) (<http://bergelson.uchicago.edu/wp-content/uploads/2015/04/Justins-360-lines.xls>). This population has been genotyped as described in (Atwell *et al.*, 2010).

All accessions were screened with two replicates in a completely randomized design. Hereto, *Arabidopsis* was grown in a mini rhizotron system, essentially as described by others (Gurney *et al.*, 2006; Cissoko *et al.*, 2011) with small modifications. Briefly, a 5 mm hole was punctured through lid and bottom on one side of a 14.5 cm diameter round Petri dish, containing a slice of rockwool (14.5 cm diameter, 1.5 cm in thickness) covered with a piece of 12 cm diameter glass-fibre filter and a piece of 14.5 cm diameter nylon mesh. The rhizotron system was supplied with sterile 1/2-strength Hoagland solution.

*Arabidopsis* seeds were placed on wet filter paper under dark at 4°C for 3 d. Then five *Arabidopsis* seeds for each accession were sown on river sand (with a thin layer of soil on the top) and grown for 2 w at 21°C, 60% RH, 100  $\mu\text{mol m}^{-2} \text{s}^{-1}$  light intensity, 12 h:12 h L:D photoperiod. After 2 w, two replicates of healthy *Arabidopsis* seedlings for each accession were randomly selected, surface-sterilized with 70% ethanol for 5 s and washed with sterile demi-water and placed in the rhizotron system by fitting the plant

in the hole of the Petri dish. The leaves and shoots of the seedlings were kept outside of the Petri dishes. The roots were carefully spread out on the nylon mesh by forceps. Subsequently, the *Arabidopsis* was grown in the vertically placed rhizotron system at 21°C, 60% RH, 100  $\mu\text{mol m}^{-2} \text{s}^{-1}$  light intensity, 12 h:12 h L: D photoperiod for another 2 w.

In parallel, *P. ramosa* seeds were sterilized and spread on 5cm-diameter glass-fiber filter discs (Whatman GF/A paper), which were prewetted with 0.8 ml sterilized demi-water and placed in a 9 cm-diameter Petri dish. The Petri dish was sealed with parafilm and then kept in the dark in a growth chamber at 20°C for 12 d, the preconditioning period. Preconditioned *P. ramosa* seeds were then air-dried and treated with 0.8 ml strigolactone analog GR24 at the concentration of  $3.3 \times 10^{-3} \mu\text{M}$  for 1 d in the dark at 25°C. GR24 treatment triggered the initial germination of *P. ramosa*. After 1 d, GR24 was washed off using sterile demi-water. The pre-germinated *P. ramosa* seeds were spread along the roots of 4 w old *Arabidopsis* seedlings in the rhizotron system with a sterile painting brush. The rhizotron Petri dish was subsequently sealed with tape and wrapped in aluminium foil to keep the roots in darkness. The plates were then put back vertically under light at 21°C in a growth chamber. Plants were grown under the same conditions for another 4 w. Rhizotron Petri dishes were completely randomized in trays and their positions rearranged randomly every 3 d.

### Image analysis

Photos of *P. ramosa*-infested roots in the rhizotron system were taken at three time points: time point 1 (T1, 2 w after infection), time point 2 (T2, 3 w after infection) and time point 3 (T3, 4 w after infection) by using a Canon camera EOS 60D DSLR (with EF-S 18-135 mm IS Lens). Image processing was first optimised with the software Adobe Lightroom 4 and Adobe Photoshop CC. By using the image analysis software ImageJ (version 1.50e), tubercle diameter (Dia) on each host plant was measured. For the tubercles that had differentiated adventitious roots and shoots, the longest stretch across the center of the organ was considered the diameter. The numbers of tubercles (Nr) as well as numbers of germinated *P. ramosa* seeds that are in close vicinity to the roots (within 5 mm) were counted. The total area of tubercle occupation (Area) was estimated by summing up calculated areas of each tubercle based on diameter, assuming the shape of a tubercle is a circle.

### Statistical analysis

Mean values of replicates were calculated for each phenotypic trait.

Normality for each trait was evaluated by Shapiro-Wilk normality test and QQ-plot. All the measured and estimated traits (Nr, Dia and Area) across the three time-points were log-transformed since the majority of the data did not exhibit a normal distribution. A normal quantile transformation was performed to remove outliers as suggested (Guan and Stephens, 2010).

Since the outcome of parasite infection is highly dependent on how many pre-germinated *P. ramosa* seeds were spread along the host roots, linear regression was done with each log-transformed resistance parameter to the log-transformed number of pre-germinated *P. ramosa* seeds. The residue was then used as the value for the parameter.

Principal component analysis (PCA) was conducted to reduce the dimension of data, both on combining all single traits (Nr, Dia and Area) across three time-points and separately on each trait (Nr, Dia and Area) across time-points. The first principal component (PC1) was then taken for further use in GWA analysis, including PC1 of the combined PCA (Comb\_PC1), Nr (Nr\_PC1), Dia (Dia\_PC1) and Area (Area\_PC1) across all time points.

In order to investigate tubercle growth, growth rate of each tubercle parameter (Nr, Dia and Area) was calculated as  $[\log(X_j) - \log(X_i)] / T_{j-i}$  ( $X_j$ , the phenotypic value at the time-point  $j$ ;  $X_i$ , the phenotypic value at the time-point  $i$ ;  $T_{j-i}$ , time interval (days) between time point  $i$  and  $j$ ).

Descriptions for all the phenotypic parameters are given in **Table 1**. Spearman's rank correlation and other statistical analyses were implemented in the software Minitab and R (R Development Core Team, version 3.0).

### Genome-wide association mapping and heritability calculation

After removing data from plants that failed to grow properly or were contaminated with fungi, phenotypic values of the remaining 239 accessions were subjected to GWA analysis, including each tubercle parameter across different time points as well as PCA-based parameters. GWA analysis was performed with the EMMA software package by using a mixed model to correct for population structure based on a kinship matrix of all SNPs (Kang *et al.*, 2010). The model we adopted is as follows:

$$Y_i = \mu + X_{i\beta} + G_i + E_i \quad (i = 1, \dots, n) \quad G \sim N(0, \sigma_A^2 K), E_i \sim N(0, \sigma_E^2).$$

Where  $n$  is the number of accessions,  $Y_i$  is the phenotypic value of

accession  $i$ ,  $\mu$  is the intercept,  $X_i$  is the marker score,  $\beta$  is the marker effect,  $K$  is the kinship matrix. Genotypic effects  $G = (G_1, \dots, G_n)$  follow a  $N(0, \sigma_A^2 K)$  distribution. The random error effects  $E_i$  follow  $N(0, \sigma_E^2)$  distribution. The estimation of variance components  $\sigma_A^2$  and  $\sigma_E^2$  were obtained with the method of residual maximum likelihood (REML) by using the commercial R package 'ASREML' (Butler *et al.*, 2009) based on the methodology of EMMAX (Kang *et al.*, 2010). The significance of the marker effect  $\beta$  was tested with generalized least-squares (GLS) calculations by using the command line program 'scan-GLS' (El-Soda *et al.*, 2015). Single nucleotide polymorphisms (SNPs) with minor allele frequency (MAF) below 0.05 were excluded from the analysis. The broad-sense heritability ( $H^2$ ) and marker-based narrow-sense heritability ( $h^2$ ) were estimated by using the R package 'heritability' (El-Soda *et al.*, 2015).

### **Assignment of candidate genes, gene annotation, gene ontology (GO) analysis and prioritization of candidates**

After performing GWA analysis, a list of associated SNPs with a  $-\log_{10}(P)$  value above the arbitrarily set significance threshold of 4 was selected. This threshold has been used in previous GWA analysis in *Arabidopsis* (El-Soda *et al.*, 2015; Davila Olivas *et al.*, 2016; Kooke *et al.*, 2016). The SNPs in the  $\pm 10$ kb neighboring region around the identified significant SNPs in close LD (LD cutoff threshold  $r^2 > 0.4$ ) were obtained based on both the 250K array (Baxter *et al.*, 2010; Li *et al.*, 2010; Horton *et al.*, 2012) and resequencing data (1001genomes.org) as previously described (Bac-Molenaar *et al.*, 2015a; Kooke *et al.*, 2016). The search window was thus defined by the first and last SNP in close LD with the significant SNPs. All the genes within the search window were considered as a priori candidate genes. Gene annotation, gene expression patterns and predicted gene networks were obtained from The *Arabidopsis* Information Resource (TAIR), the *Arabidopsis* eFP browser and GeneMania (Warde-Farley *et al.*, 2010), respectively.

The a priori list of candidate genes was submitted to the gene list analysis tool in the PANTHER (Protein Annotation Through Evolutionary Relationship) classification system (<http://www.pantherdb.org/>). The analysis was based on GO Ontology database version 11.0 released 2016-07-15. Genes were then classified according to their functional categories based on gene ontology (GO) terms and PANTHER protein class (Mi *et al.*, 2012; Mi *et al.*, 2013). An overrepresentation test on the PANTHER website was also run on the a priori candidate list to identify whether there are



overrepresented functional categories among these candidates. Bonferroni correction was used for multiple testing (if no results were retrieved, no Bonferroni correction was applied). The Gene Functional Classification Tool from the DAVID Bioinformatics Resources 6.8 (Beta) was used to perform gene enrichment and produce classified gene clusters (Huang *et al.*, 2009a; Huang *et al.*, 2009b). The default medium classification stringency was applied to the gene functional classification test. If the medium stringency gave no clusters, then the low classification stringency was applied instead. Only group results with  $P < 0.05$  were retrieved. In addition, in order to see whether there are differences in GO term enrichment between traits, we separately compared PANTHER overrepresentation test results and DAVID gene functional classified groups based on a priori list of all the traits, traits for tubercle number, traits for tubercle diameter, traits for estimated tubercle area and traits for tubercle developmental rate.

A number of significant SNPs are in LD with each other and therefore are likely representing a single QTL. Individual genes were considered as the most promising candidate genes if they had at least two significant SNPs in the coding region (at least one of them in coding region of the gene), similar to the two-SNP approach used in previous studies (Chan *et al.*, 2011; Corwin *et al.*, 2016; Francisco *et al.*, 2016).

### Characterization of candidate genes

For selected candidate genes, the information of T-DNA lines was obtained by using the T-DNA Express Tool (<http://signal.salk.edu/cgi-bin/tdnaexpress>). Two T-DNA lines per candidate were obtained from NASC (The European Arabidopsis Stock Centre) (Alonso, 2003). To confirm whether the T-DNA lines are homozygous or heterozygous, PCR primers were designed by using the T-DNA Primer Design Tool (<http://signal.salk.edu/tdnaprimers.2.html>). Only homozygous T-DNA lines were used for further study. Information of these homozygous T-DNA lines and primers used are summarized in **Table S9**. For the gene RHB1A, two T3-generation mutants line GABI\_843C09 (mutation in exon) and SALK\_205476 (mutation in 3'UTR region) were included in the test. Homozygosity of GABI\_843C09 was confirmed by primers (forward primer TGGGGTTTTTATAGGGTTTGG; reverse primer TTTCGTGTTCAATGTGTTTATGC). Rhizotron experiments were performed on these T-DNA lines together with corresponding wildtypes under the same growth condition as in the GWA screening. Six biological replicates per line were included. Tubercle percentage (the percentage of tubercle number out of the number of pre-germinated seeds), average

tubercle diameter and estimated tubercle area for each line were analysed as described above.

Expression of multiple candidate genes was measured in the leaves and roots of Col-0 infected with *P. ramosa* in a time series (1 d, 1 w, 2 w, 3 w and 4 w). RNA was isolated from 20 mg of plant tissues with the Qiagen Plant RNA Mini Kit (to confirm) according to the manufacturer's instructions. For the cDNA synthesis, RNA was converted to cDNA using the iScript cDNA synthesis kit (Bio-Rad) according to the manufacturer's instructions. The cDNA was subsequently diluted to end volume for use in RT-qPCR. Absence of genomic DNA was confirmed by comparing cDNA samples with RNA samples that were not reverse transcribed (minus RT control). Multiple qPCR was performed. Primers used for multiple qPCR are summarized in **Table S9**. Six biological replicates were included. Expression of *RHBIA* was measured using the primers (forward primer TTCACCGGAGAATCACGACAACA, reverse primer TCAAGCCAGGGGATAGTAATGATGC) designed by AtRTPPrimer. Expression data were normalized to geometric mean of four reference genes (*ACTIN*, *18S*, *UBC10*, *EIF-4A2*) with the  $2^{-\Delta\Delta C_t}$  method (Livak and Schmittgen, 2001).

## Results

### Variation in *Arabidopsis* susceptibility to *P. ramosa* invasion during the post-attachment process

To assess variation in the susceptibility of *Arabidopsis* for *P. ramosa* infection, 359 *Arabidopsis* accessions, each with two biological replicates, were infested with *P. ramosa* using an *in vitro* rhizotron system. Because of infections or bad plant growth, in the end data of 239 accessions were obtained. By taking advantage of the rhizotron system, we were able to take photographs at a number of time points, and hence we could not only quantify the number and size of tubercles, but also their development through time (**Figure 1**).



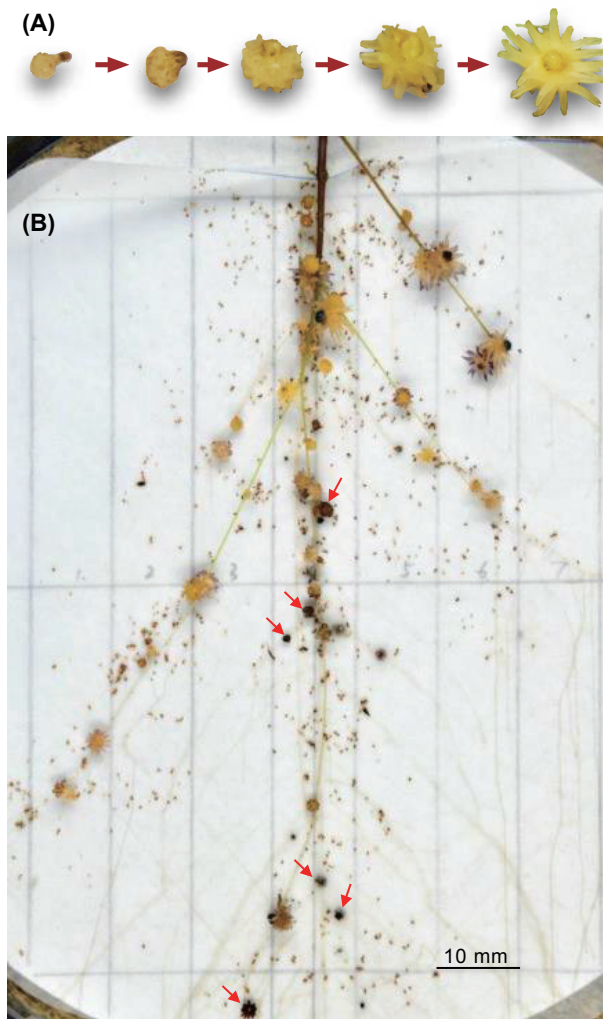


**Figure 1. Illustrations of *Phelipanche ramosa* tubercle growth (A) and rhizotron system (B).** (A) The developmental process of *P. ramosa* tubercles on host roots. After the haustorium of pre-germinated *P. ramosa* attaches to the host root, it develops into a tubercle on the surface of the host root at the attachment site. Swollen round tubercles grow bigger as the parasite stores assimilates in the tubercles. Subsequently, they develop adventitious roots and these adventitious roots grow longer so that the tubercles become “spider-like”. (B) A picture of the rhizotron system showing infection of *Arabidopsis* by *P. ramosa* and the subsequent development of tubercles. Red arrows indicate necrosed tubercles.

For each time-point we assessed three parameters to characterize the infection level: tubercle number (Nr), average tubercle diameter (Dia) and total area of tubercles (Area). The first two parameters were obtained from image analysis, whereas the total tubercle area, a measure for the overall susceptibility of the host, was calculated as the sum of the size of all attachments on a single host. On many ecotypes, necrosis or browning of the tubercles was observed (**Figure 1**). This has also been observed in other host-parasitic plant interactions and is considered to represent an incompatible host-parasite interaction (Labrousse *et al.*, 2004; Louarn *et al.*, 2016). However, preliminary tests showed that the necrosis rate was not reproducible in our rhizotron system, while the tubercle number (as percentage of germinated seeds) was (**Figure S1**). Therefore, we focused on the susceptibility of *Arabidopsis* to *P. ramosa* and only used the three above-mentioned growth indicators (**Table 1**). With these data, also the growth rates between the time-points were calculated (**Table 1**). To reduce the dimensionality of the data and support the validation of results based on single traits, PCA was performed using the three mentioned parameters describing the infection level/process of all ecotypes during all time-points. For all parameters and time points, the first principle component (PC1) explained most of the variation among the ecotypes, ranging from 62% to 90% (**Table S1**). PC1 of total number (Nr\_PC1) explained the highest variation (90%). In addition, PCA was also conducted on the combined data of number, diameter and area for all three time-points. The PC1 of this PCA (Comb\_PC1) explained 52% of the variation among the ecotypes. These PC1 parameters, as well as each single trait, all had a unimodal distribution (**Figure S2**), showing that a continuum exists from low to higher susceptibility. For all the phenotypic traits, both broad-sense ( $H^2$ ) and marker-based narrow-sense heritability ( $h^2$ ) were calculated (**Table 1**). The  $H^2$  was moderate to high, ranging from 0.49 to 0.70, while the  $h^2$  was low to moderate, ranging from 0 to 0.51. The low  $h^2$  suggests that there is a strong influence of other than direct genetic factors such as epistatic interactions.

**Table1. Descriptions and heritability for each trait.**

Trait	Trait Description <sup>1</sup>	Broad-sense Heritability (H <sup>2</sup> )	Narrow-sense Heritability (h <sup>2</sup> )
Comb_PC1	The first principal component of PCA on combining number, average diameter and estimated area of tubercles at all time-points	0.66	0.21
Nr_PC1	The first principal component of PCA on number of tubercles at all time-points	0.64	0.17
Dia_PC1	The first principal component of PCA on average diameter of tubercles at all time-points	0.51	0.04
Area_PC1	The first principal component of PCA on estimated total area of tubercles at all time-points	0.61	0.13
T1_Nr	Number of tubercles at time-point 1 (T1)	0.62	0.17
T2_Nr	Number of tubercles at time-point 2 (T2)	0.64	0.18
T3_Nr	Number of tubercles at time-point 3 (T3)	0.66	0.08
T1_Dia	Average diameter of tubercles at time-point 1 (T1)	0.49	0.15
T2_Dia	Average diameter of tubercles at time-point 2 (T2)	0.54	0.08
T3_Dia	Average diameter of tubercles at time-point 3 (T3)	0.57	0.08
T1_Area	Estimated total area of tubercles at time-point 1 (T1)	0.64	0.26
T2_Area	Estimated total area of tubercles at time-point 2 (T2)	0.62	0.08
T3_Area	Estimated total area of tubercles at time-point 3 (T3)	0.66	0.27
Nr_Rate21	Growth rate of tubercle number between time-point 1 and 2	0.56	0.00
Nr_Rate31	Growth rate of tubercle number between time-point 1 and 3	0.58	0.00
Nr_Rate32	Growth rate of tubercle number between time-point 2 and 3	0.62	0.33
Dia_Rate21	Growth rate of average tubercle diameter between time-point 1 and 2	0.70	0.49
Dia_Rate31	Growth rate of average tubercle diameter between time-point 1 and 3	0.63	0.25
Dia_Rate32	Growth rate of average tubercle diameter between time-point 2 and 3	0.55	0.10
Area_Rate21	Growth rate of total area of tubercles between time-point 1 and 2	0.70	0.51
Area_Rate31	Growth rate of total area of tubercles between time-point 1 and 3	0.65	0.40
Area_Rate32	Growth rate of total area of tubercles between time-point 2 and 3	0.59	0.13

<sup>1</sup> For individual traits (number, diameter and total area of tubercles) at a certain time-point, date was log transformed. Linear regression was done with these log-transformed data against the log-transformed number of pre-germinated *P. ramosa*

seeds. Residues were then taken as the final trait value. For growth rate traits, the growth rate was defined as the subtraction of the log-transformed trait between two time-points divided by the number of days between the two time-points.

To investigate the overall trend of tubercle growth on *Arabidopsis* accessions during the screening, the distribution of the individual parameters at each time-point as well as growth rate parameters across time intervals were plotted (**Figure 2**). Tubercle size continued to increase over time while the number remained more or less stable, from 2 w (T1) to 4 w (T3) after *P. ramosa* infection (**Figure 2A to 2C**). The increase in diameter and total area during the first period (from T1 to T2) was slightly higher than during the later period (T2 to T3) (**Figure 2E, 2F**), while the increase in tubercle number displayed an opposite trend (**Figure 2D**).

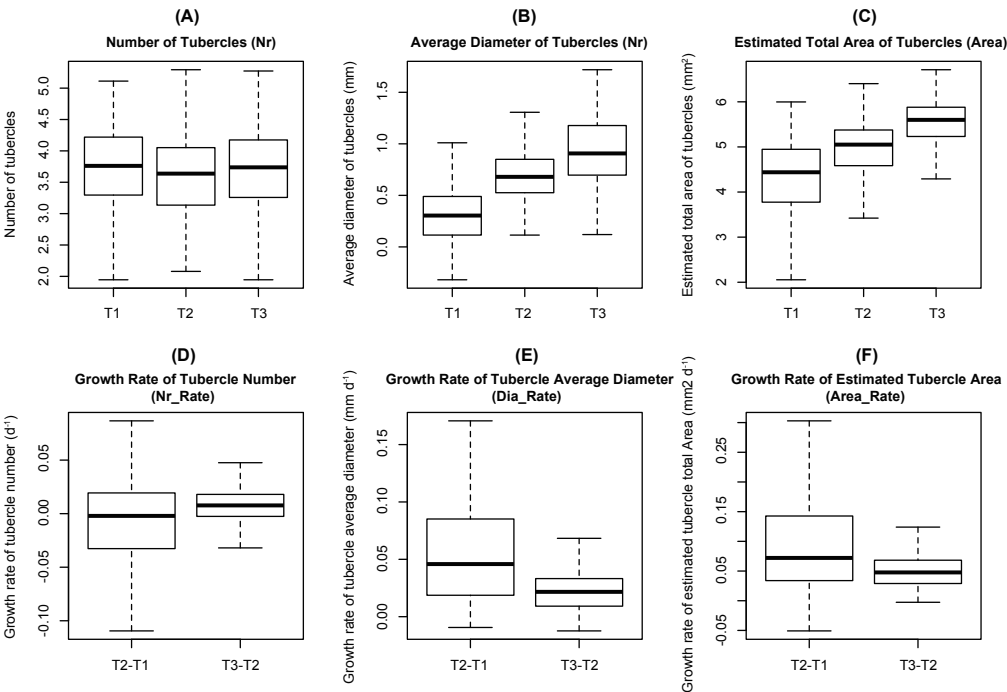


**Figure 2.** Boxplots showing the distribution of traits (tubercle number, average tubercle diameter and estimated total area of tubercles) of *Phelipanche ramosa* at different time points (T1, T2 and T3, 2 w, 3 w and 4 w (weeks) after infection, respectively) (A-C) as well as their increase during two time intervals (growth rate, D-F). The bottom and top of the box are the first and third quartiles, the bar inside the box indicates the mean value. Data were all log-transformed.

To further explore the relationship between phenotypic traits, Spearman's rank correlation analysis was performed (**Table S2**). The tubercle numbers across the three time-points were highly correlated, with correlation coefficients ( $r$ ) ranging from 0.80 to 0.94 ( $P < 0.05$ ), whereas the diameter and total area displayed a lower correlation among the time-points. Tubercle diameter showed a stronger correlation between T2 and T3 ( $r = 0.72$ ,  $P < 0.05$ ) than between T1 and T2 ( $r = 0.37$ ,  $P < 0.05$ ). Total tubercle area, which integrates information of number and size, showed moderate correlation between different time-points ( $r = 0.38$  to  $0.79$ ,  $P < 0.05$ ). The Nr\_PC1, Dia\_PC1 and Area\_PC1 were relatively highly correlated with Nr, Dia and Area at each time-point ( $r = -0.90$  to  $-0.97$ ;  $-0.43$  to  $-0.96$ ;  $-0.78$  to  $-0.97$ , at T2 and T3, respectively). The Comb\_PC1 correlated more with Nr\_PC1 ( $r = 0.97$ ,  $P < 0.05$ ) and Area\_PC1 ( $r = 0.75$ ,  $P < 0.05$ ) than with Dia\_PC1 ( $r = -0.33$ ,  $P < 0.05$ ). The Area\_PC1 correlated more with the Nr\_PC1 ( $r = 0.62$ ,  $P < 0.05$ ) than with Dia\_PC1 ( $r = 0.30$ ,  $P < 0.05$ ).

The growth rate of the tubercle (Dia\_Rate) was more correlated with the increase in the total tubercle area (Area\_Rate) ( $r = 0.76$  to  $0.86$ ,  $P < 0.05$ ) than with the increase in tubercle number (Nr\_Rate) ( $r = -0.27$  to  $-0.41$ ,  $P < 0.05$ ) during three time intervals (T2-T1, T3-T2, T3-T1). Besides, growth rate for time interval T3-T1 (Rate31) highly correlated with rate for time interval T2-T1 (Rate21) ( $r = 0.81$  to  $0.92$ ,  $P < 0.05$ ), more than with time interval T3-T2 (Rate31) ( $r = 0.36$  to  $0.78$ ,  $P < 0.05$ ), possibly because both calculations involved time point T1.

Interestingly, we also found negative correlations, for example between the tubercle number and diameter ( $r = -0.02$  to  $-0.73$ ) (**Table S2**). This trend was especially true in later stages of tubercle development at time-point 2 (T2) and time-point 3 (T3) (**Figure 3**). There was a linear relationship between tubercle number and diameter, coefficient of determination ( $R^2$ ) ranging from 0.19 at T2 ( $P < 0.001$ ) to 0.51 at T3 ( $P < 0.001$ ), while there was no linear relationship between the two at T1 ( $P > 0.05$ ). This phenomenon is likely due to the competition for nutrients among the tubercles. There was also a negative correlation between Nr\_PC1 and Dia\_PC1 ( $r = -0.50$ ,  $P < 0.05$ , **TableS2**), further indicating the nutrient competition among tubercles.

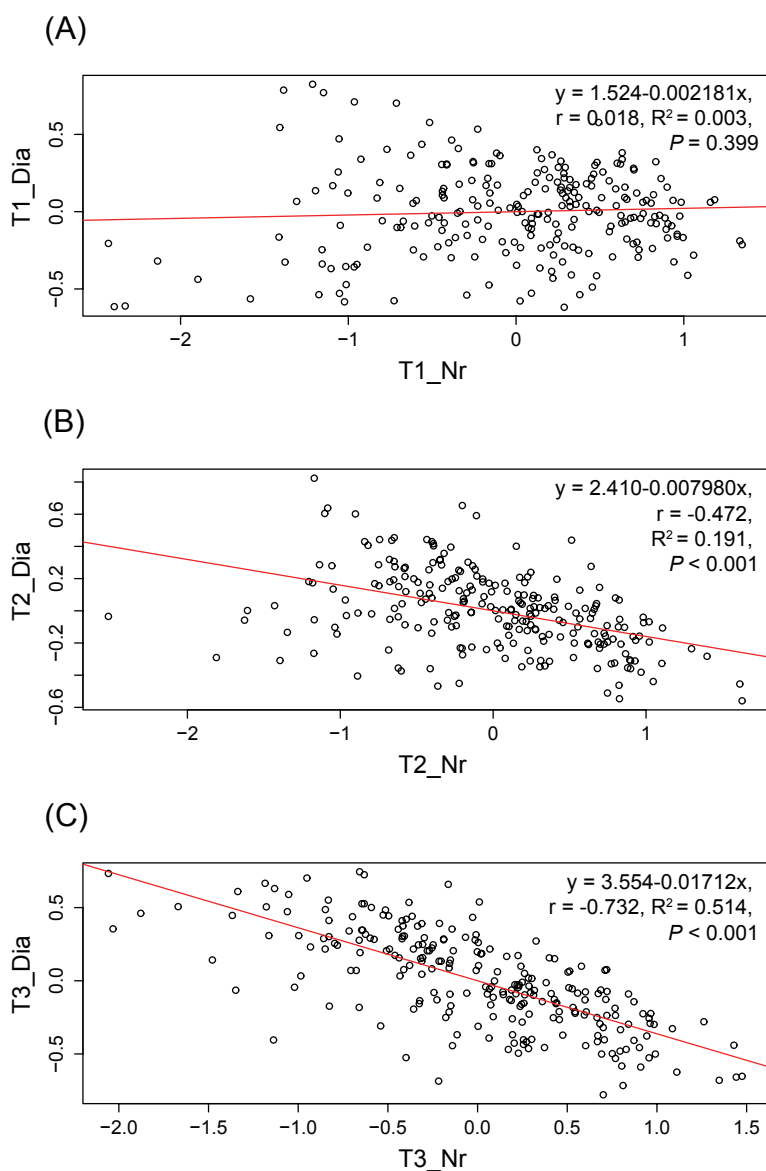


**Figure 3. Correlation between tubercle number (Nr) and tubercle diameter (Dia) of *Phelipanche ramosa* at three time-points (A) T1, 2 w after infection; (B) T2, 3 w after infection, (C) T3, 4 w after infection. The predicted linear relationship, correlation coefficient ( $r$ ) of Spearman's rank correlation test, coefficient of determination ( $R^2$ ), and  $P$  values are indicated in each figure.**

### Distinct patterns of tubercle development on a subset of *Arabidopsis* accessions

In order to study tubercle development in different *Arabidopsis* ecotypes more closely, eight *Arabidopsis* accessions were selected based on their difference in total tubercle number 4 weeks after infection (time point 3: T3\_Nr). Two of the selected accessions (T1110, Tha-1) showed relatively high tubercle numbers, one accession showed an intermediate level (RRS-10) and five other accessions only displayed a very low tubercle number during this specific time point (Bay-0, Col-0, Petergof, Knox-18, Ca-0). Comparisons between these accessions were made based on their original data including tubercle percentage (tubercle number out of number of pre-germinated *P. ramosa* seeds), diameter and total area of tubercles during a time series (**Figure 4**). The most resistant accession (Ca-0), showing the lowest final tubercle percentage and size of tubercles, also showed the lowest infection level during the earliest time point. In addition to this, this ecotype also only allowed as very low growth rate of the tubercles. From the comparisons, it could also be observed that to reach a considerable overall infection level (total area of tubercles) at the end of the parasitism, there are at least three strategies. (1) The parasite develops many small tubercles at an initial stage and maintains a slow and steady growth rate of the tubercles (eg. Tha-1, RRS-10). (2) The parasite develops a few big tubercles and maintains a slow and steady growth rate of the few tubercles (eg. Knox-18). (3) The parasite starts with a relatively low number of small tubercles however subsequent development is fast, through either increasing the number (eg. T1110) or size (eg. Bay-0, Petergof, Col-0) of the tubercles. With the latter strategy, various accessions also displayed differences in tubercle growth rates during the different timepoints. Tubercles in some accessions developed faster during the earlier stage (eg. Col-0), some faster during the later stage (eg. T1110, Petergof), whereas in one accession the fast growth rate was maintained during the entire infection process (eg. Bay-0).

Note that although growth rate of tubercles between the different *Arabidopsis* accessions varied dramatically, we observed a relatively steady increase in the total tubercle area for most accessions (**Figure 4C**), suggesting that the host cannot really restrict the parasite in withdrawing nutrients, no matter what host response is adopted. Still, some *Arabidopsis* accessions seemed more susceptible to parasite invasion than others when considering the overall tubercle area, which implies that there is variation in susceptibility to the parasite in the host *Arabidopsis*.

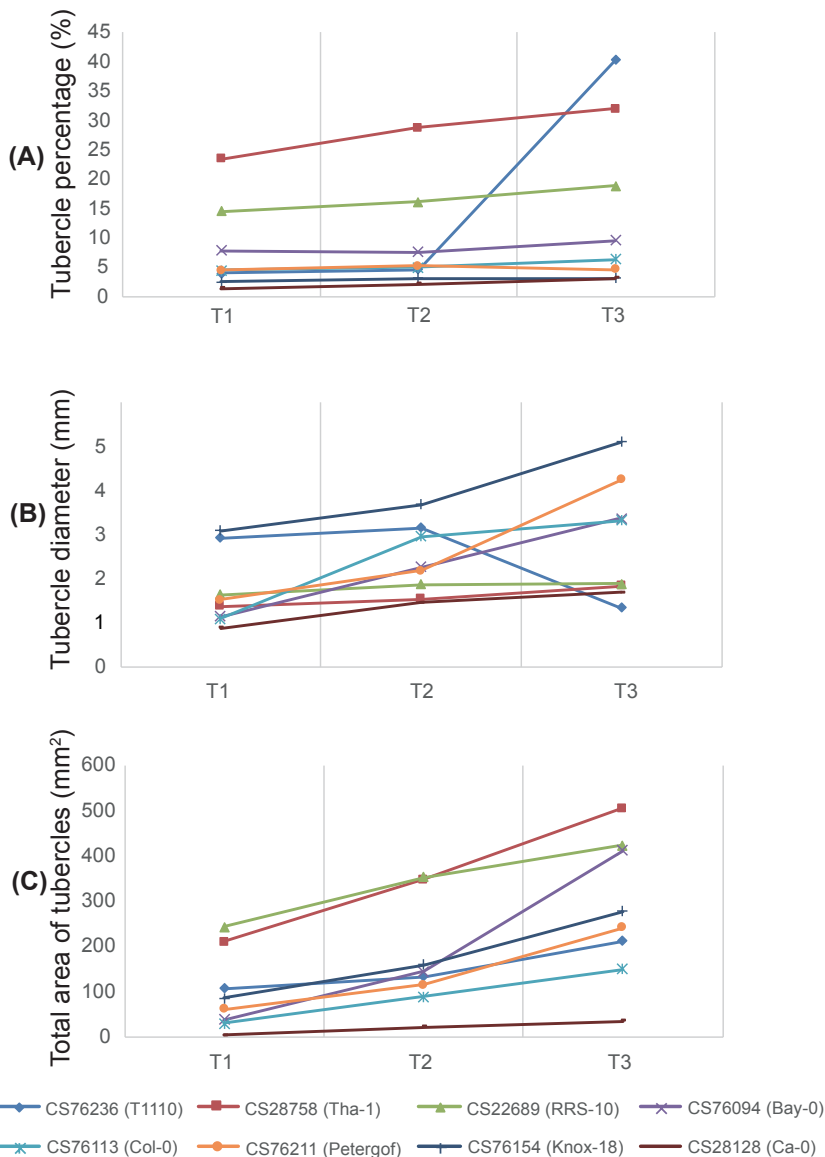


**Figure 4. *Phelipanche ramosa* infection process in eight different ecotypes of *Arabidopsis*.** (A) Tubercle percentage (tubercle number out of number of pre-germinated *P. ramosa* seeds, %), (B) average tubercle diameter (mm) and (C) total area of tubercles (mm<sup>2</sup>) in eight selected accessions at three time-points (T1=2 w, T2=3 w, T3=4 w after infection). All parameters were log-transformed. Different accessions are represented by different coloured symbols.



### Genome-wide association mapping of *Arabidopsis* susceptibility to *P. ramosa*

Subsequently, GWA analysis was performed for all individual parameters (total number, average diameter and estimated total area of tubercles) at different time-points, as well as for PC1 of each indicator. When applying an arbitrary threshold of  $-\log_{10}(P) > 4$ , a number of SNPs were found to be linked with the above described traits (**Table S3**). The chromosomal localization of these SNPs was subsequently compared between all traits (**Figure S3**).

The QTL for PC1 of combined traits (Comb\_PC1) co-localized with the QTLs for both PC1 of tubercle number (Nr\_PC1) (8 significant SNPs shared) and PC1 of tubercle area (Area\_PC1) (1 SNPs shared), but not with the QTL for PC1 of tubercle diameter (Dia\_PC1). This may be associated with the fact that PC1 of combined traits (Comb\_PC1) was more closely correlated with PC1 of tubercle number (Nr\_PC1) ( $r = 0.97$ ) and PC1 of tubercle area (Area\_PC1) ( $r = 0.76$ ) rather than with PC1 of tubercle diameter (Dia\_PC1) ( $r = -0.33$ ) (**Table S2**). Interestingly, there were no significant SNPs shared between PC1 of tubercle number (Nr\_PC1), PC1 of tubercle diameter (Dia\_PC1) and PC1 of tubercle area (Area\_PC1), suggesting that different mechanisms underlie the variation in these different tubercle development traits on the *Arabidopsis* ecotypes. In general, PC1 parameters could capture most of the SNPs that were identified in individual parameters across three time points, consistent with the finding that PC1 could explain most of the variation among *A. thaliana* ecotypes, ranging from 62% to 90% (**Table S1**). The individual indicators mostly share a few significant SNPs between time points, except that the diameter at time point 1 (T1\_Dia) had no overlapping SNPs with the diameter parameter at time point 2 and 3 (T2\_Dia and T3\_Dia) (**Figure S3**). Significant SNPs that are not shared between time points could be considered as stage-specific SNPs. GWA mapping results based on PC1 parameters and individual traits were compared to support the evaluation of candidate QTLs.

A search window for candidate QTLs was defined by including SNPs in the  $\pm 10\text{kb}$  neighbouring region around the identified significant SNPs in close LD ( $r^2 > 0.4$ ) based on both the 250K array and resequencing data (1001 genomes.org). Genes within the search window were all considered a priori candidate genes (**Table S4**). Note that all identified significant SNPs in the present study explained only a small proportion of the phenotypic variation and displayed low effect sizes (**Table S3**), suggesting that (resistance to) post-attachment parasitism is a complex trait which is associated with multiple genes with limited effect.

### Functional categorization and GO enrichment of a priori candidate genes

2 To obtain an impression on the putative mechanism(s) underlying the variation in susceptibility to an infection with *P. ramosa*, the candidate genes were annotated and categorized for *biological process*, *molecular function*, *cellular component*, *pathway* and *protein class* based on GO terms (**Table S5**). For the GO category *biological process*, the largest functional category was *metabolic process* (35.7% of the candidate genes) (**Figure 5A**), where *primary metabolic process* is the major sub-category (44.8%) (**Figure 5B**). The next major categories for the *biological process* are *cellular process* (31.5%), *localization* (13.0%), and *response to stimulus* (6.5%) (**Figure 5A**), for which *cell cycle and cell communication* (both 36.4%), *transport* (97.4%) and *response to stress* (70.6%) represent the major sub-categories, respectively. For the GO category *molecular function*, a priori candidate genes were mostly categorized in *catalytic activity* (47.9%), *binding* (24.4%) and *transporter activity* (14.3%) (**Table S5**). For the GO category *cellular component*, the a priori list of genes were mainly abundant in *cell part* (44.5%) and *organelle* (26.3%) (**Table S5**). And for the GO category *pathway*, the four major functional categories are *Insulin/IGF pathway-mitogen activated protein kinase kinase/MAP kinase* (6.3%), *ubiquitin proteasome pathway* (6.3%), *EGF receptor signalling pathway* (6.3%), *Heme biosynthesis* (6.3%), *Huntington disease* (6.3%), *FGF signalling pathway* (6.3%) (**Table S5**). For the GO category *protein class*, a priori candidate genes were mostly categorized as *nucleic acid binding* (18.2%), *hydrolase* (13.4%) and *transporter* (12.6%) (**Table S5**).

In addition, to get insight into the differences between mechanisms underlying tubercle proliferation and growth rate, we also separately performed GO enrichment analysis on the sub-lists of a priori candidate genes for these traits. The biologically functional categories of the sub-lists were then compared with each other (**Figure S4**, **Table S6**, **Table S7**). Interestingly, the candidate genes for tubercle area and growth rate seemed to be more enriched for the category *metabolic process* (10%) than the candidate genes for tubercle number and diameter, whereas tubercle number and diameter were more enriched for *localization* especially in *transport* (5%) (**Figure S4**). Besides, the GO enrichment analysis highlighted the putative importance of the category *metabolic process* for the tubercle diameter and area, and *nitrogen utilization* for growth rate, whereas the category *transport process* was highlighted for both tubercle number and diameter (**Table S6**). Although the percentages of major biological categories of candidate genes for tubercle number and diameter did not differ much, tubercle diameter had about 5% more candidate genes categorized in *response to stimulus* (**Figure S4**), suggestive of a more

prominent involvement of stress responses in the host mechanism to restrict nutrient transport to the parasitic plants. Taken together, GO enrichment analysis suggests that a variety of biological processes is related with the variation in tubercle establishment and growth on *Arabidopsis*, reflecting the complexity of the interaction between parasitic plants and their hosts.

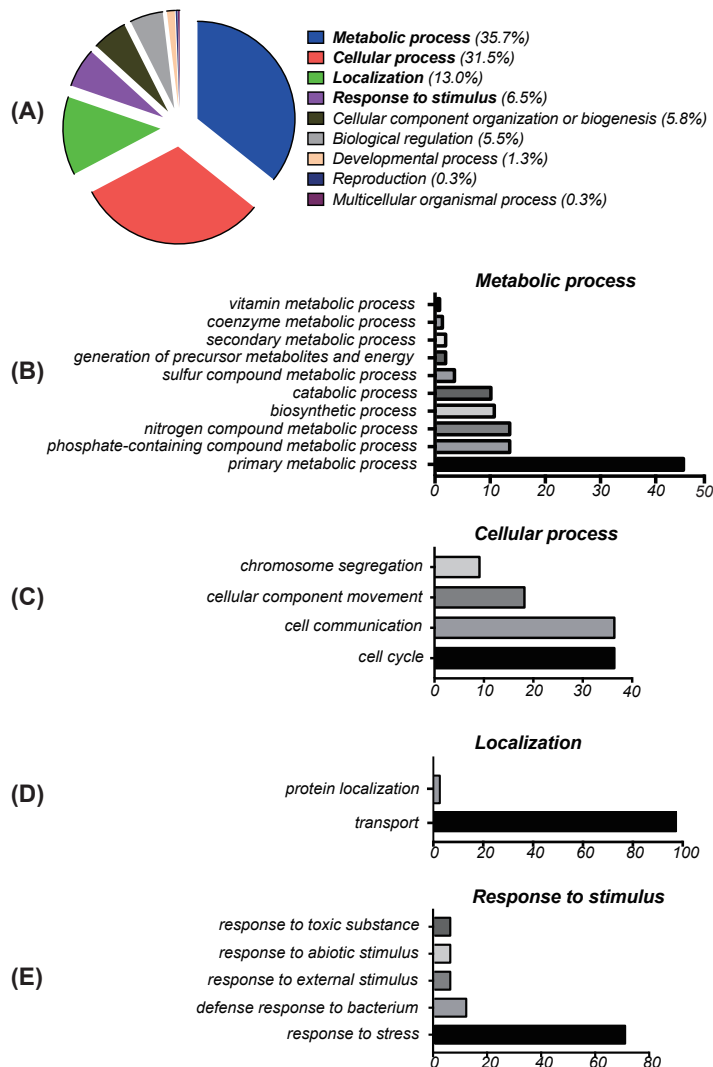


**Figure 5. Functional categorization of a priori candidate genes based on GO term analysis for *biological process*.** Pie chart of functional categories for GO category (A) *biological process* based on a priori significant SNPs in our study. Percentage of each functional

category is indicated in brackets. Sub-categorization for four top-ranked functional categories: (B) *metabolic process*, (C) *cellular process*, (D) *localization*, and (E) *response to stimulus*.

### **GWA analysis detects a number of previously identified defense response genes against *P. ramosa* and other organisms**

2 To test if the GWA analysis is able to detect genes that have previously been identified to be involved in the host defense response to *P. ramosa* or is largely identifying novel genes, we examined (the homologs of) 26 genes that have been reported to be induced in the roots of various host species in response to *P. ramosa* infection for the presence of SNPs associated with our phenotypic traits. These genes are involved in pathogenesis, phenylpropanoid and isoprenoid biosynthesis, jasmonic acid- and ethylene-related pathways, strigolactone pathway, oxidative stress, signal transduction, cell wall reinforcement and sugar transport (**Table S8**). None of the 26 genes had SNPs strongly associated ( $-\log_{10}(P) > 4$ ) with any of our traits. However, two of the 26 genes had SNPs that were moderately associated with our traits (SNPs with  $-\log_{10}(P) > 3$ ). One gene is *LOX2* (*LIPOXYGENASE 2*, AT3G45140), which is involved in wound-induced jasmonic acid biosynthesis (Bell *et al.*, 1995), with one SNP moderately associated with the first principle component of PCA for tubercle diameter Dia\_PC1 (**Table S8**). The gene expression of *LOX2* has been reported to be induced dramatically in *Arabidopsis* roots 2w after infestation by *P. ramosa* (Dos Santos *et al.*, 2003). Interestingly, expression of this gene is also induced in *Arabidopsis* leaves by aphids (Moran and Thompson, 2001), suggestive of a common host response to parasitic plants and aphids. The other gene that contained a SNP moderately associated with tubercle diameter (T1\_Dia) was *D27* (*DWARF27*, AT1G03055) (**Table S8**), which is one of strigolactone biosynthetic genes (Lin *et al.*, 2009; Waters *et al.*, 2012). In tomato, the expression of *SID27* is induced significantly at the early stage of *P. ramosa* infection and slightly higher than in the control during a later stage of infection (Torres-Vera *et al.*, 2016).

Defense against parasitic plants might be similar to defense responses against other organisms such as aphids, nematodes and pathogens. Indeed, some defense-related genes have been reported to be induced by *P. ramosa*, aphids as well as nematodes, such as pathogenesis-related protein PDF1.2 (Moran and Thompson, 2001; Dos Santos *et al.*, 2003; Kammerhofer *et al.*, 2015). To test if our GWA analysis pinpoints genes involved in resistance against other organisms, we examined gene

annotations of the a priori candidate list (**Table S4**) as well as the  $-\log_{10}(P)$  value of 22 genes reported to be involved in defense against herbivores, nematodes and pathogens (**Table S8**). Most of the a priori candidate genes could not be linked to the defense response, with a few exceptions. The gene *SOT12* (*SULPHOTRANSFERASE 12*, AT2G03760), *PERK1* (*PROLINE-RICH EXTENSIN-LIKE RECEPTOR KINASE 1*, AT3G24550), *CYP79A2* (*CYTOCHROME P450 79A2*, AT5G05260), *HPR1* (*HYPER RECOMBINATION1*, AT5G09860) and *BIR1* (*BAK1-INTERACTING RECEPTOR-LIKE KINASE 1*, AT5G48380) have been reported to contribute to resistance against pathogen infection (Silva and Goring, 2002; Brader *et al.*, 2006; Gao *et al.*, 2009; Baek *et al.*, 2010; Pan *et al.*, 2012). Among these genes, *CYP79A2*, which is involved in glucosinolate biosynthesis (Grubb and Abel, 2006), has also been suggested to be associated with the response to herbivores as its expression is induced by a phloem-feeding insect (silverleaf whitefly) and a leaf-chewing specialist (diamond back moth) (Kempema *et al.*, 2007; Ehltling *et al.*, 2008). *PERK1* is a member of the proline-rich extensin-like receptor kinase family. It has been reported that mechanical wounding stimuli result in a rapid accumulation of *PERK1* mRNA (Silva and Goring, 2002). The receptor-like kinase *BIR1*, interacts with *BAK1* (*BRI-ASSOCIATED KINASE-1*) and other ligand-binding receptor-like kinases to regulate multiple pathways, not only in cell death and immune responses but also in controlling growth of both aerial (plant height, leaf length) and below ground (root) parts of the plant (Wierzba and Tax, 2016). In addition to these genes, sugar transporter gene *SUC2* (*SUCROSE-PROTON SYMPORTER 2*, AT1G22710), which encodes a phloem-localized sucrose symporter essential for phloem loading (Srivastava *et al.*, 2008), was identified in our GWA analysis (**Table S4**, **Table S8**). It is not only involved in the response to abiotic stress in an ABA-dependent way (Gong *et al.*, 2015), but also in the plant-parasitic nematode interaction (Juergensen *et al.*, 2003). Interestingly, the predicted network of *SUC2* displays some connections with other *SUC* genes (AT1G09960 and AT2G02860), a cell-wall associated kinase protein (AT1G16260) and *C4H* (*CINNAMATE 4-HYDROXYLASE*, AT2G30490) (**Figure S5**). The latter gene *C4H*, involved in phenylpropanoid biosynthesis, has been reported to be transcriptionally up-regulated in response to an infection with *P. ramosa* (Dos Santos *et al.*, 2003). The SNPs of *SUC2* are strongly associated with the trait T3\_Area, which represents the overall tubercle development at the end point. Notably, SNPs of other sugar transport-related genes such as *STP11* (*SUGAR TRANSPORTER 11*, AT5G23270) (Schneidereit *et al.*, 2004) and AT3G02690 (Nucleotide/sugar transporter family protein) have also been found to be associated with tubercle number and tubercle area in

the present study, respectively. Another gene AT1G08890 (Major facilitator superfamily protein, with sugar: hydrogen symporter activity) is located within the LD search window of significant SNPs associated with growth rate of tubercle diameter across the first and second time points (Dia\_rate21). These findings may reflect a critical role for sucrose partitioning in the establishment and subsequent development of an infection with *P. ramosa*.

### Candidate gene prioritization and characterization

2

To prioritize candidate genes, associated SNPs and genes were not only selected based on the  $-\log_{10}(P)$  scores of individual SNPs, but also on the number of significant SNPs per gene. Furthermore, if at least one of the significant SNPs is within the predicted mRNA coding region, this gene is considered to have a higher priority. This two-SNP approach has been utilized in several previous studies in order to prioritize candidate genes and to minimize false positives (Chan *et al.*, 2011; Corwin *et al.*, 2016; Francisco *et al.*, 2016). Using this strategy, a top candidate list including 16 candidate genes was identified (**Table 2**). These genes are involved in signal transduction, metabolic process, transport, protein kinase signalling pathway, chromatin modification, proteolysis, protein myristoylation, chromatin assembly/ disassembly, reactive oxygen species, RNA binding etc. Notably, of the 16 top candidate genes, four are transporters (AT1G25380, AT2G13100, AT4G13510, AT4G18050), possibly reflecting the importance of assimilate and ion transport in the host-parasite interaction.

We preliminarily characterized several QTLs in the top candidate gene list and a few from the a priori candidate list by using T-DNA mutant lines. Most of the selected mutants for these QTLs did not display obvious differences in tubercle development when compared with their wild-types. Among these, one T-DNA line (GK-843C09) (confirmed for homozygosity), which was mutated in the exon region of *RHB1A* (RING-H2 FINGER B1A, AT4G00335), exhibited a significantly smaller total area of tubercles (**Figure 6F**), while the percentage of tubercles out of pre-germinated seeds and the average tubercle diameter did not show a difference compared with the corresponding Col-0 wildtype (**Figure 6D-E**). However, the number of tubercles during this assay was limited for both genotypes. Intriguingly, the associated QTL seems to play a role in resistance against overall growth of the tubercle and hence growth of the parasitic plant because it is associated with the trait T3\_Dia and Dia\_rate31. Several significant SNPs and SNPs within a search window of close LD and in a 20kb region are predicted to cause synonymous substitutions in the coding region or in the intron region



of the gene *RHB1A* (**Figure 6A**). Only one SNP (at the position 147388) within LD ( $r = 0.96$ ) is predicted to cause a non-synonymous substitution in the coding region of *RHB1A*. However, six haplotypes for this SNP did not show significant differences in the tubercle diameter at the time point 3 nor growth rate of the tubercle between time point 1 and 3 (**Figure 6B-C**). Besides, we also investigated the expression of *RHB1A* in Col-0 roots after *P. ramosa* infection, but it was not significantly induced although there was a tendency for an increased expression level 3 w after infection (**Figure 6G**). More efforts are still needed to validate the functions of this and other candidate genes.

**Table 2. List of top candidate genes that may be involved in determining susceptibility against an infection with *Phelipanche ramosa* in *Arabidopsis*.** Columns represent the chromosome (Chr), position (Pos), the highest  $-\log_{10}(P)$  value of the SNPs within the candidate gene, the number of SNPs and other genes within a  $\pm 10$ kb window and in LD with the significant SNP, effect size, gene ID and name of candidate genes, biological process that the candidate gene might be involved in, and the trait with which the SNPs were identified. Bold candidate gene ID and gene name indicate that there was at least one associated SNP located in the  $\pm 10$ kb window of the significant SNP for the same candidate gene.

Chr	Pos (Mb)	Max $-\log_{10}(P)$	#SNPs		#Other genes		Allele freq	Effect size	Candidate genes		
			$\pm 10$ kb	in LD	$\pm 10$ kb	in LD			Gene ID & Name	Biological Process	Trait
1	6.97	4.06	10	231	1	15	0.86	-0.84	<b>AT1G20110 (FYVE1, FYVE-DOMAIN PROTEIN 1)</b>	signal transduction	T1_Area
1	8.90	4.75	0	76	0	1	0.71	0.65	AT1G25375 (Metallo-hydrolase/oxidoreductase superfamily protein)	metabolic process	Area_rate32
1	8.91	4.79	1	74	0	1	0.77	0.70	<b>AT1G25380 (NDT2, NAD+ TRANSPORTER 2)</b>	mitochondrial transport	Area_rate32
1	21.85	4.39	0	5	0	0	0.72	0.60	AT1G59453 (B-block binding subunit of TFIIC)	unknown	T2_Area
2	2.26	4.85	1	48	0	1	0.69	-0.62	<b>AT2G05900 (SDG11, SET DOMAIN PROTEIN 11)</b>	chromatin modification	Dia_rate31
2	5.39	4.61	0	22	0	4	0.89	0.92	AT2G13100 (G3PP5, GLYCEROL-3-PHOSPHATE PERMEASE 5)	anion transport, carbohydrate transport, phosphate ion homeostasis	T1_Dia
2	11.55	5.22	1	8	1	2	0.12	-0.87	AT2G27060 (Leucine-rich repeat protein kinase family protein)	transmembrane receptor protein tyrosine kinase signalling pathway	Dia_rate32
2	15.37	4.26	4	37	1	3	0.32	-0.63	<b>AT2G36670 (Eukaryotic aspartyl protease family protein)</b>	proteolysis	Area_rate21

3	11.46	5.01	4	36	1	1	0.30	-0.68	AT3G29634 (CACTA-like transposase family)	unknown	T1_ Dia
4	0.15	4.50	2	19	0	0	0.63	0.59	AT4G00335 (RHB1A, RING-H2 FINGER B1A)	protein myristoylation	T3_ Dia, Dia_ rate31
4	7.86	5.33	0	1	0	0	0.88	0.78	AT4G13510 (AMT1;1, AMMONIUM TRANSPORTER 1;1)	ammonium transporter	Nr_ rate31
4	10.03	4.93	6	25	0	0	0.90	0.94	AT4G18050 (ABC89, ATP-BINDING CASSETTE B9)	transmembrane transport	T2_ Area, Area_ PC1
4	15.30	4.38	10	29	2	2	0.43	0.57	AT4G31570	unknown	T3_ Dia
4	17.55	4.21	14	161	4	13	0.90	-0.85	AT4G37280 (MRG1, MORF RELATED GENE 1)	chromatin assembly/ disassembly	Area_ PC1
5	20.76	4.39	2	4	0	0	0.74	0.69	AT5G51060 (RHD2, ROOT HAIR DEFECTIVE 2)	reactive oxygen species (ROS) production, root development, plant defense	T3_ Area
5	26.54	4.35	2	105	1	2	0.89	0.89	AT5G66470	RNA binding, GTP binding	Nr_ rate31

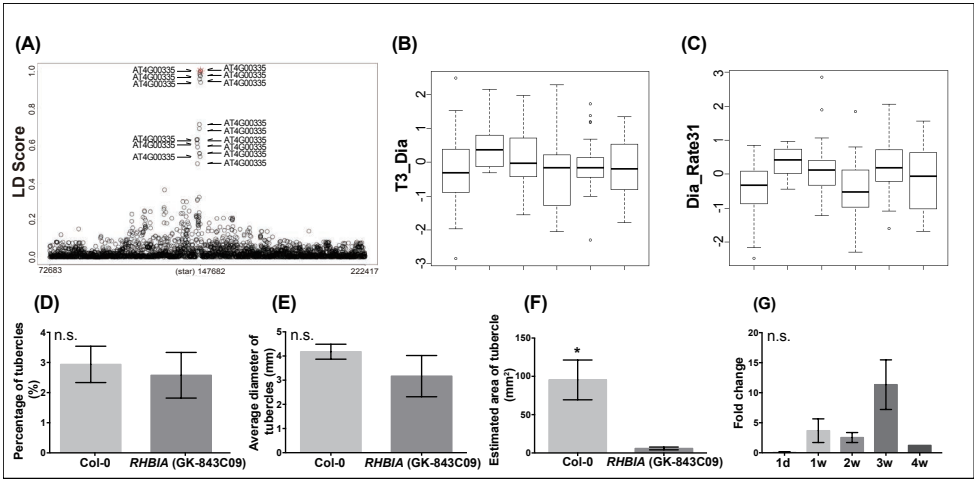


**Figure 6. Characterization of *RHB1A*.** (A) A search window of close LD with significant SNPs for *RHB1A*. (B) Haplotype effects of *RHB1A* on tubercle diameter at time point 3 (4 w after infection). (C) Haplotype effects of *RHB1A* on growth rate of tubercle diameter between time point 3 (4 w) and 1 (2 w). (D) Tubercle percentage of Col-0 and *RHB1A* T-DNA mutant GK-843C09. (E) Average tubercle diameter of Col-0 and *RHB1A* T-DNA mutant GK-843C09. (F) Total tubercle area of Col-0 and *RHB1A* T-DNA mutant GK-843C09. (G) Gene expression of *RHB1A*



in Col-0 root after *P. ramosa* infection (1 d, 1 w, 2 w, 3 w, 4 w after infection).

### Discussion

Although there have been tremendous efforts in plant breeding programs to improve resistance against parasitic weeds, our understanding of the host-parasitic plant interaction is still quite limited. By screening a population of the model plant *Arabidopsis*, we investigated the natural variation in tubercle establishment and growth on host roots. We performed a GWA analysis by exploring the association between 199589 SNPs and the number of *P. ramosa* tubercles and their subsequent development in 239 accessions. This analysis identified 637 significant SNPs (including the SNPs with strong LD within a 20kb region of the significant SNPs) divided over 227 candidate loci. Based on GO term analysis and GO term enrichment analysis, biologically functional categories were highlighted for a priori candidates. Candidates were then prioritized by a two-SNP approach and one of these top candidate genes was characterized by using a T-DNA line and gene expression assay.

### The complexity of the host-parasitic plant interaction

The interaction between host and parasitic plants is a complex process, involving multiple stages from the germination of the parasitic plant seeds to the final maturation of parasitic plant shoots and flowers. Previous studies have more focused on the initial stages such as seed germination, haustorium initiation and development. Several essential host factors involved in these processes were identified, such as germination stimulants and haustorium-inducing factors (Chang and Lynn, 1986; Xie *et al.*, 2010; Yoshida *et al.*, 2016). After the parasite has established a vascular connection with the host roots – through the haustorium - a tubercle, a swollen round organ, is formed on the surface of the connection point on the roots. As the tubercle acts as a storage reserve for further growth, the development of these tubercles is the foundation of post-attachment growth of the parasitic plant. Our study was thus focused on tubercle growth during this post-attachment process.

Tubercle growth reflects how the host plant reacts to the parasite invasion. The death or retarded growth of tubercles could be a sign of host resistance. In some cases, tubercles display necrosis or browning/darkening. The darkening of tubercles seems to be associated with lignification of the host endodermis and pericycle cells at the infection site,

resulting in xylem occlusion (Pérez-de-Luque *et al.*, 2005). Although some studies have used this trait as a resistance indicator for crop breeding (Labrousse *et al.*, 2004; Louarn *et al.*, 2016), we noticed in our study that necrosis of the tubercles on *Arabidopsis* in our hands is not reproducible. It is not clear yet how much this phenomenon is environment-dependent and/or species-dependent. On the one hand, our rhizotron system is a small open system, which could still be affected by environmental factors such as water imbalance, fungi and algae contamination, although we have tried to minimize these factors. On the other hand, as *Arabidopsis* is not a natural host of *P. ramosa*, the reaction of *Arabidopsis* to parasitic invasion might be different from that of crops. All the *Arabidopsis* accessions in our screening were susceptible to the parasitic plant infection, which confirms the results in earlier studies (Goldwasser and Yoder, 2001; Goldwasser *et al.*, 2002), in which 309 ecotypes of *Arabidopsis* all showed overall susceptibility to *O. aegytiaca*.

By using the rhizotron system, we could monitor the development of the parasitic organ on host roots in a time series. As the infection developed, the negative linear relationship between tubercle number and size became more prominent (**Figure 2**). This is consistent with previous reports that showed the size (biomass) of individual parasites (*P. ramosa*, *O. cernua*, *O. crenata*) was dependent on host resource availability especially when the severity of the infection increases (Hibberd *et al.*, 1998; Moreau *et al.*, 2016). This finding suggests the resource competition between parasites. By comparing tubercle growth on selected *Arabidopsis* accessions, we have also seen quite different patterns of tubercle development on host roots throughout time. It seems that for some host accessions, the parasite chooses to establish more small storage reserves, which slowly and steadily suck up nutrients from the host (**Figure 4**). For other host genotypes, the focus seems on first establishing only a few relatively large storage reserves and then further develop these. Also, the growth rate of tubercles on different accessions varies (**Figure 4**). These different patterns of tubercle growth reveal the complexity of the host-parasite interaction during the post-attachment stage. Further and deeper investigations are needed to explore the underlying host response mechanisms leading to these flexible invasive strategies of the parasite.

Our findings suggest that there is a risk in only looking at a single parameter at one time point, for example looking only at the number of broomrapes emerged, in breeding programs, a strategy widely adopted due to its easy practice in the field (Hausmann *et al.*, 2004; Samejima *et*

*al.*, 2016). It is likely that for some infected host accessions, broomrape emergence does not occur aboveground yet when the emergence number is counted at the end of the assay, whereas there are already many tubercles developed underground, causing considerable damage to the crop. Rather, it is advisable to integrate different resistance parameters into the breeding programs.

In addition, the low narrow-sense heritabilities and low level of phenotypic variation explained by significant SNPs indicate the large influence of environmental factors. This highlights the complexity of breeding programs that aim to improve parasitic plant resistance. Some crop genotypes that were previously identified as resistant later turned out to be susceptible (Rubiales *et al.*, 2014). It is therefore critical to look for germplasm with stable performance across environments (Rubiales *et al.*, 2014).

### **Identification of new loci involved in the *Arabidopsis* response to *P. ramosa***

By using the rhizotron system, we were able to explore the parasite development over time with the aim to discover stage-specific QTLs, a strategy also adopted in a recent QTL mapping study on sunflower resistance to *O. cumana* (Louarn *et al.*, 2016). However, different from Louarn *et al.* (2016) who primarily focused on the number of attachments, our study further investigated the tubercle size and monitored tubercle development by performing detailed image analysis. This approach offers another dimension for quantitative studies to study host-parasitic plant interaction. Interestingly, the QTLs associated with tubercle number and size that we identified in the present study are largely different from each other, indicating that the mechanisms underlying tubercle establishment and growth are also distinct from each other. It should be noted that it is still a time-consuming and labour-intensive job to perform the image analysis that was used in this study, largely due to technical difficulties to distinguish young semi-transparent tubercles from the host root and the rhizotron background using automated analysis. Our current method, to some extent, has also facilitated the identification of novel QTLs associated with the growth rate of tubercles. Still, due to the lack of ideal phenotyping tools, it is difficult to include more time points in such a large-scale screening to build a growth dynamics model which could be used in GWA analysis like in Bac-Molenaar *et al.* (2015b). Recently, a fluorescence imaging technique was published allowing the diagnosis of early broomrape infection on

sunflower in breeding programs (Ortiz-Bustos *et al.*, 2016). Techniques with stable automatic performance and high imaging resolution are expected to make an important contribution to the precise investigation of parasitism, especially in quantitative analyses.

In this study, only two genes (*LOX2* and *D27*) that were reported before to be induced by *P. ramosa*, were detected in our GWA analysis, both showing moderate association with tubercle growth. Many genes that have been reported to be involved in host-*P. ramosa* interaction did not show association with any of our phenotypes in the present study. It is likely that some of these genes are transiently expressed only in the early stage of infection such as *GST1* (*GLUTATHIONE S-TRANSFERASE 1*) of which expression is strongly induced during the first few hours after infection and decreases at later stages (Dos Santos *et al.*, 2003), so that their effects could not be easily captured in this screening. It is also not unlikely that the genes that are induced by the parasite do not contribute to the host defence or that their effect is too weak and/or is just not visible due to environmental noise.

Based on GO annotation and enrichment analysis, several biological processes have been highlighted for involvement in different aspects of tubercle growth, especially *metabolic process*, *transport* and *response to stimuli*. The mostly enriched sub-category of *metabolic process* is the *primary metabolic process*, which include *protein metabolic process*, *nucleobase-containing compound metabolic process*, *carbohydrate metabolic process*, *lipid metabolic process* and *cellular amino acid metabolic process*. One of the tested candidate gene *RHB1A*, included in the *protein metabolic process*, encodes a E3 ubiquitin-protein ligase. Although its biological function is not known, the T-DNA lines of this gene displayed a reduced level of overall tubercle area at the late stage (**Figure 6**), implying its potential role in affecting parasitism. It would be interesting to further explore the related protein interactions during the parasitism process. In addition, the enrichment for *metabolic process* and *transport* of assimilates and ions likely relates to the importance of assimilates and amino acid partitioning to the parasite. Some studies have shown that infection by *P. ramosa* could reduce aerial growth of tomato and reduce the shoot: root ratio by acting as a competing sink for assimilates and by influencing host photosynthesis (Mauromicale *et al.*, 2008). The major organic compounds transferred from the host to the broomrape have been identified as sucrose and soluble amino acid, while mineral cations (especially potassium and calcium), decreasing the osmotic potential in the

attachment organs, are also important (Abbes *et al.*, 2009b). Sucrose is metabolized to other compounds such as glucose and fructose as well as starch, which accumulate in the tubercles (Draie *et al.*, 2011). Nutritional and osmoregulation relationships have been explored on broomrape-parasitized tolerant and susceptible hosts in several studies (Abbes *et al.*, 2009a; Abbes *et al.*, 2009b). These studies have indicated that tolerant hosts have low soluble invertase activity, low osmotic potential in the infected roots and display nitrogen deficiency in the host phloem sap (Abbes *et al.*, 2009a). When broomrapes attach to these tolerant hosts, they have a reduced capacity to utilize the host-derived carbohydrates (Abbes *et al.*, 2009b). This underpins the importance of primary metabolism and osmotic regulation during parasitism. Although a number of studies have tried to decipher carbon and nitrogen relations between parasitic plants and their hosts (Hibberd *et al.*, 1999; Simier *et al.*, 2006; Gaudin *et al.*, 2014), our knowledge of how assimilate partitioning and osmotic regulation between host and parasite is achieved is still quite limited. Our GWA analysis has identified a number of candidate genes involved in metabolic processes, such as starch metabolic process (*ALPHA-AMYLASE-LIKE 3*, AT1G69830) and trehalose biosynthetic process (*TREHALOSE-6-PHOSPHATE PHOSPHATASE C*, AT1G22210), etc. (**Table S4**).

A priori candidate genes also include multiple genes involved in different transport activities, such as sugar transport (*SUCROSE-PROTON SYMPORTER 2*, AT1G22710), nitrate transport (*NITRATE TRANSPORTER 1:2*, AT1G69850), phosphate transport (*PHOSPHATE TRANSPORTER 4;4*, AT4G00370), ammonium transport (*AMMONIUM TRANSPORTER 1;1*, AT4G13510), potassium ion transport (*CA<sup>2+</sup> ACTIVATED OUTWARD RECTIFYING K<sup>+</sup> CHANNEL 4*, AT1G02510), copper ion transport (*COPPER TRANSPORTER 6*, AT2G26975), amino acid transport (*GLUTAMINE DUMPER 7*, AT5G38770) and transmembrane transport (*ATP-BINDING CASSETTE B9*, AT4G18050) etc (**Table S4**). The identification of novel candidate genes enriched in *metabolic process* and *transport* might offer a new wealth of information for further investigations on the source-sink relationships and osmotic regulation in the host-parasite interaction.

Finally, the present study has identified several candidate genes that may also be involved in defense mechanisms against other organisms such as herbivores, nematode and pathogens. This may hint at the similarities between the defence responses against parasitic plants and other biotic stresses. For instance, both parasitic plants and nematodes are able to intrude the plant root, connect to the vascular tissues and get access to host assimilates (Mitsumasu *et al.*, 2015). During the establishment of parasitism,

the parasites need to break the cell wall barrier. Pectin degrading enzymes such as pectin methylesterase (PME) have been implicated for their role as cell wall-degrading enzymes, which help cyst nematode parasitism (Hewezi *et al.*, 2008). PME has also been detected in the cell wall of *Orobanch* intrusive cells of the haustorium and in the adjacent host apoplast (Losner-Goshen, 1998), implying a role of PME in modifying host cell wall pectin to also facilitate broomrape parasitism (Mitsumasu *et al.*, 2015). Once parasitism has been established, parasites need to form a strong sink by importing assimilates via the apoplast. Interestingly, this study has identified a sugar transporter SUC2, which is also expressed in the nematode-induced feeding site (syncytial cell complex) in host roots (Juergensen *et al.*, 2003). In addition to these, one of our candidate genes, *RHD2 / RBOHC* (*ROOT HAIR DEFECTIVE 2 / RESPIRATORY BURST OXIDASE HOMOLOG C*, AT5G51060) (**Table S4**), encodes a calcium-dependent NADPH oxidase. RHD2 / RBOHC is required for the generation of reactive oxygen species (ROS) that regulate cell expansion through the activation of  $\text{Ca}^{2+}$  channels (Foreman *et al.*, 2003; Livanos *et al.*, 2012), and has been reported to be involved in the root hair elongation, mechanical sensing in root hair, response to salt stress and arsenic, cadmium-induced oxidative stresses (Macpherson *et al.*, 2008; Sakamoto *et al.*, 2008; Monshausen *et al.*, 2009; Liu *et al.*, 2012; Gupta *et al.*, 2013; Gupta *et al.*, 2017). The RBOHCs-dependent ROS signalling is critical for plant development and the defence response. Other RBOHCs have been implicated for their roles in a magnitude of signalling pathways in plant development such as bud outgrowth (Chen *et al.*, 2016) and stress responses such as the response to pathogens, wounding, osmotic stress, nutrient stress etc. (Macho *et al.*, 2012; Marino *et al.*, 2012; Baxter *et al.*, 2014). Notably, previous studies on *Striga asiatica* have shown that *S. asiatica*-generated  $\text{H}_2\text{O}_2$  is critical for host recognition and haustorium initiation (Kim *et al.*, 1998; Keyes *et al.*, 2000; Keyes *et al.*, 2007; Palmer *et al.*, 2008). It would be interesting to investigate whether broomrape infection triggers *RHD2*-dependent ROS signalling and the role of ROS signalling during the host-broomrape interaction. Future characterization of such candidate genes may increase our understanding in how far the host response to parasitic plants is similar or distinct from defence responses against other biotic and abiotic stresses. In addition, a recent study in which GWA mapping on resistance against multiple biotic and abiotic stresses was compared also offers clues about the similarities and differences in the host response to different biotic plant attackers and environmental stresses (Thoen *et al.*, 2017).



## Acknowledgements

We acknowledge funding by the Dutch Technology Foundation STW (to Carolien Ruyter-Spira; grant number 10990), the Chinese Scholarship Council (CSC; to Xi Cheng) and the Netherlands Organization for Scientific Research (NWO; VICI grant, 865.06.002 to Harro Bouwmeester). We thank Carin Helderma for technical support. We thank Willem Kruijer and Joost van Heerwaarden for giving suggestions on experimental design of GWA screening and GWA analysis. We thank Henri van de Geest and Rik Kooke for their help with the LD tool.

## References

- Abbes, Z., Kharrat, M., Delavault, P., Chaïbi, W., and Simier, P. (2009a). Osmoregulation and nutritional relationships between *Orobancha foetida* and faba bean. *Plant Signal Behav* 4(4), 336-338.
- Abbes, Z., Kharrat, M., Delavault, P., Chaïbi, W., and Simier, P. (2009b). Nitrogen and carbon relationships between the parasitic weed *Orobancha foetida* and susceptible and tolerant faba bean lines. *Plant Physiol Biochem* 47(2), 153-159.
- Alonso, J.M. (2003). Genome-wide insertional mutagenesis of *Arabidopsis thaliana*. *Science* 301(5633), 653-657.
- Atwell, S., Huang, Y.S., Vilhjálmsson, B.J., Willems, G., Horton, M., *et al.* (2010). Genome-wide association study of 107 phenotypes in *Arabidopsis thaliana* inbred lines. *Nature* 465(7298), 627-631.
- Bac-Molenaar, J.A., Fradin, E.F., Becker, F.F.M., Rienstra, J.A., van der Schoot, J., *et al.* (2015a). Genome-wide association mapping of fertility reduction upon heat stress reveals developmental stage-specific QTLs in *Arabidopsis thaliana*. *Plant Cell* 27(7), 1857-1874.
- Bac-Molenaar, J.A., Vreugdenhil, D., Granier, C., and Keurentjes, J.J.B. (2015b). Genome-wide association mapping of growth dynamics detects time-specific and general quantitative trait loci. *J Exp Bot* 66(18), 5567-5580.
- Baek, D., Pathange, P., Chung, J.S., Jiang, J., Gao, L., *et al.* (2010). A stress-inducible sulphotransferase sulphonates salicylic acid and confers pathogen resistance in *Arabidopsis*. *Plant Cell Environ* 33(8), 1383-1392.
- Bar-Nun, N., and Mayer, A.M. (2008). Methyl jasmonate and methyl salicylate, but not cis jasmonate, evoke defenses against infection of *Arabidopsis thaliana* by *Orobancha aegyptiaca*. *Weed Biol Manage* 8(2), 91-96.
- Baxter, A., Mittler, R., and Suzuki, N. (2014). ROS as key players in plant stress signaling. *J Exp Bot* 65(5), 1229-1240.
- Baxter, I., Brazelton, J.N., Yu, D., Huang, Y.S., Lahner, B., *et al.* (2010). A coastal cline in sodium accumulation in *Arabidopsis thaliana* is driven by natural variation of the

- sodium transporter AtHKT1;1. *PLoS Genet* 6(11), e1001193.
- Bell, E., Creelman, R.A., and Mullet, J.E.** (1995). A chloroplast lipoxygenase is required for wound-induced jasmonic acid accumulation in *Arabidopsis*. *Proc Natl Acad Sci U S A* 92(19), 8675-8679.
- Birschwilks, M., Sauer, N., Scheel, D., and Neumann, S.** (2007). *Arabidopsis thaliana* is a susceptible host plant for the holoparasite *Cuscuta spec.* *Planta* 226(5), 1231-1241.
- Brader, G., Mikkelsen, M.D., Halkier, B.A., and Tapio Palva, E.** (2006). Altering glucosinolate profiles modulates disease resistance in plants. *Plant J* 46(5), 758-767.
- Buschmann, H., Gonsior, G., and Sauerborn, J.** (2005a). Pathogenicity of branched broomrape (*Orobancha ramosa*) populations on tobacco cultivars. *Plant Pathol* 54(5), 650-656.
- Buschmann, H., Kömle, S., Gonsior, G., and Sauerborn, J.** (2005b). Susceptibility of oil-seed rape (*Brassica napus* ssp. *napus*) to branched broomrape (*Orobancha ramosa* L.). *Zeitschrift für Pflanzenkrankheiten und Pflanzenschutz* 112(1), 65-70.
- Butler, D.G., Cullis, B.R., Gilmour, A.R., and Gogel, B.J.** (2009). ASReml-R reference manual. *The State of Queensland, Department of Primary Industries and Fisheries, Brisbane*.
- Cagáň, L., and Tóth, P.** (2003). A decrease in tomato yield caused by branched broomrape (*Orobancha ramosa*) parasitization. *Acta Fytotechnica et Zootechnica*, 65-68.
- Chan, E.K., Rowe, H.C., Corwin, J.A., Joseph, B., and Kliebenstein, D.J.** (2011). Combining genome-wide association mapping and transcriptional networks to identify novel genes controlling glucosinolates in *Arabidopsis thaliana*. *PLoS Biol* 9(8), e1001125.
- Chang, M., and Lynn, D.G.** (1986). The haustorium and the chemistry of host recognition in parasitic angiosperms. *J Chem Ecol* 12(2), 561-579.
- Chen, X.J., Xia, X.J., Guo, X., Zhou, Y.H., Shi, K., et al.** (2016). Apoplastic H<sub>2</sub>O<sub>2</sub> plays a critical role in axillary bud outgrowth by altering auxin and cytokinin homeostasis in tomato plants. *New Phytol* 211(4), 1266-1278.
- Cissoko, M., Boissard, A., Rodenburg, J., Press, M.C., and Scholes, J.D.** (2011). New Rice for Africa (NERICA) cultivars exhibit different levels of post attachment resistance against the parasitic weeds *Striga hermonthica* and *Striga asiatica*. *New Phytol* 192(4), 952-963.
- Corwin, J.A., Copeland, D., Feusier, J., Subedy, A., Eshbaugh, R., et al.** (2016). The quantitative basis of the *Arabidopsis* innate immune system to endemic pathogens depends on pathogen genetics. *PLoS Genet* 12(2), e1005789.
- Davila Olivas, N.H., Kruijer, W., Gort, G., Wijnen, C.L., van Loon, J.J.A., et al.** (2016). Genome-wide association analysis reveals distinct genetic architectures for single and combined stress responses in *Arabidopsis thaliana*. *New Phytol* 213(2), 838-851.
- Denev, I., Deneva, B., Batchvarova, R., and Westwood, J.** (2014). Use of T-DNA activation tag *Arabidopsis* mutants in studying formation of germination stimulants for broomrapes (*Orobancha* spp.). *Biotechnol Biotechnol Equip* 21(4), 403-407.
- Díaz-Ruiz, R., Torres, A.M., Satovic, Z., Gutierrez, M.V., Cubero, J.I., et al.** (2010).



Validation of QTLs for *Orobanche crenata* resistance in faba bean (*Vicia faba* L.) across environments and generations. *Theor Appl Genet* 120(5), 909-919.

**Die, J.V., González Verdejo, C.I., Dita, M.A., Nadal, S., and Román, B.** (2009). Gene expression analysis of molecular mechanisms of defense induced in *Medicago truncatula* parasitized by *Orobanche crenata*. *Plant Physiol Biochem* 47(7), 635-641.

**Dos Santos, C.V., Letousey, P., Delavault, P., and Thalouarn, P.** (2003). Defense gene expression analysis of *Arabidopsis thaliana* parasitized by *Orobanche ramosa*. *Phytopathology* 93(4), 451-457.

**Draie, R., Péron, T., Pouvreau, J.-B., Véronési, C., Jégou, S., et al.** (2011). Invertases involved in the development of the parasitic plant *Phelipanche ramosa*: characterization of the dominant soluble acid isoform, PrSAI1. *Mol Plant Pathol* 12(7), 638-652.

**Ehlting, J., Chowrira, S.G., Mattheus, N., Aeschliman, D.S., Arimura, G.-I., et al.** (2008). Comparative transcriptome analysis of *Arabidopsis thaliana* infested by diamond back moth (*Plutella xylostella*) larvae reveals signatures of stress response, secondary metabolism, and signalling. *BMC Genomics* 9(1), 154.

**El-Soda, M., Kruijer, W., Malosetti, M., Koornneef, M., and Aarts, M.G.** (2015). Quantitative trait loci and candidate genes underlying genotype by environment interaction in the response of *Arabidopsis thaliana* to drought. *Plant Cell Environ* 38(3), 585-599.

**Fondevilla, S., Fernández-Aparicio, M., Satovic, Z., Emeran, A.A., Torres, A.M., et al.** (2009). Identification of quantitative trait loci for specific mechanisms of resistance to *Orobanche crenata* Forsk. in pea (*Pisum sativum* L.). *Mol Breeding* 25(2), 259-272.

**Foreman, J., Demidchik, V., Bothwell, J.H.F., Mylona, P., Miedema, H., et al.** (2003). Reactive oxygen species produced by NADPH oxidase regulate plant cell growth. *Nature* 422(6930), 442-446.

**Francisco, M., Joseph, B., Caligagan, H., Li, B., Corwin, J.A., et al.** (2016). Genome wide association mapping in *Arabidopsis thaliana* identifies novel genes involved in linking allyl glucosinolate to altered biomass and defense. *Front Plant Sci* 7(774), 627.

**Gao, M., Wang, X., Wang, D., Xu, F., Ding, X., et al.** (2009). Regulation of cell death and innate immunity by two receptor-like kinases in *Arabidopsis*. *Cell Host Microbe* 6(1), 34-44.

**Gaudin, Z., Cerveau, D., Marnet, N., Bouchereau, A., Delavault, P., et al.** (2014). Robust method for investigating nitrogen metabolism of <sup>15</sup>N labeled amino acids using AccQ\*Tag ultra performance liquid chromatography-photodiode array-electrospray ionization-mass spectrometry: application to a parasitic plant-plant interaction. *Anal Chem* 86(2), 1138-1145.

**Gibot-Leclerc, S., Sallé, G., Reboud, X., and Moreau, D.** (2012). What are the traits of *Phelipanche ramosa* (L.) Pomel that contribute to the success of its biological cycle on its host *Brassica napus* L.? *Flora* 207(7), 512-521.

**Goldwasser, Y., Plakhine, D., and Yoder, J.I.** (2000). *Arabidopsis thaliana* susceptibility to *Orobanche* spp. . *Weed Sci* 48(3), 342-346.

**Goldwasser, Y., Westwood, J.H., and Yoder, J.I.** (2002). The use of *Arabidopsis* to study interactions between parasitic angiosperms and their plant hosts. *Arabidopsis Book* 1,

e0035.

- Goldwasser, Y., and Yoder, J.I.** (2001). Differential induction of *Orobanchae* seed germination by *Arabidopsis thaliana*. *Plant Sci* 160(5), 951-959.
- Gong, X., Liu, M., Zhang, L., Ruan, Y., Ding, R., et al.** (2015). *Arabidopsis AtSUC2* and *AtSUC4*, encoding sucrose transporters, are required for abiotic stress tolerance in an ABA-dependent pathway. *Physiol Plant* 153(1), 119-136.
- Grubb, C.D., and Abel, S.** (2006). Glucosinolate metabolism and its control. *Trends Plant Sci* 11(2), 89-100.
- Guan, Y., and Stephens, M.** (2010). BIMBAM 1.0 User Manual.
- Gupta, D.K., Inouhe, M., Rodríguez-Serrano, M., Romero-Puertas, M.C., and Sandalio, L.M.** (2013). Oxidative stress and arsenic toxicity: role of NADPH oxidases. *Chemosphere* 90(6), 1987-1996.
- Gupta, D.K., Pena, L.B., Romero-Puertas, M.C., Hernandez, A., Inouhe, M., et al.** (2017). NADPH oxidases differentially regulate ROS metabolism and nutrient uptake under cadmium toxicity. *Plant Cell Environ* 40(4), 509-526.
- Gurney, A.L., Slate, J., Press, M.C., and Scholes, J.D.** (2006). A novel form of resistance in rice to the angiosperm parasite *Striga hermonthica*. *New Phytol* 169(1), 199-208.
- Hausmann, B.I.G., Hess, D.E., Omany, G.O., Folkertsma, R.T., Reddy, B.V.S., et al.** (2004). Genomic regions influencing resistance to the parasitic weed *Striga hermonthica* in two recombinant inbred populations of sorghum. *Theor Appl Genet* 109(5), 1005-1016.
- Hewezi, T., Howe, P., Maier, T.R., Hussey, R.S., Mitchum, M.G., et al.** (2008). Cellulose binding protein from the parasitic nematode *Heterodera schachtii* interacts with *Arabidopsis* pectin methylesterase: cooperative cell wall modification during parasitism. *Plant Cell* 20(11), 3080-3093.
- Hibberd, J.M., Quick, W.P., Press, M.C., and Scholes, J.D.** (1998). Can source-sink relations explain responses of tobacco to infection by the root holoparasitic angiosperm *Orobanchae cernua*? *Plant Cell Environ* 21(3), 333-340.
- Hibberd, J.M., Quick, W.P., Press, M.C., Scholes, J.D., and Jeschke, W.D.** (1999). Solute fluxes from tobacco to the parasitic angiosperm *Orobanchae cernua* and the influence of infection on host carbon and nitrogen relations. *Plant Cell Environ* 22(8), 937-947.
- Horton, M.W., Hancock, A.M., Huang, Y.S., Toomajian, C., Atwell, S., et al.** (2012). Genome-wide patterns of genetic variation in worldwide *Arabidopsis thaliana* accessions from the RegMap panel. *Nat Genet* 44(2), 212-216.
- Huang, D.W., Sherman, B.T., and Lempicki, R.A.** (2009a). Bioinformatics enrichment tools: paths toward the comprehensive functional analysis of large gene lists. *Nucl Acids Res* 37(1), 1-13.
- Huang, D.W., Sherman, B.T., Zheng, X., Yang, J., Imamichi, T., et al.** (2009b). Extracting biological meaning from large gene lists with DAVID. *Curr Protoc Bioinformatics* Chapter 13, Unit 13.11-13.11.13.
- Juergensen, K., Scholz-Starke, J., Sauer, N., Hess, P., van Bel, A.J.E., et al.** (2003). The

companion cell-specific *Arabidopsis* disaccharide carrier AtSUC2 is expressed in nematode-induced syncytia. *Plant Physiol* 131(1), 61-69.

- Kammerhofer, N., Radakovic, Z., Regis, J.M.A., Dobrev, P., Vankova, R., et al.** (2015). Role of stress-related hormones in plant defence during early infection of the cyst nematode *Heterodera schachtii* in *Arabidopsis*. *New Phytol* 207(3), 778-789.
- Kang, H.M., Sul, J.H., Service, S.K., Zaitlen, N.A., Kong, S.-Y., et al.** (2010). Variance component model to account for sample structure in genome-wide association studies. *Nat Genet* 42(4), 348-354.
- Kempema, L.A., Cui, X., Holzer, F.M., and Walling, L.L.** (2007). *Arabidopsis* transcriptome changes in response to phloem-feeding silverleaf whitefly nymphs. Similarities and distinctions in responses to aphids. *Plant Physiol* 143(2), 849-865.
- Keyes, W., O'Malley, R., Kim, D., and Lynn, D.** (2000). Signaling organogenesis in parasitic angiosperms: xenognosin generation, perception, and response. *J Plant Growth Regul* 19(2), 217-231.
- Keyes, W.J., Palmer, A.G., Erbil, W.K., Taylor, J.V., Apkarian, R.P., et al.** (2007). Semagenesis and the parasitic angiosperm *Striga asiatica*. *Plant J* 51(4), 707-716.
- Kim, D., Kocz, R., Boone, L., John Keyes, W., and Lynn, D.G.** (1998). On becoming a parasite: evaluating the role of wall oxidases in parasitic plant development. *Chem Biol* 5(2), 103-117.
- Kooke, R., Kruijer, W., Bours, R., Becker, F., Kuhn, A., et al.** (2016). Genome-wide association mapping and genomic prediction elucidate the genetic architecture of morphological traits in *Arabidopsis*. *Plant Physiol* 170(4), 2187-2203.
- Labrousse, P., Arnaud, M.C., Griveau, Y., Fer, A., and Thalouarn, P.** (2004). Analysis of resistance criteria of sunflower recombined inbred lines against *Orobanche cumana* Wallr. *Crop Protection* 23(5), 407-413.
- Li, J., Lis, K.E., and Timko, M.P.** (2009). Molecular genetics of race-specific resistance of cowpea to *Striga gesnerioides* (Willd.). *Pest Manag Sci* 65(5), 520-527.
- Li, Y., Huang, Y., Bergelson, J., Nordborg, M., and Borevitz, J.O.** (2010). Association mapping of local climate-sensitive quantitative trait loci in *Arabidopsis thaliana*. *Proc Natl Acad Sci U S A* 107(49), 21199-21204.
- Lin, H., Wang, R., Qian, Q., Yan, M., Meng, X., et al.** (2009). DWARF27, an iron-containing protein required for the biosynthesis of strigolactones, regulates rice tiller bud outgrowth. *The Plant Cell* 21(5), 1512-1525.
- Liu, S.G., Zhu, D.Z., Chen, G.H., Gao, X.-Q., and Zhang, X.S.** (2012). Disrupted actin dynamics trigger an increment in the reactive oxygen species levels in the *Arabidopsis* root under salt stress. *Plant Cell Rep* 31(7), 1219-1226.
- Livak, K.J., and Schmittgen, T.D.** (2001). Analysis of relative gene expression data using real-time quantitative PCR and the 2<sup>-</sup>(Delta Delta C(T)) Method. *Methods* 25(4), 402-408.
- Livanos, P., Apostolakos, P., and Galatis, B.** (2012). Plant cell division: ROS homeostasis is required. *Plant Signal Behav* 7(7), 771-778.

- Longo, A.M.G., Lo Monaco, A., and Mauromicale, G.** (2010). The effect of *Phelipanche ramosa* infection on the quality of tomato fruit. *Weed Res* 50(1), 58-66.
- Losner-Goshen, D.** (1998). Pectolytic activity by the haustorium of the parasitic plant *Orobancha* L. (*Orobanchaceae*) in host roots. *Ann Bot* 81(2), 319-326.
- Louarn, J., Boniface, M.-C., Pouilly, N., Velasco, L., Pérez-Vich, B., et al.** (2016). Sunflower resistance to broomrape (*Orobancha cumana*) is controlled by specific QTLs for different parasitism stages. *Front Plant Sci* 7, 590.
- Macho, A.P., Boutrot, F., Rathjen, J.P., and Zipfel, C.** (2012). Aspartate oxidase plays an important role in *Arabidopsis* stomatal immunity. *Plant Physiol* 159(4), 1845-1856.
- Macpherson, N., Takeda, S., Shang, Z., Dark, A., Mortimer, J.C., et al.** (2008). NADPH oxidase involvement in cellular integrity. *Planta* 227(6), 1415-1418.
- Marino, D., Dunand, C., Puppo, A., and Pauly, N.** (2012). A burst of plant NADPH oxidases. *Trends Plant Sci* 17(1), 9-15.
- Martín-Sanz, A., Malek, J., Fernández-Martínez, J.M., Pérez-Vich, B., and Velasco, L.** (2016). Increased virulence in sunflower broomrape (*Orobancha cumana* Wallr.) populations from southern Spain Is associated with greater genetic diversity. *Front Plant Sci* 7, 589.
- Mauromicale, G., Monaco, A.L., and Longo, A.M.G.** (2008). Effect of branched broomrape (*Orobancha ramosa*) infection on the growth and photosynthesis of tomato. *Weed Sci* 56(4), 574-581.
- Mi, H., Muruganujan, A., Casagrande, J.T., and Thomas, P.D.** (2013). Large-scale gene function analysis with the PANTHER classification system. *Nat Protoc* 8(8), 1551-1566.
- Mi, H., Muruganujan, A., and Thomas, P.D.** (2012). PANTHER in 2013: modeling the evolution of gene function, and other gene attributes, in the context of phylogenetic trees. *Nucl Acids Res* 41(D1), D377-D386.
- Mitsumasu, K., Seto, Y., and Yoshida, S.** (2015). Apoplastic interactions between plants and plant root intruders. *Front Plant Sci* 6, 909.
- Monshausen, G.B., Bibikova, T.N., Weisenseel, M.H., and Gilroy, S.** (2009). Ca<sup>2+</sup> regulates reactive oxygen species production and pH during mechanosensing in *Arabidopsis* roots. *Plant Cell* 21(8), 2341-2356.
- Mor, A., Mayer, A.M., and Levine, A.** (2008). Possible peroxidase functions in the interaction between the parasitic plant, *Orobancha aegyptiaca*, and its host, *Arabidopsis thaliana*. *Weed Biol Manage* 8(1), 1-10.
- Moran, P.J., and Thompson, G.A.** (2001). Molecular responses to aphid feeding in *Arabidopsis* in relation to plant defense pathways. *Plant Physiol* 125(2), 1074-1085.
- Moreau, D., Gibot-Leclerc, S., Girardin, A., Pointurier, O., Reibel, C., et al.** (2016). Trophic relationships between the parasitic plant species *Phelipanche ramosa* (L.) and different hosts depending on host phenological stage and host growth rate. *Front Plant Sci* 7, 289-212.
- Nordborg, M., and Tavaré, S.** (2002). Linkage disequilibrium: what history has to tell us. *Trends Genet* 18(2), 83-90.

- Ortiz-Bustos, C.M., Pérez-Bueno, M.L., Barón, M., and Molinero-Ruiz, L.** (2016). Fluorescence imaging in the red and far-red region during growth of sunflower plantlets. Diagnosis of the early infection by the parasite *Orobancha cumana*. *Front Plant Sci* 7(e110664), 671-610.
- Palmer, A.G., Liu, Y., Adkins, S.M., Zhang, X., Wu, I.L., et al.** (2008). The molecular language of semagenesis. *Plant Signal Behav* 3(8), 560-561.
- Pan, H., Liu, S., and Tang, D.** (2012). HPR1, a component of the THO/TREX complex, plays an important role in disease resistance and senescence in *Arabidopsis*. *Plant J* 69(5), 831-843.
- Pérez-de-Luque, A., Fondevilla, S., Pérez-Vich, B., Aly, R., Thoiron, S., et al.** (2009). Understanding *Orobancha* and *Phelipanche*-host plant interactions and developing resistance. *Weed Res* 49, 8-22.
- Pérez-de-Luque, A., Rubiales, D., Cubero, J.I., Press, M.C., Scholes, J., et al.** (2005). Interaction between *Orobancha crenata* and its host legumes: unsuccessful haustorial penetration and necrosis of the developing parasite. *Ann Bot* 95(6), 935-942.
- Pérez-Vich, B., Akhtouch, B., Knapp, S.J., Leon, A.J., Velasco, L., et al.** (2004). Quantitative trait loci for broomrape (*Orobancha cumana* Wallr.) resistance in sunflower. *Theor Appl Genet* 109(1), 92-102.
- Rodríguez-Ojeda, M.I., Pineda-Martos, R., Alonso, L.C., Fernández-Escobar, J., Fernández-Martínez, J.M., et al.** (2013). A dominant avirulence gene in *Orobancha cumana* triggers *Or5* resistance in sunflower. *Weed Res* 53(5), 322-327.
- Rubiales, D., Fernández-Aparicio, M., Pérez-de-Luque, A., Castillejo, M.A., Prats, E., et al.** (2009). Breeding approaches for crenate broomrape (*Orobancha crenata* Forsk.) management in pea (*Pisum sativum* L.). *Pest Manag Sci* 65(5), 553-559.
- Rubiales, D., Flores, F., Emeran, A.A., Kharrat, M., Amri, M., et al.** (2014). Identification and multi-environment validation of resistance against broomrapes (*Orobancha crenata* and *Orobancha foetida*) in faba bean (*Vicia faba*). *Field Crops Res* 166, 58-65.
- Sakamoto, H., Matsuda, O., and Iba, K.** (2008). ITN1, a novel gene encoding an ankyrin-repeat protein that affects the ABA-mediated production of reactive oxygen species and is involved in salt-stress tolerance in *Arabidopsis thaliana*. *Plant J* 56(3), 411-422.
- Samejima, H., Babiker, A.G., Mustafa, A., and Sugimoto, Y.** (2016). Identification of *Striga hermonthica*-resistant upland rice varieties in sudan and their resistance phenotypes. *Front Plant Sci* 7, 634.
- Schneidereit, A., Scholz-Starke, J., Sauer, N., and Büttner, M.** (2004). AtSTP11, a pollen tube-specific monosaccharide transporter in *Arabidopsis*. *Planta* 221(1), 48-55.
- Silva, N.F., and Goring, D.R.** (2002). The proline-rich, *extensin-like receptor kinase-1* (*PERK1*) gene is rapidly induced by wounding. *Plant Mol Biol* 50(4-5), 667-685.
- Simier, P., Constant, S., Degrande, D., Moreau, C., Robins, R.J., et al.** (2006). Impact of nitrate supply in C and N assimilation in the parasitic plant *Striga hermonthica* (Del.) Benth (*Scrophulariaceae*) and its host *Sorghum bicolor* L. *Plant Cell Environ* 29(4), 673-681.

- Srivastava, A.C., Ganesan, S., Ismail, I.O., and Ayre, B.G.** (2008). Functional characterization of the *Arabidopsis* AtSUC2 Sucrose/H<sup>+</sup> symporter by tissue-specific complementation reveals an essential role in phloem loading but not in long-distance transport. *Plant Physiol* 148(1), 200-211.
- Swarbrick, P.J., Scholes, J.D., Press, M.C., and Slate, J.** (2009). A major QTL for resistance of rice to the parasitic plant *Striga hermonthica* is not dependent on genetic background. *Pest Manag Sci* 65(5), 528-532.
- Thoen, M.P., Davila Olivas, N.H., Kloth, K.J., Coolen, S., Huang, P.P., et al.** (2017). Genetic architecture of plant stress resistance: multi-trait genome-wide association mapping. *New Phytol* 213(3), 1346-1362.
- Thorogood, C.J., and Hiscock, S.J.** (2010). Compatibility interactions at the cellular level provide the basis for host specificity in the parasitic plant *Orobancha*. *New Phytol* 186(3), 571-575.
- Timus, A., and Croitoru, N.** (2007). The state of tobacco culture in Republic Moldova and phytosanitary problems of tobacco production. *Rasteniev'dni Nauki* 44(3), 209-212.
- Torres-Vera, R., García, J.M., Pozo, M.J., and López-Ráez, J.A.** (2016). Expression of molecular markers associated to defense signaling pathways and strigolactone biosynthesis during the early interaction tomato-*Phelipanche ramosa*. *Physiol Mol Plant Pathol* 94, 100-107.
- Velasco, L., Pérez-Vich, B., Yassein, A.A.M., Jan, C.-C., and Fernández-Martínez, J.M.** (2011). Inheritance of resistance to sunflower broomrape (*Orobancha cumana* Wallr.) in an interspecific cross between *Helianthus annuus* and *Helianthus debilis* subsp. tardiflorus. *Plant Breeding* 131(1), 220-221.
- Warde-Farley, D., Donaldson, S.L., Comes, O., Zuberi, K., Badrawi, R., et al.** (2010). The GeneMANIA prediction server: biological network integration for gene prioritization and predicting gene function. *Nucl Acids Res* 38, 214-220.
- Waters, M.T., Brewer, P.B., Bussell, J.D., Smith, S.M., and Beveridge, C.A.** (2012). The *Arabidopsis* ortholog of rice *DWARF27* acts upstream of *MAX1* in the control of plant development by strigolactones. *Plant Physiol* 159(3), 1073-1085.
- Westwood, J.H.** (2000). Characterization of the *Orobancha*-*Arabidopsis* system for studying parasite-host interactions. *Weed Sci* 48(6), 742-748.
- Wierzba, M.P., and Tax, F.E.** (2016). An allelic series of *bak1* mutations differentially alter *bir1* cell death, immune response, growth, and root development phenotypes in *Arabidopsis thaliana*. *Genetics* 202(2), 689-702.
- Xie, X., Yoneyama, K., and Yoneyama, K.** (2010). The strigolactone story. *Ann Rev Phytopath* 8(1), 93-117.
- Yoshida, S., Cui, S., Ichihashi, Y., and Shirasu, K.** (2016). The haustorium, a specialized invasive organ in parasitic plants. *Annu Rev Plant Biol* 67(1), 643-667.
- Yoshida, S., and Shirasu, K.** (2009). Multiple layers of incompatibility to the parasitic witchweed, *Striga hermonthica*. *New Phytol* 183(1), 180-189.



## Supplementary materials:

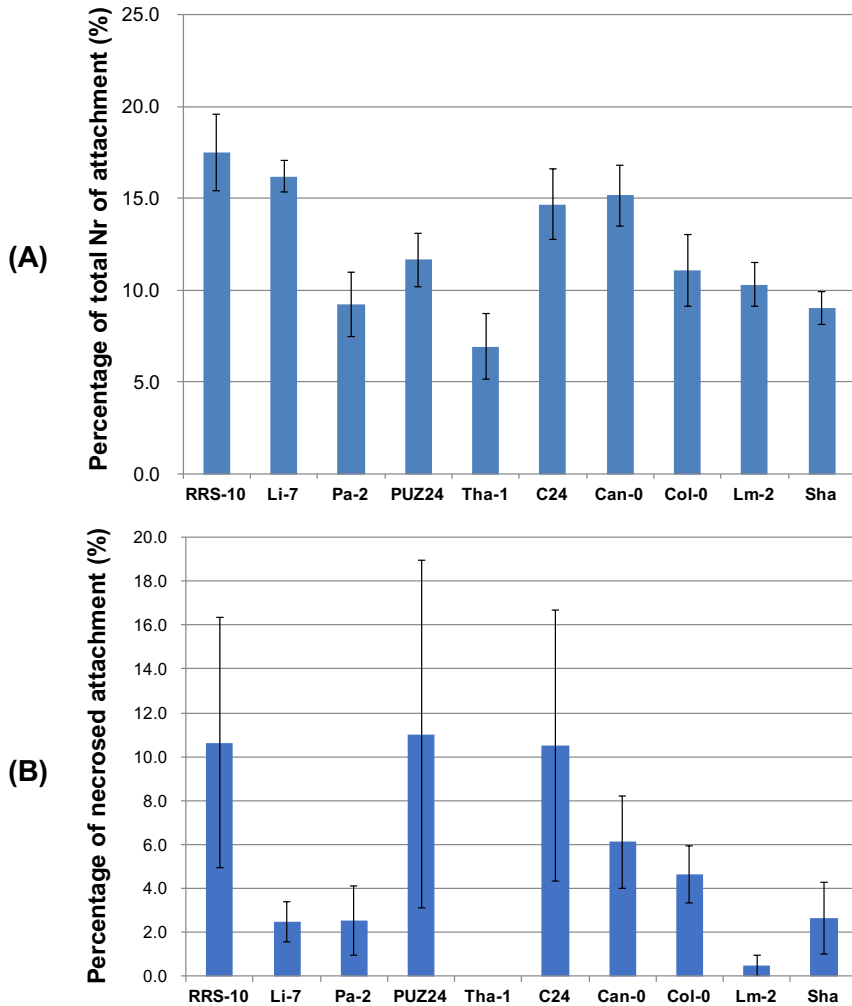
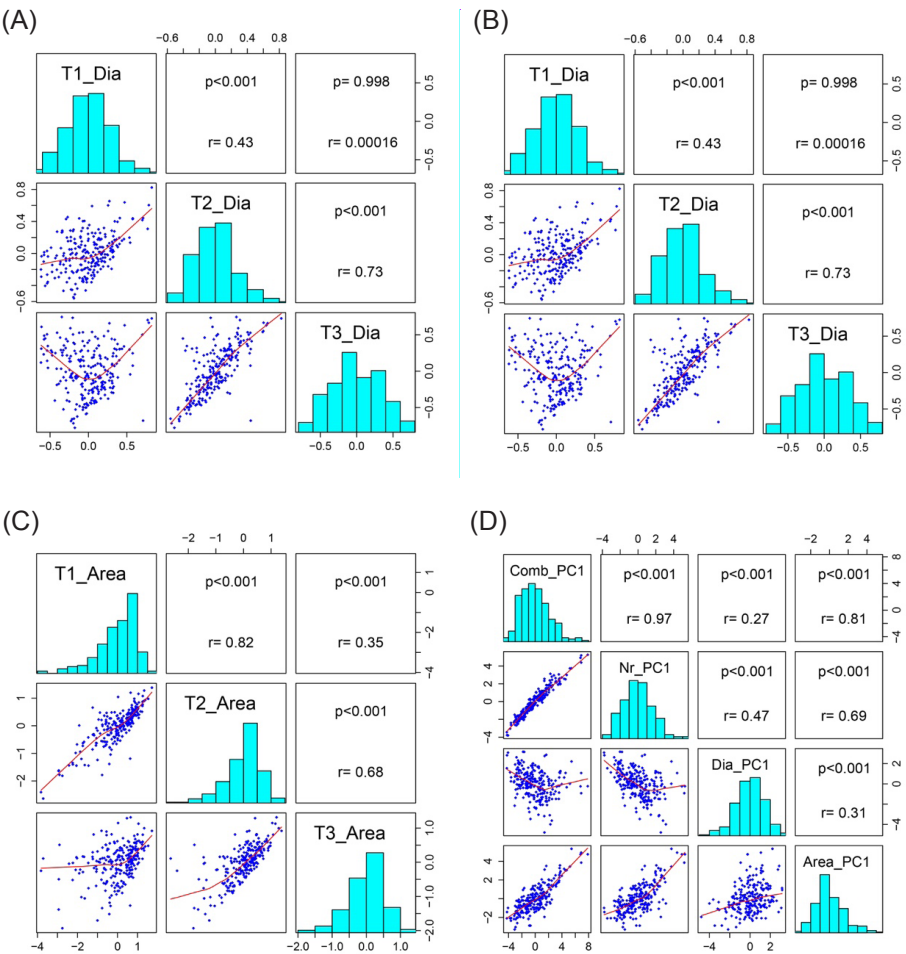


**Figure S1. A preliminary trial on ten *Arabidopsis* accessions with six replicates showing that the phenotypic parameter percentage of tubercles is a reproducible trait (A), while the percentage of necrosed tubercles is not reproducible (B).**



(continues)



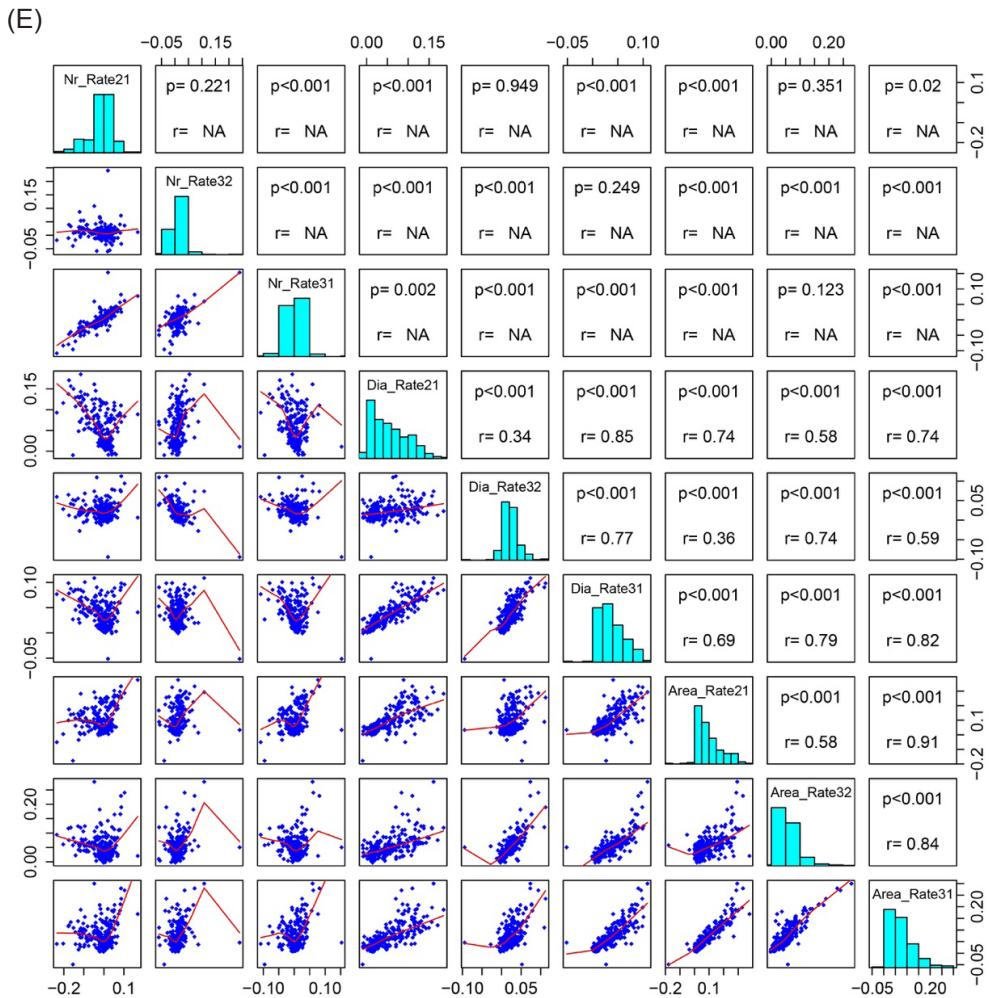


**Figure S2. Distributions (histograms on the diagonal) and correlation matrixes (scatterplots below the diagonal) of traits:** (A) tubercle number, Nr; (B) tubercle diameter, Dia; (C) total area of tubercles, Area, across at different time points (T1, T2 and T3 -- 2 w, 3 w and 4 w (weeks) after infection, respectively); (D) the first principle component of combined data (Comb\_PC1), tubercle number (Nr\_PC1), tubercle diameter (Dia\_PC1), total area of tubercles (Area\_PC1); (E) growth rate of tubercle number (Nr), tubercle diameter (Dia), total area of tubercles (Area) between time point 1 and 2 (Rate21), between time point 2 and 3 (Rate32), between 1 and 3 (Rate31). Histograms on the diagonal show the distribution of each trait. Scatterplots with a red fitted line below the diagonal show the correlation

matrix of the paired data. And the corresponding correlation coefficients ( $r$ ) and  $p$  values are shown above the diagonal.

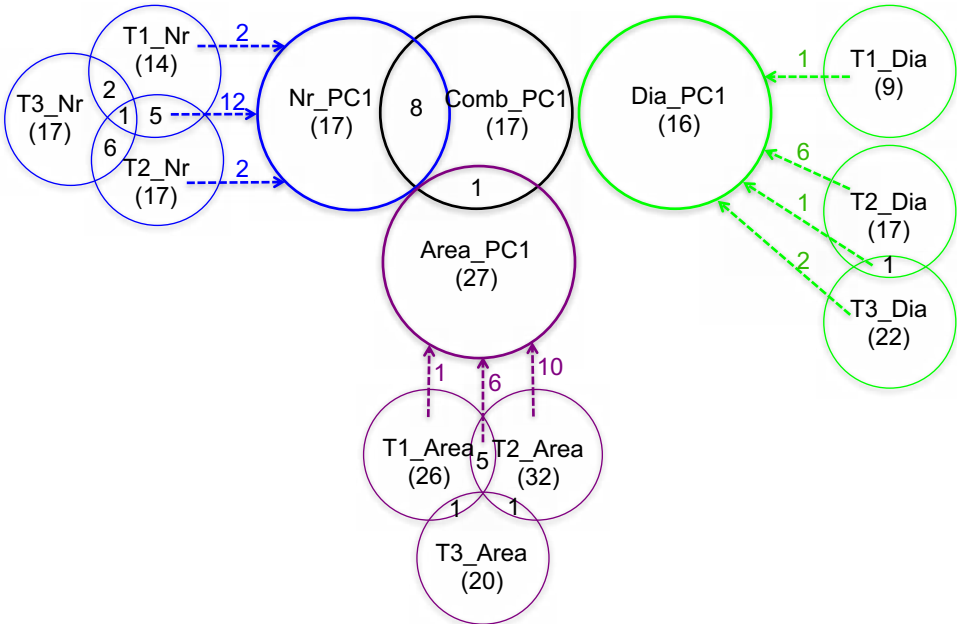


**Figure S3. Venn diagrams showing shared identified significant SNPs between traits as mentioned in Table 1.** These traits include individual traits of tubercle number (Nr), tubercle diameter (Dia), tubercle area (Area) at three time points (T1, T2, T3) and PC1 traits (Nr\_PC1, Dia\_PC1, Area\_PC1, Comb\_PC1). Comb\_PC1 is the first principal component of PCA on combining number, average diameter and estimated area of tubercles at all time-points. Numbers in brackets indicate the total number of significant SNPs associated with the corresponding trait. Numbers inside the overlapping region between two circles indicate the number of significant SNPs shared between the corresponding traits. Numbers besides the arrows indicate how many significant SNPs were shared between individual traits and PC1 traits.

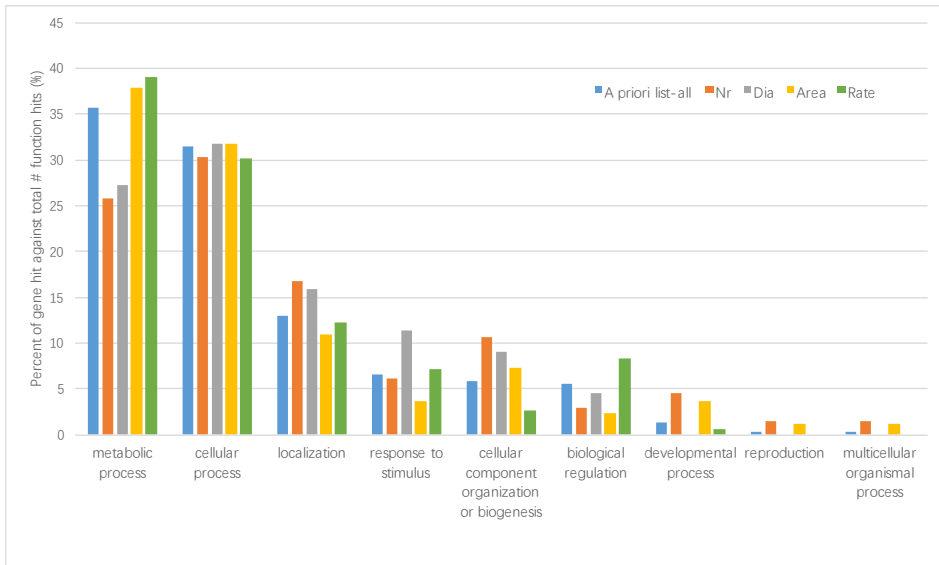


**Figure S4. Comparison of GO categories between traits based on the a priori list of candidate genes, sub-list of candidate genes for tubercle number (Nr), tubercle diameter (Dia), total area of tubercles (Area) and growth rate (Rate).**

Interaction Viewer: AT1G22710

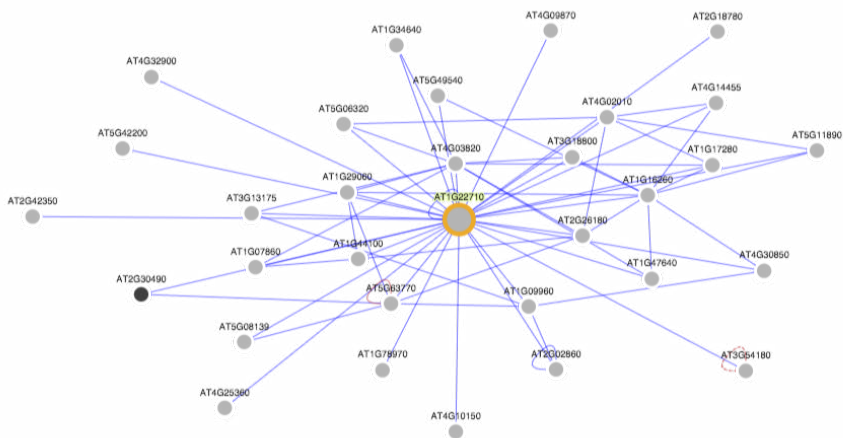


**Figure S5. Predicted protein network for SUC2 (AT1G22710, in orange circle) based GeneMania tool.**

**Table S1. PCA summary.** Proportions of variation explained by the first three components of PCA are presented in the list. (A) PCA on T1\_Nr, T2\_Nr, T3\_Nr; (B) PCA on T1\_Dia, T2\_Dia, T3\_Dia; (C) PCA on T1\_Area, T2\_Area, T3\_Area; (D) PCA on T1\_Nr, T2\_Nr, T3\_Nr, T1\_Dia, T2\_Dia, T3\_Dia, T1\_Area, T2\_Area, T3\_Area. Full descriptions of traits are included in Table 1.

**(A) PCA on T1\_Nr, T2\_Nr, T3\_Nr**

Component	Eigenvalue	Difference	Proportion	Cumulative
Comp1	2.69866	2.46506	0.8996	0.8996
Comp2	.233598	.165857	0.0779	0.9774
Comp3	.067741		0.0226	1.0000

Principal components (eigenvectors)

Variable	Comp1	Comp2	Comp3	Unexplained
T1_Nr	0.5597	0.8073	0.1870	0
T2_Nr	0.5924	-0.2320	-0.7715	0
T3_Nr	0.5795	-0.5426	0.6081	0

**(B) PCA on T1\_Dia, T2\_Dia, T3\_Dia**

Component	Eigenvalue	Difference	Proportion	Cumulative
Comp1	1.84695	.846818	0.6157	0.6157
Comp2	1.00014	.847226	0.3334	0.9490
Comp3	.15291	.	0.0510	1.0000

Principal components (eigenvectors)

Variable	Comp1	Comp2	Comp3	Unexplained
T1_Dialogres	0.3595	0.8610	0.3597	0
T2_Dialogres	0.7071	0.0001	-0.7071	0
T3_Dialogres	0.6089	-0.5085	0.6088	0

(continues)

### (C) PCA on T1\_Area, T2\_Area, T3\_Area

Component	Eigenvalue	Difference	Proportion	Cumulative
Comp1	2.25735	1.60064	0.7525	0.7525
Comp2	.656712	.570777	0.2189	0.9714
Comp3	.0859352	.	0.0286	1.0000

#### Principal components (eigenvectors)

Variable	Comp1	Comp2	Comp3	Unexplained
T1_Area	0.5661	-0.6182	0.5453	0
T2_Area	0.6476	-0.0756	-0.7582	0
T3_Area	0.5100	0.7824	0.3576	0

### (D) PCA on T1\_Nr, T2\_Nr, T3\_Nr, T1\_Dia, T2\_Dia, T3\_Dia, T1\_Area, T2\_Area, T3\_Area

Component	Eigenvalue	Difference	Proportion	Cumulative
Comp1	4.70291	2.02377	0.5225	0.5225
Comp2	2.67914	1.74511	0.2977	0.8202
Comp3	.934029	.563505	0.1038	0.9240
Comp4	.370524	.175293	0.0412	0.9652
Comp5	.195231	.09034	0.0217	0.9869
Comp6	.104891	.095691	0.0117	0.9985
Comp7	.0092004	.00619843	0.0010	0.9995
Comp8	.00300197	.00192537	0.0003	0.9999
Comp9	.0010766	.	0.0001	1.0000

#### Principal components (eigenvectors)

Variable	Comp1	Comp2	Comp3	Comp4	Comp5	Comp6	Comp7	Comp8	Comp9	Unexplained
T1_Nr	0.4016	-0.1118	0.2276	0.6443	0.0450	0.2056	0.2002	-0.3358	0.4027	0
T2_Nr	0.4385	-0.1236	0.0908	-0.1431	0.1942	-0.5383	0.3776	-0.2813	-0.4632	0
T3_Nr	0.4262	-0.1198	0.1441	-0.4036	-0.2576	0.3426	0.4323	0.4786	0.1441	0
T1_Dia	0.1913	0.3533	-0.6940	-0.2484	0.3077	0.1256	0.1709	-0.2523	0.3031	0
T2_Dia	-0.1004	0.5653	-0.0620	0.1971	-0.6267	0.0808	0.3223	-0.1791	-0.3040	0
T3_Dia	-0.2775	0.4355	0.2656	0.1871	0.4806	-0.1896	0.4179	0.4123	0.1274	0
T1_Area	0.4158	0.1485	-0.2501	0.3816	0.2082	0.2312	-0.2917	0.4209	-0.4877	0
T2_Area	0.3727	0.3304	0.0483	-0.0106	-0.2865	-0.5739	-0.3760	0.2053	0.3930	0
T3_Area	0.1714	0.4390	0.5461	-0.3468	0.2237	0.3310	-0.3102	-0.3065	-0.0982	0

**Table S2. Spearman's rank correlation matrix.** (A) Correlation matrix for total number (Nr), average diameter (Dia), estimated area (Area) of tubercles from three time points (T1, T2, T3), the first principal component of each parameter (Nr\_PC1, Dia\_PC1, Area\_PC1), as well as the first principal component for combined PCA (Comb\_PC1). (B) Correlation matrix for growth rate of Nr, Dia and Area between time points. Correlation coefficient (r) is indicated in numbers and its range is highlighted in color (the red to green scale indicate values from high to low).

(A)

	T1_Nr	T2_Nr	T3_Nr	T1_Dia	T2_Dia	T3_Dia	T1_Area	T2_Area	T3_Area	Nr_PC1	Dia_PC1	Area_PC1	Comb_PC1
T1_Nr	1												
T2_Nr	0.8233	1											
T3_Nr	0.7974	0.9389	1										
T1_Dia	0.0183	0.2477	0.2017	1									
T2_Dia	-0.3949	-0.4719	-0.4274	0.3732	1								
T3_Dia	-0.5719	-0.6946	-0.7317	-0.0295	0.7156	1							
T1_Area	0.7298	0.7581	0.7106	0.6425	-0.0446	-0.3962	1						
T2_Area	0.5029	0.6214	0.5958	0.5704	0.3108	-0.0739	0.7878	1					
T3_Area	0.2034	0.2052	0.251	0.2641	0.4735	0.4029	0.3812	0.7107	1				
Nr_PC1	-0.9086	-0.9712	-0.9642	-0.1719	0.4501	0.7037	-0.7694	-0.6055	-0.2336	1			
Dia_PC1	0.452	0.4882	0.4896	-0.4332	-0.9606	-0.8094	0.0364	-0.2848	-0.4973	-0.4984	1		
Area_PC1	-0.5541	-0.6083	-0.5954	-0.5785	-0.2978	0.0353	-0.8369	-0.966	-0.7751	0.6181	0.2949	1	
Comb_PC1	-0.8496	-0.9542	-0.9442	-0.3864	0.2956	0.6285	-0.886	-0.7392	-0.3241	0.9661	-0.3274	0.7522	1

(continues)

(B)

	Nr_Rate21	Nr_Rate32	Nr_Rate31	Dia_Rate21	Dia_Rate32	Dia_Rate31	Area_Rate21	Area_Rate32	Area_Rate31
Nr_Rate21	1								
Nr_Rate32	-0.1203	1							
Nr_Rate31	0.8123	0.3644	1						
Dia_Rate21	-0.3884	0.3513	-0.2026	1					
Dia_Rate32	-0.001	-0.413	-0.2256	0.3609	1				
Dia_Rate31	-0.2725	0.0211	-0.266	0.8737	0.7404	1			
Area_Rate21	0.1754	0.3256	0.2936	0.7797	0.3516	0.7231	1		
Area_Rate32	-0.1618	0.1423	-0.0837	0.6104	0.764	0.8042	0.527	1	
Area_Rate31	0.0716	0.2598	0.1819	0.802	0.568	0.8566	0.9227	0.7811	1



**Table S3. GWA mapping results including significant SNPs and SNPs within  $\pm 10$ kb window of significant SNPs based on 250K chip sequencing data.** Columns represent the trait, chromosome, exact position of SNPs, SNP status, candidate gene information (ID, name, descriptions, biological function), allele frequency in Col-0, the effect size (Col-0 allele is positive; non-Col-0 allele is negative) and explained genetic and phenotypic variance.

See the file in the link: <https://www.dropbox.com/sh/6sqmaovo4rjc4ep/AACX6EtKF78UugpDUGRhQhxna?dl=0>

**Table S4. A priori candidate gene list.** A search window was defined by including SNPs in the  $\pm 10$ kb neighboring region around the identified significant SNPs in close LD ( $r^2 > 0.4$ ) based on both the 250K array and resequencing data (1001genomes.org). Genes within the search window were all considered as a priori candidate genes.

See the file in the link: <https://www.dropbox.com/sh/6sqmaovo4rjc4ep/AACX6EtKF78UugpDUGRhQhxna?dl=0>

**Table S5. GO categories (biological process, cellular component, molecular function, pathway, protein class) for a priori candidate gene list.**

	Category name	Num- ber of genes	Percent of gene hit against total number of genes	Percent of gene hit against total number of func- tion hits
<b>Biological process</b>				
1	cellular component organization or biogenesis (GO:0071840)	18	4.20%	5.80%
2	cellular process (GO:0009987)	97	22.90%	31.50%
3	localization (GO:0051179)	40	9.40%	13.00%
4	biological regulation (GO:0065007)	17	4.00%	5.50%
5	reproduction (GO:0000003)	1	0.20%	0.30%
6	response to stimulus (GO:0050896)	20	4.70%	6.50%
7	developmental process (GO:0032502)	4	0.90%	1.30%
8	multicellular organismal process (GO:0032501)	1	0.20%	0.30%
9	metabolic process (GO:0008152)	110	25.90%	35.70%
<b>Molecular function</b>				
1	translation regulator activity (GO:0045182)	4	0.90%	1.80%
2	binding (GO:0005488)	53	12.50%	24.40%
3	receptor activity (GO:0004872)	10	2.40%	4.60%
4	structural molecule activity (GO:0005198)	14	3.30%	6.50%
5	signal transducer activity (GO:0004871)	1	0.20%	0.50%
6	catalytic activity (GO:0003824)	104	24.50%	47.90%
7	transporter activity (GO:0005215)	31	7.30%	14.30%
<b>Cellular component</b>				
1	membrane (GO:0016020)	19	4.50%	13.90%
2	macromolecular complex (GO:0032991)	21	5.00%	15.30%
3	cell part (GO:0044464)	61	14.40%	44.50%

(continues)

## GWA Mapping of Broomrape Parasitism

4	organelle (GO:0043226)	36	8.50%	26.30%
<b>Pathway</b>				
1	Methionine biosynthesis (P02753)	1	0.20%	3.10%
2	Tryptophan biosynthesis (P02783)	1	0.20%	3.10%
3	Axon guidance mediated by Slit/Robo (P00008)	1	0.20%	3.10%
4	Ionotropic glutamate receptor pathway (P00037)	1	0.20%	3.10%
5	Insulin/IGF pathway-mitogen activated protein kinase kinase/ MAP kinase cascade (P00032)	2	0.50%	6.30%
6	De novo pyrimidine deoxy-ribonucleotide biosynthesis (P02739)	1	0.20%	3.10%
7	Ubiquitin proteasome pathway (P00060)	2	0.50%	6.30%
8	Endothelin signalling pathway (P00019)	1	0.20%	3.10%
9	Pentose phosphate pathway (P02762)	1	0.20%	3.10%
10	EGF receptor signalling pathway (P00018)	2	0.50%	6.30%
11	DNA replication (P00017)	1	0.20%	3.10%
12	Cytoskeletal regulation by Rho GTPase (P00016)	1	0.20%	3.10%
13	PDGF signalling pathway (P00047)	1	0.20%	3.10%
14	Oxidative stress response (P00046)	1	0.20%	3.10%
15	Ras Pathway (P04393)	1	0.20%	3.10%
16	Heme biosynthesis (P02746)	2	0.50%	6.30%
17	Salvage pyrimidine ribonucleotides (P02775)	1	0.20%	3.10%
18	Salvage pyrimidine deoxyribonucleotides (P02774)	1	0.20%	3.10%
19	Huntington disease (P00029)	2	0.50%	6.30%
20	Wnt signalling pathway (P00057)	1	0.20%	3.10%
21	Synaptic vesicle trafficking (P05734)	1	0.20%	3.10%

(continues)

## CHAPTER 2

22	Transcription regulation by bZIP transcription factor (P00055)	1	0.20%	3.10%
23	5-Hydroxytryptamine degradation (P04372)	1	0.20%	3.10%
24	General transcription regulation (P00023)	1	0.20%	3.10%
25	General transcription by RNA polymerase I (P00022)	1	0.20%	3.10%
26	FGF signalling pathway (P00021)	2	0.50%	6.30%
<b>Protein class</b>				
1	extracellular matrix protein (PC00102)	1	0.20%	0.40%
2	cytoskeletal protein (PC00085)	10	2.40%	4.30%
3	transporter (PC00227)	31	7.30%	13.40%
4	transmembrane receptor regulatory/adaptor protein (PC00226)	1	0.20%	0.40%
5	transferase (PC00220)	29	6.80%	12.60%
6	oxidoreductase (PC00176)	15	3.50%	6.50%
7	lyase (PC00144)	5	1.20%	2.20%
8	cell adhesion molecule (PC00069)	1	0.20%	0.40%
9	ligase (PC00142)	10	2.40%	4.30%
10	nucleic acid binding (PC00171)	42	9.90%	18.20%
11	signalling molecule (PC00207)	2	0.50%	0.90%
12	enzyme modulator (PC00095)	13	3.10%	5.60%
13	calcium-binding protein (PC00060)	2	0.50%	0.90%
14	defense/immunity protein (PC00090)	1	0.20%	0.40%
15	hydrolase (PC00121)	31	7.30%	13.40%
16	transfer/carrier protein (PC00219)	3	0.70%	1.30%
17	membrane traffic protein (PC00150)	3	0.70%	1.30%
18	transcription factor (PC00218)	12	2.80%	5.20%
19	chaperone (PC00072)	3	0.70%	1.30%
20	storage protein (PC00210)	1	0.20%	0.40%
21	isomerase (PC00135)	4	0.90%	1.70%
22	receptor (PC00197)	11	2.60%	4.80%

**Table S6. Comparisons of PANTHER overrepresentation test results based on a priori list of all the traits, traits for tubercle number, traits for tubercle diameter, traits for estimated tubercle area, traits for tubercle developmental rate.** PANTHER Overrepresentation Test was performed based on version 11.0 Released 2016-07-15. No Bonferroni correction was applied.

Analyzed List	PANTHER GO-Slim Biological Process	Arabidopsi s (reference list)	Analyzed list				
		#	#	Expect- ed	Over/ under	Fold Enrich- ment	P-value
A priori candidate gene list for all traits	JAK-STAT cascade (GO:0007259)	2	1	0.03	+	32.25	3.05E-02
	cellular component movement (GO:0006928)	163	6	2.53	+	2.37	4.33E-02
	steroid metabolic process (GO:0008202)	317	1	4.91	-	0.2	4.26E-02
A priori candidate gene list for Nr	JNK cascade (GO:0007254)	20	1	0.05	+	20.72	4.71E-02
	cellular component morphogenesis (GO:0032989)	134	5	0.32	+	15.46	1.97E-05
	cellular component movement (GO:0006928)	163	4	0.39	+	10.17	6.77E-04
	chromosome segregation (GO:0007059)	84	2	0.2	+	9.87	1.78E-02
	exocytosis (GO:0006887)	124	2	0.3	+	6.68	3.64E-02
	intracellular protein transport (GO:0006886)	1197	8	2.89	+	2.77	8.04E-03
	protein transport (GO:0015031)	1215	8	2.93	+	2.73	8.76E-03
	cellular component organization (GO:0016043)	1048	6	2.53	+	2.37	4.07E-02
	proteolysis (GO:0006508)	1055	6	2.55	+	2.36	4.18E-02
	localization (GO:0051179)	2044	11	4.93	+	2.23	9.41E-03
	cellular component organization or biogenesis (GO:0071840)	1341	7	3.24	+	2.16	4.25E-02
	transport (GO:0006810)	1963	10	4.74	+	2.11	1.88E-02

(continues)

A priori candidate gene list for Dia	nuclear transport (GO:0051169)	110	2	0.3	+	6.63	3.70E-02
	metabolic process (GO:0008152)	7375	12	20.22	-	0.59	1.84E-02
	primary metabolic process (GO:0044238)	6057	8	16.61	-	0.48	8.22E-03
	protein metabolic process (GO:0019538)	2562	2	7.03	-	0.28	2.40E-02
A priori candidate gene list for Area	sulfur compound metabolic process (GO:0006790)	235	4	0.91	+	4.39	1.35E-02
A priori candidate gene list for Rate	JAK-STAT cascade (GO:0007259)	2	1	0.02	+	61.88	1.60E-02
	nitrogen utilization (GO:0019740)	6	1	0.05	+	20.63	4.73E-02
	cellular component organization or biogenesis (GO:0071840)	1341	4	10.84	-	0.37	1.50E-02
	cellular component organization (GO:0016043)	1048	2	8.47	-	0.24	8.61E-03

**Table S7. Comparisons of DAVID gene functional classification results (DAVID 6.8 Beta) based on a priori list of all the traits, traits for tubercle number, traits for tubercle diameter, traits for estimated tubercle area, traits for tubercle developmental rate.** The default medium classification stringency was applied to the gene functional classification test. If the medium stringency gave no clusters, then the low classification stringency was applied instead. Only results with  $P < 0.05$  was shown.

See the file in the link: <https://www.dropbox.com/sh/6sqmaovo4rjc4ep/AACX6EtKF78UugpDUGRhQhxna?dl=0>

**Table S8.  $-\log_{10}(P)$  value of defensive genes in this GWA study.**

See the file in the link: <https://www.dropbox.com/sh/6sqmaovo4rjc4ep/AACX6EtKF78UugpDUGRhQhxna?dl=0>

**Table S9. List of primers used in multiple qPCR and primers used in confirming the homozygosity of T-DNA lines.**

See the file in the link: <https://www.dropbox.com/sh/6sqmaovo4rjc4ep/AACX6EtKF78UugpDUGRhQhxna?dl=0>







# The role of endogenous strigolactones and their interaction with ABA during the infection process of the parasitic weed *Phelipanche ramosa* in tomato plants

**Running title:** Role of strigolactones in tomato broomrape interaction

**Authors:**

Xi Cheng<sup>1</sup>, Kristyna Flokova<sup>1,2</sup>, Harro Bouwmeester<sup>1,\*</sup>, Carolien Ruyter-Spira<sup>1\*</sup>

**Affiliations:**

1. Laboratory of Plant Physiology, Wageningen University, Droevendaalsesteeg 1, 6708 PB Wageningen, the Netherlands

2. Laboratory of Growth Regulators, Centre of the Region Haná for Biotechnological and Agricultural Research, Institute of Experimental Botany AS CR & Faculty of Science, Palacký University, Šlechtitelů 27, CZ-78371 Olomouc, Czech Republic

\* Present address: Plant hormone biology lab, Swammerdam Institute for Life Sciences, University of Amsterdam, Science Park 904, 1098 XH Amsterdam, the Netherlands

\*Correspondence: [carolien.ruyter@wur.nl](mailto:carolien.ruyter@wur.nl)

**This work has been published:** Cheng, X., Flokova, K., Bouwmeester, H., and Ruyter-Spira, C. (2017). The role of endogenous strigolactones and their interaction with ABA during the infection process of the parasitic weed *Phelipanche ramosa* in tomato plants. *Front Plant Sci* 8, 392. doi: 10.3389/fpls.2017.00392.

### Abstract

3 The root parasitic plant species *Phelipanche ramosa*, branched broomrape, causes severe damage to economically important crops such as tomato. Its seed germination is triggered by host-derived signals upon which it invades the host root. In tomato, strigolactones (SLs) are the main germination stimulants for *P. ramosa*. Therefore, the development of low SL-producing lines may be an approach to combat the parasitic weed problem. However, since SLs are also a plant hormone controlling many aspects of plant development, SL deficiency may also have an effect on post-germination stages of the infection process, during the parasite-host interaction. In this study, we show that SL-deficient tomato plants (*Solanum lycopersicum*; *SlCCD8* RNAi lines), infected with pre-germinated *P. ramosa* seeds, display an increased infection level and faster development of the parasite, which suggests a positive role for SLs in the host defense against parasitic plant invasion. Furthermore, we show that SL-deficient tomato plants lose their characteristic SL-deficient phenotype during an infection with *P. ramosa* through a reduction in the number of internodes and the number and length of secondary branches. Infection with *P. ramosa* resulted in increased levels of abscisic acid (ABA) in the leaves and roots of both wild type and SL-deficient lines. Upon parasite infection, the level of the conjugate ABA-glucose ester (ABA-GE) also increased in leaves of both wild type and SL-deficient lines and in roots of one SL-deficient line. The uninfected SL-deficient lines had a higher leaf ABA-GE level than the wild type. Despite the high levels of ABA, stomatal aperture and water loss rate were not affected by parasite infection in the SL-deficient line, while in wild type tomato stomatal aperture and water loss increased upon infection. Future studies are needed to further underpin the role that SLs play in the interaction of hosts with parasitic plants and which other plant hormones interact with the SLs during this process.

### Keywords

Root parasitic plant, strigolactone, abscisic acid, post-attachment resistance, plant architecture

## Introduction

During evolution, parasitic plants have evolved a mechanism to infect and rely on other plant species' water and nutrients for their growth and survival. The root parasitic *Phelipanche ramosa* (*P. ramosa*), poses a severe threat to several economically important crops, particularly *Solanaceae* spp. (Parker, 2009). In tomato (*Solanum lycopersicum*), for example, an infection with this parasite leads to a large reduction in fruit biomass, mesocarp thickness, fruit colour as well as changed contents of sugars and soluble solids in the fruits (Cagán and Tóth, 2003; Longo *et al.*, 2010).

The life cycle of *P. ramosa* consists of several different stages. Intriguingly, these parasites have evolved a mechanism ensuring that they only germinate within the hosts' rhizosphere. This feature is very important since they cannot survive long after germination unless they reach their hosts' root. Host-derived germination stimulants, such as strigolactones (SLs), have been described to be responsible for the induction of the germination of *P. ramosa* seeds (Bouwmeester *et al.*, 2003). After seed germination, *P. ramosa* makes physical contact with its host by developing an attachment organ, a haustorium, which facilitates the establishment of a vascular connection between the parasite and its host. As the development of the vascular connection proceeds, a swollen organ, called a tubercle, is formed on the surface of the host root, enabling the accumulation of nutrients supporting further development of the parasite seedling. In a later stage, adventitious roots and apical shoot buds are formed at the base of the tubercle. Finally, the shoots of mature parasitic plants emerge above the soil (Xie *et al.*, 2010; Cardoso *et al.*, 2011).

Several hormones that are major players in signalling networks during other plant defense responses have been demonstrated to also play a role in the host-parasite interaction. Several reports have shown that genes involved in the jasmonic acid (JA) and/or ethylene pathways are induced in the roots of *Arabidopsis* (*Arabidopsis thaliana*), medicago (*Medicago truncatula*), lotus (*Lotus japonica*) and tomato upon infection by *Orobanchae* and *Phelipanche* spp. (Dos Santos *et al.*, 2003a; Die *et al.*, 2007; Dita *et al.*, 2009; Hiraoka *et al.*, 2009; Torres-Vera *et al.*, 2016). In tomato and sunflower (*Helianthus annuus*), an infection with these parasites induced the expression of genes involved in the salicylic acid (SA) pathway (Torres-Vera *et al.*, 2016). In sunflower, a higher expression of these genes was found to be correlated with a more resistant phenotype (Letousey *et al.*, 2007). In addition, application of methyl jasmonate or methyl salicylate

to *Arabidopsis* seedlings was able to evoke an almost full defense response during an infection with *Phelipanche aegyptiaca*, reducing attachment and tubercle formation by 90% (Bar-Nun and Mayer, 2008). However, this process is complicated by hormonal conjugations (Bar-Nun and Mayer, 2008).

Also abscisic acid (ABA) seems to be involved in the host-parasite interaction, as expression of ABA biosynthetic as well as ABA-responsive genes was induced in tomato upon *P. ramosa* infection (Torres-Vera *et al.*, 2016). Proteomics showed that an abundance of ABA-responsive proteins is only detected in root extracts of an *O. crenata*-resistant pea (*Pisum sativum*) cultivar (Angeles Castillejo *et al.*, 2004), suggesting that ABA signalling is important for the plant's defense against broomrape. ABA levels in sorghum and maize have also been reported to be elevated upon infection by the hemiparasite *Striga hermonthica* (Taylor *et al.*, 1996; Frost *et al.*, 1997). This seems not true for the association between the hemiparasite *Rhinanthus minor* and its host barley (*Hordeum vulgare*), in which ABA levels were not affected (Jiang *et al.*, 2004; Jiang *et al.*, 2010).

The SLs are apocarotenoids like ABA, and are signalling molecules for parasitic plant seed germination and mycorrhizal symbiosis (Bouwmeester *et al.*, 2003; Akiyama *et al.*, 2005). Previously, it has been suggested that SLs and ABA influence each other's levels, and it was shown that a SL deficient tomato line (*SICCD8* RNAi) had reduced levels of ABA when compared with its wild type (López-Ráez *et al.*, 2010; Torres-Vera *et al.*, 2016). Biosynthesis of the SLs is partially elucidated and was shown to be catalyzed by a number of enzymes, including DWARF 27 (D27), CAROTENOID CLEAVAGE DIOXYGENASE 7 (CCD7)/MORE AXILLARY GROWTH 3 (MAX3), CAROTENOID CLEAVAGE DIOXYGENASE 8 (CCD8)/MORE AXILLARY GROWTH 4 (MAX4), MORE AXILLARY GROWTH 1 (MAX1) and the recently identified LATERAL BRANCHING OXIDOREDUCTASE (LBO) (Booker *et al.*, 2005; Lin *et al.*, 2009; Alder *et al.*, 2012; Kohlen *et al.*, 2012; Abe *et al.*, 2014; Zhang *et al.*, 2014; Brewer *et al.*, 2016). An F-box protein, MORE AXILLARY GROWTH2 (MAX2) / DWARF3 (D3), an  $\alpha/\beta$ -fold hydrolase DWARF14 (D14) and DWARF 53 (D53), have been recognized as the main players in the SL signalling pathway (Arite *et al.*, 2009; Mashiguchi *et al.*, 2009; Nelson *et al.*, 2011; Hamiaux *et al.*, 2012; Jiang *et al.*, 2013; Zhao *et al.*, 2013; Chevalier *et al.*, 2014; Kong *et al.*, 2014).

Tomato lines with reduced SL production, such as the *SL-ORT1* mutant and *SICCD8* RNAi lines, induce less *P. ramosa* germination, which results in reduced parasitic plant infection (Dor *et al.*, 2011; Kohlen *et al.*,

2012). Intriguingly, the expression of SL biosynthetic genes *MAX1*, *MAX3*, and *MAX4* is up-regulated in dodder pre-haustoria and haustoria (Ranjan *et al.*, 2014), implying that SLs may play a role in the process of parasitism. Recently, SLs have also been reported to be involved in plant defense and stress responses (Bu *et al.*, 2014; Ha *et al.*, 2014; Torres-Vera *et al.*, 2014; Liu *et al.*, 2015a). In addition, increased expression of SL biosynthetic genes *SID27* and *SICCD8* was observed in tomato roots after *P. ramosa* infection, suggesting activation of the SL biosynthetic pathway during the host-parasite interaction (Torres-Vera *et al.*, 2016).

The aim of the present study is to investigate the role of SLs during the interaction between the host and parasite, other than in germination. We demonstrate a protective role for endogenous SLs after attachment of *P. ramosa* to tomato by comparing two independent SL-deficient *SICCD8* RNAi lines with the corresponding wild type. We also observed that the parasite induced different phenotypic changes in the plant architecture of wild type and *SICCD8* RNAi lines. To explore the relation between SLs and ABA in the regulation of the host response during this parasitic infection, we analysed ABA levels, leaf water loss and stomatal features in the host. The role of SLs and the possible crosstalk with other hormones during the regulation of the defense response to parasitic plants is discussed.

### Materials & Methods

#### Tomato materials and plant growth

In this study, tomato wild type (cv. Craigella) and *SICCD8* RNAi lines (L04, L09), which have been described in a previous study (Kohlen *et al.*, 2012), were used. Tomato seeds were germinated on moistened filter paper at 25°C for 4 days in darkness. Germinated tomato seeds were selected and grown in moistened vermiculite, for 2 weeks for the rhizotron assay as described below, and for 3 weeks for the soil assay, under 12 h:12 h L: D photoperiod at 21°C in a growth chamber.

#### *Phelipanche ramosa* infection in a rhizotron system

A rhizotron system was adapted from previous studies on rice-*Striga* interactions (Gurney *et al.*, 2006; Cissoko *et al.*, 2011). The rhizotron was prepared by cutting a hole at one side of a 14.5 cm-diameter round Petri dish. The Petri dish was filled with a 1.5 cm thick piece of round rockwool, a round glass-fibre filter disc (Whatman GF/A paper), and finally a nylon

mesh on top. The rhizotron system was moistened with sterilized ½-strength Hoagland nutrient solution. Sterile seedlings were then moved to the rhizotron system by fitting the plant in the hole of the Petri dish. The leaves and shoots of the seedlings were kept outside while the roots were carefully separated and organized on top of the nylon mesh using forceps. The rhizotron system was placed in a vertical position at 21°C, 60% RH, 100  $\mu\text{mol m}^{-2} \text{s}^{-1}$  light intensity, in a 12 h:12 h L: D photoperiod and plants grown for another 2 weeks.

At the same time, *P. ramosa* seeds were sterilized with a 2% bleach solution and 5 drops of Tween20 for 5 min, and then washed with sterile demineralized water. Sterile *P. ramosa* seeds were dried and applied to a 5 cm-diameter glass-fiber filter paper (Whatman GF/A paper), which was pre-wetted with 0.8 ml sterile demineralized water and placed in 9 cm-diameter Petri dishes with a pre-wetted 1 cm-wide ring of filter paper to maintain moisture. The Petri dishes were sealed with parafilm and then kept in the dark in a growth chamber at 20°C for a 12 d pre-conditioning period. Pre-conditioned seeds were then dried and treated with 0.8 ml of a  $3.3 \times 10^{-3}$   $\mu\text{M}$  GR24 (synthetic strigolactone analog) solution for 24 hours in the dark at 25°C. GR24 treatment triggered the germination of *P. ramosa*. After 24 hours, GR24 was washed off with sterile demineralized water. The pre-germinated *P. ramosa* seeds were then spread along the roots of the 2-week old tomato seedlings in the rhizotron system using a sterile paint brush. The rhizotron Petri dishes were sealed with tape and covered with aluminum foil. The plates were then placed vertically again and the plants were grown under the same conditions as described above for another 4 weeks. Rhizotron Petri dishes were randomly placed in trays and their positions were randomized again every three days. Photos of *P. ramosa*-infested roots in the rhizotron were taken with a Canon digital camera EOS 60D DSLR (with EF-S 18-135 mm IS Lens) 15 and 32 days post inoculation (dpi).

### ***Phelipanche ramosa* infection assay in soil and host phenotype analysis**

Seeds of tomato wild type (cv. Craigella) and *SICCD8* RNAi line L09 (5 replicates) were germinated on moistened filter paper at 25°C for 4 days in darkness. Germinated seeds were moved onto moistened vermiculite for 2 weeks using a 12h:12h L: D photoperiod at 21°C, 60% RH, 100  $\mu\text{mol m}^{-2} \text{s}^{-1}$  light intensity in a growth chamber. Young tomato seedlings were carefully pulled out of the vermiculite substrate and their roots were cleaned with water. Pre-germinated *P. ramosa* seeds were applied to each tomato roots by using a paint brush (15 mg *P. ramosa* seeds per tomato plant). Tomato seedlings were then planted in a mixture of soil: vermiculite: sand (1: 1: 1) and grown at 25°C, 60% RH, 150  $\mu\text{mol m}^{-2} \text{s}^{-1}$  light intensity and 16 h:8 h L: D

photoperiod in the greenhouse. After 9 weeks, the number of above-ground emerging *P. ramosa* seedlings was counted. The branch number (primary and secondary branches) and internode number of *P. ramosa*-infected and uninfected tomato plants (wild type, the line L09 and L04) were counted. The length of tomato branches (primary and secondary branches) and each internode were also measured. Subsequently, the soil was washed off the tomato roots. The parasitic tubercles and shoots were carefully detached from the tomato roots. The weight of stem, leaves, shoots, branches and roots of *P. ramosa*-infected and uninfected wild type and L09 tomato plants, and the total weight of the parasitic plant biomass were measured.

### Measurement of stomatal aperture and conductance

Two leaves, of approximately similar age and not covered by other leaves, were collected from three plants for wild type and L09 with/without *P. ramosa* (5 biological replicates). To make stomatal imprints, vinylpolysiloxane dental resin was applied to the abaxial side of the leaf at midday by using a dispensing gun (Dispenser D2, Zhermack SpA, Italy) and removed after drying. The resin imprints were covered with transparent nail polish which was then peeled off after drying, giving a mirror image of the resin imprint. Photos of stomata were then taken of the imprints using a digital camera Nikon DIGITAL SIGHT DS-Fi1 (Nikon Instruments Inc.) and acquired with Nikon NIS-Elements software. Ten photos per leaf imprint were subjected to image analysis using the software package ImageJ. Stomatal aperture was calculated as the ratio of stomatal length to width. Stomatal conductance was measured directly in leaves of *P. ramosa*-infected and uninfected wild type and L09 plants using a leaf porometer (Decagon Devices, Inc.) in the afternoon between 14:00 and 17:00 hrs.

### Leaf dehydration assay

Four full-grown leaves with similar age from the top of the plant (without coverage by other leaves) were detached from seedlings of wild type and *SICCD8* RNAi line L09 with or without *P. ramosa* infection (5 biological replicates) from the soil infection experiment (8 weeks after infection). Collected leaves were placed in open Petri dishes on a bench in the growth chamber (at 21°C, 60% RH, 100  $\mu\text{mol m}^{-2} \text{s}^{-1}$  light intensity). Leaf weights were periodically measured at the indicated time points (0, 15, 30, 60, 90 min). Rate of leaf water loss was calculated as leaf weight loss divided by time.

### ABA measurements

Young leaves and roots were collected from wild type and L09 seedlings



with or without *P. ramosa* infection (5 biological replicates, 2 technical replicates) from the soil infection experiment. ABA levels were measured in these samples by Multiple Reaction Monitoring (MRM) using Ultra-Performance Liquid Chromatography coupled to tandem Mass Spectrometry (UPLC-MS/MS) using a published protocol (Floková *et al.*, 2014).

### Statistical analysis

Data are presented as mean  $\pm$  standard error of the mean (SEM). Statistical analysis was performed using Student's *t*-test (two-tailed) or analysis of variance (ANOVA) (GraphPad Prism version 7.00 for Windows). Differences between individual means were tested for significance using the *post hoc* Tukey's multiple comparison test. Percentages of differentiated and undifferentiated tubercles and total tubercle percentage from the rhizotron studies were transformed using arcsine square root transformation of the raw data prior to statistical analysis.

## Results

### Endogenous SLs inhibit parasitism

To assess the role of endogenous SLs on parasitic plant attachment in tomato, we studied the development and final number of *P. ramosa* tubercles using a rhizotron assay. In this assay, we compared the susceptibility of SL-deficient tomato *SICCD8* RNAi line L09 with its wild type. Because we were specifically interested in differences in parasite attachment levels that were not the result of differences in *P. ramosa* seed germination, the parasitic plant seeds were pre-germinated, using the synthetic strigolactone analog GR24, before they were applied to the tomato roots. A higher overall level of parasitic plant infection was observed in L09 seedlings when compared with its wild type at 32 dpi (**Figure 1A**,  $P < 0.05$ ). In addition to this, the percentage of differentiated tubercles (with adventitious roots) was also higher in the SL-deficient line L09 when compared to its wild type while the percentage of undifferentiated tubercles (without adventitious roots) was similar between wild type and L09 (**Figure 1A**,  $P < 0.05$ ), suggestive of a faster development of the parasite on L09.

In addition to this semi *in vitro* assay, a soil infection assay was conducted using two independent tomato *SICCD8* RNAi lines (L09 and L04) and the corresponding wild type. Also, in this experiment, the *P. ramosa* seeds were pre-germinated with GR24. Fresh weight of the attached parasites was measured after 9 weeks and was shown to be higher in both *SICCD8*

RNAi tomato lines compared with their wild type (**Figure 1B**). The combined results from both assays show that SL-deficient tomato plants are more susceptible to (pre-germinated) *P. ramosa* infection and sustain a faster development of the parasite.

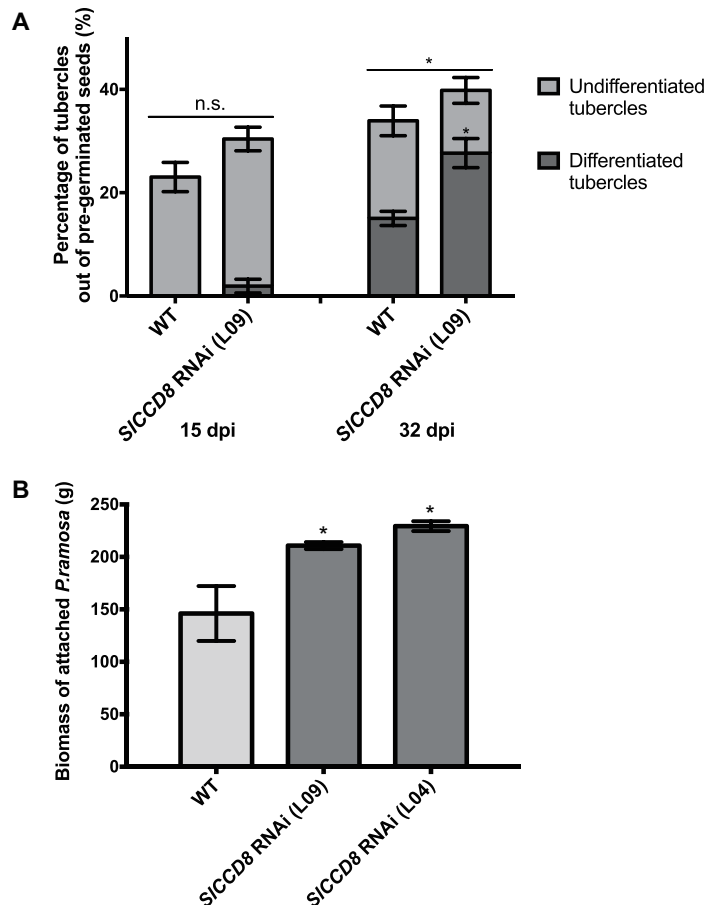


**Figure 1. Tomato strigolactone biosynthesis knock-down, *SICCD8* RNAi lines, are more susceptible to *Phelipanche ramosa* infection than wild type.** (A) Percentage of undifferentiated (in light grey color) and differentiated tubercles (in dark grey colour) (out of the total number of pre-germinated *P. ramosa* seeds applied around the host roots) that developed on wild type (WT) and *SICCD8* RNAi line L09 at 15 dpi (days post infection) and 32 dpi in the rhizotron assay. Original data was subjected to arcsine root transformation before statistical analysis. (B) Total

fresh weight (biomass) of attached parasites on tomato seedlings of WT and two *SICCD8* RNAi lines (L09 and L04) in the soil assay. Data represent the means of nine (A) or five (B) independent replicates  $\pm$  standard error (SE). Asterisks (\*) indicate statistically significant differences between WT and *SICCD8* RNAi lines (L09 and L04), respectively, according to Student's t-test. \* $P < 0.05$ .

### ***P. ramosa* infection affects tomato shoot architecture differently in WT and *SICCD8* RNAi lines**

To further explore the possible role of SLs in the host response to an infection with parasitic plants, we studied the effect of an infection with *P. ramosa* on the growth and plant architecture of the wild type and *SICCD8* RNAi tomato lines. Without infection, *SICCD8* RNAi plants (L09 and L04) displayed a more compact phenotype than the corresponding wild type, resulting from an increased number of branches and reduced plant height (**Figure 2A**). When the plants were infected with *P. ramosa* (**Figure 2A**), the shoot architecture of wild type plants became more compact due to a reduction in plant height (**Figure 2A**), while shoot branching in the *SICCD8* RNAi lines was reduced with no obvious changes in plant height (**Figure 2A**)

To further investigate the effect of a *P. ramosa* infection on plant architecture of wild type and *SICCD8* RNAi lines, parameters for shoot branching and stem growth were quantified (**Figure 2**). Compared to control conditions, the number and length of primary branches of wild type and *SICCD8* RNAi lines remained unchanged during the infection, with the exception of L04 that displayed a reduction in the length of its primary branches (**Figure 2B** and **2D**). However, the secondary branches of both *SICCD8* RNAi lines displayed a remarkable reduction in both number and length during the infection with *P. ramosa* (**Figure 2C** and **2E**,  $P < 0.001$ ). This explains the less compact appearance of the infected *SICCD8* RNAi lines observed in the pot experiment shown in **Figure 2A**. In a second pot experiment during which the *P. ramosa* infection was more severe, the same trend was observed while now also the number of primary branches of the *SICCD8* RNAi lines was reduced (data not shown). *P. ramosa* also caused a large reduction in stem length, but only in wild type plants (**Figure 2F**,  $P < 0.05$ ). This was mainly caused by a reduction in the internode length rather than a reduction in the number of internodes (**Figure 2G**, **2H**). This is consistent with the more compact and dwarf-like appearance of wild type plants upon infection with *P. ramosa* (**Figure 2A**)

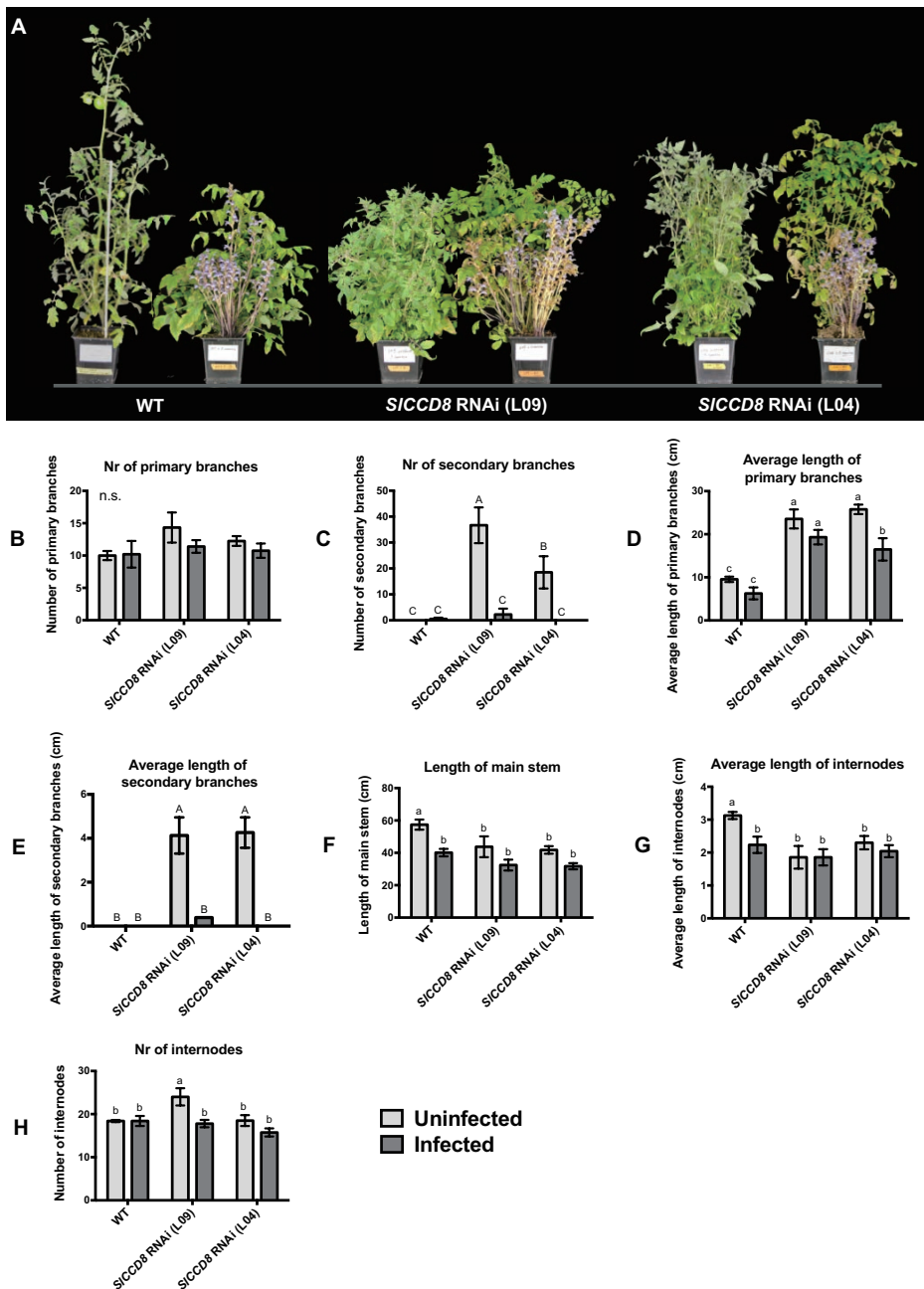


**Figure 2. Shoot architecture of wild type (WT) and *SICCD8* RNAi lines (L09 and L04) uninfected and infected with the root parasitic *Phelipanche ramosa*.** (A) Picture of the 12-week-old wild type and *SIC-*

*CD8* tomato RNAi lines, uninfected (left plant) and infected (right plant) with *P. ramosa*. (B) Number of primary branches; (C) number of secondary branches; (D) length of primary branches (cm); (E) length of secondary branches (cm); (F) length of main stem (cm); (G) average length of internode (cm); (H) number of internodes. Data represent the average of five independent replicates  $\pm$  standard error (SE). Letters (a, b, c and A, B, C) indicate statistically significant differences according to two-way ANOVA (treatment and line as factors) and Tukey's multiple comparisons tests (a, b, c;  $P < 0.05$ ; A, B, C;  $P < 0.001$ ); n.s.: no statistical significant differences for any of the comparisons in the respective graph.

3 In addition, shoot and root biomass (fresh weight) were measured in uninfected and infected wild type and the two SL deficient lines (**Figure 3**). The *P. ramosa* infection significantly reduced root biomass of wild type plants (**Figure 3B**,  $P < 0.05$ ), while shoot biomass of wild type remained unaffected (**Figure 3A**). However, the *P. ramosa* infection remarkably reduced both root and shoot biomass in both RNAi lines (although the reduction in root biomass of L04 was on the border of significance; adjusted  $P$  value = 0.069) (**Figure 3A** and **3B**). These results show that *P. ramosa* infection in wild type only reduces root biomass, while in the *SICCD8* RNAi lines both root and shoot biomass are decreased. Upon infection, both wild type and L09 displayed a reduced root-to-shoot biomass ratio (**Figure 3C**,  $P < 0.05$ ), implying that the negative effect of the infection on host root biomass is larger than the effect on shoot biomass.

In conclusion, *SICCD8* RNAi lines are more susceptible to an infection with *P. ramosa*, and show a reduction in biomass in both roots and shoots. The reduction in shoot biomass in the *SICCD8* RNAi lines is mainly caused by a reduction in the number and length of secondary shoot branches.

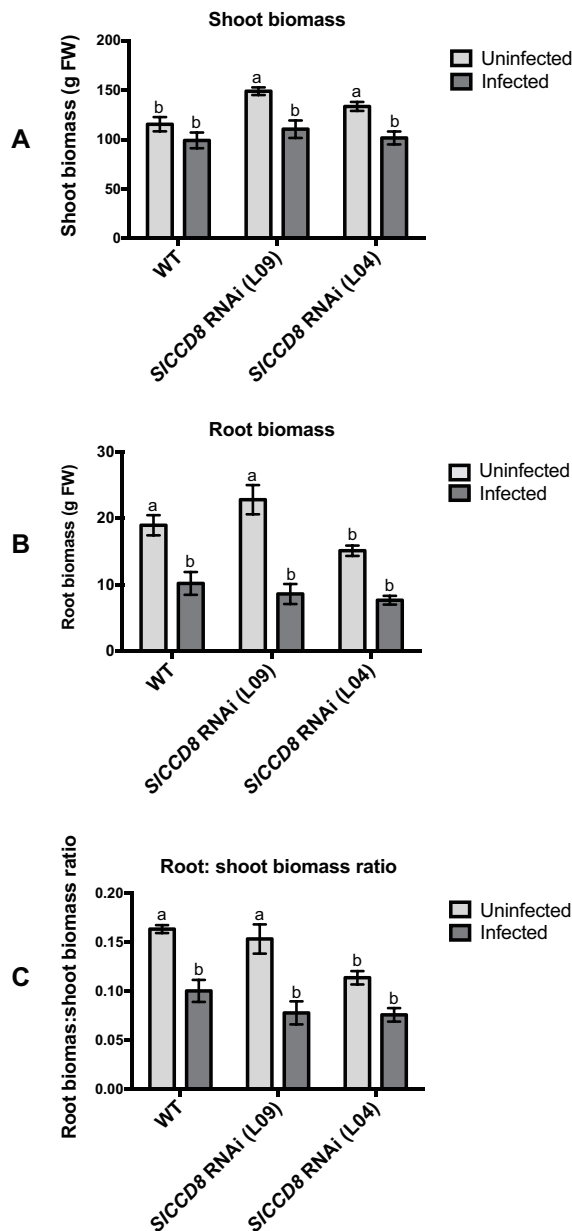


**Figure 3. Shoot biomass (A), root biomass (B) and root: shoot biomass ratio (C) of wild type (WT) and *SICCD8* RNAi lines (L09 and L04) uninfected and infected with the root parasitic plant *Phelipanche ramosa*.** Data represent the means of five independent replicates  $\pm$  standard error (SE). Letters (a, b) indicate statistically significant differences according to two-way ANOVA (treatment and line as factors)

and Tukey's multiple comparisons test ( $P < 0.05$ ).

### ***P. ramosa* infection affects ABA levels, stomata and leaf water loss**

As ABA has previously been shown to be involved in host-parasitic plant interactions (Taylor et al., 1996; Frost et al., 1997; Jiang et al., 2004a; Jiang et al., 2010), and ABA levels in the *SICCD8* RNAi line have been reported to be decreased compared to wild type (Torres-Vera et al., 2014), levels of ABA and three derived metabolites, ABA-glucosyl ester (ABA-GE), phaseic acid (PA) and dihydrophaseic acid (DPA), were measured in roots and leaves of infected and uninfected wild type and *SICCD8* RNAi lines in this study (**Figure 4**). Unexpectedly, uninfected *SICCD8* RNAi lines had similar ABA levels in roots and shoots as the uninfected wild type plants (**Figure 4A and 4B**). In response to the *P. ramosa* infection, ABA levels in these tissues increased significantly to similar levels in all lines (**Figure 4A**,  $P < 0.01$ ). As wild type and *SICCD8* RNAi lines did not remarkably differ in ABA level in the leaves and roots when they were not infected, it can be concluded that the net increase in ABA was not different between wild type and *SICCD8* RNAi lines. In contrast to ABA, the level of the major conjugate of ABA, ABA-GE, was higher in the leaves of uninfected *SICCD8* RNAi lines (L09 and L04) than in leaves of uninfected wild type plants (**Figure 4C**,  $P < 0.05$ ). Upon infection, ABA-GE levels of wild type plants and *SICCD8* RNAi lines increased to a similar level (**Figure 4C**), suggesting that *P. ramosa* infection induced a higher net increase of ABA-GE in the WT plants. Uninfected wild type and *SICCD8* RNAi lines had similar levels of ABA-GE in the roots (**Figure 4D**). Upon parasite infection, only one of the *SICCD8* RNAi lines (L09) displayed a significant increase in ABA-GE level in the roots (**Figure 4D**), suggestive of a higher net increase of ABA-GE in the line L09 upon parasite infection. Regarding ABA catabolism, uninfected wild type and *SICCD8* RNAi lines had similar levels of PA and DPA, in both leaves and roots, respectively (**Figure 4E and 4G**). Parasite infection strongly elevated the PA and DPA levels, but to a similar level in the roots of wild type and *SICCD8* RNAi lines (**Figure 4F and 4H**).

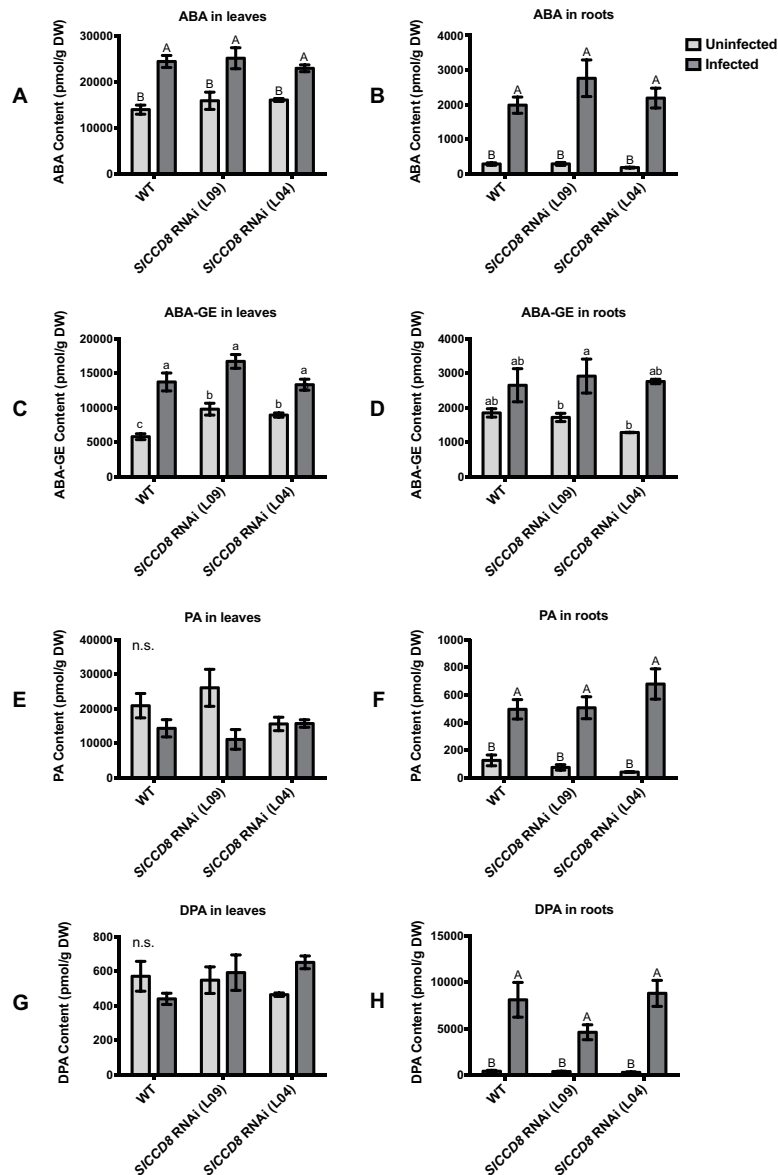


**Figure 4. Levels of abscisic acid (ABA) (A, B) and ABA metabolites (C-H) in the leaves and roots of wild type (WT) and *SICCD8* RNAi lines (L09 and L04) uninfected and infected with *Phelipanche ramosa*.** ABA metabolites measured in this study include ABA conjugate ABA-glucose ester (ABA-GE) (C-D), and two ABA degradation products phaseic acid (PA) (E-F) and dihydrophaseic acid (DPA) (G-H). Data represent the means of five independent replicates  $\pm$  standard error



(SE). Letters (a, b, c and A, B) indicate statistically significant differences according to two-way ANOVA and Tukey's multiple comparisons tests (a, b, c at the level of  $P < 0.05$ ; A, B at the level of  $P < 0.01$ ); n.s.: no significant differences for any of the comparisons in the respective graph.

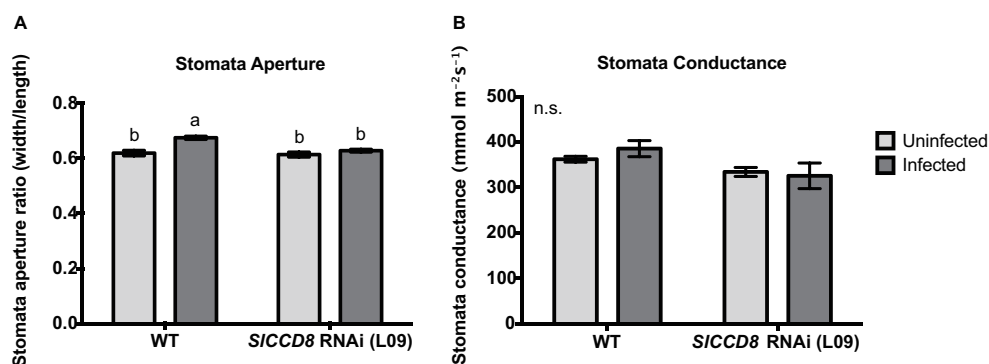


**Figure 5. Stomatal features of wild type (WT) and *SICCD8* RNAi line L09 uninfected and infected with *Phelipanche ramosa*.** Photos of stomata were taken of the leaf imprints and subjected to image analysis. (A) Stomata aperture was measured by calculating the ratio of stomatal width to length. (B) Stomatal conductance (mmol m<sup>-2</sup>s<sup>-1</sup>) was measured directly on tomato leaves by using a leaf porometer in the afternoon. Data represent the means of ten (A) and five (B) independent replicates  $\pm$  standard error (SE). Letters (a, b) indicate statistically significant differences according to two-way ANOVA and Tukey's multiple comparisons test ( $P < 0.05$ ); n.s.: no significant differences for any of the comparisons in the respective graph.

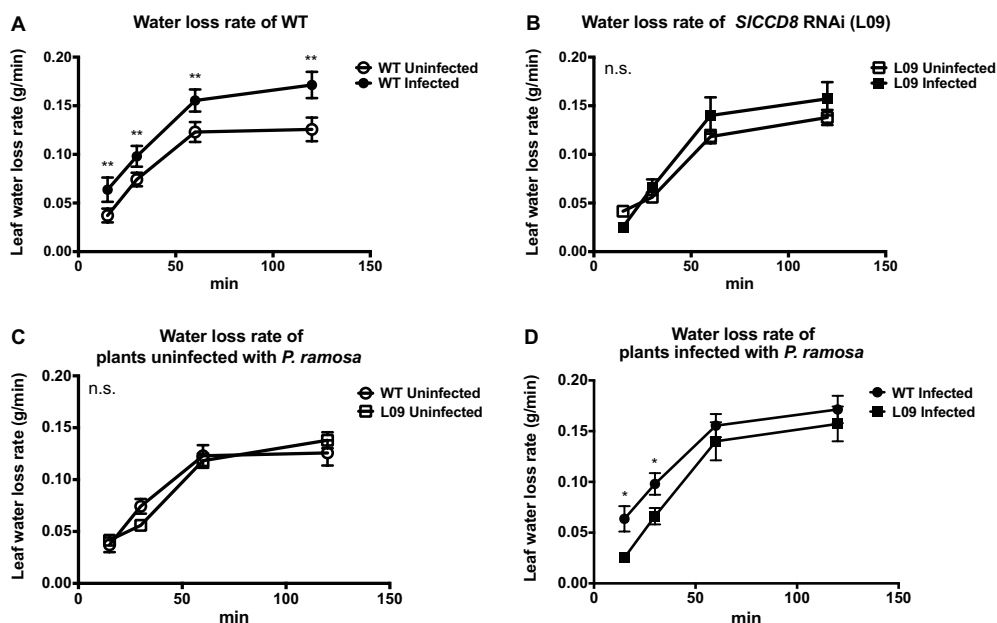


**Figure 6. Leaf water loss rate as observed in WT and *SICCD8* RNAi line L09 uninfected and infected with *Phelipanche ramosa*.** Full-expanded leaves with similar age from the top of the plant were detached from tomato plants in the soil assay (8 weeks after infection). Collected leaves were placed in open Petri dishes for a dehydration assay. Leaf weights were periodically measured at the indicated time points (0, 15, 30, 60, 90 min). Rate of leaf water loss was calculated as leaf weight loss divided by the time interval. For clarity, comparisons of leaf water loss are shown separately between (A) infected and uninfected WT; (B) infected and uninfected L09; (C) uninfected WT and L09; (D) infected WT and L09. Data represent the means of four independent replicates  $\pm$  standard error (SE). Asterisks (\*) indicate statistically significant differences based on Student's t-test performed on each two cases in (A) and (D) at each time point. \*\* $P < 0.01$ ; \* $P < 0.05$ ; n.s.: no statistical significant differences for any of the comparisons in the respective graph.

ABA regulates stomatal behavior and as a consequence water fluxes in plants. Considering the above described observation that an infection with *P. ramosa* increases ABA levels in leaves of infected plants, we also evaluated stomatal aperture, stomatal conductance and leaf water loss rate as determined by a dehydration assay. The stomatal aperture, stomatal conductance and leaf water loss rate of wild type and L09 did not statistically differ when plants were not infected with *P. ramosa* (Figures 5, 6C). Also, when wild type and L09 were infected, their stomatal conductance did not

differ nor change (**Figure 5B**). However, stomatal aperture was significantly increased by infection in wild type plants ( $P < 0.05$ ), while it was unaffected in infected L09 (**Figure 5A**). When wild type and L09 were not infected with *P. ramosa*, water loss rate of their leaves did not differ (**Figure 6C**). However, when infected with the parasite, we observed a remarkable increase in leaf water loss rate in infected wild type plants (**Figure 6A**,  $P < 0.01$ ), whereas there was no significant change in leaf water loss rate in the infected L09 plants (**Figure 6B**). During the early time points, infected wild type had a stronger leaf water loss than infected L09 (**Figure 6D**,  $P < 0.05$ ).

### Discussion

Root parasitic weeds of the Orobanchaceae family are posing a great threat to crops but are difficult to manage. Current strategies to control these weeds are not effective largely due to the fact that a substantial part of their lifecycle occurs underground. Strategies to explore resistance mechanisms against these weeds are needed. Here, we studied the effect of strigolactones on the interaction between tomato and *P. ramosa*, with specific focus on the post-attachment process of the parasitic infection and the consequences on plant architecture and aspects of water loss.

Our results show that SL deficient tomato lines display an enhanced infection and increased tubercle development rate upon inoculation with pre-germinated *P. ramosa* seeds. These results suggest that SLs play a positive role in the host defense against *P. ramosa* infection. Interestingly, it was recently reported that the expression of SL biosynthetic genes *SID27* and *SICCD8* is induced in *P. ramosa*-infected tomato roots (Torres-Vera *et al.*, 2016). The induction of the expression of *SID27* was stronger during the early stages of the infection, while the expression of *SICCD8* increased over time (Torres-Vera *et al.*, 2016). In addition, the transcription of the putative orthologue of the SL receptor, *D14*, in tomato (*SID14*) was also induced during the late stage of the infection process (Torres-Vera *et al.*, 2016). Combined with the results of the present study, this suggests that SL biosynthesis is triggered in the host plant upon infection and that SL signalling may play a role in the host defense against root parasitic plants.

One possible explanation for the high susceptibility of the *SICCD8* RNAi lines to parasite infection that was observed in the present study, may be their enhanced auxin transport capacity and altered auxin levels, as was reported for the *Arabidopsis* SL-deficient mutant *max4* (Bennett *et al.*, 2006). It was indeed shown that the tomato *SICCD8* RNAi lines have increased adventitious root formation, probably resulting from higher auxin levels in the

lower part of the stem (Kohlen *et al.*, 2012). Interestingly, it was previously shown in *Arabidopsis* that polar auxin transport directs the xylem continuity between the host root and *P. aegyptiaca* tubercles (Bar-Nun *et al.*, 2008). Perhaps the increased auxin transport capacity in *max4*, or in the present study in the *SICCD8* RNAi lines, facilitates the formation of the vascular connection between host and parasite. A higher efficiency of this process could stimulate development and shorten emergence time of the parasite. An early emergence time of *S. hermonthica* in rice resulted in shorter rice plants and reduced plant weight and was therefore negatively correlated with parasitic plant tolerance (Kaewchumnong and Price, 2008). It is of interest that the major QTL for *Striga* tolerance in the latter study was later found to co-localize with the major QTL for SL levels (Cardoso *et al.*, 2014). In both studies the same mapping population was used, and although the total number of emerged *Striga* shoots was higher on the high SL producing parent (germination was not standardized by pre-germination with GR24), the latter parent did appear to be more tolerant to an infection with *Striga*.

In addition to auxin, the recently described reduced levels of defense-related hormones JA and SA in the SL-deficient tomato *SICCD8* RNAi lines (Torres-Vera *et al.*, 2014) may also contribute to their increased susceptibility to parasite infection. Many studies have demonstrated the induction of expression of JA, SA and ethylene-dependent genes in the host (*Arabidopsis*, sunflower, tomato, Medicago) in response to an infection with *Orobancha/Phelipanche spp.* (Dos Santos *et al.*, 2003b; Letousey *et al.*, 2007; Dita *et al.*, 2009; Torres-Vera *et al.*, 2016). Further studies are still needed to reveal the possible links between SLs and (other) defence signalling pathways such as those involving JA, SA and ethylene. Moreover, these experiments should ideally be performed in a dynamic way, including different post-attachment stages, thus addressing the relative contribution of the various defence-related processes during different time windows of the infection process.

Consistent with previous reports on *O. cernua* and *S. hermonthica* (Hibberd *et al.*, 1998; Taylor and Seel, 1998), *P. ramosa* infection reduced the total biomass and plant height of its host (**Figure 2, 3**). However, unlike some other reports which showed a reduction of shoot biomass of the infected host (Barker *et al.*, 1996; Mauromicale *et al.*, 2008), total biomass of wild type plants in the present study was mainly reduced through a decrease in root biomass (**Figure 3**). This may be due to the different tomato cultivars that were used, and/or the different growing conditions. In our study, infected wild type plants displayed a more compact and dwarf-like shoot

architecture, which was caused by a decrease in internode length (**Figure 2F-2G**). Although, this phenotype resembled the SL deficient lines to some extent, the numbers of primary and secondary branches did not increase in infected wild type plants (**Figure 2B**). Total biomass of the *SICCD8* RNAi lines was also reduced upon infection (**Figure 3**). However, besides a large contribution of reduced root biomass (**Figure 3B**), the loss in biomass of *SICCD8* RNAi lines was also due to a dramatic reduction in their initially higher number of secondary branches, as well as a reduction in the length of primary and secondary branches (**Figure 2B**). The strong reduction in branching in parasitized *SICCD8* RNAi plants is likely associated with parasite-induced hormonal changes. An interesting hormone in this respect is ABA. In the present study, plant parasitism resulted in a major increase in root and shoot ABA levels of the host plant. Several reports have proposed a role for ABA in the inhibition of bud outgrowth (Suttle and Hultstrand, 1994; Emery *et al.*, 1998; Shimizu-Sato and Mori, 2001; Suttle, 2004). Moreover, reduced ABA levels were observed in the lower buds of the high branching SL signalling mutant *max2*, while ABA application in this genotype resulted in partial suppression of branch elongation (Yao and Finlayson, 2015). This would place the axillary bud outgrowth inhibiting activity of ABA downstream of SL signalling and may explain the reduction in the number of secondary branches upon parasite infection in the SL-deficient *SICCD8* RNAi tomato line observed in the present study.

Also in other studies, ABA has been considered to play a role in the interaction between the host and root parasitic plants. Increased expression of ABA biosynthetic genes and an abundance of ABA-responsive proteins were observed in tomato, pea and medicago parasitized by *P. ramosa* and *Orobancha crenata* (Angeles Castillejo *et al.*, 2004; Castillejo *et al.*, 2009; Torres-Vera *et al.*, 2016). It has been proposed that ABA biosynthesis in the host root might be triggered by local water deficiency around the haustoria (Taylor *et al.*, 1996). In the present study, we observed that both root and shoot ABA levels in wild type and *SICCD8* RNAi plants increased upon infection by the parasite to a similar extent. This ABA response can therefore not explain the observed difference in the *P. ramosa* infection level between the transgenic and WT lines. Also in uninfected plants, ABA levels in *SICCD8* RNAi and wild type plants were similar which is in contrast to a previous study, where the SL deficient line was described to have lower levels of ABA (Torres-Vera *et al.*, 2016). However, in the present study, a higher level of the ABA conjugate, ABA-GE, was observed in the leaves of uninfected *SICCD8* RNAi lines when compared with wild type, while the level of PA and DPA were similar. Cleavage of ABA-GE has been proposed as a rapid

route for ABA production in response to drought and osmotic stress (Lee *et al.*, 2006; Xu *et al.*, 2012; Liu *et al.*, 2015b). Drought and salt stress have been found to increase ABA-GE levels in the xylem in several cases (Sauter *et al.*, 2002). Whether an increased conjugation rate of ABA in SL deficient plants could contribute to their higher susceptibility to the parasite remains a question that needs further exploration.

Besides the increase in ABA levels in the host upon infection, ABA levels have also been reported to be increased in the parasitic plants themselves. For instance, *Orobanch* spp. (i.e. *Orobanch heder**ae*) accumulate high levels of ABA in their sink organs, i.e. inflorescence, which is in high demand for phloem-transported assimilates (Ihl *et al.*, 1987). Reports on the interactions between hosts (maize and sorghum) and the hemiparasite *S. hermonthica* have shown that attached *Striga* plants accumulate much more ABA than their hosts, even though *Striga* infection also leads to increased ABA levels in the infected host (Taylor *et al.*, 1996; Frost *et al.*, 1997). Detailed modelling studies performed for the association between *R. minor* and barley suggested the formation of an ABA gradient between the parasite and host, which might contribute to an increased water flow from the host into the parasite (Jiang *et al.*, 2004; Jiang *et al.*, 2010). Intriguingly, in the present study, the increase in ABA level in the host shoot upon parasite infection did not result in stomatal closure. On the contrary, in wild type tomato an increase in stomatal aperture was observed, resulting in an increased water loss rate. Interestingly, in parasitic plants such as *R. minor*, stomata remain open despite high ABA levels (Jiang *et al.*, 2004). It has been suggested that the observed accumulation of high levels of cytokinin in leaves antagonizes ABA action, resulting in ABA insensitivity of the stomata (Jiang *et al.*, 2005). It is not clear yet if this ABA insensitivity also occurs in *Orobanch*/*Phelipanche* species and whether it would influence ABA levels and/or ABA sensitivity in the host as well. It could be that in our study, the infected tomato plants also contain high levels of cytokinin, which might antagonize the effect of ABA on stomatal closure (Blackman and Davies, 1983; Tanaka *et al.*, 2006), hereby preventing stomatal closure of the parasitized host. If so, it is of interest to point out that SLs also influence cytokinin levels. SL-deficient mutants have been reported to contain reduced levels of cytokinin in xylem sap (Beveridge *et al.*, 1994; Beveridge *et al.*, 1997; Morris *et al.*, 2001; Foo *et al.*, 2007). Putative lower cytokinin levels in the SL deficient *SICCD8* RNAi tomato line that was used in the present study would explain why the stomatal aperture in infected *SICCD8* RNAi plants was lower than in infected wild type plants, while ABA levels were similar in both genotypes.



### Conclusions

In the present study, we have explored the effect of an infection with *P. ramosa* on host plant growth and architecture, its ABA and ABA metabolite profiles, stomatal conductance and water loss. Currently, there are only few reports on the role of ABA during the interaction between the host and parasitic plants, and the role of ABA in the establishment of the water flow from host to parasite is unresolved. It is vital to study the dynamics of ABA and water flow and to build a proper model for the host-parasite association. It is also of interest to explore how the parasite prevents its host from closing its stomata regardless of the elevated ABA level in the host leaves. Intriguingly, our observations suggest that SL deficiency in tomato leads to an increased infection by parasitic plants which may have implications for future strategies on how to improve parasitic plant resistance. In this respect, the emphasis should be on the development of plants with reduced SL exudation rates or a low parasitic plant germination stimulating SL profile rather than on reducing SL content/production as a whole.

### Acknowledgment

We acknowledge funding by the Dutch Technology Foundation STW (to Carolien Ruyter-Spira; grant number 10990), the Chinese Scholarship Council (CSC; to Xi Cheng) and the Netherlands Organization for Scientific Research (NWO; VICI grant, 865.06.002 to Harro Bouwmeester). We thank Yonina Hendrikse for performing the initial in vitro rhizosphere assay.

### References

- Abe, S., Sado, A., Tanaka, K., Kisugi, T., Asami, K., *et al.* (2014). Carlactone is converted to carlactonoic acid by MAX1 in *Arabidopsis* and its methyl ester can directly interact with AtD14 in vitro. *Proc Natl Acad Sci U S A* 111(50), 18084-18089.
- Akiyama, K., Matsuzaki, K., and Hayashi, H. (2005). Plant sesquiterpenes induce hyphal branching in arbuscular mycorrhizal fungi. *Nature* 435(7043), 824-827.
- Alder, A., Jamil, M., Marzorati, M., Bruno, M., Vermathen, M., *et al.* (2012). The path from  $\beta$ -carotene to carlactone, a strigolactone-like plant hormone. *Science* 335(6074), 1348-1351.
- Angeles Castillejo, M., Amiour, N., Dumas-Gaudot, E., Rubiales, D., and Jorrín, J.V. (2004). A proteomic approach to studying plant response to crenate broomrape (*Orobanche crenata*) in pea (*Pisum sativum*). *Phytochemistry* 65(12), 1817-1828.
- Arite, T., Umehara, M., Ishikawa, S., Hanada, A., Maekawa, M., *et al.* (2009). *d14*, a strigolactone-insensitive mutant of rice, shows an accelerated outgrowth of tillers. *Plant*

*Cell Physiol* 50(8), 1416-1424.

- Bar-Nun, N., and Mayer, A.M.** (2008). Methyl jasmonate and methyl salicylate, but not cisjasmonate, evoke defenses against infection of *Arabidopsis thaliana* by *Orobanche aegyptiaca*. *Weed Biol Manage* 8(2), 91-96.
- Bar-Nun, N., Sachs, T., and Mayer, A.M.** (2008). A role for IAA in the infection of *Arabidopsis thaliana* by *Orobanche aegyptiaca*. *Ann Bot* 101(2), 261-265.
- Barker, E.R., Press, M.C., Scholes, J.D., and Quick, W.P.** (1996). Interactions between the parasitic angiosperm *Orobanche aegyptiaca* and its tomato host: growth and biomass allocation. *New Phytol* 133(4), 637-642.
- Bennett, T., Sieberer, T., Willett, B., Booker, J., Luschnig, C., et al.** (2006). The *Arabidopsis* MAX pathway controls shoot branching by regulating auxin transport. *Curr Biol* 16(6), 553-563.
- Beveridge, C.A., Ross, J.J., and Murfet, I.C.** (1994). Branching mutant *rms-2* in *pisum sativum* (grafting studies and endogenous indole-3-acetic acid levels). *Plant Physiol* 104(3), 953-959.
- Beveridge, C.A., Symons, C.M., Murfet, I.C., Ross, J.J., and Rameau, C.** (1997). The *rms1* mutant of pea has elevated indole-3-acetic acid levels and reduced root-sap zeatin riboside content but increased branching controlled by graft-transmissible signal(s). *Plant Physiol* 115(3), 1251-1258.
- Blackman, P.G., and Davies, W.J.** (1983). The effects of cytokinins and ABA on stomatal behaviour of maize and *Commelina*. *J Exp Bot* 34(12), 1619-1626.
- Booker, J., Sieberer, T., Wright, W., Williamson, L., Willett, B., et al.** (2005). *MAX1* encodes a cytochrome P450 family member that acts downstream of *MAX3/4* to produce a carotenoid-derived branch-inhibiting hormone. *Dev Cell* 8(3), 443-449.
- Bouwmeester, H.J., Matusova, R., Zhongkui, S., and Beale, M.H.** (2003). Secondary metabolite signalling in host-parasitic plant interactions. *Curr Opin Plant Biol* 6(4), 358-364.
- Brewer, P.B., Yoneyama, K., Filardo, F., Meyers, E., Scaffidi, A., et al.** (2016). *LATERAL BRANCHING OXIDOREDUCTASE* acts in the final stages of strigolactone biosynthesis in *Arabidopsis*. *Proc Natl Acad Sci U S A* 113(22), 6301-6306.
- Bu, Q., Lv, T., Shen, H., Luong, P., Wang, J., et al.** (2014). Regulation of drought tolerance by the F-box protein MAX2 in *Arabidopsis*. *Plant Physiol* 164(1), 424-439.
- Cagán, L., and Tóth, P.** (2003). A decrease in tomato yield caused by branched broomrape (*Orobanche ramosa*) parasitization. *Acta Fytotechnica et Zootechnica*, 65-68.
- Cardoso, C., Ruyter-Spira, C., and Bouwmeester, H.J.** (2011). Strigolactones and root infestation by plant-parasitic *Striga*, *Orobanche* and *Phelipanche* spp. *Plant Sci* 180(3), 414-420.
- Cardoso, C., Zhang, Y., Jamil, M., Hepworth, J., Charnikhova, T., et al.** (2014). Natural variation of rice strigolactone biosynthesis is associated with the deletion of two MAX1 orthologs. *Proc Natl Acad Sci U S A* 111(6), 2379-2384.
- Castillejo, M.A., Maldonado, A.M., Dumas-Gaudot, E., Fernandez-Aparicio, M., Susin,**



- R., et al.** (2009). Differential expression proteomics to investigate responses and resistance to *Orobanche crenata* in *Medicago truncatula*. *BMC Genomics* 10(1), 294.
- Chevalier, F., Nieminen, K., Sánchez-Ferrero, J.C., Rodríguez, M.L., Chagoyen, M., et al.** (2014). Strigolactone promotes degradation of DWARF14, an  $\alpha/\beta$  hydrolase essential for strigolactone signaling in *Arabidopsis*. *Plant Cell* 26(3), 1134-1150.
- Cissoko, M., Boissard, A., Rodenburg, J., Press, M.C., and Scholes, J.D.** (2011). New Rice for Africa (NERICA) cultivars exhibit different levels of post-attachment resistance against the parasitic weeds *Striga hermonthica* and *Striga asiatica*. *New Phytol* 192(4), 952-963.
- Die, J.V., Dita, M.A., Krajinski, F., González Verdejo, C.I., Rubiales, D., et al.** (2007). Identification by suppression subtractive hybridization and expression analysis of *Medicago truncatula* putative defence genes in response to *Orobanche crenata* parasitization. *Physiol Mol Plant Pathol* 70(1-3), 49-59.
- Dita, M.A., Die, J.V., Román, B., Krajinski, F., Küster, H., et al.** (2009). Gene expression profiling of *Medicago truncatula* roots in response to the parasitic plant *Orobanche crenata*. *Weed Res* 49, 66-80.
- Dor, E., Yoneyama, K., Wininger, S., Kapulnik, Y., Yoneyama, K., et al.** (2011). Strigolactone deficiency confers resistance in tomato line *SL-ORT1* to the parasitic weeds *Phelipanche* and *Orobanche* spp. *Phytopathology* 101(2), 213-222.
- Dos Santos, C.V., Delavault, P., Letousey, P., and Thalouarn, P.** (2003a). Identification by suppression subtractive hybridization and expression analysis of *Arabidopsis thaliana* putative defence genes during *Orobanche ramosa* infection. *Physiol Mol Plant Pathol* 62(5), 297-303.
- Dos Santos, C.V., Letousey, P., Delavault, P., and Thalouarn, P.** (2003b). Defense gene expression analysis of *Arabidopsis thaliana* parasitized by *Orobanche ramosa*. *Phytopathology* 93(4), 451-457.
- Emery, R.J.N., Longnecker, N.E., and Atkins, C.A.** (1998). Branch development in *Lupinus angustifolius* L. II. Relationship with endogenous ABA, IAA and cytokinins in axillary and main stem buds. *J Exp Bot* 49(320), 555-562.
- Floková, K., Tarkowská, D., Miersch, O., Strnad, M., Wasternack, C., et al.** (2014). UH-PLC-MS/MS based target profiling of stress-induced phytohormones. *Phytochemistry* 105, 147-157.
- Foo, E., Morris, S.E., Parmenter, K., Young, N., Wang, H., et al.** (2007). Feedback regulation of xylem cytokinin content is conserved in pea and *Arabidopsis*. *Plant Physiol* 143(3), 1418-1428.
- Frost, D.L., Gurney, A.L., Press, M.C., and Scholes, J.D.** (1997). *Striga hermonthica* reduces photosynthesis in sorghum: the importance of stomatal limitations and a potential role for ABA? *Plant Cell Environ* 20(4), 483-492.
- Gurney, A.L., Slate, J., Press, M.C., and Scholes, J.D.** (2006). A novel form of resistance in rice to the angiosperm parasite *Striga hermonthica*. *New Phytol* 169(1), 199-208.
- Ha, C.V., Leyva-González, M.A., Osakabe, Y., Tran, U.T., Nishiyama, R., et al.** (2014). Positive regulatory role of strigolactone in plant responses to drought and salt stress.

*Proc Natl Acad Sci U S A* 111(2), 851-856.

- Hamiaux, C., Drummond, R.S., Janssen, B.J., Ledger, S.E., Cooney, J.M., et al.** (2012). DAD2 is an alpha/beta hydrolase likely to be involved in the perception of the plant branching hormone, strigolactone. *Curr Biol* 22(21), 2032-2036.
- Hibberd, J.M., Quick, W.P., Press, M.C., and Scholes, J.D.** (1998). Can source-sink relations explain responses of tobacco to infection by the root holoparasitic angiosperm *Orobancha cernua*? *Plant Cell Environ* 21(3), 333-340.
- Hiraoka, Y., Ueda, H., and Sugimoto, Y.** (2009). Molecular responses of *Lotus japonicus* to parasitism by the compatible species *Orobancha aegyptiaca* and the incompatible species *Striga hermonthica*. *J Exp Bot* 60(2), 641-650.
- Ihl, B., Jacob, F., Meyer, A., and Sembdner, G.** (1987). Investigations on the endogenous levels of abscisic acid in a range of parasitic phanerogams. *J Plant Growth Regul* 5(4), 191-205.
- Jiang, F., Jeschke, W.D., and Hartung, W.** (2004). Absciscic acid (ABA) flows from *Hordeum vulgare* to the hemiparasite *Rhinanthus minor* and the influence of infection on host and parasite abscisic acid relations. *J Exp Bot* 55(406), 2323-2329.
- Jiang, F., Jeschke, W.D., Hartung, W., and Cameron, D.D.** (2010). Interactions between *Rhinanthus minor* and its hosts: a review of water, mineral nutrient and hormone flows and exchanges in the hemiparasitic association. *Folia Geobotanica* 45(4), 369-385.
- Jiang, F., Veselova, S., Veselov, D., Kudoyarova, G., Jeschke, W.D., et al.** (2005). Cytokinin flows from *Hordeum vulgare* to the hemiparasite *Rhinanthus minor* and the influence of infection on host and parasite cytokinins relations. *Functional Plant Biol* 32(7), 619.
- Jiang, L., Liu, X., Xiong, G., Liu, H., Chen, F., et al.** (2013). DWARF 53 acts as a repressor of strigolactone signalling in rice. *Nature* 504(7480), 401-405.
- Kaewchumngong, K., and Price, A.H.** (2008). A study on the susceptibility of rice cultivars to *Striga hermonthica* and mapping of *Striga* tolerance quantitative trait loci in rice. *New Phytol* 180(1), 206-216.
- Kohlen, W., Charnikhova, T., Lammers, M., Pollina, T., Tóth, P., et al.** (2012). The tomato *CAROTENOID CLEAVAGE DIOXYGENASE8 (SICCD8)* regulates rhizosphere signaling, plant architecture and affects reproductive development through strigolactone biosynthesis. *New Phytol* 196(2), 535-547.
- Kong, X., Zhang, M., and Ding, Z.** (2014). D53: the missing link in strigolactone signaling. *Mol Plant* 7(5), 761-763.
- Lee, K.H., Piao, H.L., Kim, H.Y., Choi, S.M., Jiang, F., et al.** (2006). Activation of glucosidase via stress-induced polymerization rapidly increases active pools of abscisic acid. *Cell* 126(6), 1109-1120.
- Letousey, P., De Zélicourt, A., Vieira Dos Santos, C., Thoiron, S., Monteau, F., et al.** (2007). Molecular analysis of resistance mechanisms to *Orobancha cumana* in sunflower. *Plant Pathol* 56(3), 536-546.
- Lin, H., Wang, R., Qian, Q., Yan, M., Meng, X., et al.** (2009). DWARF27, an iron-containing protein required for the biosynthesis of strigolactones, regulates rice tiller bud

outgrowth. *Plant Cell* 21(5), 1512-1525.

- Liu, J., He, H., Vitali, M., Visentin, I., Charnikhova, T., et al.** (2015a). Osmotic stress represses strigolactone biosynthesis in *Lotus japonicus* roots: exploring the interaction between strigolactones and ABA under abiotic stress. *Planta* 241(6), 1435-1451.
- Liu, Z., Yan, J.P., Li, D.K., Luo, Q., Yan, Q., et al.** (2015b). UDP-glucosyltransferase71c5, a major glucosyltransferase, mediates abscisic acid homeostasis in *Arabidopsis*. *Plant Physiol* 167(4), 1659-1670.
- Longo, A.M.G., Lo Monaco, A., and Mauromicale, G.** (2010). The effect of *Phelipanche ramosa* infection on the quality of tomato fruit. *Weed Res* 50(1), 58-66.
- López-Ráez, J.A., Kohlen, W., Charnikhova, T., Mulder, P., Undas, A.K., et al.** (2010). Does abscisic acid affect strigolactone biosynthesis? *New Phytol* 187(2), 343-354.
- Mashiguchi, K., Sasaki, E., Shimada, Y., Nagae, M., Ueno, K., et al.** (2009). Feed-back-regulation of strigolactone biosynthetic genes and strigolactone-regulated genes in *Arabidopsis*. *Biosci Biotechnol Biochem* 73(11), 2460-2465.
- Mauromicale, G., Monaco, A.L., and Longo, A.M.G.** (2008). Effect of branched broomrape (*Orobancha ramosa*) infection on the growth and photosynthesis of tomato. *Weed Sci* 56(4), 574-581.
- Morris, S.E., Turnbull, C.G., Murfet, I.C., and Beveridge, C.A.** (2001). Mutational analysis of branching in pea. Evidence that *Rms1* and *Rms5* regulate the same novel signal. *Plant Physiol* 126(3), 1205-1213.
- Nelson, D.C., Scaffidi, A., Dun, E.A., Waters, M.T., Flematti, G.R., et al.** (2011). F-box protein MAX2 has dual roles in karrikin and strigolactone signaling in *Arabidopsis thaliana*. *Proc Natl Acad Sci U S A* 108(21), 8897-8902.
- Parker, C.** (2009). Observations on the current status of *Orobancha* and *Striga* problems worldwide. *Pest Manag Sci* 65(5), 453-459.
- Ranjan, A., Ichihashi, Y., Farhi, M., Zumstein, K., Townsley, B., et al.** (2014). De novo assembly and characterization of the transcriptome of the parasitic weed dodder identifies genes associated with plant parasitism. *Plant Physiol* 166(3), 1186-1199.
- Sauter, A., Dietz, K.J., and Hartung, W.** (2002). A possible stress physiological role of abscisic acid conjugates in root-to-shoot signalling. *Plant Cell Environ* 25(2), 223-228.
- Shimizu-Sato, S., and Mori, H.** (2001). Control of outgrowth and dormancy in axillary buds. *Plant Physiol* 127(4), 1405-1413.
- Suttle, J.C.** (2004). Physiological regulation of potato tuber dormancy. *Am J Potato Res* 81(4), 253-262.
- Suttle, J.C., and Hultstrand, J.F.** (1994). Role of endogenous abscisic acid in potato micro-tuber dormancy. *Plant Physiol* 105(3), 891-896.
- Tanaka, Y., Sano, T., Tamaoki, M., Nakajima, N., Kondo, N., et al.** (2006). Cytokinin and auxin inhibit abscisic acid-induced stomatal closure by enhancing ethylene production in *Arabidopsis*. *J Exp Bot* 57(10), 2259-2266.
- Taylor, A., Martin, J., and Seel, W.E.** (1996). Physiology of the parasitic association between maize and witchweed (*Striga hermonthica*): is ABA involved? *J Exp Bot* 47(8),

1057-1065.

- Taylor, A., and Seel, W.E.** (1998). Do *Striga hermonthica*-induced changes in soil matrix potential cause the reduction in stomatal conductance and growth of infected maize plants? *New Phytol* 138(1), 67-73.
- Torres-Vera, R., García, J.M., Pozo, M.J., and López-Ráez, J.A.** (2014). Do strigolactones contribute to plant defence? *Mol Plant Pathol* 15(2), 211-216.
- Torres-Vera, R., García, J.M., Pozo, M.J., and López-Ráez, J.A.** (2016). Expression of molecular markers associated to defense signaling pathways and strigolactone biosynthesis during the early interaction tomato-*Phelipanche ramosa*. *Physiol Mol Plant Pathol* 94, 100-107.
- Xie, X., Yoneyama, K., and Yoneyama, K.** (2010). The strigolactone story. *Ann Rev Phytopathol* 48(1), 93-117.
- Xu, Z.Y., Lee, K.H., Dong, T., Jeong, J.C., Jin, J.B., et al.** (2012). A vacuolar beta-glucosidase homolog that possesses glucose-conjugated abscisic acid hydrolyzing activity plays an important role in osmotic stress responses in *Arabidopsis*. *Plant Cell* 24(5), 2184-2199.
- Yao, C., and Finlayson, S.A.** (2015). Abscisic acid is a general negative regulator of *Arabidopsis* axillary bud growth. *Plant Physiol* 169(1), 611-626.
- Zhang, Y., van Dijk, A.D., Scaffidi, A., Flematti, G.R., Hofmann, M., et al.** (2014). Rice cytochrome P450 MAX1 homologs catalyze distinct steps in strigolactone biosynthesis. *Nat Chem Biol* 10(12), 1028-1033.
- Zhao, L.H., Zhou, X.E., Wu, Z.S., Yi, W., Xu, Y., et al.** (2013). Crystal structures of two phytohormone signal-transducing alpha/beta hydrolases: karrikin-signaling KAI2 and strigolactone-signaling DWARF14. *Cell Res* 23(3), 436-439.



## The interaction between strigolactones and other plant hormones in the regulation of plant development

---

**Authors:**

Xi Cheng, Carolien Ruyter-Spira, Harro Bouwmeester<sup>\*, \*</sup>

**Affiliations:**

Laboratory of Plant Physiology, Wageningen University, Droevendaalsesteeg 1, 6708 PB Wageningen, the Netherlands

<sup>\*</sup> Present address: Plant hormone biology lab, Swammerdam Institute for Life Sciences, University of Amsterdam, Science Park 904, 1098 XH Amsterdam, the Netherlands

<sup>\*</sup> Correspondence: [h.j.bouwmeester@uva.nl](mailto:h.j.bouwmeester@uva.nl), tel. +31 620387674

**This work has been published:**

Cheng, X., Ruyter-Spira, C., and Bouwmeester, H. (2013). The interaction between strigolactones and other plant hormones in the regulation of plant development. *Front Plant Sci* 4, 199.

### Abstract

Plant hormones are small molecules derived from various metabolic pathways and are important regulators of plant development. The most recently discovered phytohormone class comprises the carotenoid-derived strigolactones (SLs). For a long time, these compounds were only known to be secreted into the rhizosphere where they act as signalling compounds, but now we know they are also active as endogenous plant hormones and they have been in the spotlight ever since. The initial discovery that SLs are involved in the inhibition of axillary bud outgrowth, initiated a multitude of other studies showing that SLs also play a role in defining root architecture, secondary growth, hypocotyl elongation and seed germination, mostly in interaction with other hormones. Their coordinated action enables the plant to respond in an appropriate manner to environmental factors such as temperature, shading, day length and nutrient availability. Here, we will review the current knowledge on the crosstalk between SLs and other plant hormones – such as auxin, cytokinin, abscisic acid, ethylene and gibberellins – during different physiological processes. We will furthermore take a bird's eye view of how this hormonal crosstalk enables plants to respond to their ever-changing environments.

### Key words

strigolactone, auxin, cytokinin, ethylene, gibberellins, hormone crosstalk, root and shoot architecture, phenotypic plasticity

## 1. Introduction

Plant hormones are small molecules derived from various essential metabolic pathways. They play critical roles during all developmental stages in plants, from early embryogenesis to senescence. Research on plant hormones started as early as the beginning of the last century and has resulted in the discovery of auxins, ethylene (ET), cytokinins (CK), gibberellins (GA), abscisic acid (ABA), brassinosteroids (BRs), jasmonic acid (JA), salicylic acid (SA) and the recently identified strigolactones (SLs). The biosynthetic pathways of these plant hormones have been mostly elucidated, with some minor exceptions, such as some missing steps in SL biosynthesis. Generally, plant hormones exert their effect locally at or near the site of biosynthesis or are mobile between different tissues. The mechanisms of hormone crosstalk can be diverse. Hormone signalling pathways are known to interact at the level of gene expression. A common crosstalk strategy is to control specific key components of signalling pathways of other hormones (Santer *et al.*, 2009). In this way, hormones might regulate synthesis (hormone levels), sensitivity (hormone response) and transport (hormone distributions) of other hormones.

During the last decade, we have witnessed remarkable breakthroughs in plant hormone research, especially with the discovery of the SLs. With this discovery, plant scientists not only got a new tool to study hormonal regulation of plant development but were also triggered to critically assess existing hypotheses on hormone crosstalk mechanisms. SLs were known as host-derived germination stimulants for root parasitic plants such as the witchweeds (*Striga* spp.) and broomrapes (*Orobanche* and *Phelipanche* spp.) since the sixties of last century (Bouwmeester *et al.*, 2003). Their function, as allelochemicals in symbiosis with arbuscular mycorrhizal (AM) fungi, was discovered only recently (Akiyama *et al.*, 2005). SLs promote the establishment of mycorrhizal symbiosis which mainly facilitates the phosphate acquisition from the soil. Later, SLs were found to play a key role in shoot branching inhibition and thus were identified as a new group of plant hormones (Gomez-Roldan *et al.*, 2008; Umehara *et al.*, 2008). Their biological functions were further explored and it was discovered that they also exert their effects on different developmental processes including root development, seed germination, hypocotyl elongation and secondary growth. Their conserved functions between different plant species are indicative of their indispensability in regulating plant development.

This review will focus on the current knowledge on the SLs and their



hormonal crosstalk with other plant hormones such as auxin, CK, ABA, ET and GA during bud outgrowth, root development, secondary growth and seeds germination. We will furthermore take a bird's eye view of how this hormonal crosstalk enables the plant to respond to its ever-changing environment, including shade and nutrient deprivation.

### 2. SL biosynthesis and perception

So far, at least 15 SLs have been structurally identified. They are typically composed of four rings (A-D). The A and B rings vary due to different side groups, while the C and D rings are highly conserved and seem to play an essential role in biological activity (Xie *et al.*, 2010). Like ABA, SLs are also derived from the carotenoid pathway from which they are hypothesised to diverge at  $\beta$ -carotene (Matusova *et al.*, 2005; Lopez-Raez *et al.*, 2008; Rani *et al.*, 2008) (see **Figure 1**). Interestingly, especially considering their common biosynthetic origin, a correlation between ABA levels and SLs production was observed in the ABA mutants *notabilis*, *sitiens* and *flacca* and in plants treated with AbaminSG, an inhibitor of the ABA biosynthetic enzyme 9-*cis*-epoxycarotenoid dioxygenase (NCED). It was suggested that ABA may regulate SL biosynthesis (Lopez-Raez *et al.*, 2010).

Several mutants with increased shoot branching phenotype have been identified in several plant species, including *more axillary growth* (*max*) in *Arabidopsis* (*Arabidopsis thaliana*), *ramosus* (*rms*) in pea (*Pisum sativum*), *dwarf* (*d*) or *high-tillering dwarf* (*htd*) in rice (*Oryza sativa*) and *decreased apical dominance* (*dad*) in petunia (*Petunia hybrida*). All these mutants are defective in strigolactone biosynthesis or signalling. They form the basis for the discovery of genes involved in the SL biosynthetic and downstream signalling pathways. Key catalytic enzymes in the SL biosynthetic pathway include DWARF27 (D27) (Lin *et al.*, 2009; Waters *et al.*, 2012a), CAROTENOID CLEAVAGE DIOXYGENASE 7 and 8 (CCD7 and CCD8), and MAX1 (Booker *et al.*, 2005; Kohlen *et al.*, 2011) (see **Figure1**). CCD7 and CCD8 are respectively encoded by the genes *MAX3/RMS5/D17(HTD1)/DAD3* (Morris *et al.*, 2001; Booker *et al.*, 2004; Zou *et al.*, 2006; Drummond *et al.*, 2009) and *MAX4/RMS1/D10/DAD1* (Foo *et al.*, 2001; Sorefan *et al.*, 2003; Snowden *et al.*, 2005; Arite *et al.*, 2007). Both the F-box protein MAX2/RMS4/D3 (Stirnberg *et al.*, 2007; Yoshida *et al.*, 2012) and the  $\alpha/\beta$ -fold hydrolase D14/D88/HTD2/DAD2 (Arite *et al.*, 2009; Liu *et al.*, 2009; Gaiji *et al.*, 2012; Hamiaux *et al.*, 2012) have been shown to be involved in SL downstream signalling. More aspects about SLs biosynthesis, perception and signalling as well as structure-function relationships have been nicely

addressed and updated in several recent reviews (Janssen and Snowden, 2012; Ruyter-Spira *et al.*, 2013; Zwanenburg and Pospisil, 2013).

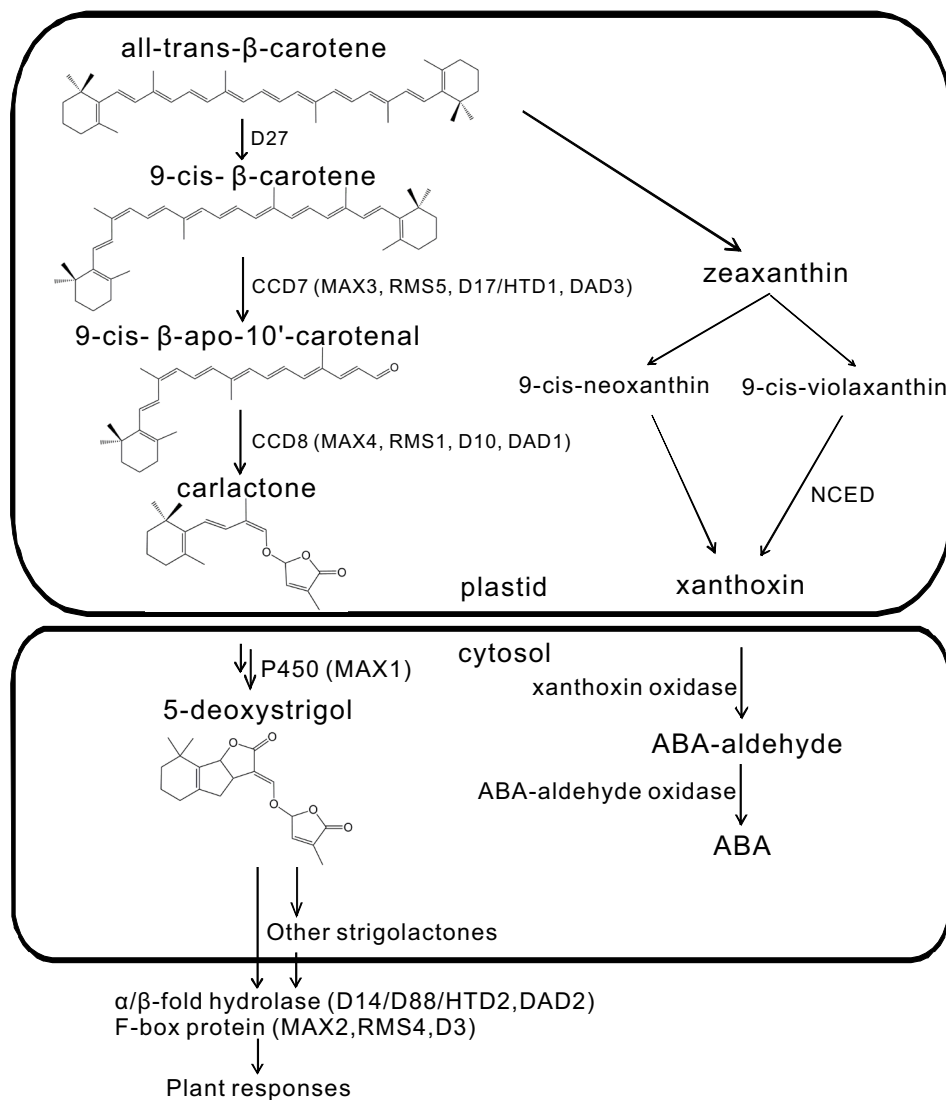


**Figure 1. Strigolactone and ABA biosynthetic pathways share a common origin at  $\beta$ -carotene.** Adapted and modified from Ruyter-Spira *et al.* 2013.

### 3. Interactions between auxin, SLs and cytolinin in the control of bud outgrowth.

Auxin plays a crucial role in the regulation of bud outgrowth. Auxin is produced mostly in the shoot apex and young leaves (Ljung *et al.*, 2001) and is transported basipetally towards the root apex in the stem through the polar auxin transport (PAT) stream (Petrasek and Friml, 2009) (**Figure 2A-D**). The PINFORMED (PIN) proteins, a family of plasma membrane auxin efflux carriers, determine the direction of this PAT stream. The PINs export auxin out of the cell across the cell membrane into the apoplast from where it is taken up by the next cell after which the whole process is repeated (Galweiler *et al.*, 1998; Wisniewska *et al.*, 2006).

Based on the pioneering work of Sachs (Sachs, 1968), one hypothesis concerning the regulation of bud outgrowth (canalization-based model) proposes that an initial auxin flux from an auxin source (shoot apex or buds) to an auxin sink (root) is gradually canalized into cell files with a large amount of PINs. These cell files will subsequently differentiate into vascular tissue through which auxin will be transported (Sachs, 1981; Domagalska and Leyser, 2011). Auxin export from buds is correlated with the initiation of bud outgrowth and therefore it is believed that buds need to export auxin in order to be activated (reviewed by Muller and Leyser (2011)). In this model, all buds compete for the release of their auxin into the common main PAT stream in the stem. Auxin exported from active buds (auxin source) reduces the auxin sink strength of the PAT stream in the stem and inhibits other buds from auxin export into the PAT stream (Sachs, 1981; Domagalska and Leyser, 2011). In pea, it was indeed observed that active axillary buds of decapitated stems rapidly triggered PIN1 polarization thus enabling directional auxin export from the buds (Balla *et al.*, 2011). Auxin application on the apex of the decapitated stem inhibited this PIN polarization and also prevented the canalization of laterally applied auxin (simulated as the secondary auxin source) (Balla *et al.*, 2011).

SLs can inhibit shoot branching via its regulation on auxin transport. In *Arabidopsis*, *max* mutants (*max1*, *max2*, *max3*, *max4*) shown increased transcript levels of the *PIN1/3/4/6* genes and an increased auxin transport capacity in the primary stem when compared to wild type plants (Bennett *et al.*, 2006). Treatment with N-1-naphthylphthalamic acid (NPA), an auxin transport inhibitor, led to a remarkable inhibition of bud outgrowth in *max* mutants in *Arabidopsis* and *dwarf* mutants in rice (Ishikawa *et al.*, 2005; Bennett *et al.*, 2006; Arite *et al.*, 2007; Lin *et al.*, 2009). Basal application of the synthet-

ic SL GR24 reduced basipetal auxin transport and PIN1 accumulation in the plasma membrane of xylem parenchyma cells in wild type and biosynthetic *max* mutants but not in *max2* (Crawford *et al.*, 2010). These results suggest that SLs dampen the PAT stream in a *MAX2*-dependent manner (Crawford *et al.*, 2010).

To understand how SLs regulate auxin transport, Leyser's group performed a computer modeling study, in which different processes affecting PAT were simulated. The results from this study suggested that SLs may modulate PIN cycling between the plasma membrane and endosomes (Prusinkiewicz *et al.*, 2009). More recent computer modeling work provided additional support for the canalization-based model for shoot branching control (Shinohara *et al.*, 2013). In this study, the relationship between PIN1 accumulation, auxin transport and shoot branching was explored in three *Arabidopsis* mutants that show excessive shoot branching: *max2*, *gnom* (*gn*) and *transport inhibitor resistant3* (*tir3*) (Shinohara *et al.*, 2013). Although all three mutants are highly branched, *max2* plants show high PIN1-GFP levels at the basal plasma membrane of stem parenchyma cells, accompanied by a high PAT capacity, while *tir3* and *gn* mutants show the opposite due to low PIN1 insertion rates at their plasma membranes (Shinohara *et al.*, 2013). SL action was simulated to increase the PIN1 removal rate from the plasma membrane in these three excessive shoot branching mutants (Shinohara *et al.*, 2013). Interestingly, the model predicted that, different concentrations of GR24 treatment can either inhibit or stimulate shoot branching, depending on the auxin transport status and concentration of the treated plant (Shinohara *et al.*, 2013). This was confirmed to occur in *tir3*, in which a low concentration of GR24 promoted shoot branching (10 nM) while a higher GR24 concentration (0.1 to 1  $\mu$ M) reduced branching (Shinohara *et al.*, 2013). An explanation for this (maybe unexpected) induced shoot branching resulting from GR24 application is that, assuming that SLs systemically remove PIN1 from plasma membranes, auxin transport capacity is also systemically reduced. A slight reduction in auxin transport in tissue through which auxin is exported from the buds, would still allow bud outgrowth. However, due to this slight decrease, more buds can simultaneously participate in this auxin export process, hereby increasing the number of shoot branches that grow out. The above observation perfectly fits within the canalization theory for the regulation of shoot branching. Finally, the presumed SL mediated reduction in PIN1 endocytosis, used in the computer model, was finally experimentally confirmed and was shown to occur through a clathrin-dependent mechanism (Shinohara *et al.*, 2013).

Consistent with the idea that SLs do not need to directly exert their branching-inhibiting function in the buds, *MAX2* in *Arabidopsis* is expressed throughout the plant, and particularly high in the vasculature of developing tissues (Stirnberg *et al.*, 2007). Similarly, the other component involved in SL signalling, the  $\alpha/\beta$ -fold hydrolase *D14*, is also expressed in vasculature tissues, especially in xylem parenchyma cells in leaves and stems in close vicinity to axillary buds (Arite *et al.*, 2009). Taken together, depending on auxin transport status, SLs systemically regulate competition between buds to release their auxin into the stem, finally determining how many buds can be activated (Prusinkiewicz *et al.*, 2009; Crawford *et al.*, 2010; Shinohara *et al.*, 2013).

An argument against the above described model is the fact that in *Arabidopsis* and pea, both wild type and SL biosynthetic mutants rapidly transport additional exogenously applied auxin, suggesting that their auxin transport capacity is not saturated (Brewer *et al.*, 2009). In addition to this, another simulation study recently shown that the increase in auxin transport capacity in the main stem as a result of decapitation occurs too slow to explain the increased bud outgrowth (Renton *et al.*, 2012). Rather, this simulation study suggested that if auxin canalization accounts for bud outgrowth, enhanced auxin levels in the bud itself may be the main driving force (Renton *et al.*, 2012).

SLs as well as CKs are considered acropetally mobile signals that can enter the buds and directly regulate bud activity (second-messenger model) (**Figure 2B**). Controversial to the canalization-based model, this model emphasizes the local action of SLs. Expression patterns of SL biosynthetic genes reveal that SLs are likely synthesized in the vascular tissue of both roots and shoots. Root derived SLs can be transported acropetally through the xylem sap stream (Kohlen *et al.*, 2011). This is in accordance with grafting studies which already shown that branching-inhibitors can move from the roots to the shoot since the bushy phenotype of SL biosynthesis mutants can be rescued by grafting mutant shoots on wild type roots (Morris *et al.*, 2001; Turnbull *et al.*, 2002; Simons *et al.*, 2007). However, grafting of wild type shoots on SL deficient roots shown that this SL transport is not a prerequisite for branching inhibition, emphasizing the importance of local SL production in the stem. Besides, auxin upregulates the transcription of SL biosynthetic genes such as *CCD7* and *CCD8* whereas decapitation results in decreased expression of these genes (Sorefan *et al.*, 2003; Johnson *et al.*, 2006; Arite *et al.*, 2007; Brewer *et al.*, 2009; Liang *et al.*, 2010). According to Dun *et al.* (2013), the GR24 signal was profoundly perceived

in the axillary buds rather than adjacent leaves in pea, supporting the direct local inhibitory effect of SLs in axillary buds. They also shown that the inhibitory effect of GR24 was not permanent, which is consistent with SLs' transient signalling role in mediating rapid plant developmental responses (Dun *et al.*, 2013). The recently discovered SL transporter gene, petunia *PLEIOTROPIC DRUG RESISTANCE 1* (*PhPDR1*), is particularly expressed in the vasculature and nodal tissues near the axillary buds (Kretzschmar *et al.*, 2012), consistent with the fact that cellular transport of SLs is likely needed in this specific region. Indeed, shoot branching in the *Petunia pdr1* mutant is increased compared with the wild type, however not to the extent observed for SL biosynthetic mutants (Kretzschmar *et al.*, 2012). This may point to a SL export-independent bud outgrowth inhibitory process. Considering the co-localization of the expression of *PIN1* and SL biosynthetic genes in vascular parenchyma cells, this SL export-independent process is potentially represented by the SL-mediated inhibition of the PAT capacity. Similar to SL, CKs are mostly synthesized in the roots, albeit with some biosynthesis also occurring in the shoot, and are also transported acropetally through the xylem (Chen *et al.*, 1985; Nordstrom *et al.*, 2004; Tanaka *et al.*, 2006). In contrast to SLs, however, CKs promote bud outgrowth directly and auxin inhibits CK biosynthesis by suppressing the cytokinins biosynthetic gene *IPT* (*ADENOSINE PHOSPHATE-ISOPENTENYL TRANSFERASE*) (Tanaka *et al.*, 2006). Accordingly, decapitation or application of an auxin transport inhibitor led to enhanced expression of CK biosynthetic genes in nodal stem and increased CK levels in pea (Tanaka *et al.*, 2006).

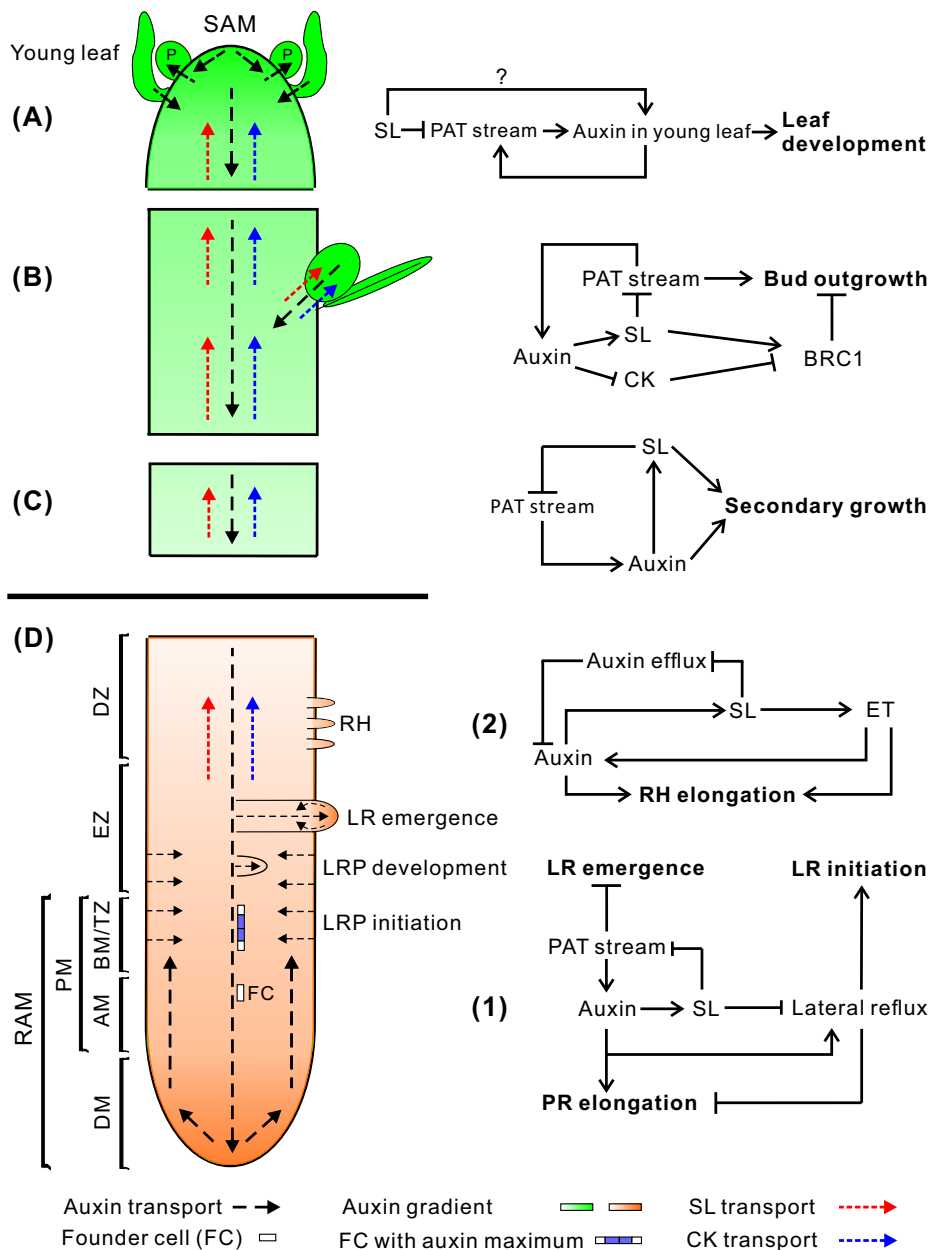


**Figure 2. An overview of auxin, SL and CK transport within the plant (left) and hormone interactions during the regulation of shoot and root development (right).** Auxin, SL and CK transport are represented by black, red and blue dotted line, respectively. For hormone interactions (right), arrows represent promotion, while flat-ended lines



indicate inhibition.

(A) Auxin, produced in the shoot apical meristem (SAM) and young leaves, is transported basipetally through the stem in the polar auxin transport (PAT) stream towards the root apical meristem (RAM). Here, but probably also throughout the entire vasculature of the plant, it positively regulates SL biosynthesis (Hayward *et al.* 2009). As shown by GR24 feeding experiments, SLs transported through the xylem from the root to the shoot down-regulate the free auxin level in young leaves in a MAX2-dependent manner hereby controlling their development (Ruyter-Spira *et al.* 2011). SLs in the vasculature negatively affect PAT capacity (Crawford *et al.* 2010), as observed for NPA (Ljung *et al.* 2001), which negatively feeds back on auxin levels at the sites of biosynthesis. This long-distance SL-auxin feedback mechanism, affects plant developmental processes as described below.

(B) During the regulation of bud outgrowth, SLs reduce the capacity of the PAT stream in the main stem, leading to enhanced competition between buds to release their auxin into the stem (Crawford *et al.* 2010; Shinohara *et al.* 2013). On the other hand, SLs and CK are transported acropetally through the xylem and act directly in the buds to control their outgrowth through the joint regulation of TCP transcription factor BRC1 (Braun *et al.* 2012; Dun *et al.* 2012).

(C) SLs have a direct positive effect on secondary growth by activating cell division in the vascular cambium in which they act downstream of auxin. The fact that the *max1* mutant still displays some residual cambium activity might point to a SL independent response to auxin. However, this remaining activity could also be due to residual SLs in these mutants (Agusti *et al.* 2011). (D) Hormone interactions during primary root (PR) elongation, lateral root (LR) initiation and development (1) and root hair (RH) elongation (2). (1) Auxin imported from the main PAT stream into the root stimulates SL production. SL export into the xylem and down regulation of the PAT stream feedback on auxin levels in the shoot as described under (A). SL biosynthesis genes are specifically expressed in vascular tissue and the cortex of the proximal meristem of the root, through which the lateral auxin reflux towards the main PAT stream takes place. Therefore, it is likely that locally synthesized SLs are controlling the efficiency of this reflux. Primary root elongation and lateral root initiation are determined by the auxin gradient inside the root tip, which is determined by auxin levels imported through the PAT stream, auxin synthesized in the root tip, and local auxin transport, including the auxin lateral reflux. Lateral root development and emergence are controlled by auxin derived from the shoot for which the SL controlled PAT stream capacity and lateral auxin influx into the developing LRP are the main determinants. Although in the flow diagram auxin is depicted as a positive regulator of root growth, auxin displays a dose-response curve with an optimum, such that supra-optimal auxin concentrations will have a negative effect (Ruyter-Spira *et al.* 2011). (2) The effect of SLs on RH elongation is dependent on both auxin and ET biosynthesis and signalling. It has been suggested that SLs negatively regulate auxin efflux (Koltai *et al.* 2010). If this would specifically occur in RH cells this would result in increased local auxin levels which stimulates RH elongation. This local action of SLs has not been proven yet. Alternatively, it may be that SLs affect auxin transport in the PAT stream and/or the root tip hereby indirectly affecting the auxin concentration in RH cells. ET acts downstream of SLs and has a direct effect on RH elongation but also interacts with



the auxin pathway (Kapulnik *et al.* 2011).

Abbreviations: P: primordium; SAM: shoot apical meristem; DM: distal meristem; PM: proximal meristem; AM: apical meristem; BM: basal meristem; TZ: transition zone; EZ: elongation zone; DZ: differentiation zone; FC: founder cell; RAM: root apical meristem; PR: primary root; RH: root hairs; LR: lateral root; LRP: lateral root primordia; SL: strigolactone; CK: cytokinin; ET: ethylene; PAT: polar auxin transport.

Consistent with the second-messenger model, SLs and CK, mediated by auxin, act antagonistically and locally in the buds to control bud outgrowth (Brewer *et al.*, 2009; Ferguson and Beveridge, 2009; Dun *et al.*, 2012). Based on decapitation and girdling experiments, it was hypothesized that growing axillary branches/buds affect auxin sink strength and also bud responsiveness to SLs (Ferguson and Beveridge, 2009). Auxin levels in the stem negatively regulate bud outgrowth by maintaining local high SL and low CK levels (Ferguson and Beveridge, 2009). Once buds are activated, auxin is exported into the stem to allow vasculature development (Ferguson and Beveridge, 2009). Recent research suggests that both SLs and CK can interact directly in buds to control bud outgrowth, converging at a common target in the bud, possibly a TCP transcription factor, BRANCHED1 (BRC1) (Dun *et al.*, 2012). In eudicots such as *Arabidopsis* and pea, BRC1 has been suggested to be expressed in axillary buds and act downstream of SLs signalling during shoot branching inhibition (Aguilar-Martinez *et al.*, 2007; Braun *et al.*, 2012; Dun *et al.*, 2012). The expression of the pea *PsBRC1* mostly occurred in the axillary buds and was up-regulated by application of GR24 and down-regulated by CK treatment (Braun *et al.*, 2012; Dun *et al.*, 2012). However, overexpression of *BRC1* ortholog *FC1* (*FINE CULM 1*) in rice could only partially rescue the tillering phenotype of the SL signalling mutant *d3* (Minakuchi *et al.*, 2010). GR24 treatment did not significantly affect the expression of *FC1* whereas CK treatment did down-regulate its expression (Minakuchi *et al.*, 2010). In maize, it seems that *BRC1* ortholog *TB1* (*TEOSINTE BRANCHED 1*) has evolved independent from SL signalling which may be explained by the fact that maize domestication is associated with a gain-of-function mutation in the *TB1* gene (Guan *et al.*, 2012). Further research is still needed to clarify the regulatory mechanisms of the *BRC1* gene family and to find out whether additional factors in the axillary bud are involved in the regulation of bud outgrowth. Recent findings have shed some light on how other factors interact with FC1 in rice, targeting D14 to control shoot branching (Guo *et al.*, 2013). Their results shown that OsMADS57, which is one of the transcription factors from the MADS-domain family, directly suppressed D14 transcription to control rice tillering, while FC1 could disturb this inhibitory effect of OsMADS57 on D14 by binding to

the OsMADS57 (Guo *et al.*, 2013).

Although second-messenger and canalization-based models look controversial, they can also be compatible since both local and systemic action of SL signalling are needed for adaptive plant responses. **Figure 2** presents an overview of auxin, SLs and CK transport within the plant (left) and interactions between these hormones during the regulation of shoot and root development (right).

### 4. Strigolactone interplay with other hormones in regulating root development

Plant root system displays a large plasticity which is required to guarantee resource acquisition in response to changing environments. Most dicot species have a typical allorhizic root system with a primary (tap) root (PR) and several orders of lateral roots (LR) (Osmont *et al.*, 2007). Adventitious roots (AR) are initiated from non-root tissues such as the hypocotyl or stem. Most monocot species are characterized by a secondary homorhizic root system including the embryonic PR, post-embryonic shoot-borne crown roots and LRs (Osmont *et al.*, 2007). On a micro scale, the root system architecture also includes root hairs (RH) that expand the root surface area and hence the capacity of plants to withdraw nutrients and water from the soil (Gilroy and Jones, 2000).

#### 4.1 Primary root development

PR growth is mainly determined by the activity of the root apical meristem (RAM). This is a complex region of the root tip including a stem cell niche (SCN), a proximal meristem (PM) and a distal meristem (DM) (**Figure 2D**). Cell division, elongation and differentiation in the RAM are tightly controlled by plant hormones. In this process, auxin is the main player. Different levels of cellular auxin have a different effect on gene expression, which determines cell fate. In roots, high auxin levels tend to stimulate cell division whereas lower levels favor cell expansion (Doerner, 2008). Auxin is mostly synthesized in the young leaves at the shoot apex (Ljung *et al.*, 2001) and directionally transported through the vascular cambium of the shoot towards the RAM (Blilou *et al.*, 2005; Petrasek and Friml, 2009). In roots, auxin is particularly accumulated in the quiescent center (QC), the columella initials and lateral root cap where auxin maxima are formed (Blilou *et al.*, 2005; Petersson *et al.*, 2009; Petrasek and Friml, 2009; Brunoud *et al.*, 2012). Besides the auxin that is imported from the shoot, local auxin biosynthesis

in the root also contributes to auxin homeostasis in the root tip (Chen and Xiong, 2009; Petersson *et al.*, 2009). A major determinant of root growth is the auxin concentration gradient which is formed along the longitudinal axis of the root meristem. This concentration gradient is established due to the directional action of auxin transporters including auxin influx carriers such as AUXIN RESISTANT1(AUX1) and LIKE-AUX1 family and efflux carriers such as PINs and ATP-BINDING CASSETTE (ABC) transporters (Blilou *et al.*, 2005; Kleine-Vehn *et al.*, 2006; Grieneisen *et al.*, 2007; Zazimalova *et al.*, 2010). The directionality of the auxin flux is determined by the polar subcellular localization of these auxin efflux proteins (Sauer *et al.*, 2006; Wisniewska *et al.*, 2006; Petrasek and Friml, 2009). In the primary root, basally localized PIN1, PIN3 and PIN7 in the stele facilitate the acropetal auxin transport towards the root apex (Petrasek and Friml, 2009) (**Figure 2D**). In the columella, PIN3 and PIN7 redirect the auxin flow laterally towards the epidermis and the lateral root cap. PIN2 then facilitates the auxin flow from there upwards to the elongation zone (Petrasek and Friml, 2009). In addition, PIN2 in the cortex is also functional and fine-tunes both the rootward and shootward auxin flux, thus helps maintain auxin maxima at the root tip (Rahman *et al.*, 2010). Finally, in the elongation zone, auxin is transported back into the main PAT stream through a lateral auxin reflux in the endodermis/cortex (as reviewed in (Petrasek and Friml, 2009) (**Figure 2D**).

SLs are suggested to modulate the auxin gradient in the PR tip. The PR length of SL biosynthesis mutants (*max1*, *max3* and *max4*) and SL signalling mutant (*max2*) is shorter than in wild-type plants (Ruyter-Spira *et al.*, 2011). Application of GR24 (2.5  $\mu$ M) rescued the short root phenotype of SL-deficient mutants but not of SL-insensitive mutant *max2* (Ruyter-Spira *et al.*, 2011). The increased PR length was associated with an expansion of the meristem and transition zone sizes, through a higher number of smaller cells in both zones (Ruyter-Spira *et al.*, 2011). Previously, modeling in which a reduction of the lateral auxin reflux was simulated shown a similar cellular patterning in the primary root tip (Grieneisen *et al.*, 2007). This suggests that SLs may reduce the efficiency of the auxin lateral reflux into the main PAT stream which would affect auxin levels in both meristem and transition zones (Ruyter-Spira *et al.*, 2011). Also consistent with these results, it has been demonstrated that expression of MAX2 under endodermis-specific SCARECROW (SCR) promoter in *max2* led to a wild-type level concerning meristem cell number, LR density and RH elongation (Koren *et al.*, 2013). Since PIN3-mediated auxin transport through the endodermis plays an important role in LR initiation (Marhavy *et al.*, 2013), SLs' effects on PR growth and LR formation may indeed act through mediating auxin flux in the root tip (Koren

*et al.*, 2013). Interestingly, there was also evidence showing that *SHORT HYPOCOTYL 2 (SHY2)*, which is the central mediator between auxin-CK antagonistic interaction in balancing cell differentiation with cell division in the meristem (Dello Iorio *et al.*, 2008; Perilli *et al.*, 2012), may be involved in endodermal SL signalling to regulate meristem size (Koren *et al.*, 2013). Thus, *SHY2* seems the converging point for auxin, CK as well as SLs. SLs may regulate PIN-based auxin flux via *MAX2* and/or *SHY2* (Koren *et al.*, 2013); however, it is still not clear how SLs regulate *SHY2*. Besides, both *max2* and *shy2-31* mutants shown reduced sensitivity to CK treatment, suggesting that *MAX2* and *SHY2* participate in CK signalling in the root (Koren *et al.*, 2013).

It has been suggested that the regulatory role of SLs in PR growth is mediated through their inhibitory effect on auxin-efflux carriers (Koltai *et al.*, 2010; Ruyter-Spira *et al.*, 2011; Koren *et al.*, 2013). As mentioned in the previous part, SLs signalling has recently been found to rapidly trigger PIN1 depletion from plasma membrane of xylem parenchyma cells. However, compared to the shoot, the effect of SLs on PIN1 depletion in root is less drastic and less specific. No obvious short-term effect of GR24 on PIN1 accumulation was observed in the root tip even within 2d (Shinohara *et al.*, 2013). Only in the longer term (6d), the inhibitory effect by GR24 treatment could be detected in the provascular region (Ruyter-Spira *et al.*, 2011). This could be explained by SLs' feedback inhibition on auxin biosynthesis in young leaves and auxin transport capacity in the stem, which would lead to reduced auxin supply to the root (Ruyter-Spira *et al.*, 2011). However, if the short term inhibitory effects of SLs on PINs are only expected to specifically occur in the endodermis cells of the transition zone, visualization of this process is technically challenging.

### 4.2 Lateral root initiation and development

LR originates from a few auxin-primed pericycle founder cells (FC) located opposite of the xylem poles in the basal meristem of the parental root (Peret *et al.*, 2009) (**Figure 2D**). LR formation is subsequently initiated through a series of anticlinal and periclinal cell divisions - controlled by auxin - in the primed FC. This process is promoted by the auxin reflux in the transition zone (Casimiro *et al.*, 2001; De Smet *et al.*, 2007; Dubrovsky *et al.*, 2008; Marhavy *et al.*, 2013). Particularly, PIN3, which is transiently induced in the endodermis during early stages of LR initiation, enables proper auxin gradient for transition from FC to LR initiation (Marhavy *et al.*, 2013). LR initiation is followed by tightly regulated cell divisions leading to subsequent LR

primordial (LRP) development and finally LR emergence (Peret *et al.*, 2009; De Smet, 2012) (**Figure 2D**). As LRP develop, auxin efflux carriers promote the accumulation of auxin in the tips of the multilayered LRP. The formation of a proper auxin maximum is a crucial event during LR development (Petrásek and Friml, 2009) (**Figure 2**). The accumulated auxin in developing LR tips also serves as a local signal to remodel adjacent cells by inducing the expression of auxin influx carrier LAX3 (LIKE AUX1 3) in cortical and epidermal cells, which leads to cell separation in LRP overlaying tissues, thus enabling LR emergence (Swarup *et al.*, 2008).

While LR initiation is dependent on auxin which is circling inside the root tip (and is derived from both the shoot and the root) (Reed *et al.*, 1998; Casimiro *et al.*, 2001; Marchant *et al.*, 2002; Wu *et al.*, 2007), subsequent LR development is solely sustained by shoot derived auxin transported to the parent root and into the LRP through the PAT stream (Casimiro *et al.*, 2001; Bhalerao *et al.*, 2002; Chhun *et al.*, 2007; Wu *et al.*, 2007). Inherent to these different auxin sources, the regulatory mechanisms controlling LR initiation and subsequent development are also different; however, in both cases the control of PINs plays an important role.

SLs act as regulators for LR initiation and LRP development (**Figure 2D**). SL-deficient (*max3* and *max4*) and SL-insensitive (*max2*) mutants shown increased density of LRs compared with wild type (Kapulnik *et al.*, 2011a). Treatment of *Arabidopsis* seedlings with increasing concentrations of GR24 shown that LR density is reduced when 2.5  $\mu\text{M}$  GR24 is applied, however LR initiation is only reduced with 5  $\mu\text{M}$  GR24 (Ruyter-Spira *et al.*, 2011). Therefore, it was concluded that the reduction in LR density observed with 2.5  $\mu\text{M}$  GR24 results from a delay in LR development (Ruyter-Spira *et al.*, 2011). Indeed, a LR developmental study shown a specific accumulation of LR stage V primordia (according to the LR developmental scale of Malamy and Benfey (1997)). The arrested primordia displayed reduced levels of auxin reporter DR5-GUS and pPIN1-PIN1-GFP, suggesting that reduced auxin levels inside LRP are responsible for their delayed development or arrest (Ruyter-Spira *et al.*, 2011). Auxin is provided to the developing primordia by a PIN1-dependent auxin influx from the PAT stream in the stem into the LRP interior toward the LR cap. It has been shown that GR24 application to the roots of *Arabidopsis* reduced auxin levels in young leaves (Ruyter-Spira *et al.*, 2011). Possibly, the SL-mediated reduction in auxin transport in the PAT stream temporarily increases auxin levels in vascular tissue throughout the plant, which negatively feeds back on auxin production in young leaves (or positively on auxin degradation), similar to what has been observed upon

application of the auxin transport inhibitor NPA (Ljung *et al.*, 2001). The role of SL signalling in lateral root development may also involve *SHY2* (Koren *et al.*, 2013), which has been suggested to suppress LR initiation but promotes LR development by mediating PIN activity and auxin homeostasis (Goh *et al.*, 2012). Endodermis-specific expression of *SCR: MAX2* in *max2* background restored LR density to a wild-type level. As PIN3-dependent auxin reflux between endodermis and pericycle has a critical function in LR initiation (Marhavy *et al.*, 2013), the fact that *MAX2*-mediated endodermal SL signalling is sufficient to confer sensitivity to LR formation implies that SL signalling may regulate LR formation via modulating auxin flux in the elongation zone (Koren *et al.*, 2013). Hence the mechanism underlying the GR24 mediated reduction of LR initiation is likely similar to the one described above for PR growth, i.e. a reduction in auxin reflux through the transition zone. In addition, the above described reduction in shoot derived auxin likely also contributes to the reduction in both PR growth and LR initiation (**Figure 2D**).

### 4.3 Root hair elongation

RHs are tip-growing, tube-like outgrowths that help to anchor roots in the soil and assist in the uptake of nutrients and water (Gilroy and Jones, 2000). In the differentiation zone of the root, root hairs emerge at the base of the epidermis cells. RH development can be divided into two stages: determination of hair/nonhair cells and hair morphogenesis (Lee and Cho, 2009). A cell in contact with two cortex cells will develop into a hair cell. RH initiation has been suggested to be directly mediated by optimal auxin levels and signalling, whereas ET's effect is indirect and likely to act through regulating intracellular auxin levels (Muday *et al.*, 2012). RH elongation requires an optimal intracellular auxin level which is regulated by auxin efflux and influx carriers. Auxin efflux PIN2 facilitates auxin supply through basipetal auxin transport from the root apex to the RH differentiation zone (Cho *et al.*, 2007). PIN2 in the cortex has recently been shown to fine-tune both the rootward and shootward auxin flux (Rahman *et al.*, 2010). Modeling of the auxin flow suggests that auxin influx carrier AUX1-dependent transport through non-hair cells can maintain auxin supply for developing hair cells and sustain RH outgrowth (Jones *et al.*, 2009). ET also plays a positive role in regulating RH elongation (Tanimoto *et al.*, 1995; Rahman *et al.*, 2002). Both the *Arabidopsis ein2* (*ethylene insensitive 2*) mutant and ethylene-resistant mutant *aux1* exhibited decreased RH length (Rahman *et al.*, 2002). Application of a low concentration of 1-naphthaleneacetic acid (NAA) (10 nM) could restore RH length of ethylene-resistant mutant *aux1* (Rahman *et al.*, 2002).



However, a much higher level of NAA (100 nM) was needed to recover RH length of *ein2* to the wild-type level, suggesting that the loss of ET signalling makes roots less sensitive to auxin (Rahman *et al.*, 2002). SLs interact with auxin and ET in regulating RH elongation (**Figure 2D**). In tomato, a high dose of exogenous GR24 (27  $\mu$ M) resulted in shorter and fewer root hairs than in the control (Koltai *et al.*, 2010). The authors suggested that the effect of SLs is mediated via an effect on auxin efflux carriers (Koltai *et al.*, 2010). In *Arabidopsis*, treatment with a low dose of GR24 increases the RH length in WT and in *max3* and *max4* mutants but not in *max2*, indicating the positive regulatory role of SLs in RH elongation, mediated via the MAX2 protein (Kapulnik *et al.*, 2011b). Concerning RH elongation, SL signalling mutant *max2* has a similar sensitivity to ET precursor ACC as wild type, whereas ET signalling mutants *ein2-1* and *etr1-1* (*ethylene resistant1-1*) show reduced sensitivity to GR24, suggesting that SL signalling is not necessary for the ET response but ET signalling is involved in the SL response (Kapulnik *et al.*, 2011b). Furthermore, SL application stimulates expression of ET biosynthetic genes (Kapulnik *et al.*, 2011b). Taking together, these results suggest that ET biosynthesis is necessary for SLs to have an effect on RH elongation and that ET acts downstream of SLs (**Figure 2D**). The relationship between SLs and auxin in RH formation was also explored by the same authors. RH elongation upon IAA application in *max2* was similar to that of wild type, suggesting that SL signalling is not necessary for the auxin response. In contrast, auxin perception mutant *tir1-1* exhibited a reduced response to GR24 compared with the wild type, implying that auxin perception is needed for the SL response (Kapulnik *et al.*, 2011b). However, the reduced sensitivity of *tir1-1* to GR24 may also be due to its reduced response to ET since *tir1-1* also shows reduced sensitivity to ACC. Moreover, the double mutant *aux1-7ein2-1* (insensitive to auxin and ET) shows reduced sensitivity to GR24 compared with the wild type upon RH elongation. Therefore, the effect of SLs on RH elongation is dependent on both auxin and ET biosynthesis and signalling while ET signalling also directly interacts with the auxin pathway (Kapulnik *et al.*, 2011b) (**Figure 2D**).

As mentioned above, RH initiation and elongation takes place in epidermis cells (Lee and Cho, 2009). Endodermal SL signalling, mediated by MAX2, is still sufficient to confer sensitivity for RH elongation, suggesting the effect of SLs on RH elongation is likely to occur in a non-cell-autonomous manner (Koren *et al.*, 2013).

### 4.4 Adventitious root formation

ARs are post-embryonic roots that arise from non-root tissues. They can be induced by direct organogenesis from differentiated cells or from callus formed upon mechanical damage such as a cutting (Li *et al.*, 2009). The formation of ARs in tomato occurs in the lower part of the hypocotyl as well as from the shoot-root junction. IAA application enhances AR formation in tomato hypocotyls in a dose-dependent manner (Negi *et al.*, 2010). In rice calli, overexpression of auxin biosynthetic gene *YUCCA1* (*YUC1*), results in increased numbers of ARs (crown roots) as well as active crown root formation in the elongated node of the stem, suggesting that increased auxin production promotes AR development from both callus and stem (Yamamoto *et al.*, 2007). Interestingly, in the stem, *OsYUC1-GUS* is expressed in the parenchyma cells surrounding the vascular bundles, suggesting local auxin biosynthesis in the vasculature of the stem (Yamamoto *et al.*, 2007). In addition, AR emergence and development in rice are significantly suppressed in *OsPIN1* RNAi lines (Xu *et al.*, 2005), suggesting an essential role of PIN1-dependent PAT during the process of AR initiation and development. Since SLs have been found to trigger PIN1 depletion from xylem parenchyma cells in the stem (Shinohara *et al.*, 2013), it is also plausible to predict their inhibitory effect on PAT and thus AR development.

Indeed, studies on *Arabidopsis* and pea (*Pisum sativum*) show that SLs negatively regulate AR formation (Rasmussen *et al.*, 2012a; Rasmussen *et al.*, 2012b). SL biosynthetic and signalling mutants of both species displayed increased number of AR compared with wild type. It was suggested that SLs suppress adventitious root formation by inhibiting the very early divisions of founder cells (Rasmussen *et al.*, 2012b). When *MAX2* is expressed in *max2* under the control of a xylem-specific promoter *NST3* (*NAC SECONDARY WALL THICKENING PROMOTING FACTOR3*), the AR formation is restored to the wild type level. This is consistent with the fact that *MAX2* is expressed in vasculature tissues throughout the plant. The authors suggest that SL signalling in the xylem is sufficient to mediate the formation of pericycle-derived AR. Interestingly, etiolation is known to induce AR formation in hypocotyls and this process is stimulated in all *max* mutants. The expression of *MAX3* and *MAX4* in wild type hypocotyls is induced upon light exposure, suggesting that local SL biosynthesis is involved in the regulation of AR formation during the process of de-etiolation (Rasmussen *et al.*, 2012b). SL treatment of *Arabidopsis* wild type and *max* biosynthesis mutants (but not the signalling mutant *max2*), results in a reduction in AR number even in the presence of elevated auxin levels (such as in 35S: *YUC1* plants). The auxin response mutant *auxin resistant 1* (*axr1*) and the *axr1max1-4* double mutants hardly form ARs. Auxin application (although



not all concentrations) increases the number of ARs in *max* mutants (Rasmussen *et al.*, 2012b). These findings indicate that SLs can at least partially revert the positive effect of auxin on AR formation and *AXR1* functions upstream of SLs in the early stages of AR initiation (Rasmussen *et al.*, 2012b). The authors also investigated possible crosstalk between SLs and CK in regulating AR development as CK are known to suppress AR formation. CK responsiveness is not impaired in the SL mutants and CK mutants are also SL-responsive, indicating that SLs and CK act independently in AR formation (Rasmussen *et al.*, 2012b).

### 5. SLs and auxin action during secondary growth

Plant growth initiated by apical meristems leads to development of primary tissues such as epidermis, vascular bundles and leaves. In addition to primary growth, plants, especially tree species, also display secondary growth during which they expand their growth axes laterally. Secondary growth depends on the activity of the vascular cambium which originates from the procambium and parenchyma cells (Ye *et al.*, 2002). The vascular cambium has the capacity to divide and form a continuous ring of meristem cells located between the primary xylem and the phloem in the vascular bundles (Ursache *et al.*, 2013). The cylindrical layer of cambium undergoes cell division, resulting in new xylem on the inside and new phloem on the outside (Ye *et al.*, 2002; Ursache *et al.*, 2013). There is strong evidence that procambium patterning is regulated by PIN1-dependent polar auxin transport (Scarpella *et al.*, 2004; Scarpella *et al.*, 2006). Also secondary xylem differentiation was shown to be associated with reduced polar auxin transport. The *Arabidopsis interfascicular fiber* mutant (*ifl1*) displays reduced secondary growth (Zhong and Ye, 2001). The authors shown that reduced expression of auxin efflux carriers and the resulting reduced PAT along the inflorescence stems and hypocotyls in this mutant lead to a block of vascular cambium activity (Zhong and Ye, 2001).

SLs have recently been proven to positively regulate secondary growth (**Figure 2C**). SL biosynthetic and signalling mutants all displayed reduced cambium activity compared with wild type. Local application of GR24 stimulates cell division in the interfascicular cambium in wild type and all *Arabidopsis* SL biosynthetic *max* mutants and to a lesser extent in the *max2* signalling mutant (Agusti *et al.*, 2011). Remarkably, the *max2* mutant is still slightly responsive to GR24 which is not consistent with its complete insensitivity in other processes such as shoot branching and root development. This suggests that there may also be other factors involved in the transduc-

tion of the SL signal in this particular physiological process (Agusti *et al.*, 2011). In this study of Agusti *et al.* (2011), shoot branching is not affected by GR24 application showing that the effect of SLs on cambium development in inflorescence stems is mechanistically independent from the effect they have on shoot branching (Agusti *et al.*, 2011). Interestingly, although the *max1* mutant displays reduced secondary growth, its auxin concentration, signalling and transport are enhanced. This suggests that the effect of SLs on secondary growth is direct and independent of auxin accumulation (Agusti *et al.*, 2011). In addition to this, local NPA application, which reduces the initially enhanced auxin transport capacity observed in the *max* mutants, does not restore secondary growth, suggesting that SL biosynthesis and signalling are required for auxin to stimulate cambium activity. This conclusion is supported by the fact that GR24 application to the auxin insensitive *axr1-3* mutant results in a similar increase in cambial activity as observed for wild type and the *max* mutants. Collectively, these results suggest that SLs function downstream of auxin in the regulatory pathway of secondary growth in *Arabidopsis* (Agusti *et al.*, 2011). However, the observed remaining cambium activity in *max1* cannot be ignored. It would suggest that either auxin also has a direct effect or that residual SLs are still present in the *max1* mutant background.

### 6. SLs and other hormones during seeds germination

SLs have been identified as germination stimulants for seeds of parasitic plants *Orobancha spp.* and *Striga spp.* These parasitic plants seeds are usually dormant in soil and germinated only when they are close to host roots. Previous studies shown that ABA levels decrease during seeds pre-conditioning of *O. minor* (Chae *et al.*, 2004). Still, seed dormancy release depends on an additional reduction of ABA levels which was recently shown to be mediated through ABA catabolism which is triggered by GR24 application (Lechat *et al.*, 2012). Other hormones such as CK and ET can promote parasitic plant seeds germination in the absence of SLs (Logan and Stewart, 1991; Babiker *et al.*, 1993; Babiker *et al.*, 1994; Sugimoto *et al.*, 2003), suggesting that they may act downstream of SLs; whereas CK promotes germination by enhancing ET biosynthesis (Babiker *et al.*, 1993). Furthermore, GA is necessary but not sufficient to trigger *Striga* seeds germination (Toh *et al.*, 2012).

Currently, model plant *Arabidopsis* is also being used to explore hormone interactions, including SLs, during seed germination. Based on thermoinhibition experiments, a positive role of SLs in *Arabidopsis* seeds

4 germination was revealed (Toh *et al.*, 2012). Both SLs biosynthetic and signalling mutants shown enhanced sensitivity to high temperature which is a constraint for normal germination (Toh *et al.*, 2012). GR24 could not only alleviate thermoinhibition by decreasing ABA levels and increasing GA levels, but also break secondary dormancy in *Arabidopsis*. Nice comparisons were made between hormone interactions occurring during the alleviation of thermoinhibition in parasitic and non-parasitic seeds germination (Toh *et al.*, 2012). In both cases, SLs reduce the ABA:GA ratio, leading to enhanced germination activity. To trigger *Striga* seed germination, SLs also positively regulate CK which contributes to ET production (not proven for *Arabidopsis* yet) (Toh *et al.*, 2012). However, as expected when considering the difference in germination behavior between parasitic plants and *Arabidopsis*, differences between hormone signalling networks were also reported. GA, for instance, is sufficient to counteract thermoinhibition in *Arabidopsis* seeds but is not sufficient to do so in parasitic plants seeds (Chae *et al.*, 2004; Toh *et al.*, 2012). Besides, parasitic plants seeds are very sensitive to SLs that are exuded from host plants, suggesting their evolutionary dependence on hormone interaction (Toh *et al.*, 2012). Light signalling related topics concerning seeds germination will be discussed in the following 7.1 section. Interestingly, a smoke-derived compound, karrikin, has similar effects on seed germination in a MAX2-dependent manner (Nelson *et al.*, 2011). The *kai2* (karrikin insensitive 2) mutant seeds are insensitive to GR24. It was suggested that there is a butenolide-based signalling mechanism via KAI2 which is distinct from SL signalling, providing an adaptive response to smoke (Waters *et al.*, 2012b).

### 7. Hormones interactions in response to environmental stimuli

Plants, unlike animals, are sessile organisms and hence require phenotypic plasticity, which is the ability of a certain genotype to produce different phenotypes in response to varying environmental conditions (Pfennig *et al.*, 2010). Meristem development is of vital importance for the adaptation of plants to changes in the environment. Regulation of axillary meristem outgrowth, for example, is one of the major strategies that plants adopt to adjust their body plan, leading to changes in shoot branching. Another mechanism to modify the body plan is to alter secondary growth of stems and roots by regulating development of lateral meristem tissue, especially the vascular cambium (Agusti and Greb, 2013), allowing plants to regulate root and shoot thickness. Collectively, all plant meristems are closely coordinated to face environmental challenges during plant development. In the following paragraphs, we will elaborate on how SLs and other plant hormones are involved

in the regulation of two different environmentally regulated physiological processes, the response to light and the response to nutrient shortage.

### 7.1 The response to light

Light is a highly variable environmental factor affecting plant growth and development. Changes in light quality and intensity affect multiple processes in plants, such as intensively studied shade avoidance syndrome (SAS). During this response, plants are able to detect a decrease in the R:FR and initiate morphological changes that help plants to compete with their neighbours (Franklin, 2008), such as elongation of internodes, hypocotyls and petioles, reduced shoot branching and leaf development, inhibited root growth, early flowering and reduced seed set in the long term (Ruberti *et al.*, 2012). The stimulation of the elongation responses can be as rapid as a few minutes and the process is reversible. The photoreceptors responsible for the response to changes in light quality in the red and far-red regions are the phytochromes, including PhyA to PhyE in higher plants.

Light also affects the levels of plant hormones and in turn, plant hormones affect the photoreceptor signal transduction (Wang *et al.*, 2013). Shade has been reported to induce a rapid increase in auxin levels, its PIN-based transport (i.e. PIN1 and PIN3) and auxin signalling, resulting in enhanced elongation growth (Tao *et al.*, 2008) (Keuskamp *et al.*, 2010; Hornitschek *et al.*, 2012). Notably, it has been shown that *PIN1* expression was regulated by the photomorphogenesis repressor COP1 (CONSTITUTIVE PHOTOMORPHOGENIC 1), which is suppressed by light-activated PHYB. COP1 not only controlled the transcription of *PIN1* and the capacity of the PAT stream in the hypocotyls but also affected PIN1 and PIN2 intracellular distribution in the root tip thus affecting root elongation. This suggests that COP1 efficiently coordinates both root and shoot growth under changing light conditions (Sassi *et al.*, 2012).

SLs were shown to be essential components of the low R:FR mediated reduction of bud outgrowth. In *Arabidopsis* it was shown that both *BRC1* and the SL biosynthetic and downstream signalling genes *MAX4* and *MAX2* were needed to suppress branching during low R:FR conditions (Finlayson *et al.*, 2010). In addition to this, functional *AXR1*, was also essential for the control of shoot branching under low R:FR conditions, confirming that auxin signalling is important during shade avoidance reactions (Tao *et al.*, 2008) and is probably needed to induce SL biosynthesis. Indeed, auxin was shown to induce SL biosynthetic gene expression under normal light condition

(Hayward *et al.*, 2009). It's very likely that it's the similar case under shade: auxin levels and PAT stream are promoted under shade, which may enhance SL biosynthesis, leading to reduced bud outgrowth.

A low R:FR and/or inactive PHYB also induce an elongation response in branches. Interestingly, the *Arabidopsis max2* mutation inhibited the elongation response of rosette branches in the presence of the *phyB* mutation, while *axr1-12* and *max4* maintained the elongation response of branches in the *phyB* mutant (Finlayson *et al.*, 2010). Also for other light regulated plant growth characteristics, such as decreased hypocotyl growth and de-etiolation, MAX2 dependency has been observed while the SL biosynthetic mutants did not display the corresponding photomorphogenic phenotypes. For instance, while *max2* is hyposensitive to red, far-red and blue light, leading to longer hypocotyls (Stirnberg *et al.*, 2002; Shen *et al.*, 2007; Nelson *et al.*, 2011), this was not the case for *max1*, *max3* and *max4* (Shen *et al.*, 2012). Therefore, it was suggested that MAX2 regulates photomorphogenesis in a SL-independent manner, and may form complexes consisting of different ligands and/or substrates. In this respect, it is intriguing that not only the response to SLs, but also to smoke derived compounds called karrikins, requires MAX2 (Nelson *et al.*, 2011). An alternative explanation could be that the SL biosynthetic mutants tested in these studies are leaky, and still produce sufficient SLs to result in different phenotypes when compared to the signalling mutant. Based on altered expression patterns of GA and ABA biosynthesis and catabolic genes in *Arabidopsis max2* seeds, in combination with a *max2* specific germination phenotype, it was hypothesized that MAX2 would also affect photomorphogenesis by modulating hormonal levels in a non-SL dependent manner (Shen *et al.*, 2012). However, again, it could be that the hormonal levels in the SL biosynthetic mutants are not enough reduced to result in a phenotype. It would therefore be interesting to include SL biosynthetic double or triple mutants in these experiments. A direct link between SLs and photomorphogenesis has been suggested (Tsuchiya *et al.*, 2010). It was shown that SLs inhibit hypocotyl elongation in the dark. However, it must be noted that non-physiological levels of GR24 (50  $\mu$ M) were applied. A mechanistic explanation for the MAX2/SL role in photomorphogenesis was provided with the discovery that GR24 (10  $\mu$ M) mediates nuclear exclusion of COP1, which leads to the stabilization of HY5 (ELONGATED HYPOCOTYL 5) and reduced hypocotyl elongation (Tsuchiya *et al.*, 2010). This led to the intriguing conclusion that SL application can mimic light under dark conditions (Tsuchiya *et al.*, 2010). However, in contrast to above results (Tsuchiya *et al.*, 2010), it was recently found that HY5 is not necessarily required for MAX2-dependent SL regulation of hypocotyl

growth (Waters and Smith, 2013). It was proposed that HY5 and MAX2 act in separate signalling pathways during early light-mediated seedling development and that they may subsequently interact, in later developmental stages, downstream of auxin and light signalling (Waters and Smith, 2013).

### 7.2 The response to nutrient deprivation

Nutrient deprivation is another important abiotic stress frequently encountered by plants. Phosphorus (P), for example, is one of the essential macronutrients required by plants but only the inorganic phosphate (Pi) is the phosphorus form which is accessible for plants. As roots are the main site for Pi acquisition, plant roots usually cope with Pi-limiting conditions by investing more energy into root growth, resulting in reduced shoot/root ratio (including inhibited shoot branching), inhibited PR elongation and enhanced LR and RH growth (Williamson *et al.*, 2001; Linkohr *et al.*, 2002; Niu *et al.*, 2012). It has been shown that the root tip is involved in sensing low Pi (Svistoonoff *et al.*, 2007).

In *Arabidopsis*, the *phosphorus starvation-insensitive (psi)* mutant, displaying reduced inhibition of PR growth and reduced LR and RH growth under Pi-limited conditions, shown less sensitivity to auxin and enhanced ability to sustain auxin response in the root tip than wild type plants under low Pi, suggesting that low Pi can increase the sensitivity of roots to auxin (Wang *et al.*, 2010). The enhanced auxin sensitivity induced by Pi deprivation is conferred by an increased expression of *TIR1*, which accelerates the degradation of AUX/IAA proteins (Perez-Torres *et al.*, 2008).

In addition to auxin, SLs are also important regulators of root architecture under Pi-limiting conditions. SL production in roots is promoted by Pi starvation (Yoneyama *et al.*, 2007; Lopez-Raez *et al.*, 2008; Jamil *et al.*, 2011). Interestingly, while LR development in *Arabidopsis* SL biosynthetic and signalling mutants was increased during normal Pi conditions, LR outgrowth was decreased during Pi starvation (Ruyter-Spira *et al.*, 2011). Similarly, in rice, crown root elongation in wild type was increased in Pi-deficient media while *d10* and *d14* mutant plants did not show such response (Arite *et al.*, 2012). Particularly the results in *Arabidopsis* suggest that the increase in SL production under Pi-limited conditions is necessary for the expansion of the root system, allowing the plant to explore a larger area of the soil for nutrients. That this is due to an interaction with auxin is suggested by the results of an experiment in which GR24 was applied to *Arabidopsis* plants growing on medium also containing auxin (NAA) which resulted in a more



rapid elongation of lateral roots than in the absence of GR24 (Ruyter-Spira *et al.*, 2011). Moreover, GR24 application to plants grown with sufficient Pi caused a more severe reduction in lateral root number compared with plants grown under Pi starvation (Ruyter-Spira *et al.*, 2011). Because Pi starvation increases auxin sensitivity (Perez-Torres *et al.*, 2008; Koltai, 2012) and GR24 application was shown to decrease auxin levels in the leaves, it is likely that the final effect of GR24 (or SLs in general) in the low Pi response depends on the auxin status of the plant, as affected by the environment (Pi level) of the plant.

The effect of SL on Pi starvation-mediated changes in root hair density also sheds light on the mechanism by which SL affect auxin signalling. *Arabidopsis* SL biosynthetic and signalling mutants shown a remarkably lower RH density, than wild type plants and only the response of the SL biosynthetic mutant *max4*, not that of *max2*, could be rescued by exogenous treatment with GR24 (Koltai, 2012; Mayzlish-Gati *et al.*, 2012). These results could be explained by the absence of low Pi mediated induction of TIR1 in *max2* while TIR1 expression is induced in wild type plants. This would render SL mutant plants less sensitive to auxin during Pi starvation. Moreover, this SL-mediated RH response to low Pi was suggested to be independent or downstream of the ET signalling pathway, while only auxin, and not ET was able to restore the relatively low RH density in the *max2* mutant (Koltai, 2012; Mayzlish-Gati *et al.*, 2012).

The expression of SL exporter *PDR1* is also induced by Pi deprivation. *PDR1* is localized in the plasma membrane of sub-epidermal cells of roots, facilitating SL exudation into the rhizosphere and promotes the symbiotic interaction with AM fungi and hence Pi uptake by the plant (Kretzschmar *et al.*, 2012). SL production in the root is relatively high. A part of this SL pool is transported upwards to the shoot. It has been shown in *Arabidopsis* and tomato that under low Pi, increased levels of SLs travel through the xylem (Kohlen *et al.*, 2011). This systemic mode of action allows SLs to rapidly regulate aboveground architecture by altering PIN accumulation (Shinohara *et al.*, 2013), thus facilitates nutrient re-allocation. However, under Pi deficiency, transcript levels of SL biosynthetic genes were also slightly increased in the shoot (Umehara *et al.*, 2010), suggesting that local SL biosynthesis in the shoot also contributes to the branching inhibition observed during low Pi conditions. However, currently it is not known to what extent this local production is sufficient, and if it is, why SLs are transported to the shoot through the xylem. One explanation could be that long-distance transport of SLs provides a feedback mechanism for auxin levels (through



production and/or degradation) in auxin producing tissues in the shoot, as was demonstrated to occur upon GR24 application in *Arabidopsis* seedlings (Ruyter-Spira *et al.*, 2011). In conclusion, SLs play multiple roles in the response of plants to low Pi conditions. They not only improve Pi acquisition by improving AM fungi symbiosis but also act as long-distance signal to optimize shoot architecture in a nutrient-limited environment and regulate root architecture in such a way that Pi uptake can be improved.

In summary, plants have evolved multiple adaptive mechanisms to achieve phenotypic plasticity, not only by regulating whole plant architecture, but also by balancing nutrient allocation among different organs in response to changing environments. Plant hormones play a crucial role in these adaptive responses and their intricate interaction enables fine-tuned responses to many different changes in the environment.

### 8. Perspective

Plants exhibit a high degree of plasticity, which is defined by their ability to adjust their development to changes in the environment. Hormone interactions can fine-tune the plant response and determine plant architecture when plants are challenged by environmental stimuli such as nutrient deprivation and canopy shade. One of the essential nutrients plants strongly respond to is phosphate. Modern agriculture is highly dependent on its application, and its finite resource is worrying and deserves immediate attention. Future strategies need to focus on lower phosphate fertiliser application accompanied by improved phosphate use efficiency (PUE) by agricultural crops. Improved phosphate use efficiency is a highly desirable trait to which also root architecture contributes. Since SLs are involved in different plant developmental processes leading to plant architectural changes, including root architecture, more knowledge about their role, particularly under phosphate limiting conditions, is highly desirable. This includes the low phosphate mediated regulation of SL transport within the plant and the exudation to the rhizosphere as well as the local regulation of SL biosynthesis and transport in close vicinity to the buds.

SL crosstalk with other plant hormones is still a research area in its infancy, certainly at the cellular and genetic level. As we have pointed out in this review, a common target for many plant hormones is the regulation of auxin levels and gradients through their effect on PINs. The exact mechanism of how SLs do this however still needs to be resolved. Because different hormonal and environmental signals also interact with each other this is very complex. Computational modelling and simulations may facilitate the interpretation of complicated datasets, leading to predictions or the estab-

lishment of new models.

Finally, the intriguing structural diversity in SLs observed in plants and its relevance for differential regulation of various plant developmental processes is of great interest. Improved knowledge about SL perception and downstream signalling mechanisms will shed more light on the biological relevance of this structural diversity. The discovery of genetic variation and favourable alleles of genes involved in SL diversification and downstream signalling processes would be an interesting asset to future breeding programs as it will help to fine-tune SL action in such a way that maximum benefit is obtained in agriculture (improved PUE, better crop architecture, etc.), without negative side effects (germination of parasitic weeds).

### Acknowledgements

We acknowledge funding by the Dutch Technology Foundation STW (to CR; grant number 10990), the Chinese Scholarship Council (CSC; to XC) and the Netherlands Organization for Scientific Research (NWO; VICI grant, 865.06.002 to HB). HB was co-financed by the Centre for BioSystems Genomics (CBSG) which is part of the Netherlands Genomics Initiative/ Netherlands Organization for Scientific Research.

### References

- Aguilar-Martinez, J.A., Poza-Carrion, C., and Cubas, P.** (2007). *Arabidopsis* BRANCHED1 acts as an integrator of branching signals within axillary buds. *Plant Cell* 19(2), 458-472.
- Agusti, J., and Greb, T.** (2013). Going with the wind--adaptive dynamics of plant secondary meristems. *Mech Dev* 130(1), 34-44.
- Agusti, J., Herold, S., Schwarz, M., Sanchez, P., Ljung, K., et al.** (2011). Strigolactone signaling is required for auxin-dependent stimulation of secondary growth in plants. *Proc Natl Acad Sci U S A* 108(50), 20242-20247.
- Akiyama, K., Matsuzaki, K., and Hayashi, H.** (2005). Plant sesquiterpenes induce hyphal branching in arbuscular mycorrhizal fungi. *Nature* 435(7043), 824-827.
- Arite, T., Iwata, H., Ohshima, K., Maekawa, M., Nakajima, M., et al.** (2007). DWARF10, an RMS1/MAX4/DAD1 ortholog, controls lateral bud outgrowth in rice. *Plant J* 51(6), 1019-1029.
- Arite, T., Kameoka, H., and Kyojuka, J.** (2012). Strigolactone positively controls crown root elongation in rice. *J Plant Growth Regul* 31(2), 165-172.
- Arite, T., Umehara, M., Ishikawa, S., Hanada, A., Maekawa, M., et al.** (2009). *d14*, a strigolactone-insensitive mutant of rice, shows an accelerated outgrowth of tillers. *Plant*

*Cell Physiol* 50(8), 1416-1424.

- Babiker, A.G.T., Butler, L.G., Ejeta, G., and Woodson, W.R.** (1993). Enhancement of ethylene biosynthesis and germination by cytokinins and 1-aminocyclopropane-1-carboxylic acid in *Striga asiatica* seeds. *Physiol Plant* 89(1), 21-26.
- Babiker, A.G.T., Cai, T., Ejeta, G., Butler, L.G., and Woodson, W.R.** (1994). Enhancement of ethylene biosynthesis and germination with thidiazuron and some selected auxins in *Striga asiatica* seeds. *Physiol Plant* 91(3), 529-536.
- Balla, J., Kalousek, P., Reinohl, V., Friml, J., and Prochazka, S.** (2011). Competitive canalization of PIN-dependent auxin flow from axillary buds controls pea bud outgrowth. *Plant J* 65(4), 571-577.
- Bennett, T., Sieberer, T., Willett, B., Booker, J., Luschnig, C., et al.** (2006). The *Arabidopsis* MAX pathway controls shoot branching by regulating auxin transport. *Curr Biol* 16(6), 553-563.
- Bhalerao, R.P., Eklof, J., Ljung, K., Marchant, A., Bennett, M., et al.** (2002). Shoot-derived auxin is essential for early lateral root emergence in *Arabidopsis* seedlings. *Plant J* 29(3), 325-332.
- Blilou, I., Xu, J., Wildwater, M., Willemsen, V., Paponov, I., et al.** (2005). The PIN auxin efflux facilitator network controls growth and patterning in *Arabidopsis* roots. *Nature* 433(7021), 39-44.
- Booker, J., Auldridge, M., Wills, S., McCarty, D., Klee, H., et al.** (2004). MAX3/CCD7 is a carotenoid cleavage dioxygenase required for the synthesis of a novel plant signaling molecule. *Curr Biol* 14(14), 1232-1238.
- Booker, J., Sieberer, T., Wright, W., Williamson, L., Willett, B., et al.** (2005). MAX1 encodes a cytochrome P450 family member that acts downstream of MAX3/4 to produce a carotenoid-derived branch-inhibiting hormone. *Dev Cell* 8(3), 443-449.
- Bouwmeester, H.J., Matusova, R., Sun, Z.K., and Beale, M.H.** (2003). Secondary metabolite signalling in host-parasitic plant interactions. *Curr Opin Plant Biol* 6(4), 358-364.
- Braun, N., de Saint Germain, A., Pillot, J.P., Boutet-Mercey, S., Dalmais, M., et al.** (2012). The pea TCP transcription factor PsBRC1 acts downstream of strigolactones to control shoot branching. *Plant Physiol* 158(1), 225-238.
- Brewer, P.B., Dun, E.A., Ferguson, B.J., Rameau, C., and Beveridge, C.A.** (2009). Strigolactone acts downstream of auxin to regulate bud outgrowth in pea and *Arabidopsis*. *Plant Physiol* 150(1), 482-493.
- Brunoud, G., Wells, D.M., Oliva, M., Larrieu, A., Mirabet, V., et al.** (2012). A novel sensor to map auxin response and distribution at high spatio-temporal resolution. *Nature* 482(7383), 103-106.
- Casimiro, I., Marchant, A., Bhalerao, R.P., Beeckman, T., Dhooge, S., et al.** (2001). Auxin transport promotes *Arabidopsis* lateral root initiation. *Plant Cell* 13(4), 843-852.
- Chae, S.H., Yoneyama, K., Takeuchi, Y., and Joel, D.M.** (2004). Fluridone and norflurazon, carotenoid-biosynthesis inhibitors, promote seed conditioning and germination of the holoparasite *Orobancha minor*. *Physiol Plant* 120(2), 328-337.

- Chen, C.M., Ertl, J.R., Leisner, S.M., and Chang, C.C.** (1985). Localization of cytokinin biosynthetic sites in pea plants and carrot roots. *Plant Physiol* 78(3), 510-513.
- Chen, H., and Xiong, L.** (2009). Localized auxin biosynthesis and postembryonic root development in *Arabidopsis*. *Plant Signal Behav* 4(8), 752-754.
- Chhun, T., Uno, Y., Taketa, S., Azuma, T., Ichii, M., et al.** (2007). Saturated humidity accelerates lateral root development in rice (*Oryza sativa* L.) seedlings by increasing phloem-based auxin transport. *J Exp Bot* 58(7), 1695-1704.
- Cho, M., Lee, S.H., and Cho, H.T.** (2007). P-Glycoprotein4 displays auxin efflux transporter-like action in *Arabidopsis* root hair cells and tobacco cells. *Plant Cell* 19(12), 3930-3943.
- Crawford, S., Shinohara, N., Sieberer, T., Williamson, L., George, G., et al.** (2010). Strigolactones enhance competition between shoot branches by dampening auxin transport. *Development* 137(17), 2905-2913.
- De Smet, I.** (2012). Lateral root initiation: one step at a time. *New Phytol* 193(4), 867-873.
- De Smet, I., Tetsumura, T., De Rybel, B., Frey, N.F., Laplace, L., et al.** (2007). Auxin-dependent regulation of lateral root positioning in the basal meristem of *Arabidopsis*. *Development* 134(4), 681-690.
- Dello Ioio, R., Nakamura, K., Moubayidin, L., Perilli, S., Taniguchi, M., et al.** (2008). A genetic framework for the control of cell division and differentiation in the root meristem. *Science* 322(5906), 1380-1384.
- Doerner, P.** (2008). Plant roots: recycled auxin energizes patterning and growth. *Curr Biol* 18(2), R72-74.
- Domagalska, M.A., and Leyser, O.** (2011). Signal integration in the control of shoot branching. *Nat Rev Mol Cell Biol* 12(4), 211-221.
- Drummond, R.S.M., Martínez-Sánchez, N.M., Janssen, B.J., Templeton, K.R., Simons, J.L., et al.** (2009). *Petunia hybrida* CAROTENOID CLEAVAGE DIOXYGENASE7 is involved in the production of negative and positive branching signals in *Petunia*. *Plant Physiol* 151(4), 1867-1877.
- Dubrovsky, J.G., Sauer, M., Napsucially-Mendivil, S., Ivanchenko, M.G., Friml, J., et al.** (2008). Auxin acts as a local morphogenetic trigger to specify lateral root founder cells. *Proc Natl Acad Sci U S A* 105(25), 8790-8794.
- Dun, E.A., de Saint Germain, A., Rameau, C., and Beveridge, C.A.** (2012). Antagonistic action of strigolactone and cytokinin in bud outgrowth control. *Plant Physiol* 158(1), 487-498.
- Dun, E.A., de Saint Germain, A., Rameau, C., and Beveridge, C.A.** (2013). Dynamics of strigolactone function and shoot branching responses in *Pisum sativum*. *Mol Plant* 6(1), 128-140.
- Ferguson, B.J., and Beveridge, C.A.** (2009). Roles for auxin, cytokinin, and strigolactone in regulating shoot branching. *Plant Physiol* 149(4), 1929-1944.
- Finlayson, S.A., Krishnareddy, S.R., Kebrom, T.H., and Casal, J.J.** (2010). Phytochrome regulation of branching in *Arabidopsis*. *Plant Physiol* 152(4), 1914-1927.

- Foo, E., Turnbull, C.G., and Beveridge, C.A.** (2001). Long-distance signaling and the control of branching in the *rms1* mutant of pea. *Plant Physiol* 126(1), 203-209.
- Franklin, K.A.** (2008). Shade avoidance. *New Phytol* 179(4), 930-944.
- Gaiji, N., Cardinale, F., Prandi, C., Bonfante, P., and Ranghino, G.** (2012). The computational-based structure of Dwarf14 provides evidence for its role as potential strigolactone receptor in plants. *BMC Res Notes* 5, 307.
- Galweiler, L., Guan, C., Muller, A., Wisman, E., Mendgen, K., et al.** (1998). Regulation of polar auxin transport by AtPIN1 in *Arabidopsis* vascular tissue. *Science* 282(5397), 2226-2230.
- Gilroy, S., and Jones, D.L.** (2000). Through form to function: root hair development and nutrient uptake. *Trends Plant Sci* 5(2), 56-60.
- Goh, T., Kasahara, H., Mimura, T., Kamiya, Y., and Fukaki, H.** (2012). Multiple AUX/IAA-ARF modules regulate lateral root formation: the role of *Arabidopsis* SHY2/IAA3-mediated auxin signalling. *Philos Trans R Soc Lond B Biol Sci* 367(1595), 1461-1468.
- Gomez-Roldan, V., Feras, S., Brewer, P.B., Puech-Pages, V., Dun, E.A., et al.** (2008). Strigolactone inhibition of shoot branching. *Nature* 455(7210), 189-194.
- Grieneisen, V.A., Xu, J., Maree, A.F.M., Hogeweg, P., and Scheres, B.** (2007). Auxin transport is sufficient to generate a maximum and gradient guiding root growth. *Nature* 449(7165), 1008-1013.
- Guan, J.C., Koch, K.E., Suzuki, M., Wu, S., Latshaw, S., et al.** (2012). Diverse roles of strigolactone signaling in maize architecture and the uncoupling of a branching-specific subnetwork. *Plant Physiol* 160(3), 1303-1317.
- Guo, S., Xu, Y., Liu, H., Mao, Z., Zhang, C., et al.** (2013). The interaction between OsMADS57 and OsTB1 modulates rice tillering via DWARF14. *Nat Commun* 4, 1566.
- Hamiaux, C., Drummond, R.S., Janssen, B.J., Ledger, S.E., Cooney, J.M., et al.** (2012). DAD2 is an alpha/beta hydrolase likely to be involved in the perception of the plant branching hormone, strigolactone. *Curr Biol* 22(21), 2032-2036.
- Hayward, A., Stirnberg, P., Beveridge, C., and Leyser, O.** (2009). Interactions between auxin and strigolactone in shoot branching control. *Plant Physiol* 151(1), 400-412.
- Hornitschek, P., Kohnen, M.V., Lorrain, S., Rougemont, J., Ljung, K., et al.** (2012). Phytochrome interacting factors 4 and 5 control seedling growth in changing light conditions by directly controlling auxin signaling. *Plant J* 71(5), 699-711.
- Ishikawa, S., Maekawa, M., Arite, T., Onishi, K., Takamure, I., et al.** (2005). Suppression of tiller bud activity in tillering dwarf mutants of rice. *Plant Cell Physiol* 46(1), 79-86.
- Jamil, M., Charnikhova, T., Cardoso, C., Jamil, T., Ueno, K., et al.** (2011). Quantification of the relationship between strigolactones and *Striga hermonthica* infection in rice under varying levels of nitrogen and phosphorus. *Weed Res* 51(4), 373-385.
- Janssen, B.J., and Snowden, K.C.** (2012). Strigolactone and karrikin signal perception: receptors, enzymes, or both? *Front Plant Sci* 3, 296.

- Johnson, X., Bricch, T., Dun, E.A., Goussot, M., Haurogne, K., et al.** (2006). Branching genes are conserved across species. Genes controlling a novel signal in pea are coregulated by other long-distance signals. *Plant Physiol* 142(3), 1014-1026.
- Jones, A.R., Kramer, E.M., Knox, K., Swarup, R., Bennett, M.J., et al.** (2009). Auxin transport through non-hair cells sustains root-hair development. *Nat Cell Biol* 11(1), 78-84.
- Kapulnik, Y., Delaux, P.M., Resnick, N., Mayzlish-Gati, E., Wininger, S., et al.** (2011a). Strigolactones affect lateral root formation and root-hair elongation in *Arabidopsis*. *Planta* 233(1), 209-216.
- Kapulnik, Y., Resnick, N., Mayzlish-Gati, E., Kaplan, Y., Wininger, S., et al.** (2011b). Strigolactones interact with ethylene and auxin in regulating root-hair elongation in *Arabidopsis*. *J Exp Bot* 62(8), 2915-2924.
- Keuskamp, D.H., Pollmann, S., Voesenek, L.A., Peeters, A.J., and Pierik, R.** (2010). Auxin transport through PIN-FORMED 3 (PIN3) controls shade avoidance and fitness during competition. *Proc Natl Acad Sci U S A* 107(52), 22740-22744.
- Kleine-Vehn, J., Dhonukshe, P., Swarup, R., Bennett, M., and Friml, J.** (2006). Sub-cellular trafficking of the *Arabidopsis* auxin influx carrier AUX1 uses a novel pathway distinct from PIN1. *Plant Cell* 18(11), 3171-3181.
- Kohlen, W., Charnikhova, T., Liu, Q., Bours, R., Domagalska, M.A., et al.** (2011). Strigolactones are transported through the xylem and play a key role in shoot architectural response to phosphate deficiency in nonarbuscular mycorrhizal host *Arabidopsis*. *Plant Physiol* 155(2), 974-987.
- Koltai, H.** (2012). Strigolactones activate different hormonal pathways for regulation of root development in response to phosphate growth conditions. *Ann Bot* 112(2), 409-415.
- Koltai, H., Dor, E., Hershenhorn, J., Joel, D.M., Weininger, S., et al.** (2010). Strigolactones' effect on root growth and root-hair elongation may be mediated by auxin-efflux carriers. *J Plant Growth Regul* 29(2), 129-136.
- Koren, D., Resnick, N., Gati, E.M., Belausov, E., Weininger, S., et al.** (2013). Strigolactone signaling in the endodermis is sufficient to restore root responses and involves SHORT HYPOCOTYL 2 (SHY2) activity. *New Phytol* 198(3), 866-874.
- Kretschmar, T., Kohlen, W., Sasse, J., Borghi, L., Schlegel, M., et al.** (2012). A petunia ABC protein controls strigolactone-dependent symbiotic signalling and branching. *Nature* 483, 341-344.
- Lechat, M.M., Pouvreau, J.B., Peron, T., Gauthier, M., Montiel, G., et al.** (2012). *PrCY-P707A1*, an ABA catabolic gene, is a key component of *Phelipanche ramosa* seed germination in response to the strigolactone analogue GR24. *J Exp Bot* 63(14), 5311-5322.
- Lee, S., and Cho, H.T.** (2009). Auxin and root hair morphogenesis. *Root Hairs*, 45-64.
- Li, S., Xue, L., Xu, S., Feng, H., and An, L.** (2009). Mediators, Genes and signaling in adventitious rooting. *Bot Rev* 75(2), 230-247.
- Liang, J., Zhao, L., Challis, R., and Leyser, O.** (2010). Strigolactone regulation of shoot branching in chrysanthemum (*Dendranthema grandiflorum*). *J Exp Bot* 61(11), 3069-



3078.

- Lin, H., Wang, R., Qian, Q., Yan, M., Meng, X., et al.** (2009). DWARF27, an iron-containing protein required for the biosynthesis of strigolactones, regulates rice tiller bud outgrowth. *Plant Cell* 21(5), 1512-1525.
- Linkohr, B.I., Williamson, L.C., Fitter, A.H., and Leyser, H.M.O.** (2002). Nitrate and phosphate availability and distribution have different effects on root system architecture of *Arabidopsis*. *Plant J* 29(6), 751-760.
- Liu, W., Wu, C., Fu, Y., Hu, G., Si, H., et al.** (2009). Identification and characterization of *HTD2*: a novel gene negatively regulating tiller bud outgrowth in rice. *Planta* 230(4), 649-658.
- Ljung, K., Bhalerao, R.P., and Sandberg, G.** (2001). Sites and homeostatic control of auxin biosynthesis in *Arabidopsis* during vegetative growth. *Plant J* 28(4), 465-474.
- Logan, D.C., and Stewart, G.R.** (1991). Role of Ethylene in the Germination of the Hemiparasite *Striga hermonthica*. *Plant Physiol* 97(4), 1435-1438.
- Lopez-Raez, J.A., Charnikhova, T., Gomez-Roldan, V., Matusova, R., Kohlen, W., et al.** (2008). Tomato strigolactones are derived from carotenoids and their biosynthesis is promoted by phosphate starvation. *New Phytol* 178(4), 863-874.
- Lopez-Raez, J.A., Kohlen, W., Charnikhova, T., Mulder, P., Undas, A.K., et al.** (2010). Does abscisic acid affect strigolactone biosynthesis? *New Phytol* 187(2), 343-354.
- Malamy, J.E., and Benfey, P.N.** (1997). Organization and cell differentiation in lateral roots of *Arabidopsis thaliana*. *Development* 124(1), 33-44.
- Marchant, A., Bhalerao, R., Casimiro, I., Eklof, J., Casero, P.J., et al.** (2002). AUX1 promotes lateral root formation by facilitating indole-3-acetic acid distribution between sink and source tissues in the *Arabidopsis* seedling. *Plant Cell* 14(3), 589-597.
- Marhavy, P., Vanstraelen, M., De Rybel, B., Zhaojun, D., Bennett, M.J., et al.** (2013). Auxin reflux between the endodermis and pericycle promotes lateral root initiation. *EMBO J* 32(1), 149-158.
- Matusova, R., Rani, K., Verstappen, F.W., Franssen, M.C., Beale, M.H., et al.** (2005). The strigolactone germination stimulants of the plant-parasitic *Striga* and *Orobanch* spp. are derived from the carotenoid pathway. *Plant Physiol* 139(2), 920-934.
- Mayzlish-Gati, E., De-Cuyper, C., Goormachtig, S., Beeckman, T., Vuylsteke, M., et al.** (2012). Strigolactones are involved in root response to low phosphate conditions in *Arabidopsis*. *Plant Physiol* 160(3), 1329-1341.
- Minakuchi, K., Kameoka, H., Yasuno, N., Umehara, M., Luo, L., et al.** (2010). FINE CULM1 (FC1) Works downstream of strigolactones to inhibit the outgrowth of axillary buds in rice. *Plant Cell Physiol* 51(7), 1127-1135.
- Morris, S.E., Turnbull, C.G., Murfet, I.C., and Beveridge, C.A.** (2001). Mutational analysis of branching in pea. Evidence that *Rms1* and *Rms5* regulate the same novel signal. *Plant Physiol* 126(3), 1205-1213.
- Muday, G.K., Rahman, A., and Binder, B.M.** (2012). Auxin and ethylene: collaborators or competitors? *Trends Plant Sci* 17(4), 181-195.



- Muller, D., and Leyser, O.** (2011). Auxin, cytokinin and the control of shoot branching. *Ann Bot* 107(7), 1203-1212.
- Negi, S., Sukumar, P., Liu, X., Cohen, J.D., and Muday, G.K.** (2010). Genetic dissection of the role of ethylene in regulating auxin-dependent lateral and adventitious root formation in tomato. *Plant J* 61(1), 3-15.
- Nelson, D.C., Scaffidi, A., Dun, E.A., Waters, M.T., Flematti, G.R., et al.** (2011). F-box protein MAX2 has dual roles in karrikin and strigolactone signaling in *Arabidopsis thaliana*. *Proc Natl Acad Sci U S A* 108(21), 8897-8902.
- Niu, Y., Chai, R., Jin, G., Wang, H., Tang, C., et al.** (2012). Responses of root architecture development to low phosphorus availability: a review. *Ann Bot* 112(2), 391-408.
- Nordstrom, A., Tarkowski, P., Tarkowska, D., Norbaek, R., Astot, C., et al.** (2004). Auxin regulation of cytokinin biosynthesis in *Arabidopsis thaliana*: a factor of potential importance for auxin-cytokinin-regulated development. *Proc Natl Acad Sci U S A* 101(21), 8039-8044.
- Osmont, K.S., Sibout, R., and Hardtke, C.S.** (2007). Hidden branches: developments in root system architecture. *Annu Rev Plant Biol* 58, 93-113.
- Peret, B., De Rybel, B., Casimiro, I., Benkova, E., Swarup, R., et al.** (2009). *Arabidopsis* lateral root development: an emerging story. *Trends Plant Sci* 14(7), 399-408.
- Perez-Torres, C.A., Lopez-Bucio, J., Cruz-Ramirez, A., Ibarra-Laclette, E., Dharmasiri, S., et al.** (2008). Phosphate availability alters lateral root development in *Arabidopsis* by modulating auxin sensitivity via a mechanism involving the TIR1 auxin receptor. *Plant Cell* 20(12), 3258-3272.
- Perilli, S., Di Mambro, R., and Sabatini, S.** (2012). Growth and development of the root apical meristem. *Curr Opin Plant Biol* 15(1), 17-23.
- Petersson, S.V., Johansson, A.I., Kowalczyk, M., Makoveychuk, A., Wang, J.Y., et al.** (2009). An auxin gradient and maximum in the *Arabidopsis* root apex shown by high-resolution cell-specific analysis of IAA distribution and synthesis. *Plant Cell* 21(6), 1659-1668.
- Petrasek, J., and Friml, J.** (2009). Auxin transport routes in plant development. *Development* 136(16), 2675-2688.
- Pfennig, D.W., Wund, M.A., Snell-Rood, E.C., Cruickshank, T., Schlichting, C.D., et al.** (2010). Phenotypic plasticity's impacts on diversification and speciation. *Trends Ecol Evol* 25(8), 459-467.
- Prusinkiewicz, P., Crawford, S., Smith, R.S., Ljung, K., Bennett, T., et al.** (2009). Control of bud activation by an auxin transport switch. *Proc Natl Acad Sci U S A* 106(41), 17431-17436.
- Rahman, A., Hosokawa, S., Oono, Y., Amakawa, T., Goto, N., et al.** (2002). Auxin and ethylene response interactions during *Arabidopsis* root hair development dissected by auxin influx modulators. *Plant Physiol* 130(4), 1908-1917.
- Rahman, A., Takahashi, M., Shibasaki, K., Wu, S., Inaba, T., et al.** (2010). Gravitropism of *Arabidopsis thaliana* roots requires the polarization of PIN2 toward the root tip in

meristematic cortical cells. *Plant Cell* 22(6), 1762-1776.

- Rani, K., Zwanenburg, B., Sugimoto, Y., Yoneyama, K., and Bouwmeester, H.J.** (2008). Biosynthetic considerations could assist the structure elucidation of host plant produced rhizosphere signalling compounds (strigolactones) for arbuscular mycorrhizal fungi and parasitic plants. *Plant Physiol Biochem* 46(7), 617-626.
- Rasmussen, A., Beveridge, C.A., and Geelen, D.** (2012a). Inhibition of strigolactones promotes adventitious root formation. *Plant Signal Behav* 7(6), 694-697.
- Rasmussen, A., Mason, M.G., De Cuyper, C., Brewer, P.B., Herold, S., et al.** (2012b). Strigolactones suppress adventitious rooting in *Arabidopsis* and pea. *Plant Physiol* 158(4), 1976-1987.
- Reed, R.C., Brady, S.R., and Muday, G.K.** (1998). Inhibition of auxin movement from the shoot into the root inhibits lateral root development in *Arabidopsis*. *Plant Physiol* 118(4), 1369-1378.
- Renton, M., Hanan, J., Ferguson, B.J., and Beveridge, C.A.** (2012). Models of long-distance transport: how is carrier-dependent auxin transport regulated in the stem? *New Phytol* 194(3), 704-715.
- Ruberti, I., Sessa, G., Ciolfi, A., Possenti, M., Carabelli, M., et al.** (2012). Plant adaptation to dynamically changing environment: The shade avoidance response. *Biotech Adv* 30(5), 1047-1058.
- Ruyter-Spira, C., Al-Babili, S., van der Krol, S., and Bouwmeester, H.** (2013). The biology of strigolactones. *Trends Plant Sci* 18(2), 72-83.
- Ruyter-Spira, C., Kohlen, W., Charnikhova, T., van Zeijl, A., van Bezouwen, L., et al.** (2011). Physiological effects of the synthetic strigolactone analog GR24 on root system architecture in *Arabidopsis*: another belowground role for strigolactones? *Plant Physiol* 155(2), 721-734.
- Sachs, T.** (1968). On the determination of the pattern of vascular tissue in peas. *Ann Bot* 32(4), 781-790.
- Sachs, T.** (1981). The control of the patterned differentiation of vascular tissues. *Adv Bot Res* 9, 151-262.
- Santner, A., Calderon-Villalobos, L.I., and Estelle, M.** (2009). Plant hormones are versatile chemical regulators of plant growth. *Nat Chem Biol* 5(5), 301-307.
- Sassi, M., Lu, Y., Zhang, Y., Wang, J.Y., Dhonukshe, P., et al.** (2012). COP1 mediates the coordination of root and shoot growth by light through modulation of PIN1- and PIN2-dependent auxin transport in *Arabidopsis*. *Development* 139(18), 3402-3412.
- Sauer, M., Balla, J., Luschnig, C., Wisniewska, J., Reinohl, V., et al.** (2006). Canalization of auxin flow by Aux/IAA-ARF-dependent feedback regulation of PIN polarity. *Genes Dev* 20(20), 2902-2911.
- Scarpella, E., Francis, P., and Berleth, T.** (2004). Stage-specific markers define early steps of procambium development in *Arabidopsis* leaves and correlate termination of vein formation with mesophyll differentiation. *Development* 131(14), 3445-3455.
- Scarpella, E., Marcos, D., Friml, J., and Berleth, T.** (2006). Control of leaf vascular pat-

turning by polar auxin transport. *Genes Dev* 20(8), 1015-1027.

**Shen, H., Luong, P., and Huq, E.** (2007). The F-box protein MAX2 functions as a positive regulator of photomorphogenesis in *Arabidopsis*. *Plant Physiol* 145(4), 1471-1483.

**Shen, H., Zhu, L., Bu, Q.Y., and Huq, E.** (2012). MAX2 affects multiple hormones to promote photomorphogenesis. *Mol Plant* 5(3), 750-762.

**Shinohara, N., Taylor, C., and Leyser, O.** (2013). Strigolactone can promote or inhibit shoot branching by triggering rapid depletion of the auxin efflux protein PIN1 from the plasma membrane. *PLoS Biol* 11(1), e1001474.

**Simons, J.L., Napoli, C.A., Janssen, B.J., Plummer, K.M., and Snowden, K.C.** (2007). Analysis of the DECREASED APICAL DOMINANCE genes of petunia in the control of axillary branching. *Plant Physiol* 143(2), 697-706.

**Snowden, K.C., Simkin, A.J., Janssen, B.J., Templeton, K.R., Loucas, H.M., et al.** (2005). The *decreased apical dominance1/Petunia hybrida CAROTENOID CLEAVAGE DIOXYGENASE8* gene affects branch production and plays a role in leaf senescence, root growth, and flower development. *Plant Cell* 17(3), 746-759.

**Sorefan, K., Booker, J., Haurogne, K., Goussot, M., Bainbridge, K., et al.** (2003). *MAX4* and *RMS1* are orthologous dioxygenase-like genes that regulate shoot branching in *Arabidopsis* and pea. *Genes Dev* 17(12), 1469-1474.

**Stirnberg, P., Furner, I.J., and Ottoline Leyser, H.M.** (2007). MAX2 participates in an SCF complex which acts locally at the node to suppress shoot branching. *Plant J* 50(1), 80-94.

**Stirnberg, P., van de Sande, K., and Leyser, H.M.O.** (2002). *MAX1* and *MAX2* control shoot lateral branching in *Arabidopsis*. *Development* 129(5), 1131-1141.

**Sugimoto, Y., Ali, A.M., Yabuta, S., Kinoshita, H., Inanaga, S., et al.** (2003). Germination strategy of *Striga hermonthica* involves regulation of ethylene biosynthesis. *Physiol Plant* 119(1), 137-145.

**Svistoonoff, S., Creff, A., Reymond, M., Sigoillot-Claude, C., Ricaud, L., et al.** (2007). Root tip contact with low-phosphate media reprograms plant root architecture. *Nat Genet* 39(6), 792-796.

**Swarup, K., Benkova, E., Swarup, R., Casimiro, I., Peret, B., et al.** (2008). The auxin influx carrier LAX3 promotes lateral root emergence. *Nat Cell Biol* 10(8), 946-954.

**Tanaka, M., Takei, K., Kojima, M., Sakakibara, H., and Mori, H.** (2006). Auxin controls local cytokinin biosynthesis in the nodal stem in apical dominance. *Plant J* 45(6), 1028-1036.

**Tanimoto, M., Roberts, K., and Dolan, L.** (1995). Ethylene is a positive regulator of root hair development in *Arabidopsis thaliana*. *Plant J* 8(6), 943-948.

**Tao, Y., Ferrer, J.L., Ljung, K., Pojer, F., Hong, F., et al.** (2008). Rapid synthesis of auxin via a new tryptophan-dependent pathway is required for shade avoidance in plants. *Cell* 133(1), 164-176.

**Toh, S., Kamiya, Y., Kawakami, N., Nambara, E., McCourt, P., et al.** (2012). Thermoinhibition uncovers a role for strigolactones in *Arabidopsis* seed germination. *Plant Cell*

*Physiol* 53(1), 107-117.

- Tsuchiya, Y., Vidaurre, D., Toh, S., Hanada, A., Nambara, E., et al.** (2010). A small-molecule screen identifies new functions for the plant hormone strigolactone. *Nat Chem Biol* 6(10), 741-749.
- Turnbull, C.G., Booker, J.P., and Leyser, H.M.** (2002). Micrografting techniques for testing long-distance signalling in *Arabidopsis*. *Plant J* 32(2), 255-262.
- Umehara, M., Hanada, A., Magome, H., Takeda-Kamiya, N., and Yamaguchi, S.** (2010). Contribution of strigolactones to the inhibition of tiller bud outgrowth under phosphate deficiency in rice. *Plant Cell Physiol* 51(7), 1118-1126.
- Umehara, M., Hanada, A., Yoshida, S., Akiyama, K., Arite, T., et al.** (2008). Inhibition of shoot branching by new terpenoid plant hormones. *Nature* 455(7210), 195-200.
- Ursache, R., Nieminen, K., and Helariutta, Y.** (2013). Genetic and hormonal regulation of cambial development. *Physiol Plant* 147(1), 36-45.
- Wang, Q., Zhu, Z., Ozkardesh, K., and Lin, C.** (2013). Phytochromes and phytohormones: The shrinking degree of separation. *Mol Plant* 6(1), 5-7.
- Wang, X., Du, G., Wang, X., Meng, Y., Li, Y., et al.** (2010). The function of *LPR1* is controlled by an element in the promoter and is independent of SUMO E3 ligase SIZ1 in response to low Pi stress in *Arabidopsis thaliana*. *Plant Cell Physiol* 51(3), 380-394.
- Waters, M.T., Brewer, P.B., Bussell, J.D., Smith, S.M., and Beveridge, C.A.** (2012a). The *Arabidopsis* ortholog of rice *DWARF27* acts upstream of *MAX1* in the control of plant development by strigolactones. *Plant Physiol* 159(3), 1073-1085.
- Waters, M.T., Nelson, D.C., Scaffidi, A., Flematti, G.R., Sun, Y.K., et al.** (2012b). Specialisation within the *DWARF14* protein family confers distinct responses to karrikins and strigolactones in *Arabidopsis*. *Development* 139(7), 1285-1295.
- Waters, M.T., and Smith, S.M.** (2013). *KAI2*- and *MAX2*-mediated responses to karrikins and strigolactones are largely independent of *HY5* in *Arabidopsis* seedlings. *Mol Plant* 6(1), 63-75.
- Williamson, L.C., Ribrioux, S.P.C.P., Fitter, A.H., and Leyser, H.M.O.** (2001). Phosphate availability regulates root system architecture in *Arabidopsis*. *Plant Physiol* 126(2), 875-882.
- Wisniewska, J., Xu, J., Seifertova, D., Brewer, P.B., Ruzicka, K., et al.** (2006). Polar PIN localization directs auxin flow in plants. *Science* 312(5775), 883.
- Wu, G., Lewis, D.R., and Spalding, E.P.** (2007). Mutations in *Arabidopsis* multidrug resistance-like ABC transporters separate the roles of acropetal and basipetal auxin transport in lateral root development. *Plant Cell* 19(6), 1826-1837.
- Xie, X., Yoneyama, K., and Yoneyama, K.** (2010). The strigolactone story. *Annu Rev Phytopathol* 48, 93-117.
- Xu, M., Zhu, L., Shou, H., and Wu, P.** (2005). A PIN1 family gene, *OsPIN1*, involved in auxin-dependent adventitious root emergence and tillering in rice. *Plant Cell Physiol* 46(10), 1674-1681.
- Yamamoto, Y., Kamiya, N., Morinaka, Y., Matsuoka, M., and Sazuka, T.** (2007). Auxin

biosynthesis by the *YUCCA* genes in rice. *Plant Physiol* 143(3), 1362-1371.

**Ye, Z.H., Freshour, G., Hahn, M.G., Burk, D.H., and Zhong, R.** (2002). Vascular development in *Arabidopsis*. *Int Rev Cytol* 220, 225-256.

**Yoneyama, K., Xie, X., Kusumoto, D., Sekimoto, H., Sugimoto, Y., et al.** (2007). Nitrogen deficiency as well as phosphorus deficiency in sorghum promotes the production and exudation of 5-deoxystrigol, the host recognition signal for arbuscular mycorrhizal fungi and root parasites. *Planta* 227(1), 125-132.

**Yoshida, S., Kameoka, H., Tempo, M., Akiyama, K., Umehara, M., et al.** (2012). The D3 F-box protein is a key component in host strigolactone responses essential for arbuscular mycorrhizal symbiosis. *New Phytol* 196(4), 1208-1216.

**Zazimalova, E., Murphy, A.S., Yang, H.B., Hoyerova, K., and Hosek, P.** (2010). Auxin transporters - why so many? *Cold Spring Harb Perspect Biol* 2(3), a001552.

**Zhong, R., and Ye, Z.H.** (2001). Alteration of auxin polar transport in the *Arabidopsis ifl1* mutants. *Plant Physiol* 126(2), 549-563.

**Zou, J., Zhang, S., Zhang, W., Li, G., Chen, Z., et al.** (2006). The rice *HIGH-TILLERING DWARF1* encoding an ortholog of *Arabidopsis MAX3* is required for negative regulation of the outgrowth of axillary buds. *Plant J* 48(5), 687-698.

**Zwanenburg, B., and Pospisil, T.** (2013). Structure and activity of strigolactones: new plant hormones with a rich future. *Mol Plant* 6(1), 38-62.







## The tomato *MAX1* homolog-*SIMAX1* - is involved in the conversion of carlactone to orobanchol

### Authors:

Yanxia Zhang<sup>1,‡</sup>, Xi Cheng<sup>1,a</sup>, Yanting Wang<sup>1,a</sup>, Kristyna Flokova<sup>1,†</sup>, Carmen Díez-Simón<sup>1</sup>, Andrea Bimbo<sup>1</sup>, Harro J. Bouwmeester<sup>1,†,\*</sup>, Carolien Ruyter-Spira<sup>1</sup>

### Affiliations:

<sup>1</sup> Laboratory of Plant Physiology, Wageningen UR, P.O. Box 658, 6700 AR Wageningen, the Netherlands

<sup>a</sup> These authors contributed equally to this work.

<sup>‡</sup> Current address: Plant Cell Biology, Swammerdam Institute for Life Sciences, University of Amsterdam, Science Park 904, 1090 GE Amsterdam, The Netherlands

<sup>†</sup> Current address: Plant hormone biology, Swammerdam Institute for Life Sciences, University of Amsterdam, Science Park 904, 1098 XH Amsterdam, The Netherlands

\* Correspondence: [h.j.bouwmeester@uva.nl](mailto:h.j.bouwmeester@uva.nl), tel. +31 6 20387674

### Abstract

Strigolactones (SLs) are rhizosphere signalling molecules exuded by plants that induce seed germination of root parasitic weeds and hyphal branching of arbuscular mycorrhizal fungi. They are also phytohormones regulating plant architectures. *MORE AXILLARY GROWTH 1 (MAX1)* and its homologs encode cytochrome P450 enzymes that catalyse the conversion of the strigolactone precursor carlactone to canonical strigolactones in rice, and to a SL-like compound in *Arabidopsis*. In this study, we characterized the tomato *MAX1* homolog, *SIMAX1*. Targeting Induced Local Lesions in Genomes (TILLING) was used to obtain *Simax1* mutants, which exhibited strongly reduced production of strigolactones (orobanchol, solanacol and didehydro-orobanchol isomers). This resulted in a severe mutant phenotype in vegetative and reproductive development. Transient expression of *SIMAX1* in *N. benthamiana* showed that *SIMAX1* catalyses the formation of carlactonic acid from carlactone. *In vivo* plant feeding assays showed that carlactone, but not 4-deoxy-orobanchol, is the precursor of orobanchol, which in turn is the precursor of solanacol and two of the three didehydro-orobanchol isomers. The third seems to be derived from *epi*-orobanchol. Inhibitor studies suggest that an oxoglutarate-dependent dioxygenase is involved in orobanchol biosynthesis from carlactonic acid and cytochrome P450s in the formation of solanacol and didehydro-orobanchol isomers from orobanchol in tomato.

### 5

### Key Words

Cytochrome P450 (CYP450), *MORE AXILLARY GROWTH 1 (MAX1)*, didehydro-orobanchol isomers, orobanchol, tomato, strigolactones **Introduction**

## Introduction

Strigolactones (SLs) were originally discovered as rhizosphere signalling molecules secreted by plants into the soil that stimulate seed germination of root parasitic plants of the *Orobanchaceae* (*Striga*, *Phelipanche* and *Orobanche* genera) (Cook *et al.*, 1966). Many years later they were demonstrated to promote hyphal branching of beneficial arbuscular mycorrhizal fungi (AMF) (Cook *et al.*, 1966; Akiyama *et al.*, 2005). Recently, they were identified as a new class of phytohormones regulating plant architecture, including shoot branching and several aspects of root development (Gomez-Roldan *et al.*, 2008; Umehara *et al.*, 2008; Ruyter-Spira *et al.*, 2011; Kapulnik and Koltai, 2014; Sun *et al.*, 2015). Interestingly, in and between plant species there is extensive variation in the decoration of in the typical SL structure of which the backbone consists of a butenolide D-ring attached to a tricyclic ABC-lactone ring. The SLs are distributed into two groups: the orobanchol and the strigol type (Zwanenburg and Pospisil, 2013a). More recently, non-canonical SL-LIKE structures with a non-cyclized BC-ring were discovered in *Arabidopsis* and sunflower, namely methyl carlactonoate (MeCLA) and heliolactone (Abe *et al.*, 2014; Ueno *et al.*, 2014). The different SL and SL-LIKE molecules may all display different activities with regard to the stimulation of parasitic plant seed germination, AMF hyphal branching or the inhibition of plant axillary bud outgrowth (Akiyama *et al.*, 2010; Boyer *et al.*, 2012; Nomura *et al.*, 2013; Zwanenburg and Pospisil, 2013a). However, to better understand the biological significance of all the different SLs, manipulation of their content would be desirable, for which knowledge of their biosynthetic pathway is required.

The biosynthesis of SLs has been partially unraveled, with the identification of a number of enzymes that were characterized in several plant species. More than a decade ago, genetics studies in *Arabidopsis* showed that *MORE AXILLARY GROWTH 1* (*MAX1*), *MORE AXILLARY GROWTH 3* (*MAX3*) and *MORE AXILLARY GROWTH 4* (*MAX4*) are required for the biosynthesis of a shoot branching inhibiting signal which was later shown to be strigolactone (Stirnberg *et al.*, 2002; Sorefan *et al.*, 2003; Booker *et al.*, 2004; Booker *et al.*, 2005; Gomez-Roldan *et al.*, 2008; Umehara *et al.*, 2008). The homologs of *MAX3* and *MAX4* were characterized also in rice (*DWARF 17* and *DWARF 10*), pea (*RAMOSUS 5* and *RAMOSUS 1*) and petunia (*DECREASED APICAL DOMINANCE 3* and *DECREASED APICAL DOMINANCE 1*) (Morris *et al.*, 2001; Sorefan *et al.*, 2003; Zou *et al.*, 2006; Arite *et al.*, 2007; Simons *et al.*, 2007; Drummond *et al.*, 2009). *MAX3* and *MAX4* are encoding two *CAROTENOID CLEAVAGE DIOXYGENASEs* 7

and 8 (*CCD7* and *CCD8*), respectively. Together with a  $\beta$ -carotene isomerase, *DWARF 27* (*D27*), these three genes are catalyzing the conversion of  $\beta$ -carotene to the C19 SL precursor, carlactone (CL) (Lin *et al.*, 2009; Alder *et al.*, 2012). The gene acting downstream of CL, which should encode the formation of a SL from CL, was unclear although a cytochrome P450 (CYP), encoded by *MAX1*, was postulated to be involved in the required cyclization of CL and the lactone ring formation, typical for the SLs (Booker *et al.*, 2005; Alder *et al.*, 2012). Recent studies showed that CL can be oxidized by *MAX1* homologs from *Arabidopsis* (*AtMAX1*) and rice (*Os900*) to carlactonoic acid (CLA) and 4-deoxyorobanchol (4DO), respectively (Abe *et al.*, 2014; Seto *et al.*, 2014; Zhang *et al.*, 2014). Intriguingly, *MAX1* in monocots and certain dicot species usually occurs in multiple copies (Challis *et al.*, 2013). For example, there are five *MAX1*s in rice with one of the most divergent members - *Os1400* - encoding the orobanchol synthase catalysing orobanchol formation from 4DO (Zhang *et al.*, 2014). The major function of other rice *MAX1* homologs is not entirely clear, and they might be involved in the formation of the other SLs reported in rice or SL precursors (Abe *et al.*, 2014) Jamil *et al.*, 2012; Seto *et al.*, 2014; Zhang *et al.*, 2014). In contrast, in many dicot species such as *Arabidopsis*, *MAX1* exists as one copy (Challis *et al.*, 2013).

In tomato, there is also only one *MAX1* homolog present (hereafter called *SIMAX1*) according to the public tomato genomic database (Sol Genomics Network: <https://solgenomics.net/>), but the molecular function of *SIMAX1* is uncharacterized. On the basis of the biochemical function of *MAX1* in rice and *Arabidopsis* (Abe *et al.*, 2014; Zhang *et al.*, 2014), we hypothesized that *SIMAX1* is required for the oxidation of the SL precursor CL. However, there are great differences between *Arabidopsis* and tomato in the reported SL profiles. In tomato, many different SLs such as orobanchol, solanacol, several dihydro-orobanchol (DDH) isomers, orobanchyl acetate, 7-oxoorobanchol and 7-hydroxyorobanchol were identified (Koltai *et al.*, 2010; Vogel *et al.*, 2010; Kohlen *et al.*, 2012; Kohlen *et al.*, 2013). The two basic SL pathway enzymes *CCD7* and *CCD8* have been characterized in tomato (Vogel *et al.*, 2010; Kohlen *et al.*, 2012). However, the biochemical mechanism by which SL diversification in tomato is created remains elusive. In the present study, we use a tomato *max1* mutant to show that *SIMAX1* is required for the oxidation of CL to form orobanchol likely via CLA. In addition, we provide evidence that one of the main dihydro-orobanchol isomers (DDH1) is a strigol-type SL - implying that there are both orobanchol-type and strigol-type SLs present in tomato - and that solanacol and one of the other predominant dihydro-orobanchol isomers (DDH2) are formed from orobanchol.

### Materials and Methods

#### Plant growth conditions and treatments

Targeting Induced Local Lesions in Genomes (TILLING) was carried out to obtain the mutants of *SIMAX1* - *SImax1* by using a cultivated wild-type tomato cultivar as described (Kurowska *et al.*, 2011). The mutation of *SIMAX1* was confirmed by PCR and sequencing. Two M3 *SImax1* homozygous lines 13539-02 and 13539-03, containing a pre-mature stop codon in the genomic sequence (at position +466), were used in this study.

For phenotype characterization of young seedlings, germinated wild-type and *SImax1* seeds (13539-02 and 13539-03) were grown in trays filled with vermiculite. After 10 days, photos were taken of the roots of these young seedlings to perform further image analysis of hypocotyl and root phenotypes.

To characterize the phenotype of adult plants, pre-germinated plants were transferred to pots containing a mixture of soil and vermiculite (2:1) and grown under 16/8h photoperiod at 25°C (60% humidity) in the greenhouse. After 10 weeks, number and length/diameter of nodes, shoot branches, flowers and fruits were scored and measured.

To examine the SL levels, pre-germinated wild-type and *SImax1* (13539-02) seeds were grown on moistened vermiculites for one week under a 12h/ 12h photoperiod at 22°C. Young seedlings were then grown hydroponically for another week to get sufficient root development before they were moved to an X-stream 20 aeroponics system (Nutriculture, Lancashire, UK) in the greenhouse (16h/ 8h photoperiod, 25°C/ 22°C, 60% humidity). The plants were continuously supplied with ½ strength Hoagland solution for 18 days after which phosphorus (P) deficiency (by using 1/2 strength Hoagland solution without phosphorus) was applied to induce the production of SLs (Lopez-Raez *et al.*, 2008). Root exudates of wild-type tomato and the *SImax1* mutant were collected every day during phosphorus deficiency treatment. After 15 days of P-starvation, plant roots were harvested, frozen in liquid nitrogen and stored at -80°C for further analysis. Four plants were pooled as one biological replicate.

For gene expression analysis, wild-type and *SImax1* tomato seeds were pre-germinated in darkness at 25°C for 4 days. Seedlings were transferred to rockwool or water-agar blocks in an Eppendorf vial from which the bottom was cut and grown in hydroponic trays supplied with 1/2 strength

Hoagland solution under 16/8h photoperiod at 25°C in the greenhouse for 3 weeks followed by a one-week phosphorus deficiency treatment. During this treatment, roots and several other tissues were collected at different time intervals (day 3, day 5, and day 7) for further analysis.

### Biosynthetic intermediate feeding assays

Biosynthetic intermediate feeding assays with 4-deoxyorobanchol (4DO), carlactone and orobanchol isomers (orobanchol and *ent*-2'-*epi*-orobanchol) were carried out on 18-day old plants according to a previously published protocol with modifications (Motonami *et al.*, 2013). The plants were pre-grown in 1/2 strength Hoagland solution (under 16/ 8h photoperiod, 25°C, 60% humidity) for 14 days. Then they were grown in tap water (to mimic the P-starvation) supplemented with 1  $\mu$ M fluridone (the inhibitor of phytoene desaturase, a key-step in carotenoid biosynthesis) (Matusova *et al.*, 2005), which effectively inhibits SL biosynthesis. After 3 days, the plants were transferred to fresh tap water (containing again 1  $\mu$ M fluridone) supplemented with the CL or SLs (at the required concentration). The plant root exudates were collected after 24 h feeding and concentrated through a C18-fast column (Grace, 500 mg/3mL). All substrate SLs, CL, 4DO and two orobanchol isomers (orobanchol and *ent*-2'-*epi*-orobanchol) were applied with the same concentrations (0.05  $\mu$ M) separately to plants in the same developmental stage. Enzyme inhibitors, uniconazole-P and prohexadione, were applied at 50  $\mu$ M. All chemicals and SLs with the exception of uniconazole-P were prepared in a master stock in acetone with the exception of uniconazole-P that was dissolved in DMSO, before they were diluted for the treatment and the control plants were treated with an equal amount of acetone/DMSO. Three to five biological replicates were used for each treatment. Two plants were pooled for each biological replicate.

### Molecular cloning

The cDNA sequences of *SID27*, *SICCD7*, *SICCD8* and *SIMAX1* were obtained from SGN (Sol Genomics Network: <https://solgenomics.net/>) by using protein sequences of the *Arabidopsis* homologs as baits (tblastn) or from previously published reports (**Table S1**) (Kohlen *et al.*, 2012). Primers were designed to clone the full-length genes from cDNA of tomato M82 (**Table S2**). Cloning for agro-infiltration was conducted as previously described into a pBIN19-plus binary vector (Zhang *et al.*, 2014). Primers were designed with restriction sites included (**Table S2**).

## Gene expression analysis

Total RNA was extracted using TriPure isolation reagent (Sigma) combined with a Qiagen RNeasy mini kit following the manufacture's manual. For all samples 800 ng total RNA was used to synthesize cDNA using the iScript cDNA Synthesis kit (Bio-Rad). Real-time qPCR was performed with the CFX Connect Real-Time PCR Detection System (Bio-Rad) using primers as shown in **Table S2**. Tomato housekeeping genes were selected based on the stability as previously described (Dekkers *et al.*, 2012). Relative expression of transcripts in different plant tissues was normalized to the average expression level of two housekeeping genes as listed in **Table S2**. To compare gene expression in wild-type and mutants/transgenic lines (*Slmax1* or *CCD8-RNAi* line), the expression levels were normalized to the expression levels in the wild-type plants.

## Transient expression in *Nicotiana benthamiana*

For transient expression, 4-week old *Nicotiana benthamiana* plants were used for agro-infiltration. The preparation of the *Agrobacterium* (AGL0) strains (OD=0.5) was performed as previously described (Zhang *et al.*, 2014). To compensate for differences in numbers of constructs per treatment, strains carrying empty vectors were used. The TBSV P19 gene was co-infiltrated to prevent gene silencing (Voinnet *et al.*, 2003). The bacterial suspension was injected into the abaxial side of the leaf by using a 1 mL syringe without needle. After 6 days, the infiltrated leaves were harvested and frozen into liquid nitrogen and stored at -80°C until further analysis. Six biological replicates were used for each gene combination.

## Plant hormone extraction and measurement

To analyse SL levels in the root exudates, the nutrient solution from aeroponically or hydroponically grown plants were concentrated using C18 columns (Grace, C18-fast/5000mg) as previously described (Kohlen *et al.*, 2012). SLs in root tissue and *N. benthamiana* leaves were extracted and further analysed by MRM-LC-MS/MS as previously described (Lopez-Raez *et al.*, 2011; Zhang *et al.*, 2014).

Carlactone detection in *N. benthamiana* leaves was carried out as previously described (Zhang *et al.*, 2014). For CLA analysis in *N. benthamiana* leaves, 500 mg fresh *N. benthamiana* leaves were ground and extracted with 4 mL ethyl acetate. Subsequently, the ethyl acetate was evaporated



with a speedvac until dryness, then the sample were re-dissolved in 100  $\mu$ L 50% acetonitrile (in MQ water) before injection. Then LC-MS profiling of crude plant extracts was performed as previously described (De Vos *et al.*, 2007), using an LC-Orbitrap-FTMS instrument consisting of an Acquity HPLC with PDA (photodiode array) detection (Waters) interfaced to an LTQ ion trap/Orbitrap hybrid mass spectrometer (Thermo Fisher Scientific) equipped with an ESI source (van der Hooft *et al.*, 2012). The sample injection volume was 5  $\mu$ L. A Luna RP-C18 analytical column (2.0 mm diameter, 150 mm length, 100 Å pore size and spherical particles of 3  $\mu$ m, Phenomenex, USA) was used for chromatographic separation. The mobile phase consisted of a binary eluent solvent system of degassed ultra-pure water (solvent A) and acetonitrile (solvent B), both containing 0.1% v/v formic acid, with a flow rate of 0.19 ml.min<sup>-1</sup> and a column temperature of 40°C. The HPLC gradient started at 5% B and linearly increased to 75% B across a period of 45 min. The column was re-equilibrated for 15 min following the separation of each sample. CLA further confirmation by the MRM-LC-MS/MS was done according to previously published with modifications (Zhang *et al.*, 2014) (Flokova *et al.*, 2016, unpublished).

### Software and statistics for data analysis

Image analysis of root phenotypes was performed by using ImageJ. Gene expression data analysis was done with Bio-Rad CFX Manager 3.0 combined with Microsoft Excel. Masslynx 4.1 software and Xcalibur software (combined with Microsoft Excel) were used for compound identification and quantification from MRM-LC-MS/MS and LC-orbitrap-FTMS, respectively. PCR efficiencies of qPCR were calculated using LinReg PCR software (Dekkers *et al.*, 2012). Statistical analysis was performed using one-way ANOVA of Prism (version 6.0) or student's t-test of Microsoft Excel.

### Results

#### The cloning and characterization of *SIMAX1*

A homology search approach was employed to get the DNA sequence of *SIMAX1*. Hereto the protein sequence of the *Arabidopsis MAX1* homolog was BLASTed against the SGN (Sol Genomics Network). The DNA sequence of *SIMAX1* is 3300 bp long and contains a coding region of 1560 bp (**Table S1**) (519 aa). A sequence alignment shows that *SIMAX1* has 72%, 62% and 64% amino acid identity with *AtMAX1* and the two functionally characterized rice *MAX1* homologs, *Os900* and *Os1400*, respectively (**Figure S1A**). *SIMAX1* is clustered into the dicot *MAX1* clade as indicated

by the phylogenetic alignment with *MAX1* homologs from other plant species including monocots and dicots plants (**Figure 1A**).

To characterize the biological function of *SIMAX1*, we obtained M3 homozygous mutant lines using Targeting Induced Local Lesions in Genomes (TILLING). This method allows the detection of point mutations, usually introduced through EMS treatment, in the genome sequence of the target genes, in this case *SIMAX1*. The mutant lines that were identified are carrying a pre-mature stop codon in the genomic sequences (G → T at position +466bp downstream of the transcription start site) (**Figure S1B**). Two independent homozygous lines carrying this mutation were obtained and they exhibited an average 90% reduction in *SIMAX1* transcripts levels compared with the wild-type tomato plants (**Figure S1C**).

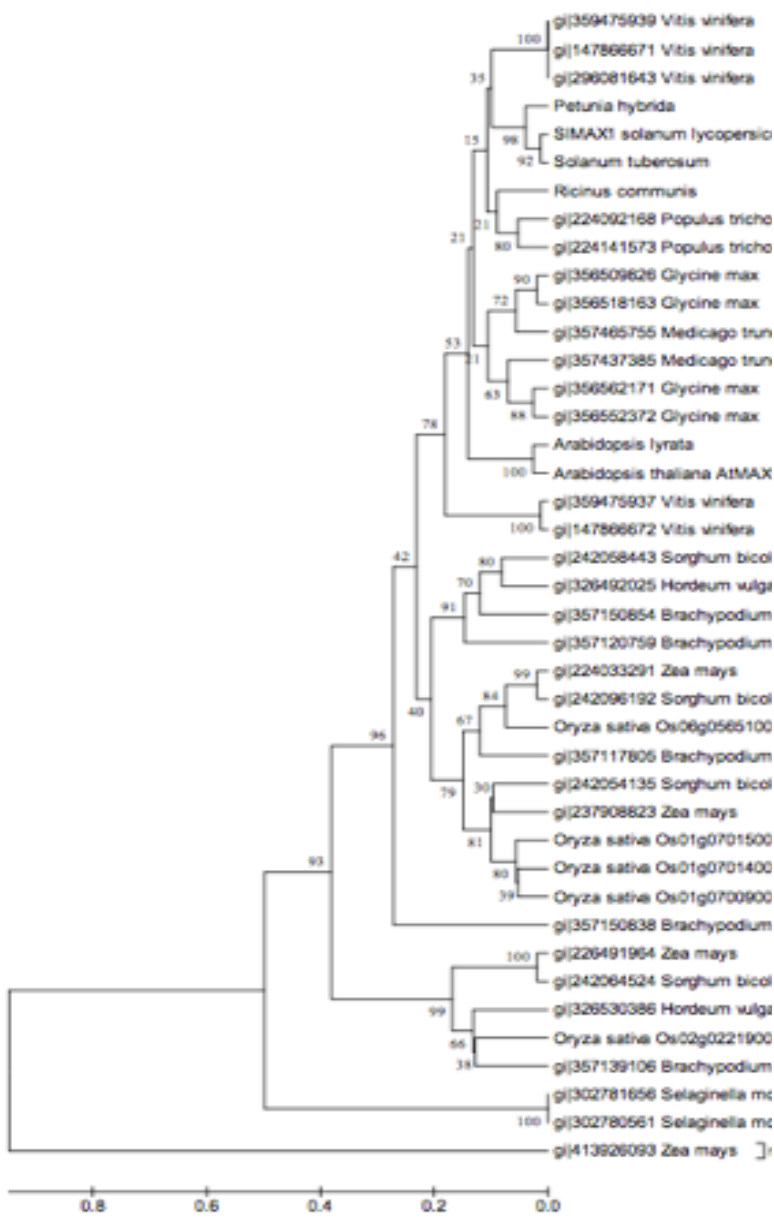


**Figure 1. Phylogenetic relationship of MAX1 homologs from different plant species.** The phylogeny was inferred using the UPGMA method. The optimal tree with the sum of branch length = 6.1112455 is shown. The percentage of replicate trees in which the associated taxa clustered together in the bootstrap test (500 replicates) are shown next

to the branches. The tree is drawn to scale, with branch lengths in the same units as those of the evolutionary distances used to infer the phylogenetic tree. The evolutionary distances were computed using the Poisson correction method (Rosset, 2007) and are in the units of the number of amino acid substitutions per site. The analysis involved 41 amino acid sequences. All positions containing gaps and missing data were eliminated. There were a total of 80 positions in the final dataset. Evolutionary analyses were conducted in MEGA6.

### The mutation of *SIMAX1* reduces strigolactone production

*MAX1* homologs in both *Arabidopsis* and rice have been shown to be involved in the production of non-canonical (MeCLA) and canonical SLs (4DO and orobanchol) (Abe *et al.*, 2014; Zhang *et al.*, 2014). To gain insight into whether *SIMAX1* is playing a role in the biosynthesis of SLs in tomato, we analysed the SL content of both wild-type tomato and the *simax1* mutant. We pre-grew both genotypes aeroponically with 100% P before a P-starvation treatment was applied to induce the production of SLs and then examined SL levels in the root exudates constantly for several days, starting from the 11<sup>th</sup> until the 15<sup>th</sup> day of P-starvation. In the root exudates and root extracts of wild-type tomato, solanacol, orobanchol and three isomers of DDH were detected (**Figure 2A, B and Figure S2A**), while there were hardly any detectable SLs in both root extracts and root exudates of the *Simax1* mutants (**Figure 2A, B**). These data are clearly demonstrating that *SIMAX1* is a key enzyme in the biosynthesis of the tomato SLs.

Consistent with what was previously described (Kohlen *et al.*, 2013), the three DDH isomers - DDH1, DDH2, and DDH3- exhibit a different pattern in the root exudates and root extracts (**Figure S2A**). DDH1 is predominantly present in the exudate (**Figure S2B**), while in the root extract its level is much lower than that of DDH2 (**Figure S2C**). The amount of DDH3 is much less in both root exudate and root extract is much lower than that of DDH1 and DDH2 (**Figure S2B, C**).

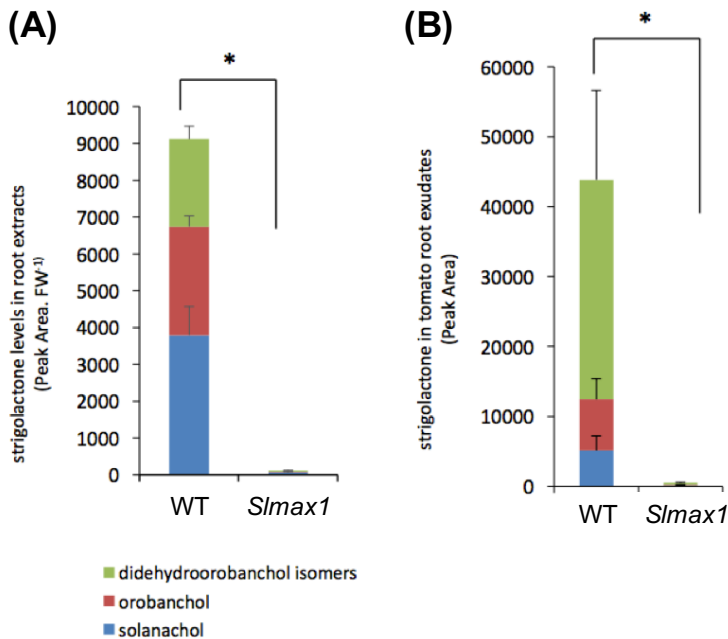


**Figure 2. Strigolactone accumulation in wild-type tomato and *Slmax1* mutant after P-starvation.** (A) The level of strigolactones (solanachol, orobanchol and didehydro-orobanchol isomers) in the root extracts after 15 days of P-starvation (n=3). The Y axis shows the peak area from MRM-LC-MS/MS analysis corrected by sample fresh weight. (B) The level of solanachol, orobanchol and didehydroorobanchol isomers in the root exudates of tomato plants combining the collections of day 11 through day 15 after P-starvation (n=3). The Y axis is representing the peak area from MRM-LC-MS/MS analysis. The green, red and blue bars represent the production of didehydroorobachol isomers, orobanchol and solanachol, respectively. Error bars represent means ± SEM. \* indicates the significant difference at 0.01 < P < 0.05 evaluated by student's t-test.

## ***SIMAX1* mutation results in alterations in plant architecture and development**

To examine the effect of the *SIMAX1* mutation on plant architecture and development, plant phenotypic data at different developmental stages were recorded for *Slmax1* mutants and corresponding wild-type plants. Growth of the *Slmax1* lines was impaired compared with the wild-type tomato plants (**Figure 3A**). *Slmax1* lines (13539-02 and 13539-03) exhibit significantly increased branch numbers (5.75 to 7.25-fold higher than that in

the wild-type) and average lateral branch length (27.8 to 58-fold longer than in the wild type) compared with the wild-type plants (**Figure 3B, C**). To gain more insights into how *SIMAX1* regulates the shoot architecture of tomato, the stem length and number of internodes were scored. Wild-type plants showed significantly longer stem length (1.9 to 2.7-fold longer than in *Slmax1* mutants) with fewer internodes (10% less than in *Slmax1* mutants) (**Figure 3D and S3A**). The mutant line 13539-02 exhibited a reduction in total root length (decreased by 23%) and average lateral root length (decreased by 30%) during the seedling stage (**Figure S3B and C**). The mutation in *SIMAX1* also caused defects in the reproductive stage of the plants and results in reduced flower length and fruit size in the *Slmax1* mutant (**Figure 3E and Figure S3D**).

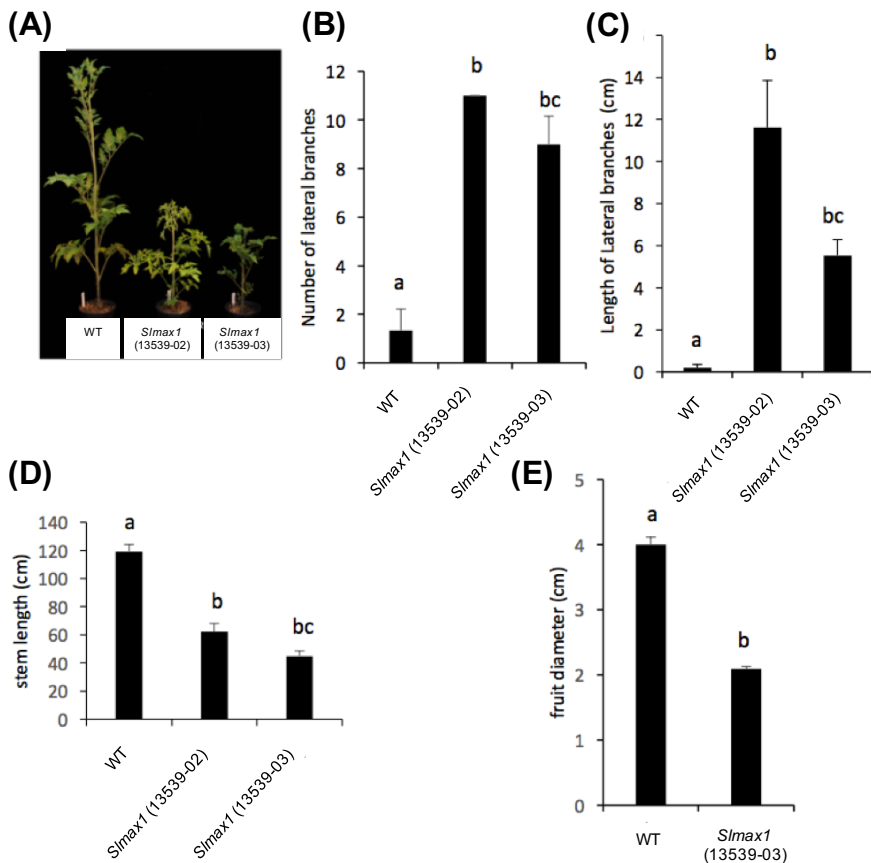


**Figure 3. Characterization of the plant phenotypes affected by *SIMAX1* mutation.** (A) Global plant phenotypes of *Slmax1* mutants (line

13539-02 and 13539-03) in comparison with the corresponding wild-type plant. (B) The average number of lateral branches of *SImax1* mutants and the wild-type (1st order, > 2mm) on 10-week old plants (n = 3). (C) The average length of lateral branches in *SImax1* mutants and wild-type plants (n = 3). (D) The average stem length of the wild-type and *SImax1* mutants (n = 3). (E) Diameters of mature red fruits of wild-type plants and *SImax1* mutants (n=14~21). Values in (B) through (E) are means  $\pm$  SEM. Data significance was determined by one-way ANOVA in Prism 6,  $P < 0.05$ .

### ***SIMAX1* expression is induced by phosphate starvation**

The expression of SL biosynthetic genes was shown to respond to P deficiency in several plant species (Umehara *et al.*, 2010; Liu *et al.*, 2015; van Zeijl *et al.*, 2015). We analysed the expression of *SIMAX1* and the SL biosynthetic genes upstream (*SID27*, *SICCD7*, *SICCD8*) under P-starvation in tomato. Initially, we checked the expression of the phosphate starvation marker gene *LePS2* (*Lycopersicon esculentum* phosphate starvation-induced gene) at different time intervals during the P deficiency treatment (3 days, 5 days and 7 days), which reveals the P-starvation status of the plant (Baldwin *et al.*, 2001). After 7 days of P-starvation, we observed a strong increase in *LePS2* expression in all the tested tissues (root, adventitious root, leaf and leaf petiole) except for the flower buds, which indicates the success of the P-starvation treatment (**Figure S4A and S4B**). At this time point, *SIMAX1* transcripts were up-regulated up to 1.8-fold in root tissue but not in other tested plant tissues (**Figure 4A**). The expression of *SIMAX1* was at least 3-fold lower in the leaves and flower buds than in the root and other tested tissues (adventitious root, stem and leaf petiole) under normal P conditions (**Figure 4A**). The expression of the three SL biosynthetic genes upstream of *SIMAX1* was also up-regulated by the P-starvation treatment in the roots and their expression was low or absent in leaf and flower bud (**Figure S4C-E**). However, unlike *SIMAX1*, expression of these three genes was also induced in adventitious roots and the stem by P-starvation (**Figure S4C-E**). In the leaf petiole, the expression of *SID27* was strongly induced by P-starvation, while expression of *SIMAX1*, *SICCD8* and *SICCD7* did not change in response to P-starvation (**Figure 4A and S4C-E**).

We were also interested in whether there is feedback regulation in the expression of the three upstream biosynthetic genes in the *SImax1* mutant. The expression of *SID27* and *SICCD7*, but not that of *CCD8* was up-regulated in the *SImax1* mutant by 90 and 153%, respectively, compared with wildtype after 7 days of P-starvation (**Figure 4B**). Furthermore, we



examined *SIMAX1* expression in the *CCD8*-RNAi line and corresponding wild-type (Kohlen *et al.*, 2012), and this showed that *SIMAX1* is significantly induced in the *CCD8*-RNAi line (**Figure S4F**). These data further support the involvement of *SIMAX1* in tomato SL biosynthesis together with *SID27*, *SICCD7* and *SICCD8*.

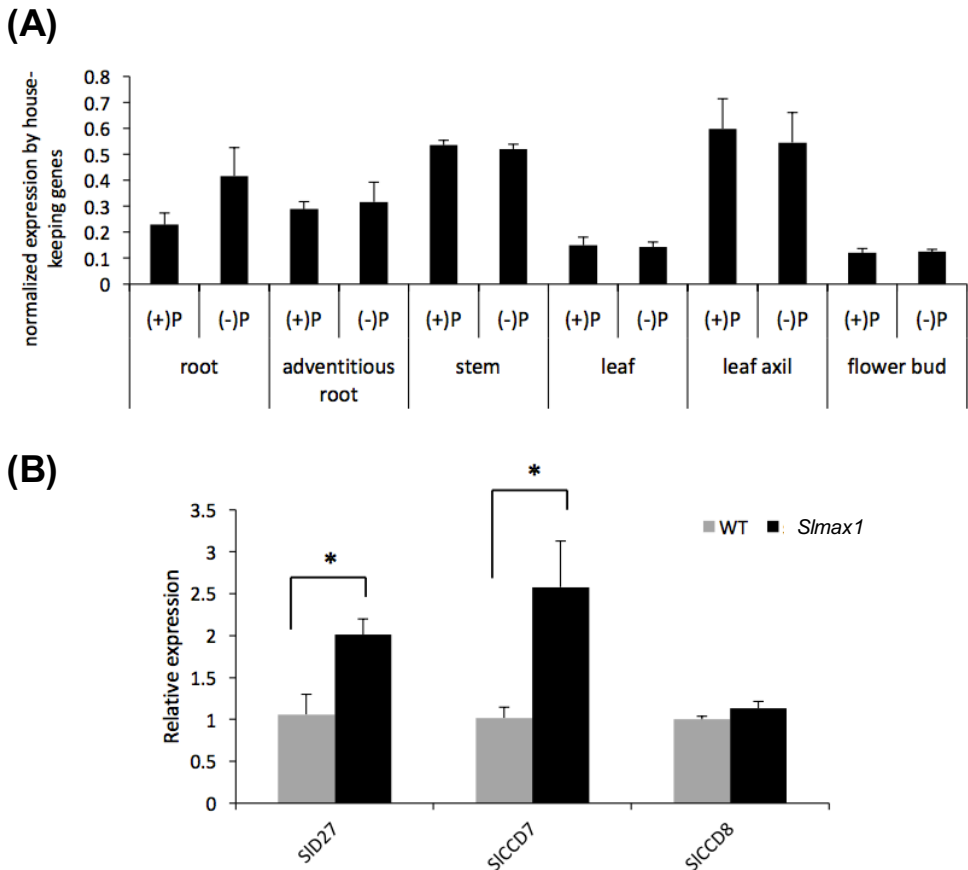


**Figure 4. Expression of *SIMAX1* in different tissues of wild-type tomato as affected by P-starvation and strigolactone biosynthetic genes upstream of *SIMAX1* in the *slmax1* mutant.** (A) Normalized gene expression of *SIMAX1* in different tissues of wild-type tomato under normal and P-starvation conditions (n=3). P-starvation was applied for 7 days. (B) Relative expression of strigolactone biosynthetic genes (*SID27*, *SICCD7* and *SICCD8*) in the roots of *slmax1* mutants after 7 days of P-starvation (n=3). The gene expression level in wild-type tomato was set to 1. Error bars represent means  $\pm$  SEM (\*,  $0.01 < P < 0.05$ ).

SGN-U584254 and SGN-U563892 are the two housekeeping genes used for normalization of target genes (Dekkers *et al.*, 2012).

### **SIMAX1 is involved in the oxidation of carlactone *in vivo* and *in vitro***

To further assess the role of *SIMAX1* in the SL biosynthetic pathway of tomato, we reconstituted the tomato SL biosynthetic pathway in *Nicotiana benthamiana*. Hereto we used the published sequence of *CCD7* and *CCD8* and we identified the putative tomato *D27*, *SID27* based on its homology with *Arabidopsis D27* (**Table S1**). Subsequently, we transformed all three upstream genes and *SIMAX1* individually to *Agrobacterium tumefaciens* and co-infiltrated these into the leaves of *N. benthamiana* for transient expression as described before (Zhang *et al.*, 2014). We analysed the level of CL in leaf extracts of *N. benthamiana* after transient expression. When expressing *SID27*, *SICCD7* and *SICCD8* simultaneously, there was a strong accumulation of CL in the *N. benthamiana* leaves (**Figure 5A**). However, co-infiltration of *SIMAX1* with *SID27*, *SICCD7* and *SICCD8* greatly decreased the level of CL, suggesting that *SIMAX1* catalyses the conversion of CL to something else (**Figure 5A**). Since in *Arabidopsis* *AtMAX1* catalyses the conversion of CL to the SL intermediate CLA (Abe *et al.*, 2014), we analysed leaf extracts for the presence of possible CL derivatives (19-hydroxy-CL, 19-oxo-CL or CLA) and screened the known canonical SLs by liquid chromatography coupled to a Thermo Orbitrap Fourier Transform Mass Spectrometer (LC-FTMS). CLA was present in the samples in which *SIMAX1* was co-infiltrated with *SID27*, *SICCD7* and *SICCD8*, but no known canonical SLs were detected (**Figure 5B-C**). These results indicate that *SIMAX1* is catalysing the oxidation of CL to CLA in tomato.

To gain a higher sensitivity for SLs, screening by multiple reaction monitoring (MRM)-LC/MS/MS was carried out in *N. benthamiana* leaves after co-infiltration of *SIMAX1* with the three CL biosynthetic pathway genes, showing that trace amounts of 4DO and 5DS were produced, but no other known tomato SLs (**Figure S5A, B**). This is consistent with the fact that *SIMAX1* is required for the formation of CLA from CL (**Figure 5**) and also similar to what we observed for co-infiltration of some of the rice *MAX1* homologs (such as *Os5100* and *Os1900*) and *AtMAX1* individually with the CL biosynthetic genes (Zhang *et al.*, 2014). In the same study, two other rice *MAX1* homologues, *Os900* and *Os1400*, were shown to sequentially catalyse the conversion of CL to 4DO and 4DO to orobanchol, respectively (Zhang *et al.*, 2014). Orobanchol is one of the major SLs in tomato yet oro-

banchol nor its direct precursor 4Do were formed in any appreciable amount by *SIMAX1* from CL (**Figure 2**). To investigate whether *SIMAX1* perhaps plays a role in the conversion of 4DO to orobanchol, we produced 4DO as substrate for *SIMAX1* in *N. benthamiana* by co-infiltrating *Os900* with the tomato CL biosynthetic genes. The latter resulted in the production of 4DO (**Figure S5C**). However, co-expression of *SIMAX1* neither resulted in the production of orobanchol nor a significant reduction in amount of 4DO (**Figure S5C**). Taken together, these results show that *SIMAX1* catalyses the formation of CLA, and not 4DO, from CL, and that 4DO is not the substrate of *SIMAX1* for the production of orobanchol.

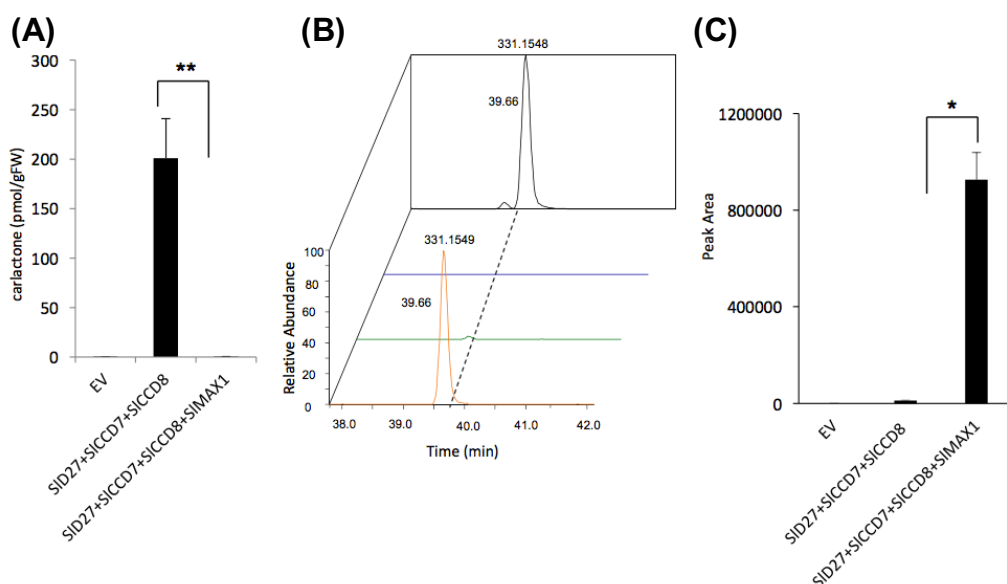


**Figure 5. Biochemical characterization of *SIMAX1* in transient expression assays.** (A) The reduction of carlactone level by co-expression of *SIMAX1* with the carlactone biosynthetic genes (*SID27*, *SICCD7* and *SICCD8*) in *N. benthamiana* transient expression (transition  $m/z$  303 > 207). The measurement was conducted using MRM-LC-MS/MS ( $n = 6$ ). (B) Representative chromatogram of the production of carlactonic acid in *N. benthamiana* transient expression as analysed by LC-Orbitrap-FTMS ( $n = 6$ ). (C) The abundance of carlactonic acid by simultaneously expressing *SIMAX1* with *SID27*, *SICCD7* and *SICCD8* in *N. benthamiana* detected by LC-Orbitrap-FTMS ( $n = 2$ ). Error bars in (A) and (C) represent means  $\pm$  SE. \* and \*\* indicate significant difference at  $0.01 < P < 0.05$  and  $0.001 < P < 0.01$ , respectively.

## Carlactone, but not 4DO, is the preferred direct precursor for SL formation in tomato

To further confirm the substrate of SIMAX1 and gain more insight into the origin of the tomato SLs, we performed plant feeding assays with SL precursors while inhibiting endogenous SL production with the carotenoid pathway inhibitor fluridone (Matusova *et al.*, 2005; Motonami *et al.*, 2013). In rice, it was shown that orobanchol is derived from 4DO by the orobanchol synthase (Os1400) (Zhang *et al.*, 2014). However, 4DO has never been detected in tomato plants to date. To investigate whether 4DO is an intermediate for tomato SLs (orobanchol, solanacol and didehydro-orobanchol isomers), we fed plants with an equal concentration (0.05  $\mu$ M) of 4DO or the SL precursor CL. Upon CL feeding, there was a significant production of orobanchol in the root exudates, and it was more than 25-fold higher than that after 4DO feeding (**Figure 6A**). Similar results were observed in root extracts (**Figure S6a**). Addition of the CYP inhibitor uniconazole-P in the feeding assay was able to suppress the bioconversion of CL to orobanchol likely through inhibition of the activity of SIMAX1 (**Figure 6B**). Upon CL feeding, we were able to detect a trace of *epi*-orobanchol, likely *ent*-2'-*epi*-orobanchol (the other naturally occurring orobanchol stereoisomers), using non-chiral MRM-LC/MS/MS analysis (**Figure S6B-C**), which has not been identified in tomato as a natural SL to date. *Ent*-2'-*epi*-orobanchol has been reported to be present in other Solanaceae, such as tobacco (Xie *et al.*, 2013), so it is not unlikely that it can also be produced in tomato.

It is well known that 2-oxoglutarate and Fe(II)-dependent dioxygenase (2-OGD) family genes are involved in various oxidation and hydroxylation reactions in the plant kingdom (Kawai *et al.*, 2014). To investigate whether this type of enzyme is also involved in tomato SL production, we supplemented the 2-OGD inhibitor prohexadione during the CL feeding assay. Intriguingly, in the tomato root exudates, the level of orobanchol derived from CL feeding is reduced by prohexadione but to a much lower extent compared to the inhibition by the same concentration of CYP inhibitor (**Figure 6B**). Additionally, also in root extracts the inhibitor caused a slight but non-significant reduction in orobanchol amount (**Figure S6D**), implying that a 2-OGD enzyme might contribute to the biosynthesis of orobanchol from CL in tomato. The conversion of 4DO to a trace amount of orobanchol in our feeding assays (**Figure 6A**), was not affected by CYP 450 or 2-OGD inhibitors (**Figure S6E**). These results are in line with the results from the heterologous expression experiments using *N. benthamiana* (**Figure S5C**), suggesting that SIMAX1 uses CL as a substrate to produce CLA and that

(an)other enzyme(s) is/are required for biosynthesis of orobanchol, directly from CLA but not through 4DO.

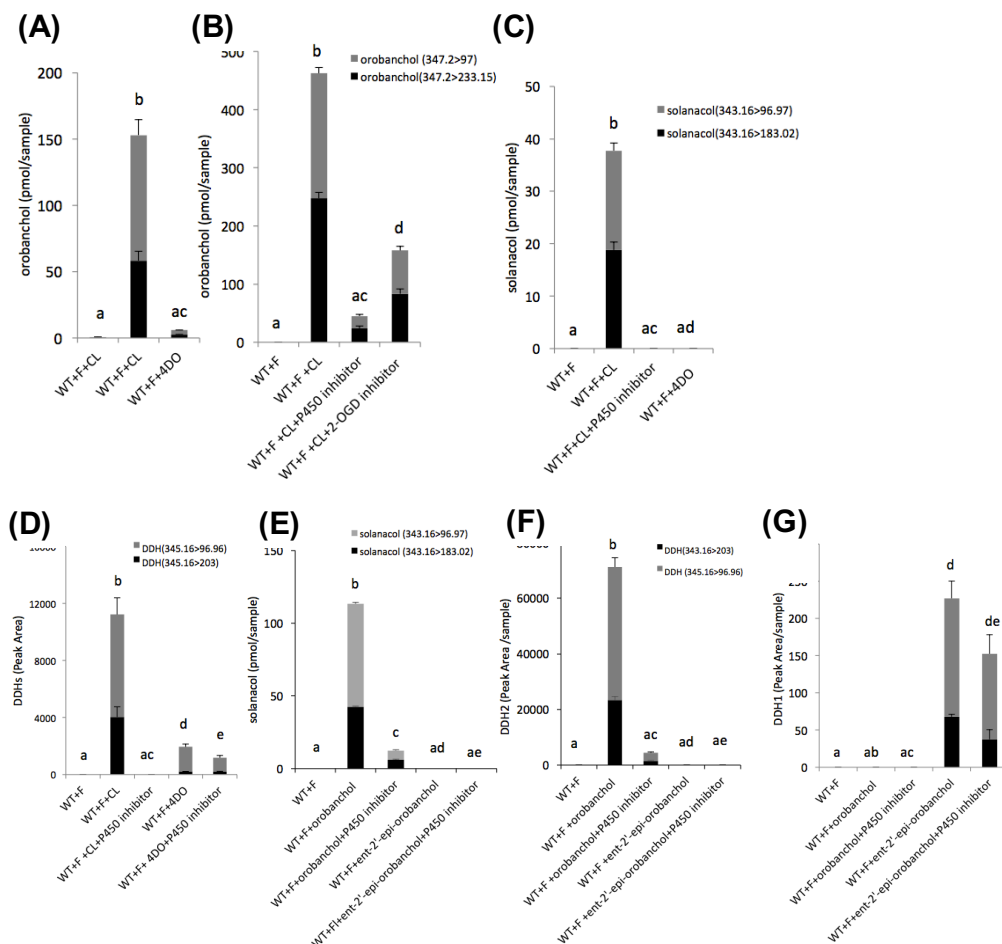


**Figure 6. Strigolactone quantification in plant feeding assays.** (A) Orobanchol production in the root exudates after feeding of carlactone (CL) and 4-deoxy-orobanchol (4DO) in the same molar concentration (0.05 $\mu$ M). (B) Orobanchol levels in the root exudates of plants supplied with CL after supplementation of enzyme inhibitors for cytochrome P450s (uniconazole-P) or 2-oxoglutarate dependent dioxygenases (prohexadione). (C) Solanacol accumulation in the root exudates of plants supplied with CL or 4DO with or without the application of uniconazole-P. (D) Quantification of total amount of didehydro-orobanchol (DDH) isomers (1 through 3) after feeding of 4DO or CL with or without the pres-

ence of uniconazole-P. The total level of all three DDH isomers were quantified by summing up the peak area of these DDHs together. (E) Accumulation of solanacol in the root exudates after feeding with orobanchol isomers (orobanchol or *ent*-2'-*epi*-orobanchol) with or without the presence of uniconazole-P. (F) Quantification of DDH2 in plants root exudates after feeding of orobanchol stereoisomers with or without the presence of uniconazole-P. (G) Abundance of DDH1 after feeding of orobanchol stereoisomers with or without the addition of uniconazole-P. Error bars in (A) through (G) represent means  $\pm$  SEM (n = 3~5). Statistical significance was determined by one way anova performed in Graphpad Prism 6, P < 0.01. F represents the carotenoid pathway inhibitor fluridone in (A) through (G).

### CYP450 enzymes are involved in the tomato strigolactone decoration

The absolute configuration of the C-ring in solanacol and medicaol (one of the DDH isomers isolated from *Medicago truncatula*) was reported to be the same as in orobanchol which is derived from 4DO in rice (Chen *et al.*, 2010; Zwanenburg and Pospisil, 2013a; Zhang *et al.*, 2014; Tokunaga *et al.*, 2015). Thus, we hypothesized that solanacol and DDH isomers in tomato share the same C-ring stereochemistry as 4DO, which might be the precursor of solanacol or DDH isomers. However, in our plant feeding experiment, solanacol was only detectable after feeding of CL but not with 4DO, therefore we could not determine its stereochemistry (**Figure 6C and Figure S6F**). The total production of all three DDH isomers showed a strong increase after feeding with CL, while the induction after feeding with 4DO was much lower (**Figure 6D**). Interestingly, the feeding of 4DO gave rise to a different DDH composition, showing predominantly an increase in DDH3, but not DDH1 and DDH2, suggesting 4DO is the substrate for DDH3 but not CL (**Figure S6G**). After CL feeding, DDH2 is the most dominant peak and it is probably masking the trace amount of DDH 1 and/or DDH3 because of the overlapping of the peaks (**Figure 6D and Figure S6G**). The production of orobanchol, solanacol and the DDH isomers from CL is inhibited by the CYP inhibitor (**Figure 6B-D**). To further support the stereochemistry of solanacol and DDH isomers in tomato, we further performed a plant feeding experiment with the two naturally occurring orobanchol stereoisomers - orobanchol and *ent*-2'-*epi*-orobanchol (**Figure S7A**). The production of solanacol was significantly induced by feeding of orobanchol (**Figure 6E and Figure S7B**). Among the DDH isomers, the DDH2 peak was predominant after orobanchol feeding (**Figure 6F and Figure S7B-C**), whereas DDH1 was induced

(though at a very low level) after feeding of *ent*-2'-*epi*-orobanchol (**Figure 6G and Figure S7B-C**). These results are suggesting that DDH1 is a strigol-type SL and is derived from *ent*-2'-*epi*-orobanchol while all other tomato SLs are orobanchol-type SLs. The production of solanacol and DDH isomers from orobanchol was dramatically suppressed after the use of the P450 inhibitor (**Figure 6D, E and Figure S7B**), suggesting that CYP enzymes are essential for the formation of solanacol and DDH isomers from orobanchol or possibly other substrates (such as 4DO or *ent*-2'-*epi*-orobanchol).

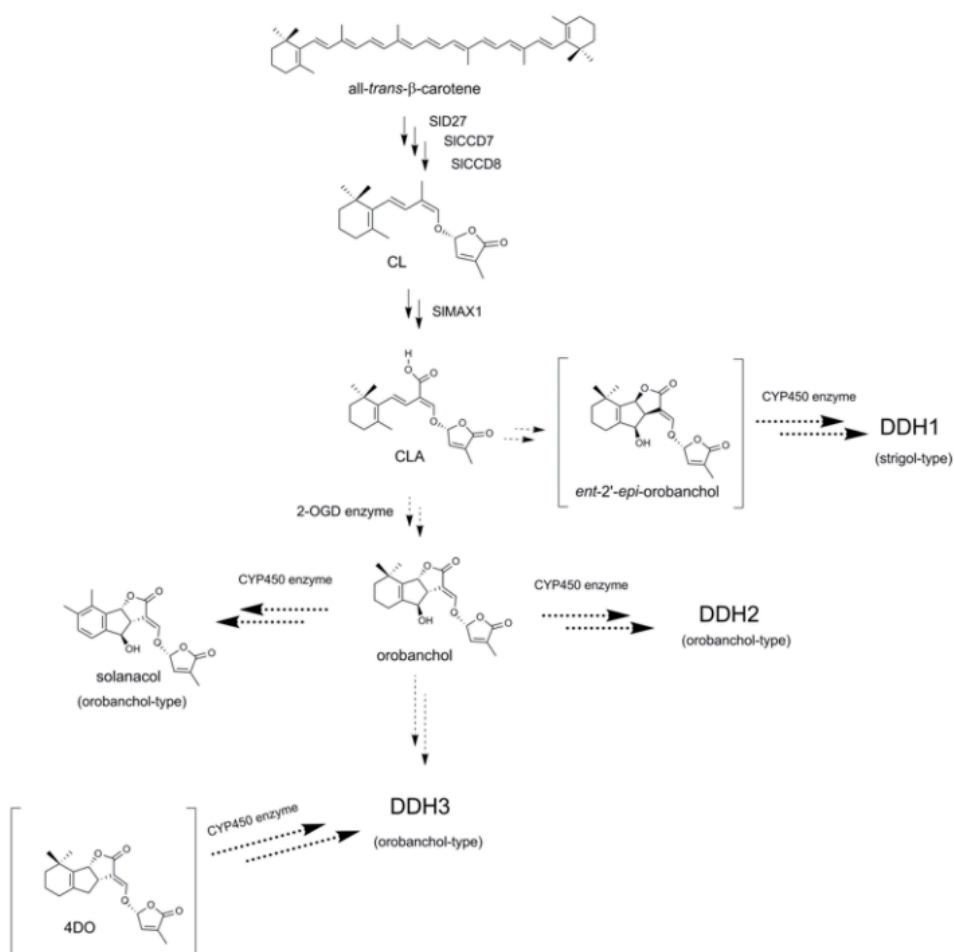


**Figure 7. The proposed strigolactone biosynthetic pathway in tomato.** SIMAX1 catalyses the oxidation of carlactone to carlactonic acid (CLA). CLA is subsequently the precursor for other canonical SL structures, such as orobanchol, solanacol and didehydro-orobanchol (DDH)



isomers. Our results suggest a 2-oxoglutarate dependent dioxygenase (2-OGD) enzyme is involved in the formation of orobanchol. Orobanchol is the precursor for solanacol and DDH isomers 2 and 3. The formation of DDH 2 and 3 from orobanchol requires cytochrome P450 enzymes. DDH 1 is produced from a strigol-type SL, possibly *ent-2'-epi*-orobanchol. SL structures that are in brackets have not been reported in tomato plants before.

### Discussion

In the present study, we show that the *MAX1* homolog in tomato, *SIMAX1*, catalyses the formation of CLA from CL (**Figure 5**). In *Arabidopsis*, CLA is an intermediate in the production of SL-LIKE1 and is produced by the oxidation of CL by *AtMAX1* (Abe *et al.*, 2014). In the present study, we did not detect the other two known intermediates in this triple oxidation reaction, 19-hydroxy-CL and 19-oxo-CL, in the *N. benthamiana* leaf samples co-expressing *SIMAX1* with the CL biosynthetic genes using untargeted LC-Orbitrap-FTMS analysis (**Figure 5A**). Our results confirm that CL is the substrate for a number of different enzymes in the production of canonical SLs (such as 4DO and orobanchol) as well as non-canonical SL-LIKE compounds, such as MeCLA in different plant species (Abe *et al.*, 2014; Zhang *et al.*, 2014; Brewer *et al.*, 2016).

It has been postulated that 5DS and 4DO are the precursors for all canonical SLs of the strigol and orobanchol type, respectively (Yoneyama *et al.*, 2010; Ruyter-Spira *et al.*, 2013). Rice *MAX1* homolog Os1400 was indeed demonstrated to act as orobanchol synthase catalyzing the conversion of 4DO to orobanchol (Zhang *et al.*, 2014). However, multiple results from the present study are indicating that *SIMAX1* does not produce 4DO from CL as an intermediate en route to orobanchol, but converts CL to CLA which is then likely the precursor in the formation of orobanchol by an as yet unknown enzyme (**Figure 5 and Figure 6A**): feeding of CL, but not 4DO, to fluridone treated plants results in orobanchol production (**Figure 6A**). The conversion of CL to orobanchol is likely a multistep-reaction mediated by multiple enzymes including *SIMAX1* (**Figure 7**). Inhibition of orobanchol production by the 2-OGD inhibitor in the feeding assay suggests that a 2-OGD may play a role in this conversion (**Figure 6B and Figure 7**). The 2-OGD gene family is widely distributed in plants, microorganisms and mammals and is involved in the oxidation of organic substrates (Aravind and Koonin, 2001). In plants, this gene family has been reported to be essential for the biosynthesis and/or metabolism of several plant hormones, such as gibberellins, auxin and ethylene (Kawai *et al.*, 2014). It is suggested that 2-OGDs

prefer more hydrophilic substrates, such as those compounds that are obtained after hydroxylation by CYPs (Kawai *et al.*, 2014). Therefore, oxidation catalyzed by 2-OGDs usually occurs after the oxidation by CPYs or the glycosylation by UPD-sugar dependent glycosyltransferases (UGTs). This has been proven to be true also in SL biosynthesis, in *Arabidopsis*, in which the 2-OGD, *LATERAL BRANCHING OXIDOREDUCTASE* (*LBO*), is involved in SL biosynthesis downstream of *AtMAX1* using MeCLA as a substrate (Brewer *et al.*, 2016). Thus, we postulate that a 2-OGD enzyme acts down stream of *SIMAX1* in the conversion of CL to orobanchol (**Figure 7**).

Generally, canonical SLs with the typical tricyclic lactone coupled to the D-ring have been classified into two groups according to the stereochemistry of the C-ring, *viz.* orobanchol type and strigol type (Xie *et al.*, 2013; Zwanenburg and Pospisil, 2013b). In rice, so far only orobanchol-type SLs, orobanchol and 4DO, were identified (Xie *et al.*, 2013), while in sorghum strigol-type SLs (sorgomol, sorgolactone and 5DS) as well as orobanchol have been reported (Yoneyama *et al.*, 2010). The solanaceous species tobacco has been shown to produce at least 11 SLs from both SL families, including two orobanchol isomers - orobanchol and *ent-2'-epi-orobanchol* - and three putative DDH isomers (Xie *et al.*, 2013). As solanaceous species, tomato has been shown to produce orobanchol-type SLs, such as orobanchol and solanacol (Kohlen *et al.*, 2012). In the present study, we have further unraveled the biosynthetic origin of several tomato SLs. Orobanchol in tomato derives from CL but not 4DO by the sequential oxidation of carlactone by *SIMAX1* and possibly a 2-OGD (**Figure 6A, B and Figure 7**). Consistent with previously published results about the absolute stereochemistry of solanacol (Chen *et al.*, 2010), we have shown that solanacol derives from orobanchol but not from *ent-2'-epi-orobanchol*; this reaction requires one or more CYPs (**Figure 6F and Figure 7**). Our findings shed new light on the biosynthesis of solanacol in plants. Unlike in tobacco, in tomato *ent-2'-epi-orobanchol* has never been detected before, but here we find that it can be produced by tomato after feeding of CL (**Figure S6B,C**), implying that the enzyme(s) responsible for *ent-2'-epi-orobanchol* production is/are present in tomato, just as in tobacco (Xie *et al.*, 2013).

In tomato, the predominant DDH isomers are DDH1 and DDH2 (**Figure S2A, B, C**). These DDH isomers are contributing to the major tomato SL profile detected by MRM-LC/MS-MS (**Figure 2**) (Liu *et al.*, 2011; Kohlen *et al.*, 2013). However, the stereochemistry and biosynthetic origin of these DDH isomers is unclear. In *Medicago truncatula*, a DDH isomer was identified as medicaol with the orobanchol-type stereochemistry (Tokunaga *et*

*al.*, 2015), which is in line with our results for the predominant production of DDH2 after orobanchol feeding (**Figure 5G**). Feeding of CL also results in a dramatic induction of DDH2, which is due to the production of orobanchol from CL and the subsequent further conversion to DDH2 (**Figure 5G and Figure 6A, F**). Our current study provides the first evidence that DDH1 may derive from a strigol-type SL, which is indicated by the accumulation of DDH1 after *ent-2'-epi-orobanchol* feeding (**Figure 6G and Figure S7C**). Although *ent-2'-epi-orobanchol* was so far not reported in tomato, our results support that tomato does have the enzymes for its production, making a strigol-type DDH isomer not unlikely. DDH3 is a minor DDH isomer as previously reported in tomato (Kohlen *et al.*, 2013). The present study shows that DDH3 is produced from 4DO, and thus is an orobanchol-type SL (**Figure S6G**).

Additionally, the composition of the DDH isomers in the root exudates differs from that is in the root extracts. DDH1 is the most abundant in root exudates and DDH2 in root extracts (**Figure S2**). Perhaps this is related to differences in the unknown biological function of these DDH isomers and/or differences in the specificity of SL transporter(s). It is intriguing that tomato and several other plant species produce specific DDH isomers and secrete them differentially into the rhizosphere (Xie *et al.*, 2013; Tokunaga *et al.*, 2015). So far, however, there are no reports about the biological activity of the DDH isomers, let alone about differences in their activities. The structures of these DDH isomers in tomato have also not been elucidated yet though in the present study we do provide evidence for their stereochemistry. The biosynthesis of these DDH isomers does not seem to be simple considering the structure of the only characterized DDH isomer, medicaol (Tokunaga *et al.*, 2015). We show here that CYPs are likely involved in their biosynthesis as the CYP inhibitor greatly suppressed their production (**Figure 6F, G**). The GRAS-type transcription factor *NODULATION SIGNALLING PATHWAY2* (*NPS2*) was demonstrated to regulate DDH isomer biosynthesis in *M. truncatula* (Liu *et al.*, 2011). Perhaps, in tomato a homolog of this transcription factor is involved in the regulation of the CYPs that catalyse the biosynthesis of the tomato DDH isomers. It would be interesting to further identify the structures of DDH isomers in tomato and investigate their biological significance.

Our study for the first time provides evidence that orobanchol originates from CL oxidation, by SIMAX1, without the formation of 4DO as an intermediate. It seems an ODD is involved in this process. We also show the evidence that CYPs are involved in the conversion of orobanchol to sola-

naicol and DDH isomers. It will be of great interest to further unravel these biosynthetic relationships such that a better insight in the biological relevance of all these different SLs can be obtained. The upregulation of tomato SLs and their biosynthetic genes by P-starvation (**Figure 2, Figure 4A and Figure S4C-E**) might be useful tools for further discovery of the biosynthetic enzymes that are catalyzing the formation of solanacol and DDH isomers.

## Acknowledgements

We acknowledge Gavin R. Flematti (School of Chemistry and Biochemistry, The University of Western Australia) and Salim Al-Babili (Center for Desert Agriculture, BESE Division, King Abdullah University of Science and Technology) for their kind supply of carlactone and carlactonic acid standards. We thank Koichi Yoneyama (Center for Bioscience Research and Education, Utsunomiya University, Utsunomiya, Japan) and Tadao Asami (Department of Applied Biological Chemistry, The University of Tokyo, Japan) for supplying SL standards.

## References

- Abe, S., Sado, A., Tanaka, K., Kisugi, T., Asami, K., *et al.* (2014). Carlactone is converted to carlactonoic acid by MAX1 in *Arabidopsis* and its methyl ester can directly interact with AtD14 in vitro. *Proc Natl Acad Sci U S A* 111(50), 18084-18089.
- Akiyama, K., Matsuzaki, K., and Hayashi, H. (2005). Plant sesquiterpenes induce hyphal branching in arbuscular mycorrhizal fungi. *Nature* 435(7043), 824-827.
- Akiyama, K., Ogasawara, S., Ito, S., and Hayashi, H. (2010). Structural requirements of strigolactones for hyphal branching in AM fungi. *Plant Cell Physiol* 51(7), 1104-1117.
- Alder, A., Jamil, M., Marzorati, M., Bruno, M., Vermathen, M., *et al.* (2012). The path from beta-carotene to carlactone, a strigolactone-like plant hormone. *Science* 335(6074), 1348-1351.
- Aravind, L., and Koonin, E.V. (2001). The DNA-repair protein AlkB, EGL-9, and lepre can define new families of 2-oxoglutarate- and iron-dependent dioxygenases. *Genome Biol* 2(3), RESEARCH0007.
- Arite, T., Iwata, H., Ohshima, K., Maekawa, M., Nakajima, M., *et al.* (2007). *DWARF10*, an *RMS1/MAX4/DAD1* ortholog, controls lateral bud outgrowth in rice. *Plant J* 51(6), 1019-1029.
- Baldwin, J.C., Karthikeyan, A.S., and Raghothama, K.G. (2001). LEPS2, a phosphorus starvation-induced novel acid phosphatase from tomato. *Plant Physiol* 125(2), 728-737.
- Booker, J., Auldrige, M., Wills, S., McCarty, D., Klee, H., *et al.* (2004). MAX3/CCD7 is a carotenoid cleavage dioxygenase required for the synthesis of a novel plant signaling molecule. *Curr Biol* 14(14), 1232-1238.

- Booker, J., Sieberer, T., Wright, W., Williamson, L., Willett, B., et al.** (2005). *MAX1* encodes a cytochrome P450 family member that acts downstream of *MAX3/4* to produce a carotenoid-derived branch-inhibiting hormone. *Dev Cell* 8(3), 443-449.
- Boyer, F.D., Germain, A.D., Pillot, J.P., Pouvreau, J.B., Chen, V.X., et al.** (2012). Structure-activity relationship studies of strigolactone-related molecules for branching inhibition in garden pea: molecule design for shoot branching. *Plant Physiol* 159(4), 1524-1544.
- Brewer, P.B., Yoneyama, K., Filardo, F., Meyers, E., Scaffidi, A., et al.** (2016). *LATERAL BRANCHING OXIDOREDUCTASE* acts in the final stages of strigolactone biosynthesis in *Arabidopsis*. *Proc Natl Acad Sci U S A* 113(22), 6301-6306.
- Challis, R.J., Hepworth, J., Mouchel, C., Waites, R., and Leyser, O.** (2013). A role for *MORE AXILLARY GROWTH1 (MAX1)* in evolutionary diversity in strigolactone signaling upstream of *MAX2*. *Plant Physiol* 161(4), 1885-1902.
- Chen, V.X., Boyer, F.D., Rameau, C., Retailleau, P., Vors, J.P., et al.** (2010). Stereochemistry, total synthesis, and biological evaluation of the new plant hormone solanacol. *Chemistry* 16(47), 13941-13945.
- Cook, C.E., Whichard, L.P., Turner, B., and Wall, M.E.** (1966). Germination of witchweed (*Striga lutea* Lour) - isolation and properties of a potent stimulant. *Science* 154(3753), 1189-1190.
- De Vos, R.C.H., Moco, S., Lommen, A., Keurentjes, J.J.B., Bino, R.J., et al.** (2007). Untargeted large-scale plant metabolomics using liquid chromatography coupled to mass spectrometry. *Nat Prot* 2(4), 778-791.
- Dekkers, B.J.W., Willems, L., Bassel, G.W., van Bolderen-Veldkamp, R.P., Ligterink, W., et al.** (2012). Identification of reference genes for RT-qPCR expression analysis in *Arabidopsis* and tomato seeds. *Plant Cell Physiol* 53(1), 28-37.
- Drummond, R.S.M., Martinez-Sanchez, N.M., Janssen, B.J., Templeton, K.R., Simons, J.L., et al.** (2009). *Petunia hybrida* *CAROTENOID CLEAVAGE DIOXYGENASE7* ss involved in the production of negative and positive branching signals in petunia. *Plant Physiol* 151(4), 1867-1877.
- Gomez-Roldan, V., Fermas, S., Brewer, P.B., Puech-Pages, V., Dun, E.A., et al.** (2008). Strigolactone inhibition of shoot branching. *Nature* 455(7210), 189-194.
- Kapulnik, Y., and Koltai, H.** (2014). Strigolactone involvement in root development, response to abiotic stress, and interactions with the biotic soil environment. *Plant Physiol* 166(2), 560-569.
- Kawai, Y., Ono, E., and Mizutani, M.** (2014). Evolution and diversity of the 2-oxoglutarate-dependent dioxygenase superfamily in plants. *Plant J* 78(2), 328-343.
- Kohlen, W., Charnikhova, T., Bours, R., Lopez-Raez, J.A., and Bouwmeester, H.** (2013). Tomato strigolactones: a more detailed look. *Plant Signal Behav* 8(1), e22785.
- Kohlen, W., Charnikhova, T., Lammers, M., Pollina, T., Toth, P., et al.** (2012). The tomato *CAROTENOID CLEAVAGE DIOXYGENASE8 (SICCD8)* regulates rhizosphere signaling, plant architecture and affects reproductive development through strigolactone biosynthesis. *New Phytol* 196(2), 535-547.

- Koltai, H., LekKala, S.P., Bhattacharya, C., Mayzlish-Gati, E., Resnick, N., *et al.* (2010). A tomato strigolactone-impaired mutant displays aberrant shoot morphology and plant interactions. *J Exp Bot* 61(6), 1739-1749.
- Lin, H., Wang, R., Qian, Q., Yan, M., Meng, X., *et al.* (2009). DWARF27, an iron-containing protein required for the biosynthesis of strigolactones, regulates rice tiller bud outgrowth. *Plant Cell* 21(5), 1512-1525.
- Liu, J.W., He, H.Z., Vitali, M., Visentin, I., Charnikhova, T., *et al.* (2015). Osmotic stress represses strigolactone biosynthesis in *Lotus japonicus* roots: exploring the interaction between strigolactones and ABA under abiotic stress. *Planta* 241(6), 1435-1451.
- Liu, W., Kohlen, W., Lillo, A., Op den Camp, R., Ivanov, S., *et al.* (2011). Strigolactone biosynthesis in medicago truncatula and rice requires the symbiotic GRAS-type transcription factors NSP1 and NSP2. *Plant Cell* 23(10), 3853-3865.
- Lopez-Raez, J.A., Charnikhova, T., Fernandez, I., Bouwmeester, H., and Pozo, M.J. (2011). Arbuscular mycorrhizal symbiosis decreases strigolactone production in tomato. *J Plant Physiol* 168(3), 294-297.
- Lopez-Raez, J.A., Charnikhova, T., Gomez-Roldan, V., Matusova, R., Kohlen, W., *et al.* (2008). Tomato strigolactones are derived from carotenoids and their biosynthesis is promoted by phosphate starvation. *New Phytol* 178(4), 863-874.
- Morris, S.E., Turnbull, C.G.N., Murfet, I.C., and Beveridge, C.A. (2001). Mutational analysis of branching in pea. Evidence that *Rms1* and *Rms5* regulate the same novel signal. *Plant Physiol* 126(3), 1205-1213.
- Motonami, N., Ueno, K., Nakashima, H., Nomura, S., Mizutani, M., *et al.* (2013). The bioconversion of 5-deoxystrigol to sorgomol by the sorghum, *Sorghum bicolor* (L.) Moench. *Phytochemistry* 93, 41-48.
- Nomura, S., Nakashima, H., Mizutani, M., Takikawa, H., and Sugimoto, Y. (2013). Structural requirements of strigolactones for germination induction and inhibition of *Striga gesnerioides* seeds. *Plant Cell Reports* 32(6), 829-838.
- Ruyter-Spira, C., Al-Babili, S., van der Krol, S., and Bouwmeester, H. (2013). The biology of strigolactones. *Trends Plant Sci* 18(2), 72-83.
- Ruyter-Spira, C., Kohlen, W., Charnikhova, T., van Zeijl, A., van Bezouwen, L., *et al.* (2011). Physiological effects of the synthetic strigolactone analog GR24 on root system architecture in *arabidopsis*: another belowground role for strigolactones? *Plant Physiol* 155(2), 721-734.
- Seto, Y., Sado, A., Asami, K., Hanada, A., Umehara, M., *et al.* (2014). Carlactone is an endogenous biosynthetic precursor for strigolactones. *Proc Natl Acad Sci USA* 111(4), 1640-1645.
- Simons, J.L., Napoli, C.A., Janssen, B.J., Plummer, K.M., and Snowden, K.C. (2007). Analysis of the *DECREASED APICAL DOMINANCE* genes of petunia in the control of axillary branching. *Plant Physiol* 143(2), 697-706.
- Sorefan, K., Booker, J., Haurogne, K., Goussot, M., Bainbridge, K., *et al.* (2003). *MAX4* and *RMS1* are orthologous dioxygenase-like genes that regulate shoot branching in *Arabidopsis* and pea. *Genes Dev* 17(12), 1469-1474.



- Stirnberg, P., van de Sande, K., and Leyser, H.M.O.** (2002). *MAX1* and *MAX2* control shoot lateral branching in *Arabidopsis*. *Development* 129(5), 1131-1141.
- Sun, H.W., Tao, J.Y., Hou, M.M., Huang, S.J., Chen, S., et al.** (2015). A strigolactone signal is required for adventitious root formation in rice. *Ann Botany* 115(7), 1155-1162.
- Tokunaga, T., Hayashi, H., and Akiyama, K.** (2015). Medicaol, a strigolactone identified as a putative dihydro-orobanchol isomer, from *Medicago truncatula*. *Phytochemistry* 111, 91-97.
- Ueno, K., Furumoto, T., Umeda, S., Mizutani, M., Takikawa, H., et al.** (2014). Heliolactone, a non-sesquiterpene lactone germination stimulant for root parasitic weeds from sunflower. *Phytochemistry* 108, 122-128.
- Umehara, M., Hanada, A., Magome, H., Takeda-Kamiya, N., and Yamaguchi, S.** (2010). Contribution of strigolactones to the inhibition of tiller bud outgrowth under phosphate deficiency in rice. *Plant Cell Physiol* 51(7), 1118-1126.
- Umehara, M., Hanada, A., Yoshida, S., Akiyama, K., Arite, T., et al.** (2008). Inhibition of shoot branching by new terpenoid plant hormones. *Nature* 455(7210), 195-200.
- van der Hooft, J.J.J., Vervoort, J., Bino, R.J., and de Vos, R.C.H.** (2012). Spectral trees as a robust annotation tool in LC-MS based metabolomics. *Metabolomics* 8(4), 691-703.
- van Zeijl, A., Liu, W., Xiao, T.T., Kohlen, W., Yang, W.C., et al.** (2015). The strigolactone biosynthesis gene *DWARF27* is co-opted in rhizobium symbiosis. *BMC Plant Biol* 15(1), 260.
- Vogel, J.T., Walter, M.H., Giavalisco, P., Lytovchenko, A., Kohlen, W., et al.** (2010). *SICC7* controls strigolactone biosynthesis, shoot branching and mycorrhiza-induced apocarotenoid formation in tomato. *Plant J* 61(2), 300-311.
- Voinnet, O., Rivas, S., Mestre, P., and Baulcombe, D.** (2003). An enhanced transient expression system in plants based on suppression of gene silencing by the P19 protein of tomato bushy stunt virus. *Plant J* 33(5), 949-956.
- Xie, X., Yoneyama, K., Kisugi, T., Uchida, K., Ito, S., et al.** (2013). Confirming stereochemical structures of strigolactones produced by rice and tobacco. *Mol Plant* 6(1), 153-163.
- Yoneyama, K., Awad, A.A., Xie, X., Yoneyama, K., and Takeuchi, Y.** (2010). Strigolactones as germination stimulants for root parasitic plants. *Plant Cell Physiol* 51(7), 1095-1103.
- Zhang, Y.X., van Dijk, A.D.J., Scaffidi, A., Flematti, G.R., Hofmann, M., et al.** (2014). Rice cytochrome P450 *MAX1* homologs catalyze distinct steps in strigolactone biosynthesis. *Nat Chem Biol* 10(12), 1028-1033.
- Zou, J.H., Zhang, S.Y., Zhang, W.P., Li, G., Chen, Z.X., et al.** (2006). The rice *HIGH-TILLERING DWARF1* encoding an ortholog of *Arabidopsis MAX3* is required for negative regulation of the outgrowth of axillary buds. *Plant J* 48(5), 687-696.
- Zwanenburg, B., and Pospisil, T.** (2013a). Structure and activity of strigolactones: new plant hormones with a rich future. *Mol Plant* 6(1), 38-62.
- Zwanenburg, B., and Pospisil, T.** (2013b). Structure and activity of strigolactones: new



plant hormones with a rich future. *Mol Plant* 6(1), 38-62.

Supplementary materials

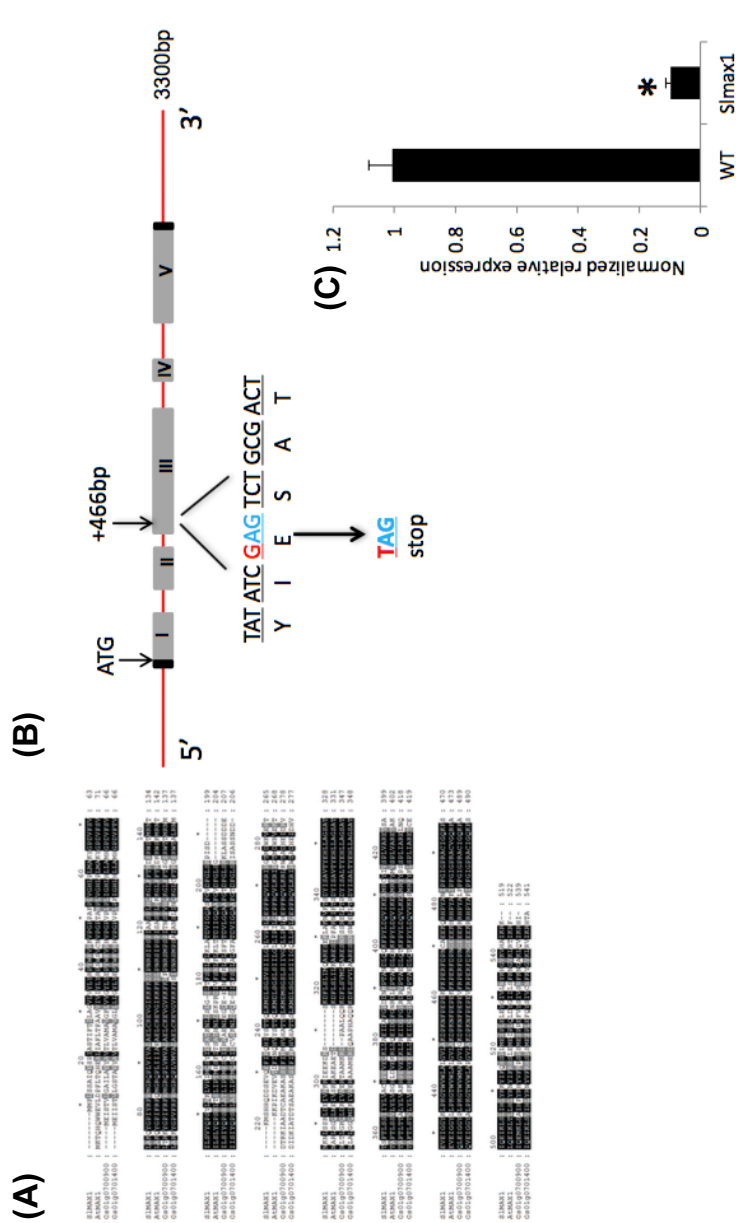
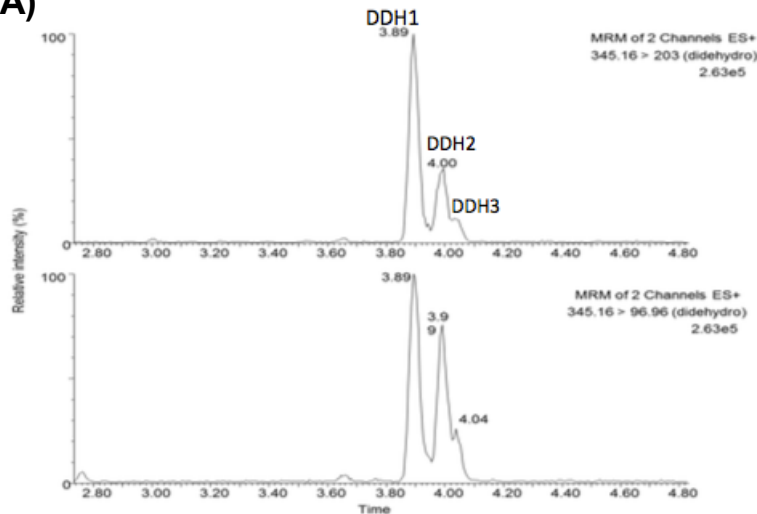
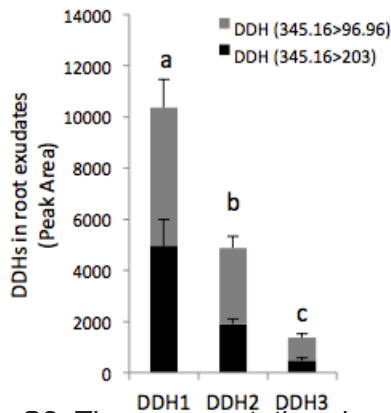


**Figure S1.** Sequence alignment of *MAX1* orthologs (A), mutation position of *SIMAX1* (B) and *SIMAX1* gene expression in wildtype (WT) and *Simax1* mutant.

(A)



(B)



(C)

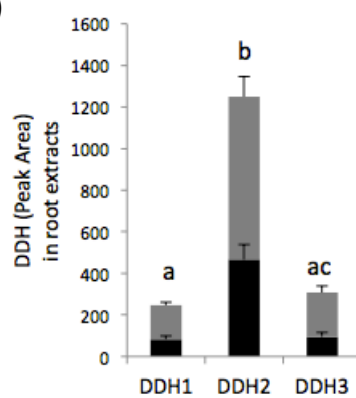


**Figure S2.** The representative chromatogram profile of three didehydro-oro-banchol (DDH) isomers (A) and level of DDH1, DDH2, DDH3 in root exudate (B) and root extracts (C) in tomato.

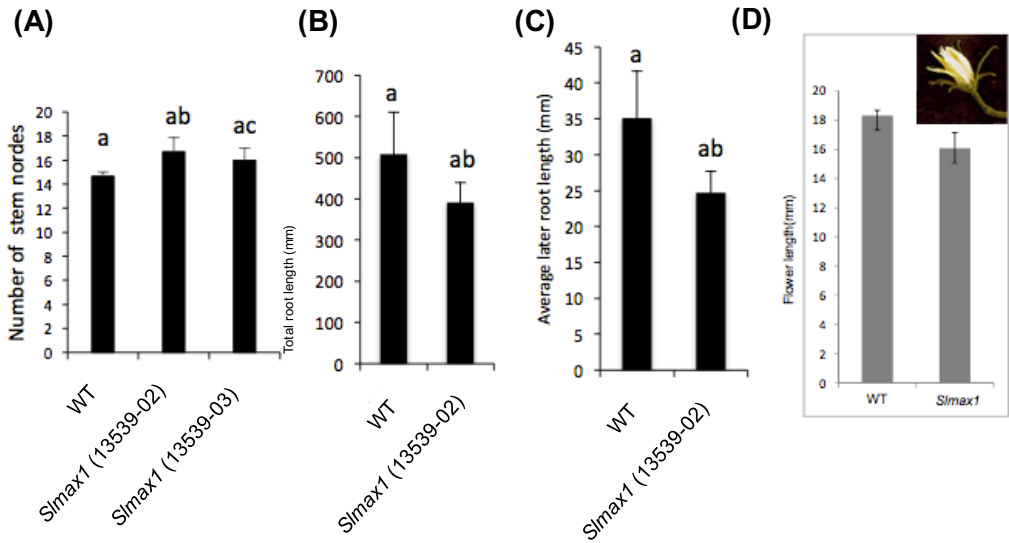


**Figure S3.** Phenotypes of *Slmax1* mutants and wildtype tomato, including number of stem nodes (A), total root length (B, mm), average lateral root length (C, mm) and flower length (D, mm).

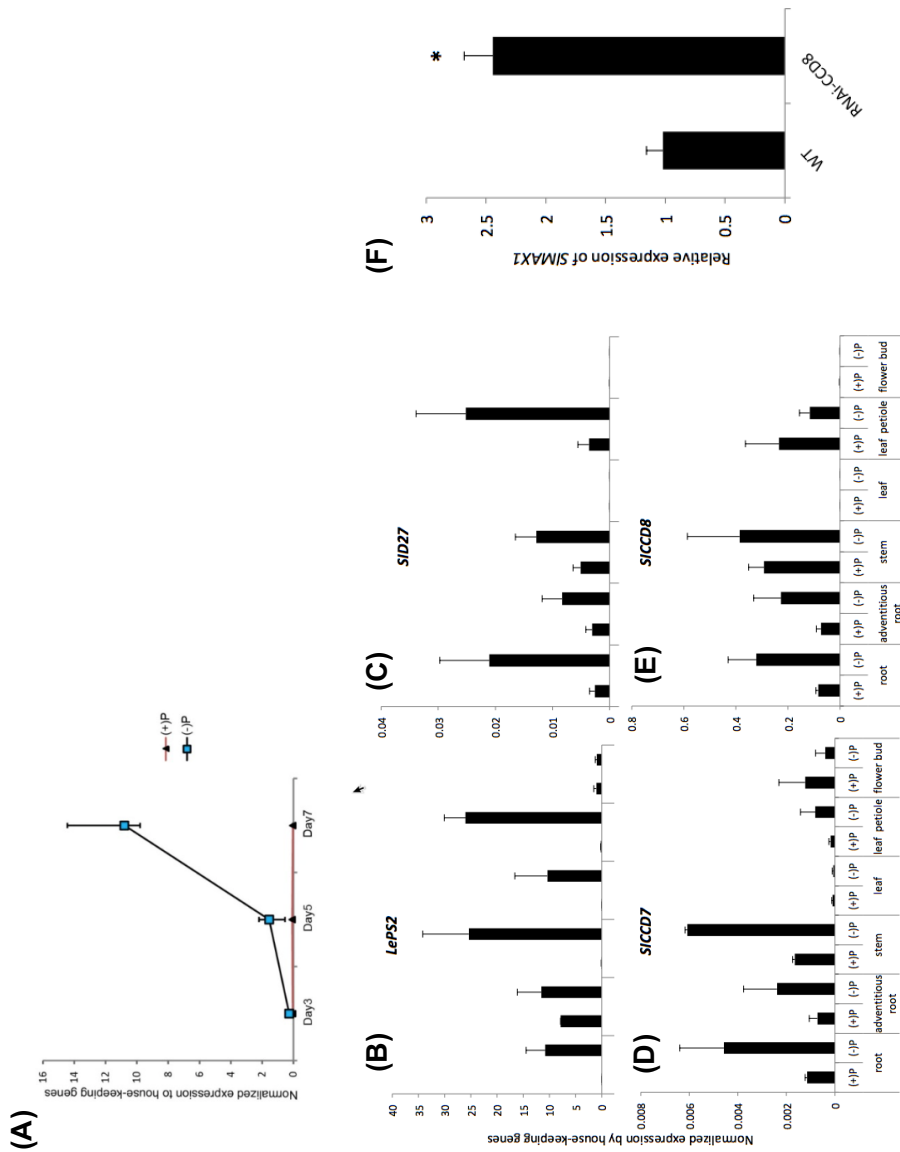


**Figure S4.** Relative gene expression of *SIMAX1* (A), *LePS2* (B), *SID27* (C), *siCCD7* (D) and *siCCD8* (E) in roots, adventitious roots, stem, leaf, leaf petiole and flower bud under control (+P) and under phosphate starvation (-P). Additionally, gene expression of *SIMAX1* in CCD8 RNAi lines is included in (F).

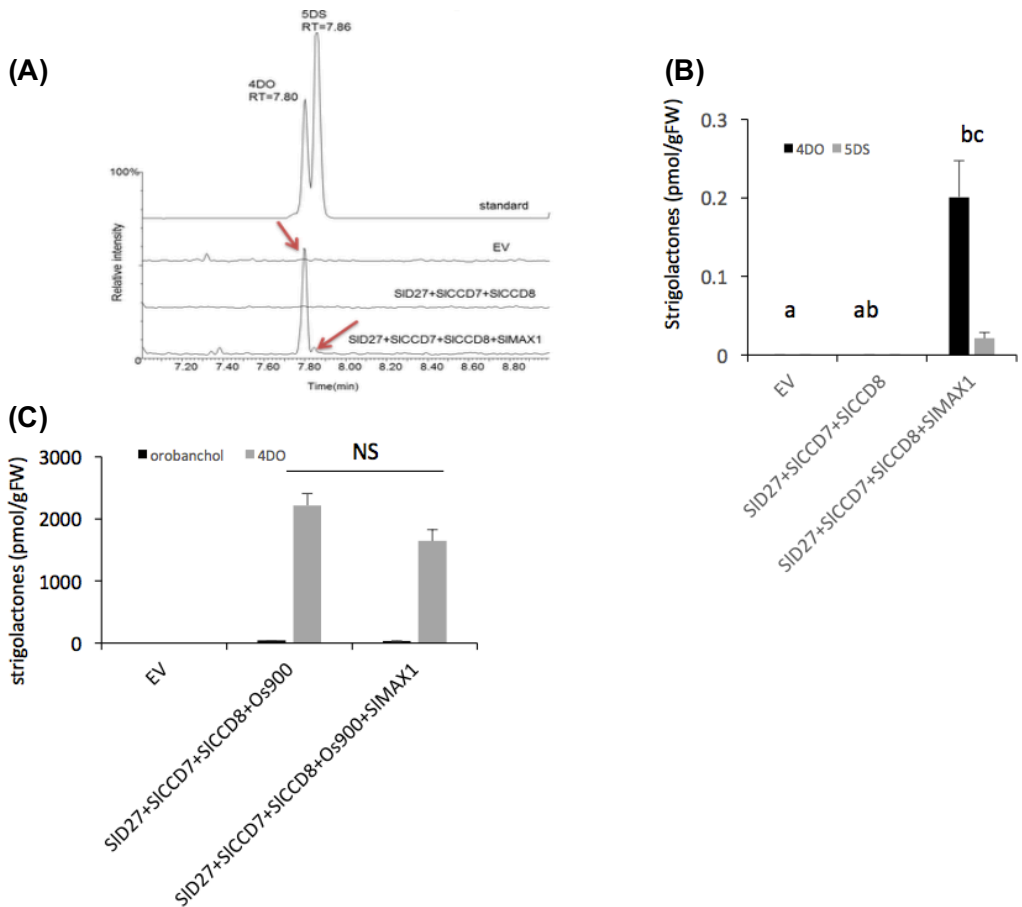


**Figure S5.** The representative chromatogram profile of 5DS and 4DO (A), strigolactone level in product by co-infiltrating *SIMAX1* with the tomato CL biosynthetic genes (B) and rice *Os900* (C) in *N. benthamiana*.

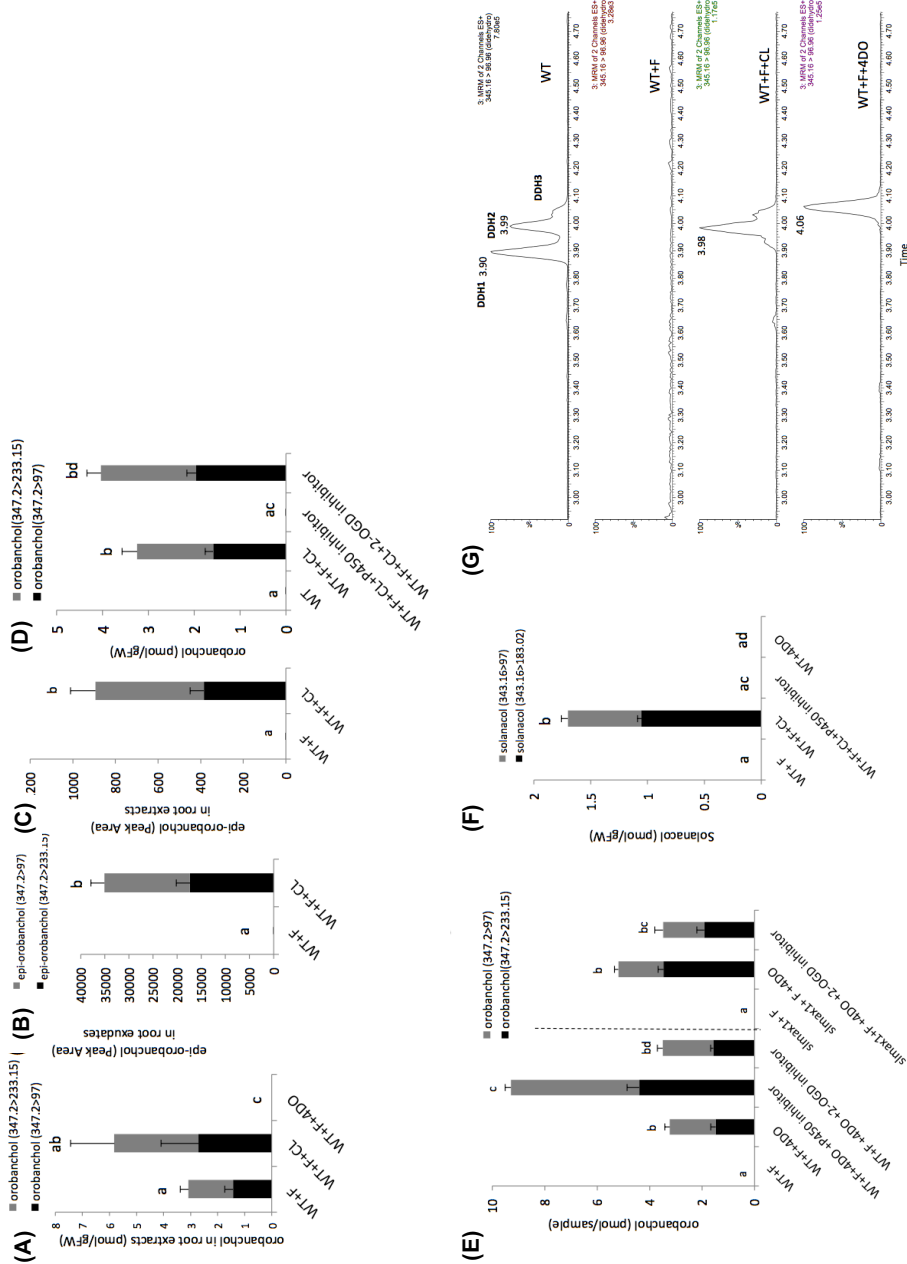


**Figure S6.** The production of strigolactones in the plant feeding assay with carlactone (CL) and 4-deoxy-orobanchol (4DO). The level of orobanchol (A, D, E), epi-orobanchol (B, C), solanacol (F) in the tomato root extracts between feeding with CL and 4DO in combination with 2-OGD inhibitor, fluridone fluridone, P450 inhibitor. The representative chromatogram profile of dihydro-orobanchol (DDH) isomers (DDH1, DDH2 and DDH3) in the tomato plant feeding assays as in (A).

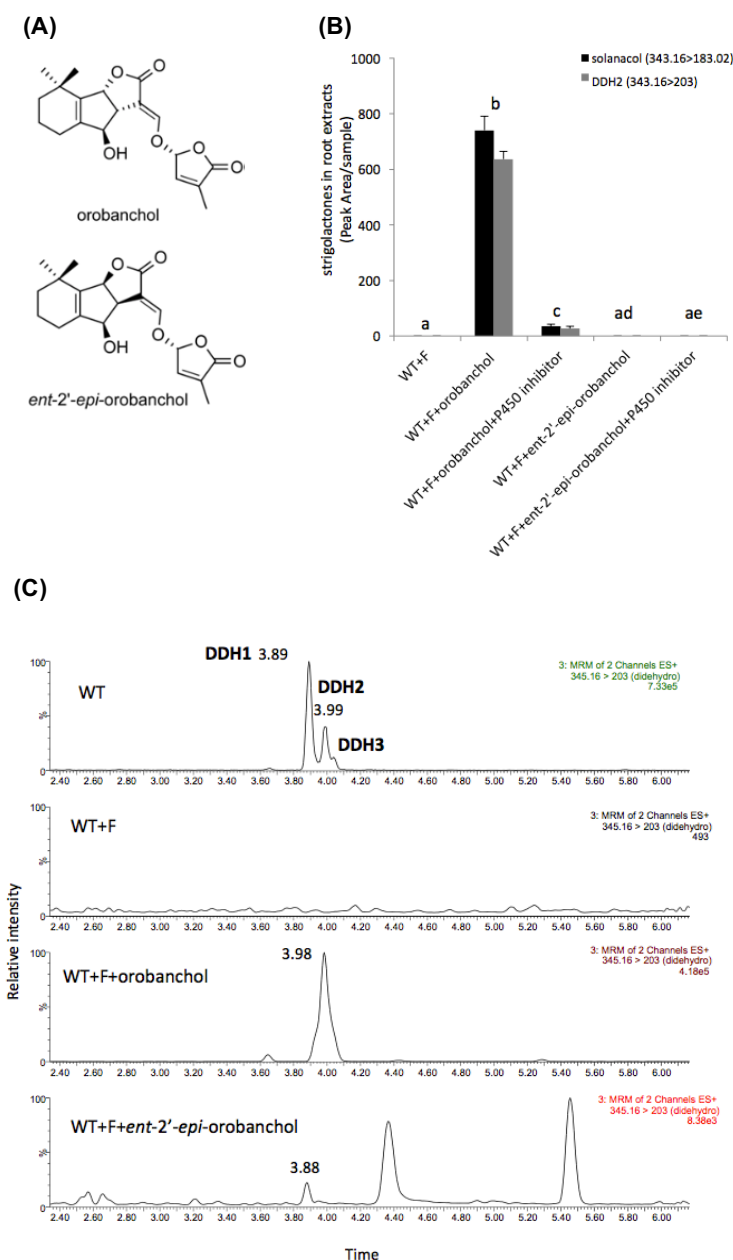


**Figure S7.** Structures of two orobanchol isomers (A), strigolactone level (B), the representative chromatogram profile of didehydro-orobanchol (DDH) isomers (DDH1, DDH2 and DDH3) (C) in the tomato plant feeding assays with orobanchol and ent-2'-epi-orobanchol.





## Dissection of hypocotyl and root response to strigolactone in darkness in a genome-wide association study

---

**Authors:**

Xi Cheng, Harro Bouwmeester<sup>\*,\*</sup> and Carolien Ruyter-Spira

**Affiliations:**

Laboratory of Plant Physiology, Wageningen University,  
Droevendaalsesteeg 1, 6708 PB Wageningen, the Netherlands

<sup>\*</sup>Present address: Plant Hormone Biology lab, Swammerdam Institute  
for Life Sciences, University of Amsterdam, Science Park 904, 1098 XH  
Amsterdam, the Netherlands

<sup>\*</sup>Correspondence: [h.j.bouwmeester@uva.nl](mailto:h.j.bouwmeester@uva.nl), tel. +31 6 20387674

### Abstract

Strigolactones are a group of carotenoid-derived plant hormones. They regulate shoot branching, root architecture and secondary growth, and are involved in plant responses to environmental factors such as light, nutrient deprivation, osmotic stress and pathogens. With regard to the plant response to light (or dark), strigolactones have been found to be regulators of photomorphogenesis (de-etiolation) and skotomorphogenesis (etiolation). Although several components of strigolactone signalling have been uncovered in recent years, the strigolactone signalling cascade during etiolation remains largely unknown. In order to gain more insight in this process, we exploited the genetic variation for the decrease in hypocotyl growth upon application of GR24, a synthetic strigolactone analog, in the dark in a large collection of *Arabidopsis* ecotypes, to perform a genome-wide association (GWA) study. In addition to this, we also explored the effect of GR24 application on root growth, and the ratio of root and hypocotyl growth. The analysis of accessions showing the most extreme response to GR24 in root and/or hypocotyl growth, revealed four distinct patterns. Based on SNP annotation, GO analysis and SNP prioritization using a newly developed scoring system, significant QTLs and corresponding candidate genes were selected for future investigation. Among the a priori candidate gene list, genes involved in sugar transport, hormone signalling and stress/disease response are highlighted. This study is the first attempt to use association mapping to explore mechanisms involved in strigolactone signalling.

### Keywords

genome-wide association study (GWAS), strigolactone signalling, etiolation, skotomorphogenesis, ethylene, sugar

### Introduction

Strigolactones have been identified as signalling molecules in the rhizosphere (Bouwmeester *et al.*, 2003, Akiyama *et al.*, 2005), as well as an important plant hormone regulating shoot branching (Gomez-Roldan *et al.*, 2008), seed germination (Toh *et al.*, 2012), hypocotyl and mesocotyl growth (Hu *et al.*, 2010, Shen *et al.*, 2012, Hu *et al.*, 2014, Jia *et al.*, 2014), root development (Kapulnik *et al.*, 2011a, Kapulnik *et al.*, 2011b, Koltai, 2011, Ruyter-Spira *et al.*, 2011, De Cuyper *et al.*, 2015), secondary growth (Agusti *et al.*, 2011) and leaf senescence (Yamada *et al.*, 2014, Ueda & Kusaba, 2015), often in response to biotic and abiotic stresses (Bu *et al.*, 2014, Kapulnik & Koltai, 2014, Torres-Vera *et al.*, 2014, Liu *et al.*, 2015, Piisila *et al.*, 2015, Stes *et al.*, 2015, Marzec, 2016, Cheng *et al.*, 2017, Decker *et al.*, 2017).

Our knowledge of strigolactone biosynthesis and signalling has expanded during the last decade. We now know that strigolactones are derived from the carotenoid pathway. Strigolactone biosynthesis is catalyzed by several key enzymes including DWARF27 (D27), MORE AXILLARY GROWTH 3 and 4 (MAX3 and MAX4), and MORE AXILLARY GROWTH1 (MAX1) (Booker *et al.*, 2005, Lin *et al.*, 2009, Alder *et al.*, 2012, Kohlen *et al.*, 2012, Abe *et al.*, 2014, Zhang *et al.*, 2014). The two known central components of strigolactone perception include an F-box protein MORE AXILLARY GROWTH2 (MAX2) in *Arabidopsis* or DWARF3 (D3) in rice (Stirnberg *et al.*, 2007, Mashiguchi *et al.*, 2009, Nelson *et al.*, 2011, Yoshida *et al.*, 2012) and an  $\alpha/\beta$  hydrolase called DWARF14 (D14). The latter serves as a strigolactone receptor (Arite *et al.*, 2009, Hamiaux *et al.*, 2012, Chevalier *et al.*, 2014). In the D14 family, the other paralog of *Arabidopsis* D14, D14 LIKE1 (D14L1)/KARRIKIN INSENSITIVE 2 (KAI2) is required for the response to karrikin-like molecules (Flematti *et al.*, 2004, Nelson *et al.*, 2010, Waters *et al.*, 2012). Karrikins are chemicals found in smoke that can promote seed germination and photomorphogenesis but are likely not the real endogenous ligand for example *Arabidopsis* D14L1. In rice, D14 and D14L1 have been found to exert inhibitory effects on mesocotyl elongation in the dark, via a strigolactone-dependent and -independent signalling pathway, respectively (Kameoka & Kyoizuka, 2015). Recently, more components of strigolactone signalling have been identified, such as DWARF 53 (D53) in rice, a repressor of strigolactone signalling, whose degradation is mediated by the strigolactone-dependent formation of the D14-D3 complex (Jiang *et al.*, 2013, Zhou *et al.*, 2013, Kong *et al.*, 2014). Interestingly, the D53 homologue in *Arabidopsis*, SUPPRESSOR OF MORE AXILLARY GROWTH2

1 (*SMAX1*), also acts downstream of *MAX2* to mediate processes such as seed germination and hypocotyl growth, but does not affect other processes such as lateral root growth, axillary shoot growth and senescence (Stanga *et al.*, 2013). Several *SMAX1-like* (*SMXL*) genes, that were found to be up-regulated in seedlings treated with the strigolactone analog GR24, may also act downstream of *MAX2* signalling to control diverse responses to strigolactones (Stanga *et al.*, 2013). In addition, there are a few other components, such as *SHY2* (*SHORT HYPOCOTYL 2*), *BES1* (*bri1-EMS-suppressor 1*) and *OsMADS57*, that have been found to act downstream of strigolactone signalling or directly/indirectly interact with strigolactone signalling (Guo *et al.*, 2013, Koren *et al.*, 2013, Wang *et al.*, 2013). *SHY2*, which is a key regulator in the auxin and cytokinin mediated control of meristem size, has been suggested to take part in strigolactone signalling to control primary root elongation and lateral root formation (Koren *et al.*, 2013). *BES1*, which is a positive regulator of brassinosteroid signalling, has been reported to be one of the direct targets of *MAX2* in the control of shoot branching (Wang *et al.*, 2013). The rice *OsMADS57* protein, that interacts with *OsTB1* (*TEOSINTE BRANCHED1*), has been shown to target strigolactone receptor *D14* to control tillering (Guo *et al.*, 2013). The discovery of all these individual components that are involved in strigolactone signalling has revealed the complexity of this process and possible crosstalk with other signalling pathways.

Light is an essential environmental factor for plant development. When seeds germinate in the soil in the absence of light, new plantlets emerge from the seed coat and show etiolated growth (skotomorphogenesis). This is characterized by rapid growth of the hypocotyl, the formation of an apical hook, closed cotyledons lacking chlorophyll accumulation and a limited root system (von Arnim & Deng, 1996, Arsoviski *et al.*, 2012). Upon reaching the soil surface, light exposure subsequently allows seedlings to reduce the elongation of their hypocotyl, to open the apical hook and to expand their cotyledons that now accumulate chlorophyll. These phenomena are described as de-etiolation (photomorphogenesis)(von Arnim & Deng, 1996, Arsoviski *et al.*, 2012). Hypocotyl elongation, is intensively studied in research that focuses on light signalling and its interaction with plant hormone signalling pathways (Vandenbussche *et al.*, 2005, Mazzella *et al.*, 2014).

It has previously been shown that strigolactones play an important role in light signalling processes regulating hypocotyl elongation. In *Arabidopsis*, strigolactones promote photomorphogenesis (Nelson *et al.*, 2011, Shen *et al.*, 2012, Waters & Smith, 2013, Jia *et al.*, 2014). Comparable to

the study in *Arabidopsis*, a recent study in rice has shown that in the dark, strigolactones also inhibit elongation of the mesocotyl, a tissue between the coleoptilar node and the base of the seminal root (Hu *et al.*, 2010, Kameoka & Kyoizuka, 2015). Thus, hypocotyl or mesocotyl elongation upon strigolactone application could be used as a trait that can accurately be measured in order to study strigolactone downstream signalling and its interaction with other hormones. Several key components of photomorphogenesis have indeed been found to act downstream of strigolactone signalling during de-etiolation of hypocotyls. Examples are the central repressor of photomorphogenesis COP1 (CONSTITUTIVE PHOTOMORPHOGENIC1), and the downstream transcription factor HY5 (ELONGATED HYPOCOTYL 5) (Tsuchiya *et al.*, 2010). Other studies on hypocotyl or mesocotyl growth have shown that plant hormones such as auxin and cytokinin may interact with strigolactone signalling (Shen *et al.*, 2012, Hu *et al.*, 2014). In a proteomics approach to identify strigolactone-responsive proteins by studying mesocotyl elongation in dark-grown rice seedlings, enzymes involved in carbohydrate metabolism, amino acid metabolism, energy supply, defense response and cytoskeleton maintenance were found to be upregulated (Chen *et al.*, 2014). However, studies that explore strigolactone downstream components using a quantitative genetics approach are rare.

Strigolactones have also been found to play a role in root elongation in *Arabidopsis* (Koltai *et al.*, 2009, Ruyter-Spira *et al.*, 2011). Low concentrations of GR24 increase primary root length while higher doses of GR24 reduce the primary root length (Koltai *et al.*, 2009, Ruyter-Spira *et al.*, 2011, Shinohara *et al.*, 2013). It has been suggested that strigolactones integrate the auxin flux and cytokinin signalling in the root tip to balance cell differentiation and cell division in the primary root meristem (Koren *et al.*, 2013). These studies using mutants (Ruyter-Spira *et al.*, 2011) and a proteomics approach (Walton *et al.*, 2016) demonstrated that the root response to GR24 is *MAX2*-dependent. However, otherwise, little is known about downstream components of strigolactone signalling during the regulation of root growth.

Genetic approaches have been widely adopted to study hypocotyl and root growth under different environmental conditions. Identification of the correlation between molecular markers and the observed phenotype, as used in quantitative trait locus (QTL) mapping, is a common and practical approach to search for causal genes that contribute to the genetic variation in various traits. In recent years, genome-wide association (GWA) studies, also known as linkage disequilibrium (LD) mapping or association mapping, have gained popularity in identifying trait-marker relationships based on LD,

which refers to the correlation between alleles in a population (Flint-Garcia *et al.*, 2003). Unlike family-based methods for linkage analysis, GWA mapping evaluates genetic diversity across natural populations to identify SNP polymorphisms that correlate with phenotypic variation, providing much higher resolution than QTL mapping to identify QTLs (Flint-Garcia *et al.*, 2003). In *Arabidopsis*, GWA mapping has for example been used to identify QTLs that contribute to shade avoidance (using a low red: far-red light ratio to mimic shade) (Filiault and Maloof 2012) and root growth of plants growing under conditions with different nutrient availabilities (Gifford *et al.*, 2013, Rosas *et al.*, 2013, Stetter *et al.*, 2015).

In the present study, we performed a genome-wide association (GWA) study by using a core set of *Arabidopsis* ecotypes to assess natural variation in the response of hypocotyl length (HL), root length (RL) and root length: hypocotyl length ratio (RL: HL Ratio) to GR24 treatment in the dark. Analysis of the most extremely performing accessions showed that four distinct patterns of hypocotyl and root response to GR24 occur. Based on the association of phenotypic variation with genetic markers, significant SNPs were identified and prioritized for future investigation. This study was the first to use GWA mapping to exploit strigolactone downstream signalling.

### Materials & Methods

#### Plant materials and plant growth

An *Arabidopsis* population consisting of a core set of 349 accessions was obtained from the Arabidopsis Biological Resource Center (Baxter *et al.* 2010; Li *et al.* 2010; Horton *et al.* 2012). Seeds of the *Arabidopsis* population were sown in eight 96-well ELISA plates, with Col-0 as reference accession on two different positions in each plate (central and marginal positions). The rac-GR24 that was used contained both the GR24<sup>5DS</sup> (GR24+) and GR24<sup>ent-5DS</sup> (GR24-) enantiomers (Scaffidi *et al.*, 2014a). Each well of the GR24 containing plates was first filled with 200  $\mu$ l  $\frac{1}{2}$  MS 0.4% sucrose-free agar medium, reaching a final GR24 concentration of 10  $\mu$ M (diluted from 10 mM stock in acetone). The control plates were filled with agar medium with 0.1% acetone added. Five seeds of each *Arabidopsis* accession were distributed evenly on the surface of the agar in each well of a 96-wells plate. The plates were then sealed with parafilm and wrapped in aluminum foil. The plates were placed in a refrigerator at 4°C for 3 d for stratification. After stratification, all plates were exposed to 100  $\mu$ mol s<sup>-1</sup>m<sup>-2</sup> of cool-white fluorescent white light for 3 h to stimulate seed germination at 20°C. Thereafter, the



plates were wrapped again in aluminum foil and were placed at 20°C in the same growth chamber for 4 days.

### Quantification of traits by image analysis

After 4 days of growth under darkness, *Arabidopsis* seedlings were placed in a refrigerator at 4°C to arrest further growth. Seedlings were then carefully removed from the ELISA plates using forceps. The seedlings were laid out on a piece of black paper to facilitate accurate image analysis. Photos of young seedlings together with a piece of scaling paper were taken using a Canon EOS 60D DSLR Camera with a lens of 18-135 mm. The hypocotyl length (HL) and root length (RL) were then measured on these photos by using the freehand tool of the image analysis software ImageJ (version 1.47). The root length: hypocotyl length ratio (RLHLRatio) was calculated by dividing RL by HL. The response of hypocotyl or root length and hypocotyl: root length ratio to GR24 treatment was calculated as the difference between the treated and control value divided by the control value: Trait Response = (Treat Trait – Control Trait) / Control Trait. Abbreviations and descriptions of all traits are listed in **Table 1**.

### Statistics and heritability calculation

Normality of data was evaluated using the Shapiro-Wilk test and Q-Q plots. Spearman's correlation analysis was performed to compare pairwise correlations between traits. In addition, linear relationships were assessed between traits of interest. All the above-mentioned statistics were implemented in R (version 3.0). The narrow-sense heritability ( $h^2$ ) was estimated as  $h^2 = \sigma_A^2 / (\sigma_A^2 + \sigma_E^2)$ , where  $\sigma_A^2$  is the additive genetic effect and  $\sigma_E^2$  is the residual variance. The calculation of heritability was based on means of trait values and was implemented in R package 'heritability' (El-Soda *et al.*, 2015).

### Selection of extreme accessions and cluster analysis

Several extreme accessions were selected separately based on the ranking of hypocotyl response, root response and response of root: hypocotyl ratio. Generally, 10 accessions with highest values and 10 with lowest values were selected for hypocotyl response and response of root: hypocotyl ratio respectively. From the root response, 17 accessions with highest values (including 7 positive values) and 10 with lowest values were included. Finally, 56 accessions were selected for cluster analysis. Values of these response traits were retrieved and scaled to exclude the effect of units before

the cluster analysis. To dissect the similarity or difference between selected extreme accessions, hierarchical clustering was performed separately on scaled trait values (hypocotyl length, root length, root length:hypocotyl length ratio) under control and treatment conditions using Ward's method (Ward Jr., 1963) in R (version 3.0).

### Genome-wide association mapping

GWA mapping was performed using 341 accessions. Genotypic data for all accessions was available for 214051 SNPs. After removal of SNPs with a minor allele frequency (MAF) below 0.05, 199589 SNPs were finally used for GWA mapping, for which the mixed model was adopted as follows:  $Y_i = \mu + X_{i\beta} + G_i + E_i$ , ( $i = 1, \dots, n$ ) with  $G \sim N(0, \sigma_A^2 K)$  and  $E_i \sim N(0, \sigma_E^2)$ ;  $n$  is the total number of accessions,  $Y_i$  is the phenotypic value of accession  $i$ ,  $\mu$  is the intercept,  $X_i$  is the marker score,  $\beta$  is the marker effect and  $K$  is the kinship matrix. Genotypic effects  $G = (G_1, \dots, G_n)$  follow a  $N(0, \sigma_A^2 K)$  distribution. The random error effects  $E_i$  follow  $N(0, \sigma_E^2)$  distribution. The estimation of variance components  $\sigma_A^2$  and  $\sigma_E^2$  were obtained with the method of residual maximum likelihood (REML) by using the commercial R package 'ASREML' (Butler *et al.*, 2009) based on the methodology of EMMAX (Kang *et al.*, 2010). The significance of the marker effect  $\beta$  was tested with generalized least-squares (GLS) calculations by using the command line program 'scan-GLS' (El-Soda *et al.*, 2015). GWA mapping was performed based on means of trait values.

### Assignment of candidate QTLs, gene annotation, gene ontology (GO) analysis and prioritization of candidates

We considered a SNP to be significantly associated with a certain phenotype when the  $-\log_{10}(P)$  was larger than 4. This threshold has been utilized in previous GWAS analyses (El-Soda *et al.*, 2015, Davila Olivas *et al.*, 2016, Kooke *et al.*, 2016). Significant SNPs are not necessarily causal and they often appear near causal genes (Li *et al.*, 2010, Civelek & Lusk, 2014). Thus, SNPs that are in tight LD ( $r^2 > 0.4$ ) with the significant SNPs within a  $\pm 10$  kb region were also considered as possible candidates based on both the 250K array (Baxter *et al.*, 2010, Li *et al.*, 2010, Horton *et al.*, 2012) and re-sequencing data (1001genomes.org) as previously described (Bac-Molenaar *et al.*, 2015, Kooke *et al.*, 2016). A search window was defined by the first and last SNPs in LD ( $r^2 > 0.4$ ) with significant SNPs in the  $\pm 10$  kb neighboring region. All the genes within the search window were considered as a priori candidate genes.

Gene annotations were retrieved from the Arabidopsis Information Resource (TAIR) database. Gene expression patterns were obtained from the *Arabidopsis* eFP Browser (Winter *et al.*, 2007) and ePlant tools (Schmid *et al.*, 2005, Fucile *et al.*, 2011). The gene/protein network was predicted by GeneMANIA (Warde-Farley *et al.*, 2010). The a priori candidate gene list was submitted to the Gene Functional Classification Tool from the DAVID Bioinformatics Resources 6.8, in order to perform gene ontology (GO) analysis (Huang *et al.*, 2009a, Huang *et al.*, 2009b). Default parameters were adopted (medium classification stringency, Kappa similarity threshold = 0.35).

Comparisons of candidate QTLs were performed between response traits (Response HL, Response RL, Response RLHLRatio), traits under control and GR24 treatment to identify which QTLs are specific to strigolactone treatment and which QTLs are common to both control and treatment conditions. Shared QTLs between response trait and trait under GR24 treatment were considered as priorities in further functional characterization. Overlapping QTLs between trait under control and GR24 treatment were not prioritized in further study.

### Characterization of prioritized candidate genes by using T-DNA lines and other mutants

For prioritized candidate genes, the information of T-DNA lines was obtained from the T-DNA Express Tool (<http://signal.salk.edu/cgi-bin/tdnaexpress>). T-DNA insertion mutant lines were ordered from the European Arabidopsis Stock Centre (Alonso *et al.*, 2003). To confirm whether the T-DNA lines are homozygous or heterozygous, PCR primers were designed using T-DNA Primer Design Tool (<http://signal.salk.edu/tdnaprimers.2.html>). Seeds of the *SWEET16*, *SWEET17* single mutants (*sweet16-1*, *sweet16-2*, *sweet17-1*, *sweet17-2*), double mutants (*sweet16-1 sweet17-1*), the transgenic over-expressor lines (35S:*SWEET16-1*, 35S:*SWEET16-2*, 35S:*SWEET16-3*, 35S:*SWEET17-1*, 35S:*SWEET17-2*, 35S:*SWEET17-6*) and corresponding wildtypes of the mutants (Col-0 (T-DNA)) and transgenic lines (Col-vector) were kindly provided by Dr. Woei-Jiun Guo (Institute of Tropical Plant Sciences, National Cheng Kung University, Taiwan)(Guo *et al.*, 2014). For the phenotypic characterization of homozygous T-DNA lines, mutants and transgenic lines, a similar procedure was followed as for the GWA screening. Five technical replicates per accession were placed in one individual well of a 96-well plate and three biological replicates (plates) were used.

### Results

### Trait distributions, correlations and heritability

A core set of the *Arabidopsis* population, which was shown to exhibit extensive genetic diversity and limited population structure (Baxter et al. 2010; Li et al. 2010; Horton et al. 2012), was used to explore the variation in hypocotyl elongation and root growth as a response to GR24 (10  $\mu$ M) application. In addition to this, the variation in changes in the ratio between root length- and hypocotyl length as a result of GR24 (10  $\mu$ M) treatment was also registered. The latter was performed to get an impression of the resource (biomass) partitioning or signalling between below-ground and above-ground tissues. The abbreviations, descriptions and heritabilities for these traits are included in **Table 1**. Phenotypic distributions during control conditions and GR24 treatment were compared (**Figure 1A-C**). Compared to the control, the hypocotyl length distribution shifted to lower values when plants were grown in the presence of GR24 (**Figure 1A**). Moreover, the response of hypocotyl elongation of all the accessions had negative values (**Figure 1D**). These results suggest an inhibitory effect of 10  $\mu$ M GR24 on hypocotyl elongation in darkness. The majority of GR24-treated plants showed a decrease in root elongation as well, when compared to the untreated control plants (**Figure 1B**). However, there were seven accessions showing a small positive root response upon GR24 treatment (**Figure 1E**). The distribution of the ratio between root and hypocotyl length showed a minor positive shift in 65% of the accessions when compared with the ratio in untreated plants (**Figure 1C**), while the other 35% displayed a decrease in that ratio (**Figure 1F**).

**Table 1. Trait abbreviations, descriptions and heritability ( $h^2$ ).**

## GWA Mapping on Strigolactone Response

Trait Abbreviation	Trait Description	Heritability ( $h^2$ )
Control HL	Hypocotyl length (HL) under control conditions	0.52
Control RL	Root length (RL) under control conditions	0.57
Control RLHLRatio	RL: HL under control conditions	0.62
Treat HL	HL upon GR24 treatment	0.77
Treat RL	RL upon GR24 treatment	0.65
Treat RLHLRatio	RL: HL ratio upon GR24 treatment	0.74
Response HL	Change in HL upon GR24 treatment	0.15
Response RL	Change in RL upon GR24 treatment	0.16
Response RLHLRatio	Change in RL: HL ratio upon GR24 treatment	0.22

The correlation and linear relationships between the phenotypic traits were explored in order to see whether the hypocotyl and root growth are independent of each other, and whether hypocotyl or root response to strigolactone depends on their initial growth under control condition (**Figure S1**). Hypocotyl length and root length are only moderately correlated with, and weakly dependent on each other, when plants are grown under the same condition (correlation coefficient  $r = 0.49$  under control,  $0.46$  under GR24 treatment; coefficient of determination  $R^2 = 0.25$  under control,  $0.23$  under treatment,  $P < 0.001$ ) (**Figure S1**). In addition, the correlation and linear relationship between the response to GR24 in root and hypocotyl growth is also low ( $r = 0.37$ ,  $R^2 = 0.11$ ,  $P < 0.001$ ) (**Figure S1**), suggesting that different mechanisms underlie the hypocotyl and root response to strigolactone. Besides, there is no correlation between hypocotyl response and hypocotyl length under control conditions (**Figure S1**). This suggests that the effect of GR24 application is not dependent on the initial growth of the plants.

To estimate to what extent the phenotypic variation can be explained by additive genotypic variation, narrow-sense heritability was calculated (**Table 1**). For single traits, such as hypocotyl length, root length and root: hypocotyl ratio under control conditions and upon GR24 treatment, heritabilities were high, ranging from  $0.52$  to  $0.77$  (**Table 1**). However, the heritabilities for hypocotyl response, root response and response of root: hypocotyl ratio to GR24 were lower, ranging from  $0.15$  to  $0.22$  (**Table 1**).

### Variation of strigolactone response in hypocotyl, root growth and root: hypocotyl ratio in *Arabidopsis* accessions

As the *Arabidopsis* population showed extensive variation in its response to GR24 with respect to both root and hypocotyl growth, it is of interest to explore the distinct patterns with which the accessions respond.

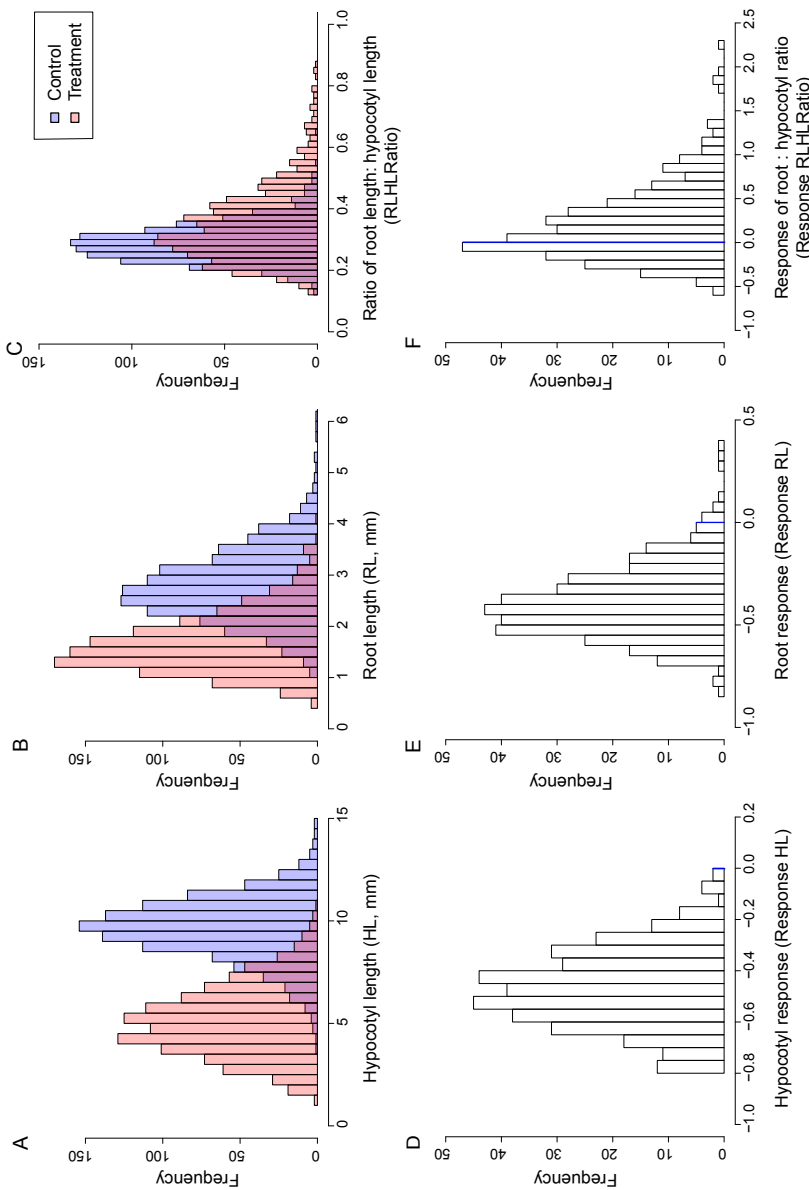


**Figure 1. Histograms displaying the distribution of traits observed within a population consisting of 349 *Arabidopsis* ecotypes.** Distributions of traits hypocotyl length (HL, mm), root length (RL, mm), ratio of root length: hypocotyl length (RL:HL Ratio) under control conditions (in blue) and GR24 treatment (in red) are displayed in (A), (B), (C), respectively. The overlap observed between both distributions under control and treatment condition is displayed in purple. Distributions of hypocotyl length response to GR24 (Response HL), root response to GR24 (Response RL), response of root: hypocotyl ratio to GR24 (Response RL:HL Ratio) are displayed in (D), (E), (F), respectively.

Therefore, 56 extreme accessions were selected based on their individual ranking of hypocotyl response, root response and their response of the observed root: hypocotyl ratio. Hierarchical clustering was then applied to the response values of these accessions, resulting in four distinct groups differing in the extent to which they respond to strigolactone (**Group 1, 2, 3 and 4**) (**Figure 1**). The accessions in **Group 1** displayed a low level of GR24-mediated inhibition of hypocotyl growth (**Figure 2** and **Figure S2**). Depending on whether their roots were sensitive to the GR24 treatment, **Group 1** was further divided into two subgroups, one subgroup having a mild root response (such as Ra-0) and the other subgroup having a very limited root response (such as accession LL-0). The accessions in **Group 2** showed the highest sensitivity to GR24 treatment, both in the root and hypocotyl length response (**Figure 2** and **Figure S1**). Probably due to the difference in the extent of hypocotyl and root growth inhibition, the response of root: hypocotyl ratio for accessions in **Group 2** is positive (eg. For accession TDr-1) or negative (eg. For accession PHW-31), resulting into two subgroups. The accessions in **Group 3** also showed a considerable inhibition of hypocotyl growth upon GR24 application, however, their root responses were variable. In addition, the effect of GR24 on the root: hypocotyl ratio for accessions in **Group 3** was generally positive because the hypocotyl response was larger than their root response (**Figure S2**). Finally, the accessions in **Group 4** have a very limited root response in combination with a mild hypocotyl response, and a mild response of the root: hypocotyl ratio. Collectively, the clustering of extreme accessions has indicated distinct response patterns to GR24 with respect to hypocotyl and root growth which needs further exploration of the underlying mechanisms.



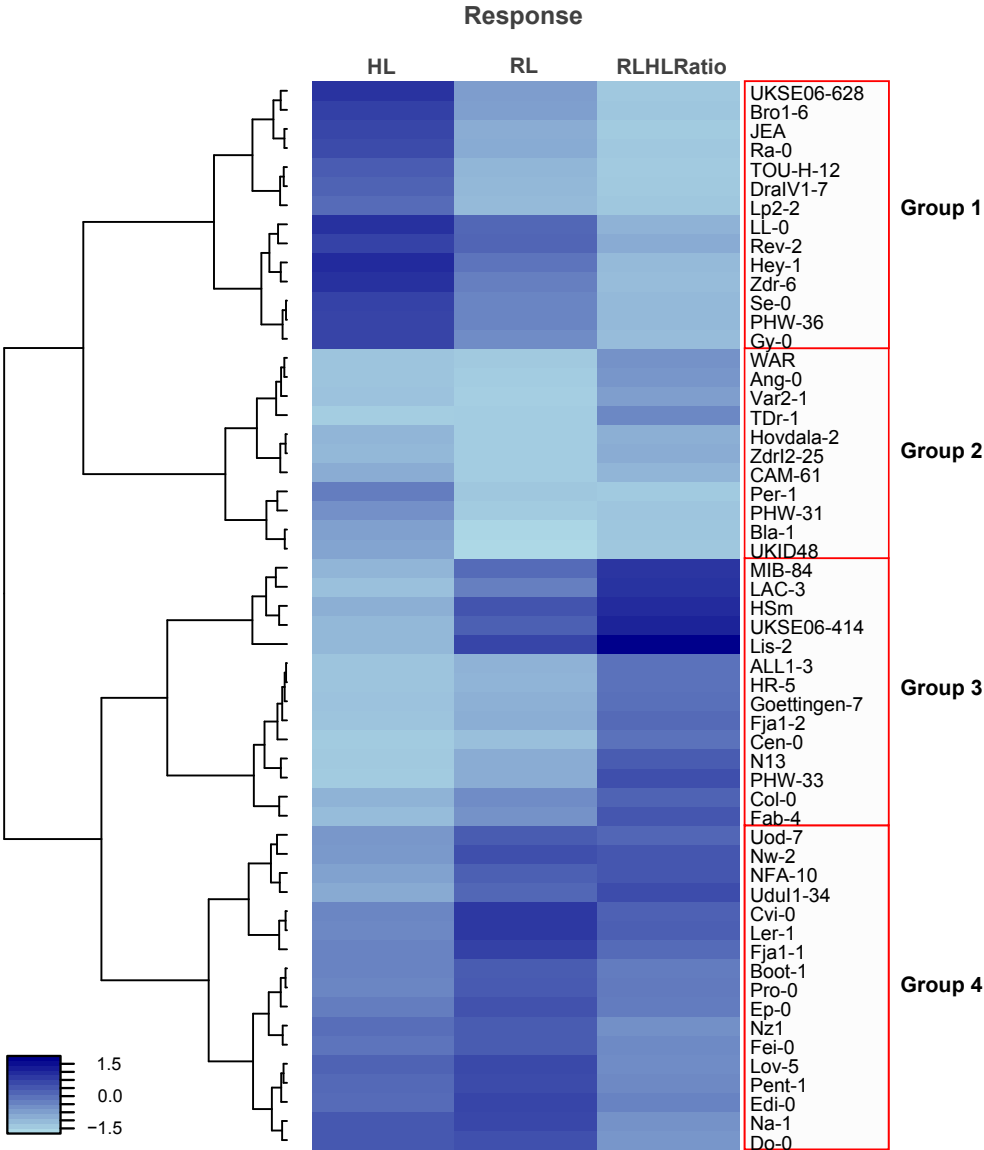


**Figure 2.** Heatmap of hierarchical clustering on strigolactone responses of 56 extreme accessions based on their individual ranking of hypocotyl response, root response and their response of root: hypocotyl ratio. The lighter the blue, the stronger the inhibitory effect of GR24 on the trait. Names of accessions are listed vertically alongside the heatmap. Trait values were scaled to get rid of the effect of units before the cluster analysis. The extreme accessions are clustered into four

groups (Group 1, 2, 3 and 4) by cluster analysis using Ward's method (Ward Jr., 1963). HL, hypocotyl length; RL, root length; RLHLRatio, the ratio of root length: hypocotyl length.

### Genome-wide association mapping and candidate QTL prioritization

To identify the regions of the *Arabidopsis* genome that are associated with the regulation of hypocotyl and root growth, and their ratio, under control conditions, GR24 treatment and the corresponding calculated responses of these traits, a genome-wide association study was performed (**Figure 3**). In this study, 199589 SNPs (Baxter *et al.*, 2010, Li *et al.*, 2010, Horton *et al.*, 2012) were used in a linear mixed model that corrects for population structure (EMMAX) (Kang *et al.*, 2010). The arbitrary threshold of  $-\log_{10}(P) = 4$  was set to focus on the QTLs with the largest explained variance. Significant SNPs are not necessarily responsible for the observed variation in the associated phenotypic traits. The real causative allele may reside adjacent to the significant SNPs in an LD block or even adjacent to the LD block (Li *et al.*, 2010, Civelek & Lusi, 2014). Therefore, SNPs with sufficient LD ( $r^2 > 0.5$ ) with the tag SNPs within a  $\pm 10$  kb region were also included in the initial candidate QTL list as described in Materials & Methods. QTLs within the search window were all considered as a priori candidate loci (**Table S1**). The a priori candidate list includes 16 QTLs for the hypocotyl response, 18 QTLs for root response and 16 QTLs for the root: hypocotyl ratio response to GR24, as well as multiple QTLs for root and hypocotyls length, and their ratio, under control and GR24 treatment (**Table S1**).

To test whether the candidate genes that are located in the QTL regions (**Table S1**) are involved in specific biological pathways possibly related to strigolactone signalling, we performed a gene functional classification test based on GO (Gene Ontology) terms for all candidate genes for hypocotyl length, root length, root: hypocotyl ratio under treatment, as well as hypocotyl response, root response and root: hypocotyl ratio response (**Table S2**) using the DAVID platform (Huang *et al.*, 2009a, Huang *et al.*, 2009b). The candidate QTLs that were associated with the strigolactone response traits were found to be enriched for disease resistance proteins, F-box proteins and galactose oxidase/kelch repeat superfamily proteins, protein kinase family proteins, transmembrane proteins and signal peptidase, transcription factors and pentatricopeptide repeat (PPR)/ tetratricopeptide repeat (TPR) superfamily proteins.

By comparing the GWA mapping results from traits under control and GR24 treatment/response traits, we concluded that most candidate QTLs were condition-specific (**Table S1**). QTLs that were found to be associated with both hypocotyl length under treatment and hypocotyl response were considered as treatment-specific candidate QTLs. Eighteen such QTLs were observed and then selected for further study (**Table 2**). In addition to this, one QTL that was observed in both the hypocotyl response and root: hypocotyl ratio response was also selected (**Table 2**).

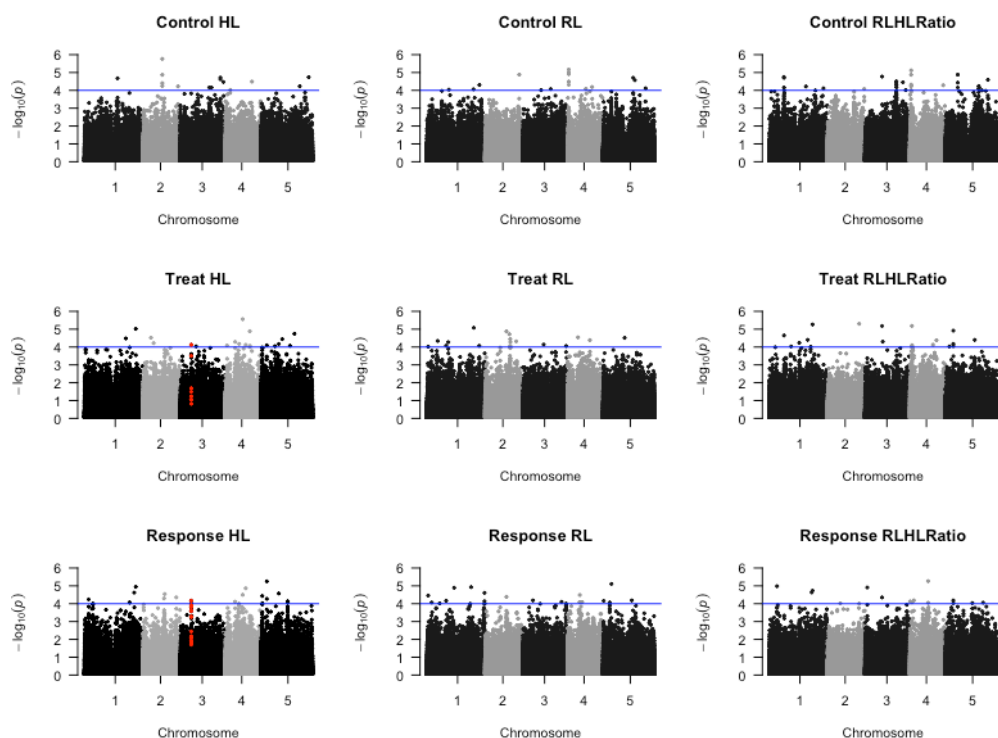


**Figure 3.** Genome-wide association analysis of hypocotyl length (HL), root length (RL), root: hypocotyl ratio (RLHLRatio) under control and GR24 treatment, and corresponding calculated response traits (Response HL, Response RL, Response RLHLRatio). The blue horizontal lines in the Manhattan plots indicate an arbitrary threshold set at  $-\log_{10}(P)=4$ . Positions highlighted by red dots are positions of SNPs identified for the *SWEET16* gene.

**Table 2. Prioritized candidate QTLs.** QTLs that were found to be associated with both hypocotyl length under treatment and hypocotyl response were considered as treatment-specific candidate QTLs. Eighteen such QTLs were included in this list. In addition, one QTL that was observed in both the hypocotyl response and response of root: hypocotyl ratio was also included. Columns represent the QTL number, chromosome (Chr), position (Pos), the highest  $-\log_{10}(P)$  value of identified significant SNPs, number of SNPs in LD with significant SNPs within  $\pm 10$  kb window, allele frequency in Col-0, effect size, information about the candidate genes (gene ID from TAIR, gene name and/or descriptions, biological process involved), and from which trait the candidate was identified. Candidate ID and names in bold indicate that there was at least one associated SNP for the same candidate gene located in the  $\pm 10$  kb window of the significant SNP. Genes highlighted in the gene ontology enrichment analysis (in **Table S2**) are underlined. NA, not available.

QTL	Chr	Pos (Mb)	SNPs in LD	Max $-\log_{10}(P)$	Allele freq	Effect size	Gene ID	Gene name/description	Biological function	Trait
1	1	23.6	15	4.03	0.57	-0.43	AT1G63560	Receptor-like protein kinase-related family protein	Unknown	Response HL, Treat HL
			8					Receptor-like protein kinase-related family protein	Unknown	Response HL, Treat HL
2	1	26.8	10	4.91	0.70	-0.53	AT1G71040	LPR2 (LOW PHOSPHATE ROOT2)	root response to phosphate starvation, meristem maintenance, oxidation-reduction process	Response HL, Treat HL
3	3	5.7	42	4.14	0.69	0.48	AT3G16690	SWEET16 (SUGARS WILL EVENTUALLY BE EXPORTED TRANSPORTER16)	Sugar transport	Response HL, Treat HL
								Fumarylacetoacetate (FAA) hydrolase family	Metabolic process	Response HL, Treat HL

(continues)

Table 2. continues

									PPR4 (PENTATRICOPEPTIDE- REPEAT 4)	AT3G16710	3.58	0.75	0.48		mRNA processing	Response HL, Treat HL
									Unknown	AT3G16712	3.77	0.75	0.49	Unknown		Response HL, Treat HL
									TL2 (TOXICOS EN LEVADU- RA 2)	AT3G16720	2.43	0.63	0.35	Defense response, pro- tein ubiquitination, re- sponse to chitin		Response HL, Treat HL
4	4	4	5.2	4		4.09	0.22	0.54	<b>ORP1C</b> <b>(OSBP(OXYSTEROL</b> <b>BINDING PROTEIN)-RE-</b> <b>LATED PROTEIN 1C)</b>	<b>AT4G08180</b>				Steroid metabolic process, signal trans- duction		Response HL, Treat HL
5	4	4	9.1	9		4.47	0.43	0.45	Calmodulin binding; tran- scription regulators	AT4G16150				Regulation of transcrip- tion		Response HL, Treat HL
6	4	4	10.8	4		4.83	0.92	0.88	Glycosyl hydrolase family protein with chitinase in- sertion domain	AT4G19770				Carbohydrate metabolic process		Response HL, Treat HL
7	5	5	0.8	19		4.40	0.48	0.45	<b>Cysteine proteinases</b> <b>superfamily protein</b>	<b>AT5G03330</b>				Proteolysis		Response HL, Treat HL
						NA	NA	NA	CDC48 (CELL DIVISION CYCLE 48C)	AT5G03340				Cell division, protein transport		Response HL, Treat HL
8	5	5	3.2	5		5.21	0.86	0.72	Major facilitator superfam- ily protein	AT5G10190				Carbohydrate transport		Response HL, Treat HL
9	5	5	9.4	1		4.54	0.60	0.47	Unknown	AT5G26790				Unknown		Response HL, Treat HL
10	5	5	14.1	22		4.05	0.19	0.56	<b>Mannose-binding lectin</b> <b>superfamily protein</b>	<b>AT5G35940</b>				Unknown		Response HL, Response RLHLRatio
						3.44	0.17	0.54	Unknown	AT5G35945				Unknown		Response HL, Response RLHLRatio
11	1	1	0.7	6		4.44	0.60	-0.48	<b>PEX6 (PEROXIN 6)</b>	<b>AT1G03000</b>				Fatty acid beta-oxida- tion, protein import into peroxisome matrix		Response RL, Treat RL
12	1	1	10.1	22		4.15	0.81	-0.57	tRNA-Pro (anticodon: TGG)	AT1G28790				Translation		Response RL, Treat RL

**Table 2.** continues

12	1	10.1	22	4.15	0.81	-0.57	AT1G28790	tRNA-Pro (anticodon: TGG)	Translation	Response RL, Treat RL
13	2	11.2	9	4.37	0.75	-0.55	AT2G26290	ARSK1 (ROOT-SPECIFIC KINASE 1)	Cell surface receptor signalling pathway, defense response, protein phosphorylation	Response RL, Treat RL
				3.13	0.72	-0.45	AT2G26310	FAP2 (FATTY-ACID-BINDING PROTEIN 2)	Fatty acid binding	Response RL, Treat RL
14	1	22.7	16	4.75	0.69	-0.50	AT1G61475	ATP binding: protein kinases	Protein amino acid phosphorylation	Response RL- HLRatio, Treat RLHLRatio
				NA	NA	NA	AT1G61480	S-locus lectin protein kinase family protein	Protein amino acid phosphorylation, recognition of pollen	Response RL- HLRatio, Treat RLHLRatio
15	2	16.6	4	4.01	0.53	-0.42	AT2G39840	TOPP4 (TYPE ONE SERINE/THREONINE PROTEIN PHOSPHATASE 4)	Protein dephosphorylation, protein phosphorylation, red light signalling pathway	Response RL- HLRatio, Treat RLHLRatio
16	3	8.9	2	4.36	0.23	0.53	AT3G24480	Leucine-rich repeat (LRR) family protein	Cell wall organization	Response RL- HLRatio, Treat RLHLRatio
17	4	1.1	1	4.09	0.81	-0.55	AT4G02420	LECRK-IV.4 (L-TYPE LECTIN RECEPTOR KINASE IV.4)	Protein amino acid phosphorylation, defense response to bacterium, defense response to oomycetes	Response RL- HLRatio, Treat RLHLRatio
18	5	4.1	7	4.20	0.11	0.70	AT5G13000	CALS3 (CALLOSE SYNTHASE 3), GSL12 (GLUCAN SYNTHASE-LIKE 12)	Cell wall organization, regulation of cell shape, (1->3)-beta-D-glucan biosynthetic process	Response RL- HLRatio, Treat RLHLRatio
				3.63	0.11	0.65	AT5G13010	CUV (CLUMSY VEIN), EMB3011 (EMBRYO DEFECTIVE 3011)	RNA splicing, defense response, seed dormancy, root hair elongation, xylem and phloem pattern formation	Response RL- HLRatio, Treat RLHLRatio

Table 2. continues

19	5	4.1	13	2.80	0.11	0.57	AT5G13050	5-FCL (5-FORMYLTETRAHY- DROFOLATE CYCLOLI- GASE)	Folic acid-containing compound biosynthet- ic process, tetrahy- drofolate metabolic process	Response RLHL Ratio, Treat RLHL- Ratio
				4.05	0.11	0.69	AT5G13060	ABAP1 (ARMADILLO BTB PRO- TEIN 1)	Cell proliferation in leaf	Response RLHL Ratio, Treat RLHL- Ratio
				3.05	0.10	0.62	AT5G13070	MSF1-like family protein	Unknown	Response RLHL Ratio, Treat RLHL- Ratio
				NA	NA	NA	AT5G13080	WRKY75 (WRKY DNA-BINDING PROTEIN 75)	Atrichoblast differenti- ation, lateral root de- velopment, regulation of transcription in re- sponse to stress, reg- ulation of response to nutrient levels	Response RLHL Ratio, Treat RLHL- Ratio



### Candidate genes involved in the hypocotyl response to strigolactone and their phenotypic characterization

We analysed the variation in hypocotyl growth in response to GR24 treatment. GWA analysis allowed the association of the variation to regions in the genome. We identified 16 and 25 QTLs for the hypocotyl response and hypocotyl length under treatment, respectively. Nine QTLs associated with both hypocotyl response and hypocotyl length under treatment were considered most promising candidates (**Table 2**).

One of the most significant QTLs (**QTL8** on chromosome 5, **Table 2**) that was associated with the hypocotyl response to GR24 contained AT5G10190 (Major facilitator superfamily protein) and AT5G10200 (ARM-repeat/Tetratricopeptide repeat (TPR)-like protein). The most significant SNP explained 6.17% of the phenotypic variance. Biological functions of both genes are still not clear, but the AT5G10190 is predicted to be involved in carbohydrate transmembrane transport. Interestingly, two other candidate genes for this trait (AT3G16690: sugar transporter gene *SWEET16* (*SUGARS WILL EVENTUALLY BE EXPORTED TRANSPORTER 16*) in **QTL3**, and AT4G19770: Glycosyl hydrolase family protein with chitinase insertion domain in **QTL6**) are also described to be involved in either carbohydrate transport or its metabolic process (**Table 2**).

**QTL3** on chromosome 3 includes 42 SNPs located within the search window between *SWEET16* and AT3G16720 (*TL2*, *TOXICOS EN LEVADURA 2*) (**Table 2**, **Figure 4A-B**). This window also contains AT3G16700 (Fumarylacetoacetate hydrolase family), AT3G16710 (*PPR4*, *PENTATRICOPEPTIDE REPEAT 4*) and AT3G16712 (unknown protein) (**Figure 4B**). While the biological functions of AT3G16710 (*PPR4*) and AT3G16712 (unknown protein) are still not clear, AT3G16700 (fumarylacetoacetate hydrolase family) is involved in metabolic processes and has copper ion binding activity (Tan et al. 2010) and AT3G16720 (*TL2*) is involved in defense responses (Serrano & Guzman, 2004, Serrano *et al.*, 2007). Phenotypic characterization of a T-DNA mutant line for AT3G16710 (*PPR4*), however, did not show any differences when compared with the corresponding wild type (**Figure S3**). For *SWEET16*, previous reports showed that overexpressor lines had an increased shoot and root biomass, indicating the positive role of *SWEET16* in shoot and root growth (Klemens *et al.*, 2013). From the expression data obtained from the eFP platform, this gene is highly expressed both in hypocotyl and root. Besides, its expression is increased in the ABA-deficient mutant *aba1* (*abscisic acid 1*) but reduced

in the hypocotyl of strigolactone-deficient mutant *max4* when compared to wild-type Col-0 (**Figure S4**). This suggests that this sugar transporter might be involved in ABA and strigolactone related processes in the hypocotyl. Based on prediction on protein interactions using the tool GeneMANIA, the SWEET16 protein may be co-localized with and physically interact with other proteins such as TCP14 (TEOSINTE BRANCHED, CYCLOIDEA AND PCF 14) (**Figure S5**), which is involved in seed germination, internode elongation and shoot branching (Kieffer *et al.*, 2011, Steiner *et al.*, 2014, Resentini *et al.*, 2015). SWEET16 has also been predicted to be co-localized with or interact with other SWEET proteins such as SWEET17 and SWEET14 based on the tool GeneMANIA (**Figure S5**). *SWEET17*, the paralog of *SWEET16*, reached a  $-\log_{10}(P)$  of 3.26 for hypocotyl length under treatment (**Table S4**), while the other paralog *SWEET14* was found in close LD with a significant SNP (search window position from 12844029 to 12855170 on chromosome 4) associated with hypocotyl length under GR24 treatment (**Table S1**). *SWEET17* is highly expressed in the cortex of roots and functions as a fructose-specific uniporter on the root tonoplast (Guo *et al.*, 2014). *SWEET14* was recently reported to be involved in mediating the response to gibberellin during germination and seedling stages (Kanno *et al.*, 2016). To explore whether *SWEET* genes are also involved in strigolactone signalling, *sweet16* and *sweet17* single and double mutants as well as 35S promoter-fused *SWEET16* and *SWEET17* over-expression lines (Guo *et al.*, 2014) were subjected to a phenotypic characterization (**Figure 4C-D**). Hypocotyl elongation of single mutants *sweet16-1*, *sweet16-2* and *sweet17-1* showed a tendency of decreased response to GR24, however not reaching statistical significance (**Figure 4C-D**). Other mutants, such as *sweet17-2* and the double mutant *sweet16-1 sweet17-1* were similar to wildtype in the hypocotyl response (**Figure 4C-D**). In contrast, 35S:*SWEET16-1* displayed remarkably enhanced responses to GR24 when compared to the wild-type (**Figure 4D**). Most of other over-expressors of *SWEET16* and *SWEET17* also showed a tendency of increased hypocotyl response to GR24 although not reaching statistical significance, except for 35S:*SWEET17-6* (**Figure 4D**).

**QTL4** (**Table 2**), containing 4 SNPs, spans over the exon and 3'-UTR region of gene AT4G08180 (*ORP1C*, *OSBP* (OXYSTEROL BINDING PROTEIN)-RELATED PROTEIN 1C). This gene was found to be highly expressed in pollen and is involved in pollen germination (Wang *et al.*, 2008). It is hardly expressed in the hypocotyl according to the eFP browser. Phenotypic characterization showed that a mutation in the exon of this gene (T-DNA mutant SALK\_089877C, **Table S3**) did not cause altered response to GR24 (**Figure S3**).

Although their functions are currently unknown, the expression of a few other candidate genes in the hypocotyl is high according to the eFP browser and ePlant platform. AT5G35940 (Mannose-binding lectin superfamily protein), a putative candidate gene underlying **QTL10** (overlapping QTL for hypocotyl response and hypocotyl length under treatment), is such an example. **QTL10** contains 22 SNPs, spanning AT5G35940 and AT5G35945 (Unknown protein). AT5G35940 is both highly expressed in hypocotyl and root, and its expression in strigolactone biosynthetic mutant *max4* and ABA biosynthetic mutant *aba1* is remarkably reduced when compared to Col-0 based on the ePlant database. A previous report showed that expression of this gene is highly induced in roots when plants are infected with root-infecting pathogens (Lyons *et al.*, 2015). In the present study, a homozygous T-DNA mutant of AT5G35940 (SALK\_045777C, **Table S3**) did not display a different response to GR24 when compared to its wild-type (**Figure S3**).

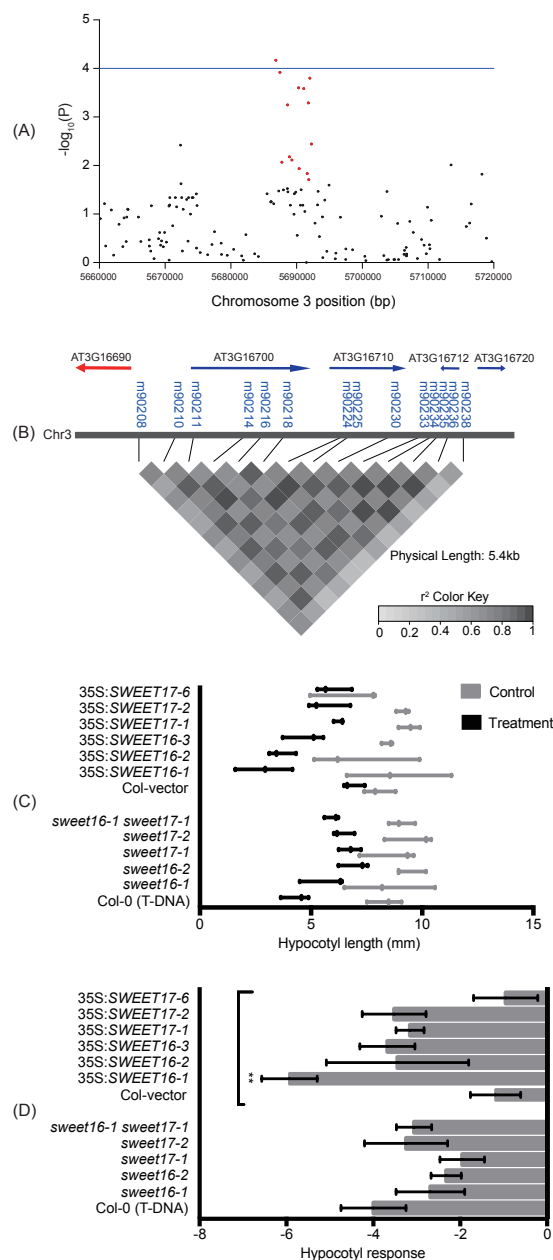


**Figure 4. SNP position, LD region of AT3G16690 (*SWEET16*) and hypocotyl response of *SWEET16*-related mutants and transgenic lines.** (A) Positions of SNPs for *SWEET16* are highlighted in red dots in a local Manhattan plot on chromosome 3. The horizontal blue line

indicates the significance threshold  $-\log_{10}(P) = 4$ . (B) LD matrix plot, showing the  $r^2$  between the SNPs in QTL3 (**Table 2**). Darker grey indicates higher  $r^2$  between two corresponding SNPs. The LD region physically spans five genes on chromosome 3, including SNPs located in the intergenic and coding region of five genes: AT3G16690 (*SWEET16*, *SUGARS WILL EVENTUALLY BE EXPORTED TRANSPORTER 16*), AT3G16700 (Fumarylacetoacetate hydrolase family), AT3G16710 (*PPR4*, *PENTATRICOPEPTIDE REPEAT 4*), AT3G16712 (unknown protein), AT3G16720 (*TL2*, *TOXICOS EN LEVADURA 2*). Marker names are indicated in blue characters. Positions and directions of the genes are indicated by arrows. The *SWEET16* gene is indicated with a red arrow. (C) Hypocotyl length of wildtype (Col-0 (T-DNA)), *sweet16* and *sweet17* single mutants (*sweet16-1*, *sweet16-2*, *sweet17-1*, *sweet17-2*), double mutant (*sweet16-1 sweet17-1*), overexpressor lines (35S: *SWEET16-1*, 35S: *SWEET16-2*, 35S: *SWEET16-3*, 35S: *SWEET17-1*, 35S: *SWEET17-2*, 35S: *SWEET17-6*) and their corresponding wildtype (Col-vector) under control conditions and GR24 treatment. Data points represent mean values and bars maximum and minimum values of three biological replicates. (D) Hypocotyl response to GR24 of wildtypes, mutants and transgenic lines. The response is calculated by subtracting hypocotyl length under control conditions from that under GR24 treatment and division by the control value ( $\pm$  standard error of means). Ordinary one-way ANOVA and Tukey's multiple comparisons test were performed to compare response traits of mutants/transgenic lines to their corresponding wildtype. \*\* indicates significant difference at  $P < 0.01$ .

### Candidate genes for the root response to strigolactones and their functional characterization

For the root response, we identified 17 QTLs for the response to GR24 and 16 QTLs for root length under GR24 treatment, with three overlapping QTLs (**Table 2** and **Table S1**). One of the three overlapping QTLs (**QTL11** on chromosome 1, **Table 2** and **Table S1**) included AT1G03000 (*PEX6*, *PEROXIN 6*) and AT1G02980 (*CUL2*, *CULLIN 2*). *PEX6* has been reported to promote peroxisomal matrix protein import which contributes to jasmonic acid (JA) biosynthesis upon wounding (Zolman & Bartel, 2004, Delker *et al.*, 2007). *CUL2* is a core component of the Skp1-Cullin-F-box (SCF) ubiquitin E3 ligase complex, which is involved in targeting proteins for degradation by the proteasome (Risseuw *et al.*, 2003). Another QTL, **QTL12** on chromosome 1, contains AT1G28700 (Nucleotide-diphospho-sugar transferase family protein), AT1G28710 (Nucleotide-diphospho-sugar transferase family protein), AT1G28720 (tRNA-Pro) and AT1G28790 (tRNA-Pro). The biological functions of the former two genes are unknown and

the latter two genes encode tRNAs which are involved in translation. The other prioritized QTL, **QTL13** on chromosome 2, spans a region covering five genes, including AT2G26280 (*CID7*, *CTC-INTERACTING DOMAIN 7*), AT2G26290 (*ARSK1*, *ROOT-SPECIFIC KINASE 1*), AT2G26300 (*GPA1*, *G PROTEIN ALPHA SUBUNIT 1*), AT2G26310 (*FAP2*, *FATTY-ACID-BINDING PROTEIN 2*), AT2G26320 (*AGL33*, *AGAMOUS-LIKE 33*). Among these genes, AT2G26290 (*ARSK1*) is specifically expressed in the root and its expression is induced by dehydration, ABA and osmotic stress (Hwang & Goodman, 1995). However, roots of a few homozygous T-DNA mutant lines for AT2G26290 (*ARSK1*) and a priori candidate genes such as AT1G08230 (*GAT1*, *GAMMA-AMINOBUTYRIC ACID TRANSPORTER 1*), AT3G54900 (*CXIP1*, *CAX INTERACTING PROTEIN 1*), AT4G10070 (KH domain-containing protein) and AT4G10090 (*ELP6*, *ELONGATOR PROTEIN 6*) (**Table S3**), did not show significantly altered sensitivity to GR24 when compared to wildtype (**Figure S3**).

### Candidate genes for the root-to-shoot ratio in response to strigolactones

For the root: hypocotyl ratio, 16 QTLs were identified for the response and 21 QTLs for the ratio under GR24 treatment (**Table S1**). There were 6 QTLs shared between the two traits. **QTL14** is located on chromosome 1, covering AT1G61475 (an ATP binding protein kinases) and AT1G61480 (S-locus lectin protein kinase family protein), both involved in protein amino acid phosphorylation. **QTL15** is located in the intergenic region of AT2G39840 (*TOPP4*, *TYPE ONE SERINE/THREONINE PROTEIN PHOSPHATASE 4*), which functions in protein dephosphorylation. Recent studies have shown that the TOPP4 protein not only regulates the stability of DELLA proteins which are key negative modulators in the gibberellin signalling pathway (Qin *et al.*, 2014), but also the phosphorylation status of PIN-FORMED1 (PIN1, an essential auxin transporter, during pavement cell interdigitation in *Arabidopsis* leaves (Guo *et al.*, 2015). Moreover, it can also modulate the stability of PIF5 (PHYTOCHROME-INTERACTING FACTOR5) during photomorphogenesis (Yue *et al.*, 2015). **QTL16** covers the coding region of AT3G24480 (Leucine-rich repeat (LRR) family protein), which is involved in cell wall organization (Baumberger *et al.*, 2003). **QTL17** contains the coding region of AT4G02420 (*LECRK-IV.4*, *L-TYPE LECTIN RECEPTOR KINASE IV.4*), which is involved in plant immunity (Wang *et al.*, 2014). **QTL18** includes AT5G13000 (*CALS3*, *CALLOSE SYNTHASE 3*) and AT5G13010 (*CUV*, *CLUMSY VEIN*). *CALS3* encodes a plasmodemata-localized callose synthase that increases callose deposition at plas-



modesmata which are cytoplasmic channels for cell-to-cell communication (Vatén *et al.*, 2011, Sevilem *et al.*, 2013, Yadav *et al.*, 2014). The *CUV* gene encodes the ortholog of DEAH-box RNA-dependent ATPase PRP16 that facilitates auxin-mediated development including embryo and vascular development, etc (Tsugeki *et al.*, 2015). Finally, QTL19 include AT5G13050 (*5-FCL*, *5-FORMYLTETRAHYDROFOLATE CYCLOLIGASE*), AT5G13060 (*ABAP1*, *ARMADILLO BTB PROTEIN 1*), AT5G13070 (MSF1-like family protein), AT5G13080 (*WRKY75*, *WRKY DNA-BINDING PROTEIN 75*). The enzyme 5-FCL, highly abundant in leaf mitochondria, has been proposed to participate in folic acid biosynthesis and metabolism (Roje *et al.*, 2002, Goyer *et al.*, 2005). *ABAP1* is involved in cell proliferation in leaves (Masuda *et al.*, 2008). *WRKY75* has been implicated in previous reports to play roles in anthocyanin accumulation, response to phosphate starvation and root development (Devaiah *et al.*, 2007, Devaiah & Raghothama, 2007, Rishma-wi *et al.*, 2014). Several T-DNA mutants were used to characterize functions of candidate genes AT2G39840 (*TOPP4*), AT4G02420 (*LECRK-IV.4*), AT5G13050 (*5-FCL*), AT5G35940 (mannose-binding lectin superfamily protein), AT5G13000 (*CALS3*) (**Figure S3**, **Table S3**). None of these T-DNA mutants displayed significantly different extent of the response of root: hypocotyl ratio from the wild type, although one mutant for *5-FCL*, with a mutation in the promotor region of the gene, showed a tendency of enhanced response to GR24, compared to its wildtype (**Figure S3**).

### Discussion

In this study, we investigated the variation of hypocotyl growth, primary root elongation and the ratio between root and hypocotyl length in response to GR24 treatment in darkness in a large collection of *Arabidopsis* accessions. Distinct strigolactone responses were identified among different accessions. GWA analysis was performed to identify candidate genes that might underlie this variation in the hypocotyl and root response to GR24.

The hypocotyl elongation of all the dark-grown *Arabidopsis* accessions was inhibited by 10  $\mu$ M GR24 (**Figure 1**). This concentration has also been shown to inhibit *Arabidopsis* hypocotyl growth in previous reports (Tsuchiya *et al.*, 2010, Jia *et al.*, 2014). Interestingly, we observed a large variation in hypocotyl length, both during control and GR24 treatment. In addition to this, we found that the response in hypocotyl growth resulting from GR24 treatment also varied between the accessions (**Figure 1**) implying a large amount of genetic variation for this trait.

Concerning root elongation, 10  $\mu$ M GR24 treatment resulted in a



reduction in root length for almost all accessions, while a few accessions displayed root elongation. It has been reported that GR24 application affects root elongation in a dose-dependent manner. In *Arabidopsis*, application of a low dose of GR24 (1.25  $\mu$ M and 2.5  $\mu$ M) increased primary root length of Col-0 plants, while higher concentrations (5 to 10  $\mu$ M) decreased primary root elongation (Ruyter-Spira et al. 2011). The latter authors hypothesized that strigolactones negatively influence local auxin levels in the root tip, while auxin, in its turn determines root growth rate. The dose-response curve for auxin induced cell elongation in the root tip is characterized by an auxin optimum. Assuming that the auxin level in control plants is higher than the optimum auxin level for root growth, the lower GR24 dose used in the latter study may have resulted in auxin levels that are closer to the optimum. Similarly, the auxin levels in plants treated with the higher dose of GR24 may already have decreased below the auxin optimum, resulting in levels that are too low to sustain maximum root growth. In the present screen, we do not know to what extent differences in endogenous auxin levels (and/or in auxin sensitivity) in root tips of the different accessions are responsible for this difference in GR24-mediated root growth rate, or to what extent this was influenced by differences in sensitivity to GR24. The few accessions showing an increased root length in response to GR24 might be the accessions with low sensitivity to GR24, which may deserve further exploration. It will be of interest to study endogenous auxin levels and auxin sensitivity in *Arabidopsis* accessions showing either a low or high GR24 response.

Several accessions with extreme hypocotyl and/or root response were identified. Detailed investigation of these accessions may help us understand the mechanism underlying variation in strigolactone responses in different tissue types. Clustering analysis of extreme accessions showed that accessions with similar performance during control conditions do not necessarily perform in the same way under treatment (**Figure 2**). In general, the strigolactone response in these extreme accessions could be divided into four types:

(1) low strigolactone response in hypocotyl and low/moderate strigolactone response in root (**Group 1 in Figure 2**);

(2) high strigolactone response in both hypocotyl and root (**Group 2 in Figure 2**);

(3) high strigolactone response in hypocotyl and moderate/high response in root (**Group 3 in Figure 2**);

(4) limited strigolactone response in both hypocotyl and root (**Group 4 in Figure 2**).

Within each clustered group also subgroups are present, indicating the com-

plex feature of the plant-wide strigolactone response. These observations may suggest different mechanisms for the strigolactone downstream signalling pathways in root and hypocotyl.

The root: hypocotyl ratio depends on both root and hypocotyl growth. Thus, variation in the response of the root: hypocotyl ratio to GR24 might indicate a role of strigolactones in mediating carbohydrate partitioning and potential regulation of plant architecture. Besides, the response of the root: hypocotyl ratio to GR24 seems more dependent on hypocotyl inhibition than on root inhibition based on correlation analysis (**Figure S1**). This suggests a higher GR24 response in the hypocotyl than in the root. In addition, the hypocotyl response/hypocotyl length under treatment and root response/root length under treatment did not correlate (**Figure S1**), once more implying different mechanisms underlying the GR24 response in these different tissues. It is still elusive whether strigolactone signalling coordinates biomass allocation and nutrient transfer between different tissues, and what factors might be involved in the hypocotyl- and root-specific strigolactone response.

In rice, *D14* and *D14L* have been suggested to work independently to inhibit mesocotyl elongation (Kameoka & Kyoizuka, 2015). However, in *Arabidopsis*, it was suggested that the strong inhibition of wildtype hypocotyl elongation by the application of the same GR24 mixture resulted from the combined activity of *AtD14* and *KAI2* (Waters *et al.*, 2012). In the present GWA results,  $-\log_{10}(P)$  values for SNPs corresponding to the *KAI2* region were all below 1 (**Table S4**), suggesting a limited effect of *KAI2* on the hypocotyl response to GR24 or limited genetic variation in this gene. Besides, note that the racemic GR24 mixture used in the present study contains non-natural stereoisomers of GR24, which could trigger *KAI2*-mediated responses (Scaffidi *et al.*, 2014b). These factors might contribute to an artefact for the GWA results concerning hypocotyl response, as the identified candidate QTLs might include both natural strigolactone-specific and -unspecific QTLs. The use of the natural GR24 stereoisomers or natural strigolactones would provide an important tool to decipher specific strigolactone downstream signalling components for future investigations.

### Identification of QTLs associated with the strigolactone response

Since the last decade, high-throughput genotyping and phenotyping techniques and next-generation sequencing platforms have facilitated GWA to dissect mechanisms underlying complex traits (Ogura & Busch, 2015). However, the identified QTLs often could only explain a small proportion of

the genetic variation, which we also found for the hypocotyl and root response to GR24 application. Overall, this is mainly due to the limited SNP effect size and existence of unexplained variation by GWA models such as epistasis (Gibson, 2010, Makowsky *et al.*, 2011, Zuk *et al.*, 2012). Therefore, it is challenging to find the true positive QTLs among the long list of candidates.

GWA analysis allowed the identification of QTLs that were associated with strigolactone responses. GO enrichment analysis on the initial candidate gene list has indicated that QTLs that were associated with strigolactone response are primarily involved in defense responses, transmembrane transport and signal transduction (**Table S2**). We tried to narrow down the strigolactone treatment-specific QTLs by identifying QTLs shared between the response of each trait and the trait value under GR24 treatment, while the QTLs shared between response/treated trait and trait under control were considered non-treatment specific QTLs which were excluded from the list of candidate QTLs. The treatment-specific QTLs were thus considered as priority for further study (**Table 2**). No overlapping QTLs were identified for hypocotyl length under control conditions and GR24 application, and most QTLs identified for root length under these two conditions did also not overlap (**Table S1**). This is consistent with the absence of a linear relationship between hypocotyl (root) length under GR24 treatment and hypocotyl (root) length during control conditions (**Figure S1**). These findings suggest that the magnitude of the strigolactone response is independent of hypocotyl (root) growth under control conditions.

Concerning the hypocotyl response to strigolactones, several candidate genes involved in metabolism were identified. Notably, two sugar transporter genes *SWEET16* (for hypocotyl response to GR24) and *SWEET14* (for hypocotyl elongation during GR24 treatment) were identified as candidate genes in two independent QTLs among the candidate list (**Table S1**). And interestingly, SNPs for the loci of *SWEET17*, the homologue of *SWEET16*, also showed association with the hypocotyl response, albeit not significant ( $3 < -\log_{10}(P) < 4$ ) (**Table S4**). *SWEET* proteins function as low-affinity sucrose transporters (Chen *et al.*, 2012). *SWEET14*, functionally redundant with *SWEET13*, is expressed in anthers, vascular tissues in leaves and roots, axillary buds and embryonic cotyledons (Kanno *et al.*, 2016). It was recently found that *SWEET14* and *SWEET13* also transport gibberellins in or out of the vascular tissues, during germination and seedling stages (Kanno *et al.*, 2016). Both *SWEET17* and *SWEET16* are vacuolar membrane-localized sugar carriers. *SWEET16* is reported to be mainly expressed in xylem parenchyma cells at a generally low level, where it is involved in

the transport of glucose, fructose and sucrose (Klemens *et al.*, 2013). It is expressed in rosette leaf, flower stalk, root (Klemens *et al.*, 2013, Guo *et al.*, 2014), and hypocotyl according to the eFP browser. During optimal conditions, *SWEET16* overexpressor lines showed an increase in shoot and root biomass, indicating the positive role of *SWEET16* in both shoot and root growth (Klemens *et al.*, 2013). Upon different types of external stimuli such as cold, low nitrogen and high nitrogen, *SWEET16* overexpressors have shown different rates of sugar accumulation (Klemens *et al.*, 2013), implying that *SWEET16* activity is dependent on different types of external stimuli. A bit different from *SWEET16*, *SWEET17* is predominantly a fructose exporter gene, which is primarily expressed in the root. Expression of *SWEET17* was found to be induced in the root elongation zone by darkness, which results in the release of vacuolar fructose to meet energy requirements. Based on our study, *SWEET16* overexpressors, especially 35S:*SWEET16-1*, displayed hypersensitivity to GR24 inhibition, while *sweet16-1*, *sweet16-2*, *sweet17-1* showed the tendency of lower sensitivity to GR24 inhibition in darkness compared to their wild-type (**Figure 4C-D**). This indicates that the two *SWEET*s are likely involved in strigolactone signalling. Besides these *SWEET* genes, two other genes involved in carbohydrate metabolism (AT4G19770: glycosyl hydrolase family protein with chitinase insertion domain and AT5G10190: major facilitator superfamily protein) were identified as candidate genes underlying the genetic variation for hypocotyl response to GR24 (**Table 2**). These findings triggered our interest to explore whether and how sugar biosynthesis, signalling and transport might play a role during strigolactone signalling. Sugars, such as sucrose and glucose, not only serve as the energy source for plant development, but also function as long-distance and local signal molecules (Smeekens *et al.*, 2010, Ljung *et al.*, 2015). In *Arabidopsis*, sugars have been found to inhibit hypocotyl elongation in the light, but promote the elongation in darkness (Zhang *et al.* 2010). In the latter process, PIFs and several hormones such as brassinosteroids and gibberellins are required (Zhang *et al.* 2010; Stewart *et al.* 2011; Liu *et al.* 2011b; Zhang *et al.* 2015b). A recent report has indicated that sugar signalling and strigolactone signalling may converge at the point of *BRC1* (*BRANCHED1*) in the control of bud outgrowth in *Rosa hybrid* (Barbier *et al.* 2015). Sucrose serves as an early signal for bud activity by up-regulating early auxin synthesis gene *YUC1* (*YUCCA 1*) and auxin efflux carrier gene *PIN1* (*PIN-FORMED 1*), and down-regulating *MAX2* and *BRC1* (Barbier *et al.* 2015). However, whether sugar signalling is also specifically involved in strigolactone-mediated etiolation of the hypocotyl is still elusive. Notably, a sucrose synthase *SUS2* (*SUCROSE SYNTHASE 2*), which is an enzyme involved in sucrose degradation and transport in root and shoot (Baro-

ja-Fernández et al. 2012), has been identified, using a proteomics approach, to be the only up-regulated protein in the mesocotyl of dark-grown strigolactone-deficient mutant *d10* rice seedlings by GR24 treatment (1  $\mu$ M) (Chen et al. 2014), suggesting that *SUS2* might be a target of strigolactone signalling. In the present study,  $-\log_{10}(P)$  values for SNPs corresponding to *SUS2* were very low for GR24 responses (**Table S4**). However, SNPs for other sugar metabolism-related genes such as *SUS6* (*SUCROSE SYNTHASE 6*) had higher  $-\log_{10}(P)$  values, even close to 3 (Table S4). It would be interesting to explore how GR24 might alter metabolism and transport of different sugars in different tissues. Interestingly, SWEET16 is predicted to be co-localized and physically interact with TCP14 (Teosinte Branched 14) (**Figure S5**), although  $-\log_{10}(P)$  values for SNPs corresponding to the TCP14 region were all low (below 2). TCP14 is a transcription factor that is playing a role in the regulation of seed germination, internode elongation, leaf shape and cytokinin-induced shoot branching and is found to be involved in stimulating cytokinin-mediated cell division (Kieffer et al. 2011b; Steiner et al. 2014; Resentini et al. 2015). In conclusion, further research into the role of strigolactones and other hormones in the orchestration of sugar signalling, metabolism and transport to facilitate plant adaptation during unfavorable conditions including abiotic and biotic stresses would be highly interesting.

Several candidate genes involved in hormone signalling were also present in our QTLs associated with hypocotyl response to GR24. One example is *EIL3* (*ETHYLENE-INSENSITIVE3-LIKE 3*), the homolog of *EIL1*. EIN3 (*ETHYLENE-INSENSITIVE3*) and EIN3-like (EIL) proteins serve as key transcription factors coordinating ethylene responses (Chao et al. 1997; An et al. 2010). They are essential for hypocotyl elongation and apical hook development (Binder et al. 2004; Zhong et al. 2009; Zhang et al. 2010; An et al. 2012; Zhang et al. 2015a), stress tolerance (Zhang et al. 2011; Shi et al. 2012; Peng et al. 2014), the jasmonate- or salicylic acid-mediated defense response (Chen et al. 2009; Zhu et al. 2011) and chlorophyll degradation during leaf senescence (Li et al. 2013; Kim et al. 2014b; Qiu et al. 2015). The identification of *EIL1* in our GWA mapping suggests the potential involvement of ethylene signalling as a response to GR24. Although strigolactones were not found to be involved in the ethylene-mediated plant response against the pathogen *Pythium irregular* (Blake et al., 2016) and ethylene regulates adventitious root initiation independently of strigolactones (Rasmussen et al., 2017), another study reported that strigolactone promotes leaf senescence by enhancing ethylene (Ueda and Kusaba 2015). Strigolactone biosynthetic and signalling mutants have shown delayed leaf senescence and expression of biosynthetic genes *MAX1*, *MAX3* and *MAX4* are induced



by dark incubation (Ueda and Kusaba 2015). In the *ein2-5* mutant, which is completely insensitive to ethylene, the transcription of *MAX1*, *MAX3* and *MAX4* was dramatically inhibited, suggesting the involvement of ethylene signalling in promoting strigolactone biosynthesis (Ueda and Kusaba 2015). The promoting effect of strigolactone on leaf senescence could not be conveyed by strigolactone alone (Ueda and Kusaba 2015). Instead, the addition of strigolactones enhanced the promoting activity of ethylene on senescence, thus implying a synergistic relationship between strigolactones and ethylene (Ueda and Kusaba 2015). Given that ethylene plays such a central role in etiolated growth, it is likely that GR24-triggered de-etiolation is dependent on ethylene signalling. None of the three *MAX* proteins (*MAX1*, *MAX3* and *MAX4*) have been found to be directly targeted by *EIN3* (Chang et al. 2013), with only *MAX4* harboring a binding site in the promoter region of *EIN3* (Ueda and Kusaba 2015). Whether hypocotyl response to strigolactone involves EIN3/EILs-dependent ethylene signalling and whether *MAX4* is targeted by EIN3/EILs during this process remain further investigations.

Concerning the root response to strigolactone, we also found candidates involved in hormone signalling, such as an auxin response factor ARF19 (AUXIN RESPONSE FACTOR 19). ARF19 and ARF7 are two functionally redundant auxin response factors that are involved in both auxin and ethylene signalling (Li et al. 2006). Interestingly, *ARF19* and *ARF7* mediated auxin signalling does not only regulate lateral root formation, emergence and leaf expansion (Wilmoth et al. 2005; Fukaki et al. 2006; Perez-Torres et al. 2008; Lee et al. 2009; Kang et al. 2013), but also acts synergistically with ethylene to control etiolation (Robles et al. 2012) and auxin-dependent root growth (Li et al. 2006). *ARF19* is expressed throughout etiolated seedlings including the hypocotyl, and is especially highly expressed in the primary root and cotyledons (Li et al. 2006). Notably, the activity of *ARF7* / *ARF19* is under negative control of *SHY2* during root elongation and gravitropism (Weijers et al. 2005), while *ARF7*/*ARF19*-mediated lateral root initiation occurs upstream of *SHY2*-mediated lateral root formation and emergence (Goh et al. 2012). *SHY2* has been suggested to be involved in *MAX2*-dependent strigolactone signalling in primary root elongation and lateral root formation, possibly controlling root meristem size and auxin flux (Koren et al., 2013). According to a previous study (Pandya-Kumar et al., 2014), GR24 treatment increases PIN2 levels and PIN2 polar localization in the plasma membrane of epidermal cells in the primary root elongation zone in a *MAX2*-dependent manner, leading to increased root hair elongation. Whether *ARF19* also contributes to this process is another intriguing question. Taken together, the identification of an auxin response factor that is possibly

involved in the root response to strigolactone in the present study, suggests that it contributes to the process of strigolactone-mediated primary root elongation which likely also involves the activity of SHY2 and other hormones such as ethylene. It would be interesting to study whether the activity of ARF19 differs between GR24-sensitive and -insensitive extreme accessions.

In line with previous reports on the positive roles of strigolactone during stress and defense responses (Bu *et al.*, 2014, Torres-Vera *et al.*, 2014, Liu *et al.*, 2015, Stes *et al.*, 2015, Blake *et al.*, 2016, Cheng *et al.*, 2017), we have also identified QTLs that include genes involved in stress - and defense responses, especially during the response of the root: hypocotyl ratio to GR24. This implies that the effect of strigolactones in plant defenses against biotic and abiotic stresses may be integrative, coordinating both aboveground and belowground growth. In some cases, it is likely that strigolactones do not directly regulate stress/defense responses but instead exert their effects by mediating other hormones (Torres-Vera *et al.*, 2014, Blake *et al.*, 2016). Still, the identification of these response candidate genes is a great addition to our understanding of strigolactone-regulated response mechanisms. For instance, jasmonic acid signalling may interact with the strigolactone pathway in the regulation of plant defenses as suggested by (Torres-Vera *et al.*, 2014). Here, one of the candidate genes *PEX6*, for instance, has been reported to promote peroxisomal matrix protein import, contributing to jasmonic acid biosynthesis upon wounding (Zolman & Bartel, 2004, Delker *et al.*, 2007). It is of interest to study whether *PEX6* is under control of strigolactone signalling

This study has identified several distinct GR24 response in hypocotyl and root of *Arabidopsis* population. Further efforts are needed to explore the underlying mechanisms of the different strigolactone responses in the extreme accessions of *Arabidopsis*. In addition, strigolactone response in the seedling is a complex trait. Several tissue-specific QTLs associated with hypocotyl and root response to GR24 treatment were identified by performing GWA mapping. Besides, the QTLs associated with response of root: hypocotyl ratio might offer some clues for future exploration on whether/how strigolactone might be involved in coordination of sink-source relationship.

### Acknowledgement

This research was funded by the Dutch Technology Foundation STW (to Carolien Ruyter-Spira; grant number 10990), the Chinese Scholarship Council (CSC; to Xi Cheng) and the Netherlands Organization for Scientific



Research (NWO; VICI grant, 865.06.002 to Harro Bouwmeester). Special thanks are given to Sanne Horst, Yunmeng Zhang and Diaan Jamar for helping with the phenotyping. We thank Binne Zwanenburg for kindly providing rac-GR24 and Dr. Woei-Jiun Guo for offering seeds of the *SWEET16*-related mutants and transgenic lines. We thank Willem Kruijer for his advice on heritability calculations.

### References

- Abe S, Sado A, Tanaka K, et al.** 2014a. Carlactone is converted to carlactonoic acid by MAX1 in *Arabidopsis* and its methyl ester can directly interact with AtD14 in vitro. *Proc Natl Acad Sci U S A* 111(50), 18084-18089.
- Agusti J, Herold S, Schwarz M, et al.** 2011. Strigolactone signaling is required for auxin-dependent stimulation of secondary growth in plants. *Proc Natl Acad Sci U S A* 108(50), 20242-20247.
- Akiyama K, Matsuzaki K, Hayashi H.** 2005. Plant sesquiterpenes induce hyphal branching in arbuscular mycorrhizal fungi. *Nature* 435(7043), 824-827.
- Alder A, Jamil M, Marzorati M, et al.** 2012. The path from  $\beta$ -carotene to carlactone, a strigolactone-like plant hormone. *Science* 335(6074), 1348-1351.
- Alonso J M, Stepanova A N, Leisse T J, et al.** 2003. Genome-wide insertional mutagenesis of *Arabidopsis thaliana*. *Science* 301(5633), 653-657.
- Arite T, Umehara M, Ishikawa S, Hanada A, Maekawa M, Yamaguchi S, Kyozuka J.** 2009. *d14*, a strigolactone-insensitive mutant of rice, shows an accelerated outgrowth of tillers. *Plant Cell Physiol* 50(8), 1416-1424.
- Arsovski A A, Galstyan A, Guseman J M, Nemhauser J L.** 2012. Photomorphogenesis. *Arabidopsis Book* 10, e0147.
- Bac-Molenaar J A, Fradin E F, Becker F F M, Rienstra J A, Van Der Schoot J, Vreugdenhil D, Keurentjes J J B.** 2015. Genome-wide association mapping of fertility reduction upon heat stress reveals developmental stage-specific QTLs in *Arabidopsis thaliana*. *Plant Cell* 27(7), 1857-1874.
- Baumberger N, Doesseger B, Guyot R, et al.** 2003. Whole-genome comparison of leucine-rich repeat extensins in *Arabidopsis* and rice. A conserved family of cell wall proteins form a vegetative and a reproductive clade. *Plant Physiol* 131(3), 1313-1326.
- Baxter I, Brazelton J N, Yu D, et al.** 2010. A coastal cline in sodium accumulation in *Arabidopsis thaliana* is driven by natural variation of the sodium transporter AtHKT1;1. *PLoS Genet* 6(11), e1001193.
- Blake S N, Barry K M, Gill W M, Reid J B, Foo E.** 2016. The role of strigolactones and ethylene in disease caused by *Pythium irregulare*. *Mol Plant Pathol* 17(5), 680-690.
- Booker J, Sieberer T, Wright W, et al.** 2005. MAX1 encodes a cytochrome P450 family member that acts downstream of MAX3/4 to produce a carotenoid-derived branch-inhibiting hormone. *Dev Cell* 8(3), 443-449.

- Bouwmeester H J, Matusova R, Zhongkui S, Beale M H.** 2003. Secondary metabolite signalling in host–parasitic plant interactions. *Curr Opin Plant Biol* 6(4), 358–364.
- Bu Q, Lv T, Shen H, et al.** 2014. Regulation of drought tolerance by the F-box protein MAX2 in *Arabidopsis*. *Plant Physiol* 164(1), 424–439.
- Butler D G, Cullis B R, Gilmour A R, Gogel B J.** 2009. ASReml-R reference manual. The State of Queensland, Department of Primary Industries and Fisheries, Brisbane.
- Chen F, Jiang L, Zheng J, Huang R, Wang H, Hong Z, Huang Y.** 2014. Identification of differentially expressed proteins and phosphorylated proteins in rice seedlings in response to strigolactone treatment. *PLoS ONE* 9(4), e93947.
- Chen L Q, Qu X Q, Hou B H, Sosso D, Osorio S, Fernie A R, Frommer W B.** 2012. Sucrose efflux mediated by SWEET proteins as a key step for phloem transport. *Science* 335(6065), 207–211.
- Cheng X, Floková K, Bouwmeester H, Ruyter-Spira C.** 2017. The role of endogenous strigolactones and their interaction with ABA during the infection process of the parasitic weed *Phelipanche ramosa* in tomato plants. *Front Plant Sci* 8(294), 392.
- Chevalier F, Nieminen K, Sánchez-Ferrero J C, Rodríguez M L, Chagoyen M, Hardtke C S, Cubas P.** 2014. Strigolactone promotes degradation of DWARF14, an  $\alpha/\beta$  hydrolase essential for strigolactone signaling in *Arabidopsis*. *Plant Cell* 26(3), 1134–1150.
- Civelek M, Lusis A J.** 2014. Systems genetics approaches to understand complex traits. *Nat Rev Genet* 15(1), 34–48.
- Davila Olivas N H, Kruijer W, Gort G, Wijnen C L, Van Loon J J A, Dicke M.** 2016. Genome-wide association analysis reveals distinct genetic architectures for single and combined stress responses in *Arabidopsis thaliana*. *New Phytol* 213(2), 838–851.
- De Cuyper C, Fromentin J, Yocco R E, De Keyser A, Guillotin B, Kunert K, Boyer F-D, Goormachtig S.** 2015. From lateral root density to nodule number, the strigolactone analogue GR24 shapes the root architecture of *Medicago truncatula*. *J Exp Bot* 66(1), 137–146.
- Decker E L, Alder A, Hunn S, et al.** 2017. Strigolactone biosynthesis is evolutionarily conserved, regulated by phosphate starvation and contributes to resistance against phytopathogenic fungi in a moss, *Physcomitrella patens*. *New Phytol* 216(2), 455–468.
- Delker C, Zolman B K, Miersch O, Wasternack C.** 2007. Jasmonate biosynthesis in *Arabidopsis thaliana* requires peroxisomal beta-oxidation enzymes--additional proof by properties of *pex6* and *aim1*. *Phytochemistry* 68(12), 1642–1650.
- Devaiah B N, Karthikeyan A S, Raghothama K G.** 2007. WRKY75 transcription factor is a modulator of phosphate acquisition and root development in *Arabidopsis*. *Plant Physiol* 143(4), 1789–1801.
- Devaiah B N, Raghothama K G.** 2007. Transcriptional regulation of Pi starvation responses by WRKY75. *Plant Signal Behav* 2(5), 424–425.
- El-Soda M, Kruijer W, Malosetti M, Koornneef M, Aarts M G.** 2015. Quantitative trait loci and candidate genes underlying genotype by environment interaction in the response of *Arabidopsis thaliana* to drought. *Plant Cell Environ* 38(3), 585–599.

- Flematti G R, Ghisalberti E L, Dixon K W, Trengove R D.** 2004. A compound from smoke that promotes seed germination. *Science* 305(5686), 977.
- Flint-Garcia S A, Thornsberry J M, Buckler E S.** 2003. Structure of linkage disequilibrium in plants. *Annu Rev Plant Biol* 54, 357-374.
- Fucile G, Di Biase D, Nahal H, et al.** 2011. ePlant and the 3D data display initiative: integrative systems biology on the world wide web. *PLoS ONE* 6(1), e15237.
- Gibson G.** 2010. Hints of hidden heritability in GWAS. *Nat Genet* 42(7), 558-560.
- Gifford M L, Banta J A, Katari M S, et al.** 2013. Plasticity regulators modulate specific root traits in discrete nitrogen environments. *PLoS Genet* 9(9), e1003760.
- Gomez-Roldan V, Fermas S, Brewer P B, et al.** 2008. Strigolactone inhibition of shoot branching. *Nature* 455, 189-194.
- Goyer A, Collakova E, Díaz De La Garza R, Quinlivan E P, Williamson J, Gregory J F, Shachar-Hill Y, Hanson A D.** 2005. 5-Formyltetrahydrofolate is an inhibitory but well tolerated metabolite in *Arabidopsis* leaves. *J Biol Chem* 280(28), 26137-26142.
- Guo S, Xu Y, Liu H, Mao Z, Zhang C, Ma Y, Zhang Q, Meng Z, Chong K.** 2013. The interaction between OsMADS57 and OsTB1 modulates rice tillering via DWARF14. *Nat Commun* 4, 1566.
- Guo W-J, Nagy R, Chen H-Y, Pfrunder S, Yu Y-C, Santelia D, Frommer W B, Martinoia E.** 2014. SWEET17, a facilitative transporter, mediates fructose transport across the tonoplast of *Arabidopsis* roots and leaves. *Plant Physiol* 164(2), 777-789.
- Guo X, Qin Q, Yan J, et al.** 2015. TYPE-ONE PROTEIN PHOSPHATASE4 regulates pavement cell interdigitation by modulating PIN-FORMED1 polarity and trafficking in *Arabidopsis*. *Plant Physiol* 167(3), 1058-1075.
- Hamiaux C, Drummond R S, Janssen B J, Ledger S E, Cooney J M, Newcomb R D, Snowden K C.** 2012. DAD2 is an alpha/beta hydrolase likely to be involved in the perception of the plant branching hormone, strigolactone. *Curr Biol* 22(21), 2032-2036.
- Horton M W, Hancock A M, Huang Y S, et al.** 2012. Genome-wide patterns of genetic variation in worldwide *Arabidopsis thaliana* accessions from the RegMap panel. *Nat Genet* 44(2), 212-216.
- Hu Z, Yamauchi T, Yang J, et al.** 2014. Strigolactone and cytokinin act antagonistically in regulating rice mesocotyl elongation in darkness. *Plant Cell Physiol* 55(1), 30-41.
- Hu Z, Yan H, Yang J, Yamaguchi S, Maekawa M, Takamure I, Tsutsumi N, Kyojuka J, Nakazono M.** 2010. Strigolactones negatively regulate mesocotyl elongation in rice during germination and growth in darkness. *Plant Cell Physiol* 51(7), 1136-1142.
- Huang D W, Sherman B T, Lempicki R A.** 2009a. Bioinformatics enrichment tools: paths toward the comprehensive functional analysis of large gene lists. *Nucl Acids Res* 37(1), 1-13.
- Huang D W, Sherman B T, Zheng X, Yang J, Imamichi T, Stephens R, Lempicki R A.** 2009b. Extracting biological meaning from large gene lists with DAVID. *Curr Protoc Bioinformatics* Chapter 13, Unit 13.11-13.11.13.
- Hwang I, Goodman H M.** 1995. An *Arabidopsis thaliana* root-specific kinase homolog is

induced by dehydration, ABA, and NaCl. *Plant J* 8(1), 37-43.

**Jia K P, Luo Q, He S B, Lu X D, Yang H Q.** 2014. Strigolactone-regulated hypocotyl elongation is dependent on cryptochrome and phytochrome signaling pathways in *Arabidopsis*. *Mol Plant* 7(3), 528-540.

**Jiang L, Liu X, Xiong G, et al.** 2013. DWARF 53 acts as a repressor of strigolactone signaling in rice. *Nature* 504(7480), 401-405.

**Kameoka H, Kyojuka J.** 2015. Downregulation of rice *DWARF 14 LIKE* suppress mesocotyl elongation via a strigolactone independent pathway in the dark. *J Genet Genomics* 42(3), 119-124.

**Kang H M, Sul J H, Service S K, Zaitlen N A, Kong S-Y, Freimer N B, Sabatti C, Eskin E.** 2010. Variance component model to account for sample structure in genome-wide association studies. *Nat Genet* 42(4), 348-354.

**Kanno Y, Oikawa T, Chiba Y, et al.** 2016. *AtSWEET13* and *AtSWEET14* regulate gibberellin-mediated physiological processes. *Nat Commun* 7, 13245.

**Kapulnik Y, Delaux P M, Resnick N, et al.** 2011a. Strigolactones affect lateral root formation and root-hair elongation in *Arabidopsis*. *Planta* 233(1), 209-216.

**Kapulnik Y, Koltai H.** 2014. Strigolactone involvement in root development, response to abiotic stress, and interactions with the biotic soil environment. *Plant Physiol* 166(2), 560-569.

**Kapulnik Y, Resnick N, Mayzlish-Gati E, Kaplan Y, Wininger S, Hershenhorn J, Koltai H.** 2011b. Strigolactones interact with ethylene and auxin in regulating root-hair elongation in *Arabidopsis*. *J Exp Bot* 62(8), 2915-2924.

**Kieffer M, Master V, Waites R, Davies B.** 2011. *TCP14* and *TCP15* affect internode length and leaf shape in *Arabidopsis*. *Plant J* 68(1), 147-158.

**Klemens P a W, Patzke K, Deitmer J, et al.** 2013. Overexpression of the vacuolar sugar carrier *AtSWEET16* modifies germination, growth, and stress tolerance in *Arabidopsis*. *Plant Physiol* 163(3), 1338-1352.

**Kohlen W, Charnikhova T, Lammers M, et al.** 2012. The tomato *CAROTENOID CLEAVAGE DIOXYGENASE8 (SICCD8)* regulates rhizosphere signaling, plant architecture and affects reproductive development through strigolactone biosynthesis. *New Phytol* 196(2), 535-547.

**Koltai H.** 2011. Strigolactones are regulators of root development. *New Phytol* 190(3), 545-549.

**Koltai H, Dor E, Hershenhorn J, et al.** 2009. Strigolactones' effect on root growth and root-hair elongation may be mediated by auxin-efflux carriers. *J Plant Growth Regul* 29(2), 129-136.

**Kong X, Zhang M, Ding Z.** 2014. D53: the missing link in strigolactone signaling. *Mol Plant* 7(5), 761-763.

**Kooke R, Kruijer W, Bours R, et al.** 2016. Genome-wide association mapping and genomic prediction elucidate the genetic architecture of morphological traits in *Arabidopsis*. *Plant Physiol* 170(4), 2187-2203.

- Koren D, Resnick N, Mayzlish Gati E, Belausov E, Weininger S, Kapulnik Y, Koltai H.** 2013. Strigolactone signaling in the endodermis is sufficient to restore root responses and involves *SHORT HYPOCOTYL 2 (SHY2)* activity. *New Phytol* 198(3), 866-874.
- Li Y, Huang Y, Bergelson J, Nordborg M, Borevitz J O.** 2010. Association mapping of local climate-sensitive quantitative trait loci in *Arabidopsis thaliana*. *Proc Natl Acad Sci U S A* 107(49), 21199-21204.
- Lin H, Wang R, Qian Q, et al.** 2009. DWARF27, an iron-containing protein required for the biosynthesis of strigolactones, regulates rice tiller bud outgrowth. *Plant Cell* 21(5), 1512-1525.
- Liu J, He H, Vitali M, et al.** 2015. Osmotic stress represses strigolactone biosynthesis in *Lotus japonicus* roots: exploring the interaction between strigolactones and ABA under abiotic stress. *Planta* 241(6), 1435-1451.
- Ljung K, Nemhauser J L, Perata P.** 2015. New mechanistic links between sugar and hormone signalling networks. *Curr Opin Plant Biol* 25, 130-137.
- Lyons R, Stiller J, Powell J, Rusu A, Manners J M, Kazan K.** 2015. *Fusarium oxysporum* triggers tissue-specific transcriptional reprogramming in *Arabidopsis thaliana*. *PLoS ONE* 10(4), e0121902.
- Makowsky R, Pajewski N M, Klimentidis Y C, Vazquez A I, Duarte C W, Allison D B, De Los Campos G.** 2011. Beyond missing heritability: prediction of complex traits. *PLoS Genet* 7(4), e1002051.
- Marzec M.** 2016. Strigolactones as part of the plant defence system. *Trends Plant Sci* 21(11), 900-903.
- Mashiguchi K, Sasaki E, Shimada Y, Nagae M, Ueno K, Nakano T, Yoneyama K, Suzuki Y, Asami T.** 2009. Feedback-regulation of strigolactone biosynthetic genes and strigolactone-regulated genes in *Arabidopsis*. *Biosci Biotechnol Biochem* 73(11), 2460-2465.
- Masuda H P, Cabral L M, De Veylder L, et al.** 2008. ABAP1 is a novel plant Armadillo BTB protein involved in DNA replication and transcription. *EMBO J* 27(20), 2746-2756.
- Mazzella M A, Casal J J, Muschietti J P, Fox A R.** 2014. Hormonal networks involved in apical hook development in darkness and their response to light. *Front Plant Sci* 5, 52.
- Nelson D C, Flematti G R, Riseborough J-A, Ghisalberti E L, Dixon K W, Smith S M.** 2010. Karrikins enhance light responses during germination and seedling development in *Arabidopsis thaliana*. *Proc Natl Acad Sci U S A* 107(15), 7095-7100.
- Nelson D C, Scaffidi A, Dun E A, Waters M T, Flematti G R, Dixon K W, Beveridge C A, Ghisalberti E L, Smith S M.** 2011. F-box protein MAX2 has dual roles in karrikin and strigolactone signaling in *Arabidopsis thaliana*. *Proc Natl Acad Sci U S A* 108(21), 8897-8902.
- Ogura T, Busch W.** 2015. From phenotypes to causal sequences: using genome wide association studies to dissect the sequence basis for variation of plant development. *Curr Opin Plant Biol* 23, 98-108.

- Pandya-Kumar N, Shema R, Kumar M, et al.** 2014. Strigolactone analog GR24 triggers changes in PIN2 polarity, vesicle trafficking and actin filament architecture. *New Phytol* 202(4), 1184-1196.
- Piisila M, Keceli M A, Brader G, Jakobson L, Joesaar I, Sipari N, Kollist H, Palva E T, Kariola T.** 2015. The F-box protein MAX2 contributes to resistance to bacterial phytopathogens in *Arabidopsis thaliana*. *BMC Plant Biol* 15(1), 53.
- Qin Q, Wang W, Guo X, Yue J, Huang Y, Xu X, Li J, Hou S.** 2014. *Arabidopsis* DELLA protein degradation is controlled by a type-one protein phosphatase, TOPP4. *PLoS Genet* 10(7), e1004464.
- Resentini F, Felipo-Benavent A, Colombo L, Blázquez M A, Alabadí D, Masiero S.** 2015. *TCP14* and *TCP15* mediate the promotion of seed germination by gibberellins in *Arabidopsis thaliana*. *Mol Plant* 8(3), 482-485.
- Rishmawi L, Pesch M, Juengst C, Schauss A C, Schrader A, Hulskamp M.** 2014. Non-cell-autonomous regulation of root hair patterning genes by *WRKY75* in *Arabidopsis*. *Plant Physiol* 165(1), 186-195.
- Risseeuw E P, Daskalchuk T E, Banks T W, Liu E, Cotelesage J, Hellmann H, Estelle M, Somers D E, Crosby W L.** 2003. Protein interaction analysis of SCF ubiquitin E3 ligase subunits from *Arabidopsis*. *Plant J* 34(6), 753-767.
- Roje S, Janave M T, Ziemak M J, Hanson A D.** 2002. Cloning and characterization of mitochondrial 5-formyltetrahydrofolate cycloligase from higher plants. *J Biol Chem* 277(45), 42748-42754.
- Rosas U, Cibrian-Jaramillo A, Ristova D, et al.** 2013. Integration of responses within and across *Arabidopsis* natural accessions uncovers loci controlling root systems architecture. *Proc Natl Acad Sci U S A* 110, 15133-15138.
- Ruyter-Spira C, Kohlen W, Charnikhova T, et al.** 2011. Physiological effects of the synthetic strigolactone analog GR24 on root system architecture in *Arabidopsis*: another belowground role for strigolactones? *Plant Physiol* 155(2), 721-734.
- Scaffidi A, Waters M T, Sun Y K, Skelton B W, Dixon K W, Ghisalberti E L, Flematti G R, Smith S M.** 2014a. Strigolactone hormones and their stereoisomers signal through two related receptor proteins to induce different physiological responses in *Arabidopsis*. *Plant Physiol* 165(3), 1221-1232.
- Scaffidi A, Waters M T, Sun Y K, Skelton B W, Dixon K W, Ghisalberti E L, Flematti G R, Smith S M.** 2014b. Strigolactone hormones and their stereoisomers signal through two related receptor proteins to induce different physiological responses in *Arabidopsis*. *Plant Physiol* 165(3), 1221-1232.
- Schmid M, Davison T S, Henz S R, Pape U J, Demar M, Vingron M, Schölkopf B, Weigel D, Lohmann J U.** 2005. A gene expression map of *Arabidopsis thaliana* development. *Nat Genet* 37(5), 501-506.
- Serrano M, Guzman P.** 2004. Isolation and gene expression analysis of *Arabidopsis thaliana* mutants with constitutive expression of *ATL2*, an early elicitor-response RING-H2 zinc-finger gene. *Genetics* 167(2), 919-929.



- Serrano M, Robatzek S, Torres M, Kombrink E, Somssich I E, Robinson M, Schulze-Lefert P.** 2007. Chemical interference of pathogen-associated molecular pattern-triggered immune responses in *Arabidopsis* reveals a potential role for fatty-acid synthase type II complex-derived lipid signals. *J Biol Chem* 282(9), 6803-6811.
- Sevilem I, Miyashima S, Helariutta Y.** 2013. Cell-to-cell communication via plasmodesmata in vascular plants. *Cell Adh Migr* 7(1), 27-32.
- Shen H, Zhu L, Bu Q-Y, Huq E.** 2012. MAX2 affects multiple hormones to promote photomorphogenesis. *Mol Plant* 5(3), 750-762.
- Shinohara N, Taylor C, Leyser O.** 2013. Strigolactone can promote or inhibit shoot branching by triggering rapid depletion of the auxin efflux protein PIN1 from the plasma membrane. *PLoS Biology* 11(1), e1001474.
- Smeekens S, Ma J, Hanson J, Rolland F.** 2010. Sugar signals and molecular networks controlling plant growth. *Curr Opin Plant Biol* 13(3), 274-279.
- Stanga J P, Smith S M, Briggs W R, Nelson D C.** 2013. SUPPRESSOR OF MORE AXIL-LARY GROWTH2 1 controls seed germination and seedling development in *Arabidopsis*. *Plant Physiol* 163(1), 318-330.
- Steiner E, Yanai O, Efroni I, Ori N, Eshed Y, Weiss D.** 2014. Class I TCPs modulate cytokinin-induced branching and meristematic activity in tomato. *Plant Signal Behav* 7(7), 807-810.
- Stes E, Depuydt S, De Keyser A, Matthys C, Audenaert K, Yoneyama K, Werbrouck S, Goormachtig S, Vereecke D.** 2015. Strigolactones as an auxiliary hormonal defence mechanism against leafy gall syndrome in *Arabidopsis thaliana*. *J Exp Bot* 66(16), 5123-5134.
- Stetter M G, Schmid K, Ludewig U.** 2015. Uncovering genes and ploidy involved in the high diversity in root hair density, length and response to local scarce phosphate in *Arabidopsis thaliana*. *PLoS ONE* 10(3), e0120604.
- Stirnberg P, Furner I J, Ottoline Leyser H M.** 2007. MAX2 participates in an SCF complex which acts locally at the node to suppress shoot branching. *Plant J* 50(1), 80-94.
- Toh S, Kamiya Y, Kawakami N, Nambara E, Mccourt P, Tsuchiya Y.** 2012. Thermoinhibition uncovers a role for strigolactones in *Arabidopsis* seed germination. *Plant Cell Physiol* 53(1), 107-117.
- Torres-Vera R, Garcia J M, Pozo M J, Lopez-Raez J A.** 2014. Do strigolactones contribute to plant defence? *Mol Plant Pathol* 15(2), 211-216.
- Tsuchiya Y, Vidaurre D, Toh S, Hanada A, Nambara E, Kamiya Y, Yamaguchi S, Mccourt P.** 2010. A small-molecule screen identifies new functions for the plant hormone strigolactone. *Nat Chem Biol* 6(10), 741-749.
- Tsugeki R, Tanaka-Sato N, Maruyama N, Terada S, Kojima M, Sakakibara H, Okada K.** 2015. CLUMSY VEIN, the *Arabidopsis* DEAH-box Prp16 ortholog, is required for auxin-mediated development. *Plant J* 81(2), 183-197.
- Ueda H, Kusaba M.** 2015. Strigolactone regulates leaf senescence in concert with ethylene in *Arabidopsis*. *Plant Physiol* 169(1), 138-147.



- Vandenbussche F, Verbelen J-P, Van Der Straeten D.** 2005. Of light and length: regulation of hypocotyl growth in *Arabidopsis*. *BioEssays* 27(3), 275-284.
- Vatén A, Dettmer J, Wu S, et al.** 2011. Callose biosynthesis regulates symplastic trafficking during root development. *Dev Cell* 21(6), 1144-1155.
- Von Arnim A, Deng X W.** 1996. Light control of seedling development. *Annu Rev Plant Biol Plant Mol Biol* 47, 215-243.
- Walton A, Stes E, Goeminne G, et al.** 2016. The response of the root proteome to the synthetic strigolactone GR24 in *Arabidopsis*. *Mol Cell Proteomics* 15(8), 2744-2755.
- Wang Y, Bouwmeester K, Beseh P, Shan W, Govers F.** 2014. Phenotypic analyses of *Arabidopsis* T-DNA insertion lines and expression profiling reveal that multiple L-type lectin receptor kinases are involved in plant immunity. *Mol Plant Microbe Interact* 27(12), 1390-1402.
- Wang Y, Sun S, Zhu W, Jia K, Yang H, Wang X.** 2013. Strigolactone/MAX2-induced degradation of brassinosteroid transcriptional effector BES1 regulates shoot branching. *Dev Cell* 27(6), 681-688.
- Wang Y, Zhang W-Z, Song L-F, Zou J-J, Su Z, Wu W-H.** 2008. Transcriptome analyses show changes in gene expression to accompany pollen germination and tube growth in *Arabidopsis*. *Plant Physiol* 148(3), 1201-1211.
- Ward Jr. J H.** 1963. Hierarchical grouping to optimize an objective function. *J AmStat Assoc* 58(301), 236-244.
- Warde-Farley D, Donaldson S L, Comes O, et al.** 2010. The GeneMANIA prediction server: biological network integration for gene prioritization and predicting gene function. *Nucl Acids Res* 38, W214-220.
- Waters M T, Nelson D C, Scaffidi A, Flematti G R, Sun Y K, Dixon K W, Smith S M.** 2012. Specialisation within the DWARF14 protein family confers distinct responses to karrikins and strigolactones in *Arabidopsis*. *Development* 139(7), 1285-1295.
- Waters M T, Smith S M.** 2013. *KAI2*- and *MAX2*-mediated responses to karrikins and strigolactones are largely independent of *HY5* in *Arabidopsis* seedlings. *Mol Plant* 6(1), 63-75.
- Winter D, Vinegar B, Nahal H, Ammar R, Wilson G V, Provart N J.** 2007. An “Electronic Fluorescent Pictograph” browser for exploring and analyzing large-scale biological data sets. *PLoS ONE* 2(8), e718.
- Yadav S R, Yan D, Seville I, Helariutta Y.** 2014. Plasmodesmata-mediated intercellular signaling during plant growth and development. *Front Plant Sci* 5, 44.
- Yamada Y, Furusawa S, Nagasaka S, Shimomura K, Yamaguchi S, Umehara M.** 2014. Strigolactone signaling regulates rice leaf senescence in response to a phosphate deficiency. *Planta* 240(2), 399-408.
- Yoshida S, Kameoka H, Tempo M, Akiyama K, Umehara M, Yamaguchi S, Hayashi H, Kyojuka J, Shirasu K.** 2012. The D3 F-box protein is a key component in host strigolactone responses essential for arbuscular mycorrhizal symbiosis. *New Phytol* 196(4), 1208-1216.

- Yue J, Qin Q, Meng S Y, Jin H, Gou X, Li J.** 2015. *TOPP4* regulates the stability of Phytochrome Interacting Factor 5 during photomorphogenesis in *Arabidopsis*. *Plant Physiol* 170(3), 1381-1397.
- Zhang Y, Van Dijk A D, Scaffidi A, et al.** 2014. Rice cytochrome P450 MAX1 homologs catalyze distinct steps in strigolactone biosynthesis. *Nat Chem Biol* 10(12), 1028-1033.
- Zhou F, Lin Q, Zhu L, et al.** 2013. D14–SCFD3-dependent degradation of D53 regulates strigolactone signalling. *Nature* 504(7480), 406-410.
- Zolman B K, Bartel B.** 2004. An *Arabidopsis* indole-3-butyric acid-response mutant defective in PEROXIN6, an apparent ATPase implicated in peroxisomal function. *Proc Natl Acad Sci U S A* 101(6), 1786-1791.
- Zuk O, Hechter E, Sunyaev S R, Lander E S.** 2012. The mystery of missing heritability: Genetic interactions create phantom heritability. *Proc Natl Acad Sci U S A* 109(4), 1193-1198.

## Supplementary materials



**Figure S1. Correlations and linear relationships between traits.** Distributions of different traits are shown as histograms in the diagonal. The correlations between traits are shown as matrices. The correlation coefficients  $r$  between traits are shown in the right part above the diagonal (a larger character size indicates a higher correlation). Linear relationships (predicted linear formulas, coefficient of determination  $R^2$  and  $P$  values) are shown in the left part underneath the diagonal.

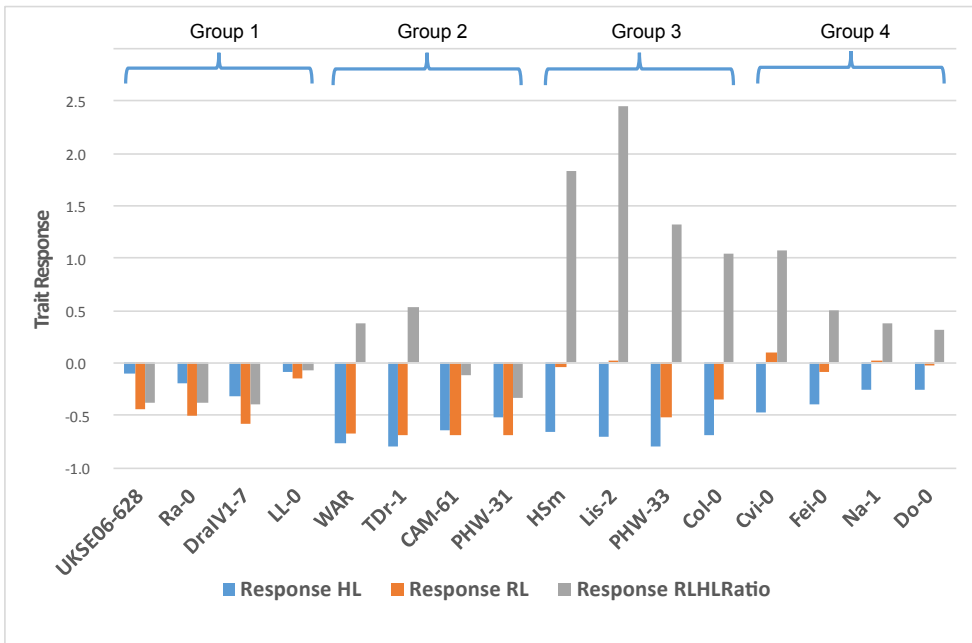


**Figure S2. Trait response of 16 *Arabidopsis* accessions.** Original trait values were scaled to get rid of the effect of units. The group name based on cluster analysis of trait responses (hypocotyl response, root response, root-to-shoot ratio response to GR24; see **Figure 2**) is indicated above the histogram.

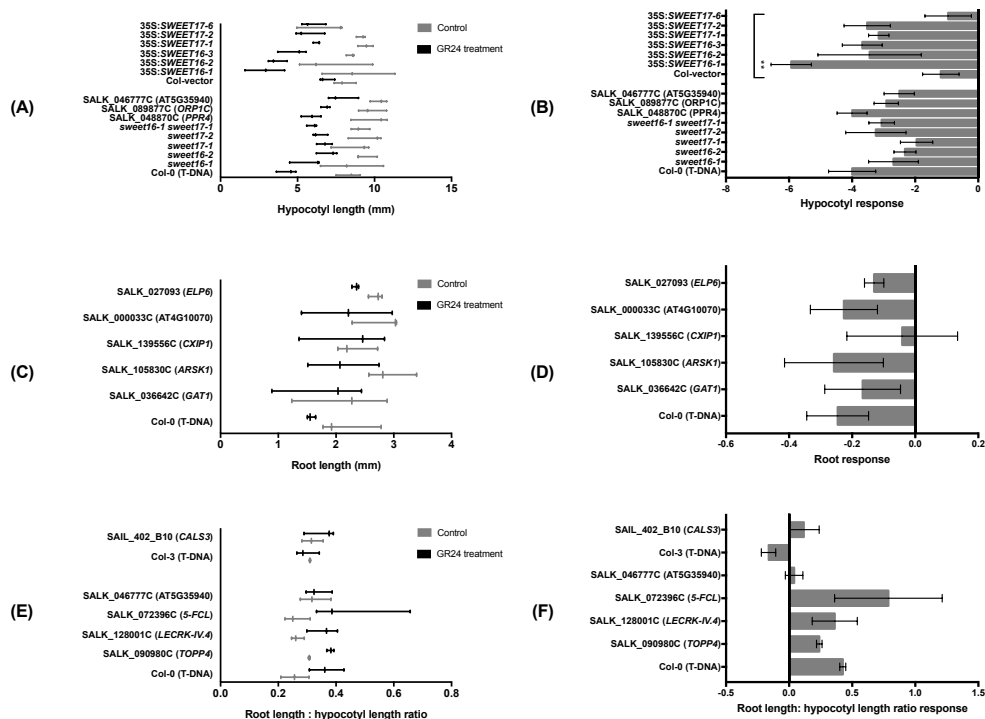


**Figure S3. Phenotype characterization of mutants and transgenic lines as described in Table S3.** (A) Hypocotyl length under control conditions and *rac*-GR24 treatment and (B) hypocotyl response to *rac*-GR24 of T-DNA mutants and transgenic lines that are related with candidate QTLs associated with hypocotyl response. These include wildtype Col-0 (T-DNA vector), *sweet16* and *sweet17* single mutants (*sweet16-1*, *sweet16-2*, *sweet17-1*, *sweet17-2*), double mutant (*sweet16-1 sweet17-1*), overexpressor lines (35S:*SWEET16-1*, 35S:*SWEET16-2*, 35S:*SWEET16-3*, 35S:*SWEET17-1*, 35S:*SWEET17-2*, 35S:*SWEET17-6*) and corresponding wildtype (Col-vector), and several T-DNA mutants for other candidate genes *PPR4*, *ORP1C*, AT5G35940. (C) Root length under control conditions and GR24 treatment, and (D) root response to GR24 of T-DNA mutants that are related with candidate QTLs associated with root response. These include wildtype Col-0 (T-DNA vector) and T-DNA mutants for candidate genes *GAT1*, *ARSK1*, *CXIP1*, AT4G10070, *ELP6*. (E) Root length: hypocotyl length ratio under control conditions and *rac*-GR24 treatment, and (F) root: hypocotyl ratio response to GR24 of mutants that are for candidate QTLs associated with root: hypocotyl ratio response of T-DNA mutants for candidate genes *TOPP4*, *LECRK-IV.4*, *PUX4*, *5-FLC*, AT4G10070 and corresponding wildtype Col-0 (T-DNA vector), T-DNA mutant for *CALS3* and its corresponding wildtype Col-3 (T-DNA vector) under control and GR24 treatment. Line plots in (A)(C)(E) represent mean values with maximum and minimum value of three biological replicates. Bar plots to the right show the response traits as the subtraction of trait values under two conditions and were subjected to division of value under control ( $\pm$  standard error of averages). Ordinary one-way ANOVA was performed and Tukey's multiple comparisons test was performed to compare response traits of mutants/transgenic lines to their corresponding wildtype.  $**P < 0.01$ . If no sign, there is no statistical significance.

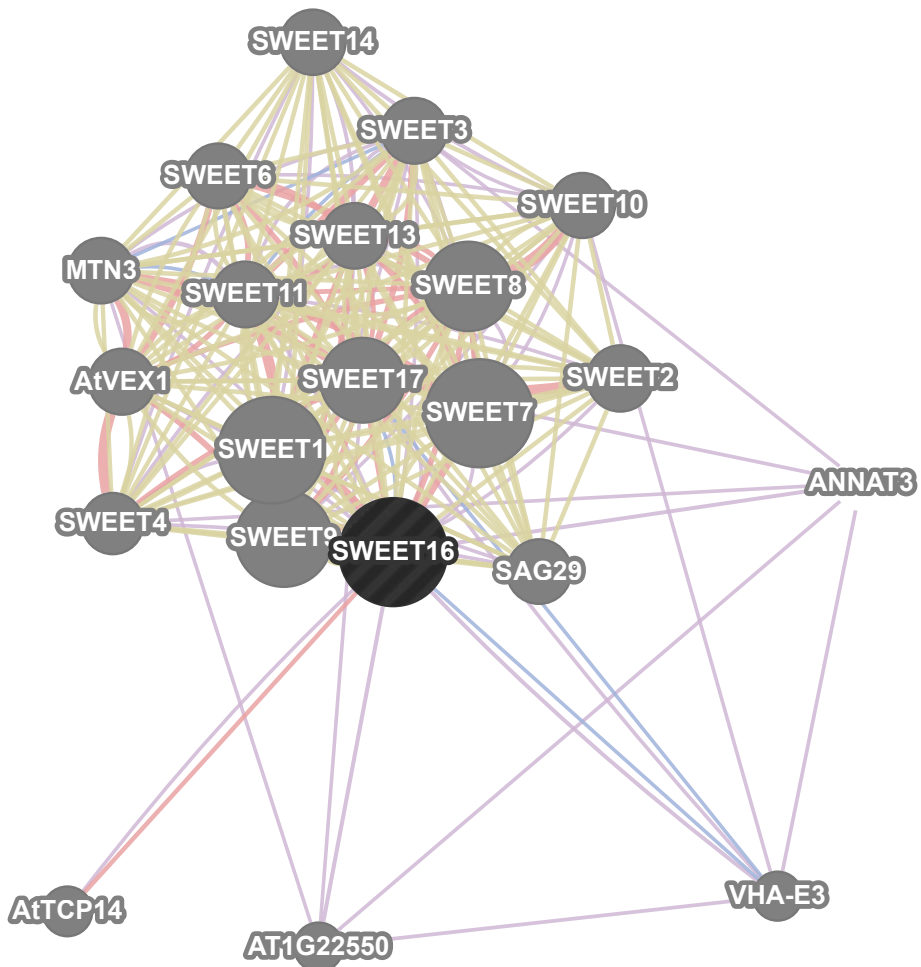
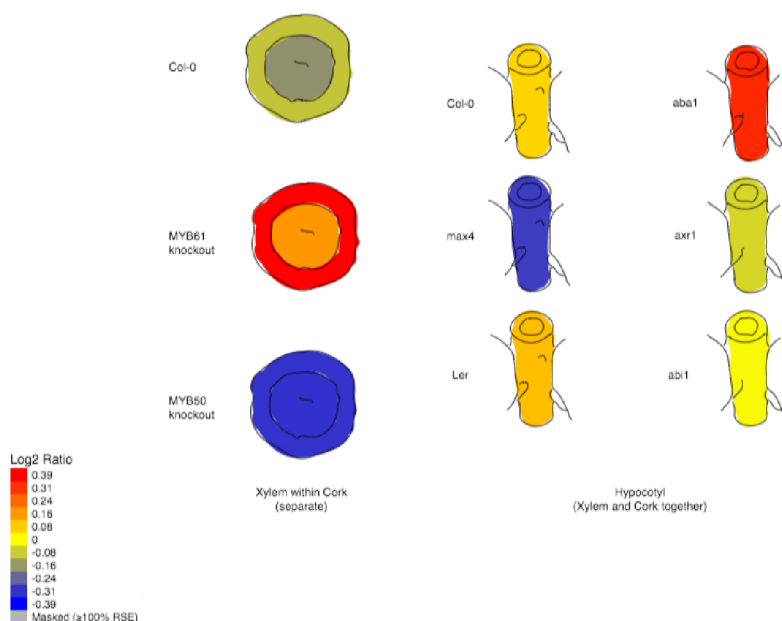


Figure S4. GeneMANIA-predicted protein network of SWEET16.

Tissue Specific Xylem And Cork eFP: AT3G16690



**Figure S5. Expression of *SWEET16* in xylem and/or cork of Col-0, Ler and several hormone-related mutants (*MYB61* knockout, *MYB50* knockout, *max4*, *aba1*, *axr1*, *abi1*) according to eFP browser. The extent of increased or decreased expression level of the gene is indicated in colors.**



**Table S1. A priori candidate QTL list.** A search window was defined by including SNPs in the  $\pm 10\text{kb}$  neighbouring region around the identified significant SNPs in close LD ( $r^2 > 0.4$ ) based on both the 250K array and resequencing data (1001genomes.org). Genes within the support window were all considered as a priori candidate genes.

See the file in the link:

<https://www.dropbox.com/sh/6sqmaovo4rjc4ep/AACX6EtKF78UugpDUGRhQhx-na?dl=0>

**Table S2. Results of Gene Ontology (GO) analysis based on candidate genes obtained from all the response traits and trait under GR24 treatment.** Gene functional classification was done by platform DAVID (version 6.8) (Huang et al., 2009b; a; Huang et al., 2009c). Default parameters were adopted (medium classification stringency, Kappa similarity threshold=0.35).

Gene Group 1    Enrichment Score: 1.55	
TAIR_ID	Gene Name
AT1G09665	Toll-Interleukin-Resistance (TIR) domain family protein(AT1G09665)
AT4G16950	Disease resistance protein (TIR-NBS-LRR class) family(RPP5)
AT4G16940	Disease resistance protein (TIR-NBS-LRR class) family(AT4G16940)
AT1G72950	Disease resistance protein (TIR-NBS class)(AT1G72950)
AT1G72940	Toll-Interleukin-Resistance (TIR) domain-containing protein(AT1G72940)
Gene Group 2    Enrichment Score: 0.95	
TAIR_ID	Gene Name
AT2G29780	Galactose oxidase/kelch repeat superfamily protein(AT2G29780)
AT1G09650	F-box and associated interaction domains-containing protein(AT1G09650)
AT2G29770	Galactose oxidase/kelch repeat superfamily protein(AT2G29770)
AT5G38386	F-box/RNI-like superfamily protein(AT5G38386)
AT1G54040	epithiospecifier protein(ESP)
Gene Group 3    Enrichment Score: 0.80	
TAIR_ID	Gene Name
AT2G30980	SHAGGY-related protein kinase dZeta(SKdZeta)
AT5G35960	Protein kinase family protein(AT5G35960)
AT1G61480	S-locus lectin protein kinase family protein(AT1G61480)
AT1G61475	ATP binding / protein kinase(AT1G61475)

(continues)

## CHAPTER 6

AT4G13020	Protein kinase superfamily protein(MHK)
AT4G02420	Concanavalin A-like lectin protein kinase family protein(AT4G02420)
AT5G06740	Concanavalin A-like lectin protein kinase family protein(AT5G06740)
AT2G42290	Leucine-rich repeat protein kinase family protein(AT2G42290)
AT5G38210	Protein kinase family protein(AT5G38210)
AT2G26290	root-specific kinase 1(ARSK1)
AT1G16440	root hair specific 3(RSH3)
<b>Gene Group 4    Enrichment Score: 0.61</b>	
TAIR_ID	Gene Name
AT4G13030	P-loop containing nucleoside triphosphate hydrolases superfamily protein(AT4G13030)
AT5G22560	transmembrane protein, putative (DUF247)(AT5G22560)
AT2G42290	Leucine-rich repeat protein kinase family protein(AT2G42290)
AT4G25030	Serine/Threonine-kinase(AT4G25030)
AT5G22555	transmembrane protein(AT5G22555)
AT5G22550	transmembrane protein, putative (DUF247)(AT5G22550)
AT4G25010	Nodulin MtN3 family protein(SWEET14)
AT3G23080	Polyketide cyclase/dehydrase and lipid transport superfamily protein(AT3G23080)
AT4G04200	Microsomal signal peptidase 25 kDa subunit (SPC25)(AT4G04200)
AT1G08230	Transmembrane amino acid transporter family protein(AT1G08230)
AT5G26790	transmembrane protein(AT5G26790)
AT4G24980	nodulin MtN21 /EamA-like transporter family protein(UMAMIT16-psi)
AT2G30933	Carbohydrate-binding X8 domain superfamily protein(AT2G30933)
AT3G61300	C2 calcium/lipid-binding plant phosphoribosyltransferase family protein(AT3G61300)
AT3G61280	O-glucosyltransferase rumi-like protein (DUF821)(AT3G61280)
AT3G61270	O-glucosyltransferase rumi-like protein (DUF821)(AT3G61270)
AT4G23000	Calcineurin-like metallo-phosphoesterase superfamily protein(AT4G23000)
AT1G72960	Root hair defective 3 GTP-binding protein (RHD3)(AT1G72960)
AT2G13650	golgi nucleotide sugar transporter 1(GONST1)
AT4G22990	Major Facilitator Superfamily with SPX (SYG1/Pho81/XPR1) domain-containing protein(AT4G22990)
AT1G28710	Nucleotide-diphospho-sugar transferase family protein(AT1G28710)
AT1G44750	purine permease 11(PUP11)
AT5G10190	Major facilitator superfamily protein(AT5G10190)
AT4G27940	manganese tracking factor for mitochondrial SOD2(MTM1)

(continues)

## GWA Mapping on Strigolactone Response

AT3G04440	Plasma-membrane choline transporter family protein(AT3G04440)
AT4G10080	transmembrane protein(AT4G10080)
AT2G31110	trichome birefringence-like protein (DUF828)(AT2G31110)
AT5G03795	Exostosin family protein(AT5G03795)
AT1G61475	ATP binding / protein kinase(AT1G61475)
<b>Gene Group 5    Enrichment Score: 0.48</b>	
TAIR_ID	Gene Name
AT1G21990	F-box/RNI-like/FBD-like domains-containing protein(AT1G21990)
AT5G38390	F-box/RNI-like superfamily protein(AT5G38390)
AT5G38386	F-box/RNI-like superfamily protein(AT5G38386)
AT1G60410	F-box family protein(AT1G60410)
<b>Gene Group 6    Enrichment Score: 0.45</b>	
TAIR_ID	Gene Name
AT4G13040	Integrase-type DNA-binding superfamily protein(AT4G13040)
AT5G13080	WRKY DNA-binding protein 75(WRKY75)
AT1G69120	K-box region and MADS-box transcription factor family protein(AP1)
AT1G19220	auxin response factor 19(ARF19)
AT4G00270	DNA-binding storekeeper protein-related transcriptional regulator(AT4G00270)
AT3G04420	NAC domain containing protein 48(NAC048)
AT1G21970	Histone superfamily protein(LEC1)
AT5G48560	basic helix-loop-helix (bHLH) DNA-binding superfamily protein(AT5G48560)
AT4G27950	cytokinin response factor 4(CRF4)
AT2G27050	ETHYLENE-INSENSITIVE3-like 1(EIL1)
AT2G42280	basic helix-loop-helix (bHLH) DNA-binding superfamily protein(FBH4)
AT2G26320	AGAMOUS-like 33(AGL33)
<b>Gene Group 7    Enrichment Score: 0.35</b>	
TAIR_ID	Gene Name
AT5G03800	Pentatricopeptide repeat (PPR) superfamily protein(EMB175)
AT2G29760	Tetratricopeptide repeat (TPR)-like superfamily protein(OTP81)
AT3G15930	Pentatricopeptide repeat (PPR) superfamily protein(AT3G15930)
AT3G16710	Pentatricopeptide repeat (PPR) superfamily protein(AT3G16710)

**Table S3. Information of T-DNA lines and primers used in this study** (gene ID, gene name, description, biological function, SALK number, NASC stock number, wildtype name, location of the gene, status of the line). HM, homozygous.

Trait	Gene ID	Gene Name	Biological function	TDNA SALK No.	TDNA NASC Stock No.	Wild type	Location of T-DNA insertion	Status of line
Response_HL	AT3G16710	PPR4	plant defense?	SALK_048870C	N679630	Col-0	exon	HM
Response_HL	AT4G08180	ORP1C	steroid metabolic process, signal transduction, abscisic acid-activated signaling pathway, cell communication, defense response	SALK_089877C	N663274	Col-0	exon	HM
Response_HL	AT5G35940	Mannose-binding lectin superfamily protein	glucosinolate catabolic process, nitrile biosynthetic process	SALK_046777C	N684021	Col-0	exon	HM
Response_RL	AT1G08230	GAT1	gamma-aminobutyric acid transport	SALK_036642C	N670551	Col-0	exon	HM
Response_RL	AT2G26290	ARSK1	root hair cell differentiation	SALK_105830C	N680100	Col-0	promoter	HM
Response_RL	AT3G54900	CXIP1	cellular stress responses, anther development, cation transport, cell redox homeostasis, cellular cation homeostasis, divalent metal ion transport, glucosinolate biosynthetic process	SALK_139556c	N653518	Col-0	promoter	HM
Response_RL	AT4G10070	KH domain-containing protein	unknown	SALK_000033C	N661238	Col-0	exon	HM
Response_RL	AT4G10090	ELP6	negative regulation of anthocyanin metabolic process, positive regulation of cell proliferation, regulation of leaf development, response to oxidative stress	SALK_027093	N869048	Col-0	promoter	HM
Response_RLHLRatio	AT2G39840	TOPP4	N-terminal protein myristoylation, protein dephosphorylation	SALK_090980C	N682645	Col-0	exon	HM
Response_RLHLRatio	AT4G02420	LECRK-IV.4	protein amino acid phosphorylation	SALK_128001C	N667278	Col-0	exon	HM
Response_RLHLRatio	AT4G04210	PUX4	unknown	SALK_027335C	N672438	Col-0	exon	HM
Response_RLHLRatio	AT5G13000	CALS3, GSL12	RNA interference, cell wall organization, cell-cell signaling	SAIL_402_B10	N860794	Col-3	intron	HM
Response_RLHLRatio	AT5G13050	5-FCL	tetrahydrofolate metabolic process	SALK_072396C	N679812	Col-0	promoter	HM

**Table S4.  $-\log_{10}(P)$  values for SNPs corresponding to genes involved in hormone biosynthesis and signalling (strigolactone, ethylene, auxin, gibberellins, abscisic acid, cytokinin, brassinosteroid), karrikin signalling, light signalling, sugar biosynthesis/metabolism/transport are listed for all the traits in the GWA study. Many listed genes have been reported to be regulated in light or darkness.**

See the file in the link: <https://www.dropbox.com/sh/6sqmaovo4rjc4ep/AACX6EtK-F78UugpDUGRhQhxna?dl=0>



# CHAPTER 7

---

## General discussion

---





### Introduction

Parasitic weeds are posing a great threat to many economically important crops in both developed and developing countries. They impose a lot of damage to crops by causing both yield loss and reducing the quality of crop products. Compared to non-parasitic weeds, parasitic weeds are difficult to control primarily due to their highly intimate association with their hosts. Control of root parasitic plants such as broomrapes (*Orobanche* and *Phelipanche* spp.) is especially problematic because the parasitism process occurs largely underground, and often remains undiagnosed until the damage to the crop has already been caused.

Currently available control methods aim to reduce the seed bank of parasitic weeds (eg. fumigation, solarization, herbicides application and biocontrol methods), to hinder the ability of parasitic weeds to detect the host (eg. induction of suicidal germination of parasite seeds) or to reduce the penetration and attachment of parasitic weeds to the host (eg. inhibition of parasite penetration and attachment) (Kohlschmid *et al.*, 2009, Rubiales *et al.*, 2009, Cimmino *et al.*, 2014, Fernández-Aparicio *et al.*, 2016, Zwanenburg *et al.*, 2016, Aybeke, 2017, Fernández-Aparicio *et al.*, 2017). Among these control measures, the use of suicidal germination is based on the use of chemical analogs of natural germination stimulants to induce suicidal germination of parasitic plant seeds without interfering with host plant growth. Examples of such germination stimulants are the strigolactones which are carotenoid-derived compounds that are secreted by the plant roots into the rhizosphere (Zwanenburg *et al.*, 2009, Mwakaboko & Zwanenburg, 2011, Kgosi *et al.*, 2012, Kannan & Zwanenburg, 2014, Kannan *et al.*, 2015, Zwanenburg *et al.*, 2016). Besides, the development of durable host resistance against parasitic weeds is potentially another effective approach for parasitic weed control. However, our knowledge of host-parasitic weeds interactions and host resistance mechanisms is still quite limited. So far, many efforts have been made to identify source of resistance against broomrapes and witchweeds and resistance mechanisms in breeding programs and quantitative genetics research (Labrousse, 2001, Román *et al.*, 2002, Rubiales *et al.*, 2003, Labrousse *et al.*, 2004, Pérez-Vich *et al.*, 2004, Valderama *et al.*, 2004, Velasco *et al.*, 2007, Fernández-Aparicio *et al.*, 2008, Fernández-Martínez *et al.*, 2008, Fernández-Aparicio *et al.*, 2009, Fondevilla *et al.*, 2009, Díaz-Ruiz *et al.*, 2010, El-Sayed *et al.*, 2012, Fernández-Aparicio *et al.*, 2012a, Gutiérrez *et al.*, 2013, Rubiales *et al.*, 2014, Brahmi *et al.*, 2016, Louarn *et al.*, 2016, Rubiales *et al.*, 2016). Proteomics, transcriptomics and metabolomics have also been used to facilitate our understanding of

parasitism and plant defense against broomrape (Castillejo *et al.*, 2009, Die *et al.*, 2009, Castillejo *et al.*, 2012, Hacham *et al.*, 2016). In addition, a few transgenic lines have been developed for host-induced gene silencing by RNAi silencing of parasitism-related genes in the parasite *Orobanchel/Phelipanche* through the production of homologous dsRNA sequences in the host plant (Aly *et al.*, 2009, Aly, 2012, Aly *et al.*, 2014).

Strigolactones not only function as host-derived signalling molecules that induce germination of parasitic weeds but they also stimulate the symbiosis with arbuscular mycorrhizal fungi (Bouwmeester *et al.*, 2003, Gomez-Roldan *et al.*, 2008, Cheng *et al.*, 2013, Bu *et al.*, 2014, Ha *et al.*, 2014, Torres-Vera *et al.*, 2014). Besides their signalling role in the rhizosphere they also act as essential plant hormones that regulate various plant developmental processes and responses to biotic and abiotic stresses (Bouwmeester *et al.*, 2003, Gomez-Roldan *et al.*, 2008, Cheng *et al.*, 2013, Bu *et al.*, 2014, Ha *et al.*, 2014, Torres-Vera *et al.*, 2014). Considering the various roles that strigolactones play, it is of great interest to explore components of the strigolactone biosynthesis and signalling pathways, in an attempt to decipher how parasitic weeds perceive host signals and how strigolactones are involved in plant development.

In this general discussion, I will discuss the main findings of this thesis and compare results with previous studies exploring host-parasitic plant interactions. First, I will focus on the germination stimulants of parasitic weed seeds -- strigolactones, concerning both biosynthesis (**Chapter 5**) and signalling (**Chapter 6**). Thereafter, I discuss the phenotyping approach that I used to study post-germination resistance. Here I will list advantages and disadvantages of the rhizotron systems that I have used to explore post-germination resistance mechanisms against the root parasitic plant *Phelipanche ramosa* in *Arabidopsis* (**Chapter 2**) and tomato (**Chapter 3**). And I will discuss the role of strigolactones in post-germination resistance in tomato (**Chapter 3**). Furthermore, I will discuss the exploration of host-parasite interactions during the post-germination infection process, based on my genome-wide association (GWA) mapping on *Arabidopsis* susceptibility to *P. ramosa* (**Chapter 2**) and a study on post-germination resistance against *P. ramosa* in tomato (**Chapter 3**). Finally, I will give some suggestions and recommendations for further studies on exploring host-parasite interactions and biosynthesis and signalling of strigolactones.

### Exploring strigolactone biosynthesis and downstream signalling

As mentioned before, strigolactones are host-derived germination

stimulants for root parasitic plants such as broomrapes (*Orobanche* and *Phelipanche* spp.) and witchweeds (*Striga* spp.) (Bouwmeester *et al.*, 2003) and at the same time play a role as plant hormones that are involved in multiple biological processes (Cheng *et al.*, 2013, Ruyter-Spira *et al.*, 2013). Strigolactones are synthesized from the carotenoid trans- $\beta$ -carotene, which is isomerized by  $\beta$ -carotene isomerase DWARF27 (D27) (Lin *et al.*, 2009, Hepworth, 2012, Waters *et al.*, 2012, Bruno & Al-Babili, 2016). The resulting product is subsequently cleaved by the carotenoid cleavage dioxygenases 7 and 8 (CCD7 and CCD8) (Bennett *et al.*, 2006, Zou *et al.*, 2006, Vogel *et al.*, 2010, Kohlen *et al.*, 2012, Liu *et al.*, 2013), and oxidized by the cytochrome P450 enzyme MORE AXILLARY GROWTH1 (MAX1) (Stirnberg *et al.*, 2002, Booker *et al.*, 2005, Bennett *et al.*, 2006, Abe *et al.*, 2014, Cardoso *et al.*, 2014, Zhang *et al.*, 2014). In *Arabidopsis*, MAX1 product is first methylated by an yet unknown methyl transferase and then oxidized by an oxidoreductase-like enzyme LATERAL BRANCHING OXIDOREDUCTASE (LBO). The D27 and two CCD enzymes convert  $\beta$ -carotene into carlactone, which is the common precursor of all SLs. In *Arabidopsis*, carlactone is oxidized by MAX1 into carlactonoic acid, which is then converted to methyl carlactonoate (Abe *et al.*, 2014). In rice, carlactone is oxidized stereoselectively by one MAX1 ortholog to ent-2'-epi-5-deoxystrigol which is the presumed precursor of rice strigolactones, and ent-2'-epi-5-deoxystrigol is then catalyzed by a second MAX1 ortholog to orobanchol (Booker *et al.*, 2005, Zhang *et al.*, 2014). In **Chapter 5**, we explored the functions of the MAX1 ortholog in tomato by characterizing tomato *Slmax1* mutants which were identified in an EMS-mutagenized M2 population using a sequencing approach. The plants of *Slmax1* mutants show a dwarf phenotype with reduced internode lengths and more first-order branches, which is similar to what has been observed in the *Arabidopsis max1* mutant (Stirnberg *et al.*, 2002). This implicates the role of SIMAX1 in branching inhibition in tomato. However, in contrast to the *Arabidopsis max1* mutation which did not affect seed germination and hypocotyl growth under normal conditions (Nelson *et al.*, 2011), the *Slmax1* mutation in tomato did result in reduced seed germination and a shortened hypocotyl (**Chapter 5**). This implies that tomato SIMAX1 might be involved in seed germination and early seedling development (or plant body plan) in tomato. However, note that we could not rule out the possibility that there are mutations other than *Slmax1* still segregating in the EMS M3 families. Therefore, it is possible that the reduced seed germination and hypocotyl elongation of *Slmax1* EMS mutant are due to other mutations rather than *Slmax1*. Concerning strigolactone biosynthesis, the *Arabidopsis max1* mutant has significantly reduced strigolactone (orobanchol) levels (Kohlen *et al.*, 2011), while carlactone was found to be accumulated (Seto *et al.*, 2014).

In tomato, in which more types of strigolactones were identified, *Slmax1* mutants exhibited significantly reduced levels of all observed strigolactones including solanachol, orobanchol and the isomers of didehydro-orobanchol (**Chapter 5**). Our study also showed that SIMAX1 oxidizes carlactone, the presumed precursor of strigolactones, into carlactonoic acid and there must be another enzyme involved in orobanchol production (**Chapter 5**). In a recent study in *Arabidopsis* it was shown that 2-oxoglutarate and Fe(II)-dependent dioxygenase (2OGD) family protein LBO acts downstream of AtMAX1 (Brewer *et al.*, 2016). From the fact that in our current study application of a 2OGD inhibitor inhibited orobanchol production in the plant feeding assay, we hypothesized that a 2OGD protein, possibly acting downstream of SlMAX1, may also be involved in the conversion of carlactone to orobanchol (**Chapter 5**). Further investigations would be needed to confirm the identity of this 2OGD enzyme. In addition, we found that in tomato orobanchol is the precursor of solanachol and didehydro-orobanchol isomers, during which process additional cytochrome P450 enzymes might be required (**Chapter 5**). Currently, the structures and biological functions of didehydro-orobanchol isomers in tomato are still unknown. It would be interesting to explore the stereochemistry and biological functions of these isomers and which cytochrome P450 proteins are involved in their biosynthesis.

Our knowledge of SL signalling is also expanding. Several central components of SL perception have been identified, such as the F-box protein MORE AXILLARY GROWTH2 (MAX2) in *Arabidopsis* or DWARF3 (D3) in rice (Stirnberg *et al.*, 2007, Nelson *et al.*, 2011, Yoshida *et al.*, 2012) and an  $\alpha/\beta$ -fold hydrolase DWARF14 (D14) (Arite *et al.*, 2009, Hamiaux *et al.*, 2012, Chevalier *et al.*, 2014), DWARF 53 (D53) in rice (Jiang *et al.*, 2013, Zhou *et al.*, 2013, Kong *et al.*, 2014) and SUPPRESSOR OF MORE AXILLARY GROWTH2 1 (SMAX1) in *Arabidopsis* (Stanga *et al.*, 2013). These components interact with other transcription factors and hormonal signalling pathways in controlling plant development such as hypocotyl/mesocotyl growth, shoot branching and root development (Nelson *et al.*, 2011, Shen *et al.*, 2012, Guo *et al.*, 2013, Koren *et al.*, 2013, Wang *et al.*, 2013b, Hu *et al.*, 2014, Jia *et al.*, 2014).

With the final aim to identify more strigolactone signalling components by using a genome wide association (GWA) study, I explored the variation in hypocotyl and root growth responses to *rac*-GR24 treatment in an *Arabidopsis* natural population in **Chapter 6**. During this study, I observed that the accessions in this population exhibited four distinct hypocotyl and root responses to GR24 (**Chapter 6**). These different SL responses in differ-

ent accessions imply the complexity of SL response. Further exploration of these accessions would be necessary to unveil the underlying mechanisms behind different SL responses in different tissues and how GR24 coordinates root-shoot signalling.

By performing a genome-wide association (GWA) analysis, several QTLs associated with the GR24 induced growth response in hypocotyl and root were identified (**Chapter 6**). Interestingly, I found that several genes involved in sugar transport and metabolism are localized in QTLs that are moderately ( $-\log_{10}(P) > 3$ ) or highly ( $-\log_{10}(P) > 4$ ) associated with GR24 induced hypocotyl growth (**Chapter 6**). A few other studies have also indicated that enzymes involved in sucrose degradation and transport in root and shoot might be targets of strigolactone signalling (Chen *et al.*, 2014). In addition, sugar signalling may interact with SL signalling in the control of bud outgrowth in *Pisum sativum* and *Rosa hybrida* (Mason *et al.*, 2014, Barbier *et al.*, 2015a, Barbier *et al.*, 2015b). Concerning hypocotyl growth, questions remain on how sugar transporters such as candidate gene *SWEET16* (*SUGARS WILL EVENTUALLY BE EXPORTED TRANSPORTER16*) coordinates sucrose fluxes in response to GR24 during early seedling development, and how hormones such as auxin and ethylene are involved during this process. Interestingly, deficiency in strigolactone-dependent and karrikin-independent *SMXL3/4/5* led to strong defects in phloem formation, altered sugar accumulation, and seedling lethality (Wallner *et al.*, 2017), implying that these SMXLs, downstream components of strigolactone signalling, mediate sugar metabolism/transport. Note that in my GWA results (see supplementary **Table S4** in **Chapter 6**), a few SNPs residing in the coding region of the *SMXL5* gene showed moderate association with hypocotyl length in darkness without GR24 treatment (control) ( $-\log_{10}(P) > 3$ ). This might imply a possible role of *SMXL5* protein during the hypocotyl elongation in the dark. Sugars, reflecting the energy status of the plant, serve as important factors regulating vegetative growth. Darkness (as control condition in the GWA screening in **Chapter 6**) could induce energy stress which results in inhibition of seedling growth (Rolland *et al.*, 2006, Baena-Gonzalez *et al.*, 2007, Baena-Gonzalez & Sheen, 2008, Baena-Gonzalez, 2010). This raises the question whether strigolactone-dependent *SMXL5* is involved in regulation of energy signalling. In addition, a recent study showed that alteration in sugar partitioning in turn affects biosynthesis and signalling of strigolactones and auxin, as overexpression lines with higher sucrose and hexose levels displayed lower expression of *MAX1*, *MAX4*, *YUCCA8*, *YUCCA9*, *BRC1* (*BRANCHED1*) genes, compared to wild type (Otori *et al.*, 2017). It would be interesting to explore whether the feedback regulation of hormone pathways



by sugar partitioning also exists during hypocotyl elongation and the hypocotyl response to strigolactone application.

In previous studies, interactions between strigolactone and other hormones such as auxin, ethylene, abscisic acid (ABA) have been described, as reviewed in **Chapter 4** (Cheng *et al.*, 2013). Also in the present GWA study on GR24 induced root and hypocotyl growth (**Chapter 6**), candidate genes involved in ABA, ethylene and auxin signalling have been identified. The identification of candidate gene *EIL1* (*ETHYLENE-INSENSITIVE3-LIKE 1*), one of the transcription factors coordinating ethylene responses (Chao *et al.*, 1997, An *et al.*, 2010), suggests the potential involvement of ethylene signalling during the hypocotyl response to GR24. Concerning the root response to GR24, candidate gene *ARF19* (*AUXIN RESPONSE FACTOR 19*) is known to be involved in auxin signalling. Interestingly, *SHY2* negatively regulates *ARF19* activity during root elongation and gravitropism (Weijers *et al.*, 2005), whereas *ARF19*-mediated lateral root initiation occurs upstream of *SHY2*-mediated lateral root formation and emergence (Goh *et al.*, 2012). As *SHY2* was shown to be involved in *MAX2*-dependent SL signalling in primary root elongation and lateral root formation (Koren *et al.*, 2013), it remains a question whether *SHY2* is possibly involved in root response to GR24 via regulation of auxin signalling. It is necessary to validate whether these hormone-related genes are truly involved in the hypocotyl /root response to strigolactone by interacting with each other. It would also be interesting to study the crosstalk between these hormone signalling pathways during distinct strigolactone responses observed in the selected extreme accessions in **Chapter 6**.

### Phenotyping tools for studying host-parasitic plants interactions during post-germination process

The interaction between host and root parasitic weeds involves a series of complex events as the parasitism lasts for a long period of time. The infection process starts with the perception of host derived signals that stimulate the germination of the parasitic plant seeds. This is followed by the initiation and development of an absorptive organ (haustorium) that subsequently develops into a nutrient-reserve organ (tubercle). Then, a shoot develops and emerges above the soil after which flowers are produced, finally leading to seed dispersal into the soil (Xie *et al.*, 2010). To study host signalling compounds such as germination stimulants and haustorium-inducing factors, root exudate and root extracts are often collected and analysed (Chang & Lynn, 1986, Chang *et al.*, 1986, Kohlen *et al.*, 2011, Fernán-



dez-Aparicio *et al.*, 2014). For the later stages, such as haustorium and tubercle development, cytochemical and histological analyses are frequently utilized to observe the host-parasite interface with the help of microscopy techniques (Pérez-de-Luque *et al.*, 2005b, Echevarría-Zomeño *et al.*, 2006, Pérez-de-Luque *et al.*, 2006, Yoshida & Shirasu, 2009). Additionally, molecular techniques such as transcript analysis and transgenic approaches are often used to study functions of genes which are involved in the host-parasite interaction (Bandaranayake *et al.*, 2010, Rehker *et al.*, 2012, Ranjan *et al.*, 2014).

In quantitative genetics and breeding, characterization of host resistance/susceptibility to parasitic weeds is an important aspect. For the identification of lines in which resistance is based on low germination stimulatory activity, germination stimulants present in root exudates collected from populations are identified and quantified using liquid chromatography, and their germination stimulatory activity determined using germination bioassays (Mangnus *et al.*, 1992, Jamil *et al.*, 2012a, Denev *et al.*, 2014, Fernández-Aparicio *et al.*, 2014). In *Arabidopsis*, a few successful high-throughput screenings of mutants and ecotypes have been reported using either germination bioassays in a 96-well format or *in vitro* bioassays using polyethylene bag systems (Goldwasser *et al.*, 2000, Westwood, 2000, Goldwasser & Yoder, 2001, Goldwasser *et al.*, 2002).

To identify resistance in the form of low haustorium inducers in breeding and research programs, it is necessary to quantify haustorium numbers of the parasitic plants during a limited time period. However, this is quite a laborious and time-consuming task. A recently published protocol describes an *in vitro* assay using haustorium-inducing chemicals and host root exudate to study haustorium formation in *Phtheirospermum japonicum* (Ishida *et al.*, 2017). Hopefully such systems can be utilized in the future for quantitative genetic screenings for resistance against haustorial attachment.

For assessment of overall resistance/susceptibility, conventional genetic screening programs have been conducted using field conditions by assessing the emergence of parasitic shoots at the end of the experiment. However, because this type of studies is prone to environmental influences (Díaz-Ruiz *et al.*, 2010), it is essential to validate results across experiments (Swarbrick *et al.*, 2009, Rubiales *et al.*, 2014). For a better control of environmental effects, greenhouse pot experiments present good alternatives (Denev *et al.*, 2014).

In this thesis, I used *in vitro* infection bioassays adapted from previous studies (Gurney *et al.*, 2006, Cissoko *et al.*, 2011) to study the host-parasitic plant interaction, specifically focused on tubercle growth during the post-attachment process of parasitic infection (**Chapter 2** and **Chapter 3**). In this rhizotron system, the host plant seedlings (*Arabidopsis* and tomato) are grown on the surface of filter paper mounted on a substrate filled with nutrient solution. Pre-germinated parasitic plant seeds are spread along the host roots. Here, I summarize several advantages of this system. First of all, using this technique it is relatively easy to apply uniform conditions to rule out environmental factors as much as possible when compared to field trials. Notably, it allows for an even distribution of parasitic seeds which is not possible in field experiments. This aspect is especially crucial for the screening of the *Arabidopsis* population for its variation in susceptibility to *P. ramosa* (**Chapter 2**). In my preliminary trials using pot infection assays, I observed that the frequency and reproducibility of parasite emergence was low despite the use of similar amounts of *P. ramosa* seeds that were evenly spread at the same depth in the pots. In contrast, the *in vitro* infection bioassays using the rhizotron system gave relatively reproducible results. Secondly, and most importantly, the *in vitro* rhizotron system allows for non-invasive image analysis of underground tissues, which is not feasible in field or pot trials. This advantage turned out to be highly beneficial for the screening of the *Arabidopsis* population (**Chapter 2**) and the study on the interaction between *P. ramosa* and tomato strigolactone-deficient lines (**Chapter 3**). In both cases, image analysis could be performed over time, making the analysis of dynamic tubercle growth possible. Thirdly, the *in vitro* system is applicable to various host species, such as *Arabidopsis*, tobacco, legumes as reported in previous studies where similar systems were used (Zhou *et al.*, 2004, González-Verdejo *et al.*, 2005, Pérez-de-Luque *et al.*, 2005b, Lozano-Baena *et al.*, 2007). Finally, compared to pot and field assays, *in vitro* assays are less costly and take less space.

7

However, there are a few disadvantages of the *in vitro* infection system that need to be mentioned. First of all, there are still some environmental influences that can hardly be ruled out, for instance, fungal infection. In my population screening, although all materials were sterilized in advance, fungal infections were inevitable during the later stages. This was probably due to the need for a small opening inside the petri dish to allow for *Arabidopsis* shoot growth during the eight-week long experiment. Previous studies reported that some fungi are virulent against *Orobanche spp.*, causing necrosis and diminishing the formation of attachments (Aybeke *et al.*, 2014). This may explain why the ratio of necrosis was not a reproducible parameter

as observed during my preliminary trials using the *in vitro* system. Secondly, automatic image analysis of parasitic haustoria and tubercles is still not possible. I made several attempts to optimize the imaging techniques for the *in vitro* system, such as using darker paper as a background to offer a stronger contrast for image analysis. However, these attempts all failed mainly due to the transparency or semi-transparency of the haustoria and early tubercles. If this problem would have been solved, an advanced computing algorithm for the recognition of various tubercle shapes could have facilitated semi-automated scoring of the infection level. Thirdly, the same *in vitro* set-up may not be applicable to all host species. For example, the system established for *Medicago truncatula* did not work well for faba bean, probably due to a difference in root susceptibility to oxygen depletion in the *in vitro* system (Rubiales *et al.*, 2006). Finally, this approach is technically very laborious, which makes it less attractive to be used for a high-throughput screening, requiring careful planning and preparation. Therefore, it is recommended to optimize the currently available rhizotron system for instance by improving and automation of the imaging techniques. A few recent attempts will be described below.

Inspired by the semi-automatic three-dimensional (3D) recovery of plant root architecture in soil using X-ray computer tomography (X-ray CT) (Mairhofer *et al.*, 2012), I attempted to expose pots with tomato seedlings infected with *P. ramosa* to an X-ray scanner with the help of CAT-AgroFood facility in Wageningen University. Unfortunately, this attempt failed to give clear images of root architecture, making it impossible to distinguish parasite attachments from host roots. The main reasons for this failure may be that the soil-sand mixture that was optimized for the *P. ramosa* infection assay in tomato was not optimal for the CT scanning. I would recommend increasing sand proportions in the soil mixture in the future, as CT scanning for tomato root architecture using more sandy soil could result in more detailed 3D images according to a previous study (Mairhofer *et al.*, 2012). Besides, it has been shown that different soil densities also have impact on plant root architecture and thus influence the CT results (Tracy *et al.*, 2011). Future work might be needed to find a suitable soil composition that is optimal for both parasite infection/host growth to give clear CT images with enough details. In addition, the current computing algorithms for CT scanning should be updated and optimized to meet the requirements allowing the use of different soil compositions. However, given that above problems were solved, it still remains a challenge to distinguish parasite attachments from the host roots. In a study on 3D measurements of nematode feeding sites (giant cells) were hand-dissected (Cabrera *et al.*, 2015). With this approach, it would be pos-

sible to perform volumetric measurements of attachment organs in parasitic plants. However, automatic tubercle dissection will be a technical challenge for the sake of high-throughput phenotyping.

Notably, multicolor fluorescence and thermal imaging have recently been used to detect the early underground stage of an infection with *Orobanche cumana* in sunflower (Ortiz-Bustos *et al.*, 2017). Compared to healthy sunflowers, blue-green fluorescence emission is decreased in *O. cumana*-parasitized hosts. At the same time, the infected plants have warmer leaves which is associated with parasite-induced stomatal closure resulting in a lower transpiration rate (Ortiz-Bustos *et al.*, 2017). Both fluorescence and thermal imaging techniques are valuable approaches to facilitate rapid non-destructive diagnosis of crop health, dynamic and continuous evaluation of crop physiology (eg. photosynthesis) and to distinguish resistant and susceptible lines in breeding programs.

### **Exploring interactions between host and root parasitic plants during the post-germination stage of the infection process**

Seeds of root parasitic plants germinate in response to host-derived germination stimulants such as strigolactones. Once the parasitic weeds have detected host-derived signals and established physical and chemical contact with the host root, their damaging influence on the crop has begun. After that, the parasite develops an absorptive organ ("haustorium") and nutrient storage organ ("tubercle"), which provides the resources for further growth of the shoot and flowers. As the damage of root parasitic plants occurs early belowground, many efforts have been made to reduce the seed bank of parasitic plants in the soil by applying fungal and plant metabolites to kill the parasite seeds, to develop chemicals to induce suicidal germination of parasitic weeds, or to look for resources that produce low levels of germination stimulants (Rubiales *et al.*, 2009, Vurro *et al.*, 2009, Aly, 2012, Fernández-Aparicio *et al.*, 2012b, Jamil *et al.*, 2012a, Jamil *et al.*, 2012b, Zwanenburg *et al.*, 2013, Cimmino *et al.*, 2014, Fernández-Aparicio *et al.*, 2014, Boari *et al.*, 2016, Cala *et al.*, 2016, Samejima *et al.*, 2016, Zwanenburg *et al.*, 2016).

In order to obtain durable and complete resistance against parasitic weeds, it would be risky to only focus on the germination stage in breeding and research programs. In recent years, some programs have used low production of germination stimulants as a major criterion for screening for or selection of sources of resistance (Jamil *et al.*, 2010, Jamil *et al.*, 2011,

Fernández-Aparicio *et al.*, 2012b, Jamil *et al.*, 2012a, Fernández-Aparicio *et al.*, 2014, Pavan *et al.*, 2016, Trabelsi *et al.*, 2017). However, the deficiency or low level of germination stimulants, mainly strigolactones, will lead to abnormal plant morphology such as increased shoot branching and reduced flower/fruit numbers (Koltai *et al.*, 2010, Kohlen *et al.*, 2012, Liu *et al.*, 2013, Sun *et al.*, 2016, Gobena *et al.*, 2017), which are unfavorable traits for economical crops. In addition, we now know that strigolactones are involved in plant defense mechanisms against bacteria, in abiotic stress responses and in the establishment of symbioses with rhizobia and arbuscular mycorrhizal fungi (Foo & Davies, 2011, Kohlen *et al.*, 2012, Foo *et al.*, 2013, Bu *et al.*, 2014, Ha *et al.*, 2014, Kapulnik & Koltai, 2014, Torres-Vera *et al.*, 2014, Liu *et al.*, 2015a, Piisila *et al.*, 2015, van Zeijl *et al.*, 2015, Akamatsu *et al.*, 2016, Borghi *et al.*, 2016, Brewer *et al.*, 2016, Pelaez-Vico *et al.*, 2016, Ruiz-Lozano *et al.*, 2016, Guillotin *et al.*, 2017). Interestingly, after excluding the germination process as a putative variable affecting the infection level by using GR24 to equally trigger *P. ramosa* germination prior to the infection assays, I found a positive role of endogenous strigolactones in the host defense against this parasite in tomato (**Chapter 3**) (Cheng *et al.*, 2017). Strigolactone-deficient tomato plants (*SICCD8* RNAi lines) are highly branched. When *SICCD8* RNAi lines were infected with pre-germinated *P. ramosa* seeds, they displayed an increased infection level and faster development of the parasite when compared to wild type tomato (**Chapter 3**) (Cheng *et al.*, 2017). This endogenous defense role of strigolactone could not be revealed in Kohlen's previous study (Kohlen *et al.*, 2012), because they directly used non-GR24-treated parasite seeds, of which no germination was induced by *SICCD8* RNAi lines due to the lack of germination stimulants. Our study (**Chapter 3**) might also explain why intermediate strigolactone-producing line (*SICCD8* RNAi line L16), which exudate induces quite an amount of *P. ramosa* germination (about 45%, significantly higher than low strigolactone-producing lines -- *SICCD8* RNAi line L09 and L04), still displayed *P. ramosa* shoot emergence that was similar to that of low strigolactone-producing lines in Kohlen's study (Kohlen *et al.*, 2012). It is likely that the endogenous strigolactone level in the intermediate strigolactone-producing line was enough to protect the host against parasitic attachment although it still induced a lot of parasitic germination. With this respect, compared to low strigolactone-producing lines, the intermediate strigolactone-producing line is presumably more favored for its higher yield potential and better quality characteristics as it is remarkably less branched and it secretes more strigolactone into the rhizosphere, where more mycorrhizal colonization is induced as reported in Kohlen's study (Kohlen *et al.*, 2012).

The ideal strategy to develop durable resistant crop cultivars is to combine resistance mechanisms throughout different infection stages. A few programs considered to explore resistance mechanisms targeting multiple stages of the parasitic plant life cycle. These studies have identified resistance mechanisms against *Orobanch*e and *Striga* spp., majorly including low stimulation of parasite seed germination, unsuccessful penetration of host roots, delay in post-attachment tubercle development, necrosis of tubercles (Ejeta & Butler, 1993, Pérez-DE-Luque *et al.*, 2005a). Analysis of resistant genotypes has also shown that resistance against parasitic plant is the result of a combination of different mechanisms, each acting at different stages of the infection (Pérez-DE-Luque *et al.*, 2005a, Castillejo *et al.*, 2009, Dita *et al.*, 2009). However, currently there is no report showing the successful development of durable resistant cultivars that combine several target resistance mechanisms during multiple stages of parasite infection.

Apart from many efforts focusing on resistance during the germination stage as mentioned above, there were also a few research programs aiming to explore resistance against parasitic weeds during the post-germination stage, mainly for *Striga* spp. (Gurney *et al.*, 2006, Cissoko *et al.*, 2011, Rodenburg *et al.*, 2015) and *Orobanch*e spp. (Louarn *et al.*, 2016). Post-germination processes include haustorium initiation, tubercle development and subsequent emergence of the parasitic shoots and flowers.

Haustrorium initiation and development are quite critical for parasitic plants to establish vascular connection to the host. A few reports have identified haustorium-inducing factors, the chemical compounds that induce haustoria, for *Striga* spp. and *Triphysaria versicolor* (Chang & Lynn, 1986, Keyes *et al.*, 2000, Bandaranayake *et al.*, 2012, Fernández-Aparicio *et al.*, 2016, Yoshida *et al.*, 2016), and recently also for *Orobanch*e spp. (*Orobanch*e *crenata* and *O. cumana*) (Fernández-Aparicio *et al.*, 2016). Auxin seems to play an essential role in the haustorium connection to the host, for both root parasites (eg. *Orobanch*e spp., *P. japonicum*, *Santalum album*) (Zhou *et al.*, 2004, Bar-Nun *et al.*, 2008, Zhang *et al.*, 2015) and shoot parasites (eg. stem holoparasite *Cuscuta* spp.) (Löffler *et al.*, 1999, Ranjan *et al.*, 2014). Most recent studies show that local auxin biosynthesis at haustoria penetration sites is crucial for the haustorium formation of the facultative parasite *P. japonicum* (Ishida *et al.*, 2016). Besides, polar auxin transport and auxin signalling are also likely important in haustorium initiation based on transcriptomics data for root hemiparasite *Santalum* and stem holoparasite *Cuscuta* (Ranjan *et al.*, 2014, Zhang *et al.*, 2015). Interestingly, the RNA-seq data suggest the involvement of other hormones such as cytokinin, gibberel-



lin and strigolactone during haustorial development of *Santalum* and *Cuscuta* (Ranjan *et al.*, 2014, Zhang *et al.*, 2015). Future investigations are needed to explore what specific roles these plant hormones might play during the establishment of the vascular connection of the parasite to the host.

After establishing attachment to the host, tubercles, swollen organs at the interface of the attachment site, serve as nutrient reserve for parasite growth. A few genetic studies have also explored resistance against these post-attachment (post-haustorial) processes. One such case is on sunflower resistance to *O. cumana* (Louarn *et al.*, 2016). QTLs specifically associated with resistance during three post-attachment stages have been identified, including (1) early attachment of the parasite to the host root; (2) young tubercles; (3) shoot emergence (Louarn *et al.*, 2016). However, no candidate genes have been functionally characterized and no breeding results have been reported to integrate these candidate QTLs in this case (Louarn *et al.*, 2016).

In my thesis, I have explored the variation in susceptibility to *P. ramosa* in a natural *Arabidopsis* population during the post-germination stage of infection (**Chapter 2**). **Chapter 2** in my thesis is part of a European STW-funded program called 'Learning from Nature' (Thoen *et al.*, 2017). This program consists of several research projects exploring natural variation in plant resistance to a range of biotic and abiotic stresses in a large collection of *Arabidopsis* ecotypes. The ultimate goal of this program is to translate the knowledge obtained in *Arabidopsis* to crops to improve biotic/abiotic stress resistance (Thoen *et al.*, 2017). As tubercles act as food reserve storage organs for parasite growth after the parasitic weeds have attached to the host roots, I used tubercle growth parameters as indicators to reveal the post-attachment growth of the parasites on the host. Using the rhizotron system, I was able to monitor tubercle development in a time series. In this screening, I observed that all tested *Arabidopsis* accessions were infected by the pre-germinated *P. ramosa* seeds (**Chapter 2**). This implies that complete resistance to *P. ramosa* does not exist in this *Arabidopsis* population. This is consistent with a previous study, in which 309 ecotypes of *Arabidopsis* all showed overall susceptibility to *O. aegytiaca* (Goldwasser & Yoder, 2001, Goldwasser *et al.*, 2002). By performing GWA mapping, several QTLs associated with tubercle number (out of pre-germinated seeds), average tubercle diameter, total tubercle area per host plant at three time points, and growth rate/increase of the above-mentioned parameters across three time intervals have been identified (**Chapter 2**). Gene ontology (GO) analysis of the candidate genes showed an enrichment with



*metabolic process, transport and response to stimuli*. After candidate prioritization, several genes were selected as top candidates, including genes involved in signal transduction, metabolic process, transport, protein kinase signalling pathway, chromatin modification, proteolysis, protein myristoylation, chromatin assembly/ disassembly, reactive oxygen species, RNA binding (**Chapter 2**). Most of these candidate genes have not yet been reported to be involved in parasitism or plant defense responses against parasitic plants, and thus need further investigation.

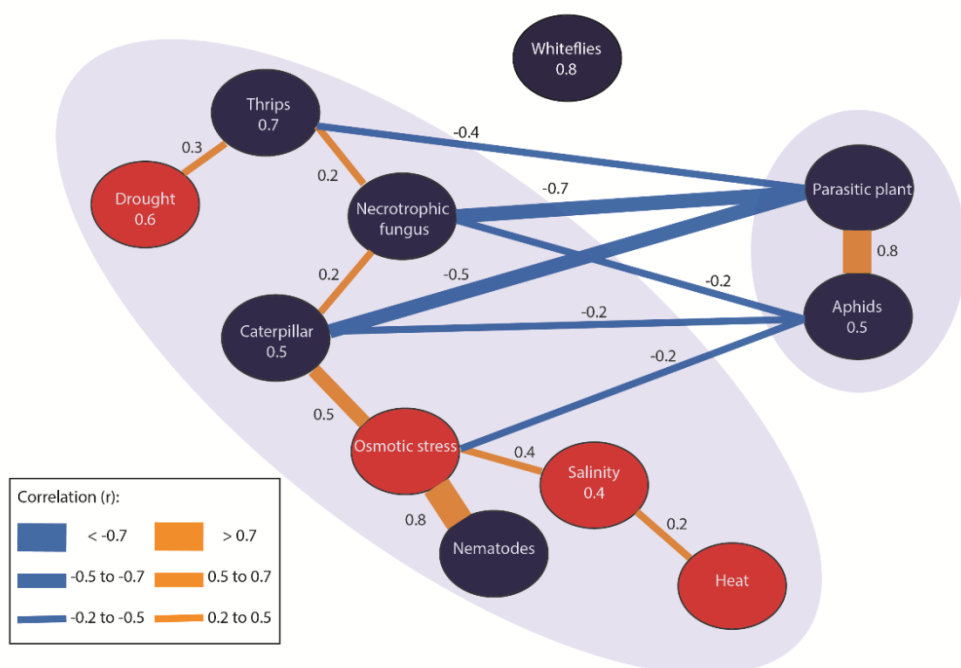


**Figure 1. Mean genetic correlations between responses of *Arabidopsis thaliana* to abiotic (red) and biotic (dark blue) plant stresses.** The thickness of lines represents the strength of mean genome-wide correlations, annotated with  $r$ -values (orange, positive; blue, negative correlation). The more shared genetic associations between stresses, the higher the absolute genetic correlation. Correlations are negative when alleles have opposite effects, resulting in increased resistance to one stress, but decreased resistance to the other stress. Values in balloons represent mean within-group correlations (not shown for groups consisting of a single trait). Mean between-group correlations are not

shown if they are below an absolute value of  $r = 0.2$ . Two clusters can be distinguished: parasitic plants and aphids; and the other stresses, except whiteflies. The figure is adapted from (Thoen *et al.*, 2017), with permission from Willey Publisher.

Notably, our joint STW project ‘Learning from Nature’ has explored variation of resistance against multiple stresses in the same *Arabidopsis* natural population (Thoen *et al.*, 2017). A multi-trait QTL mixed model (MTMM) was fitted on the set of 30 traits that were derived from resistance/susceptibility to 11 single and combined stresses (Thoen *et al.*, 2017). In this combined analysis, natural variation for parasitic plant susceptibility was also included as a form of biotic stress and was represented by the number of *P. ramosa* tubercles observed at the last time point (as described in **Chapter 2** of this thesis) (Thoen *et al.*, 2017). The result of this joint GWA mapping shows that several SNPs are significantly associated with plant defense against multiple stresses (Thoen *et al.*, 2017). However, these identified significant SNPs did not show strong association with tubercle growth traits in my **Chapter 2**. In addition, genetic correlations between *Arabidopsis* response to multiple stresses have been performed (**Figure 1**) (Thoen *et al.*, 2017). The level of the *P. ramosa* infection positively correlated with aphid behavior (probing behavior and numbers of offspring) (genetic correlation  $r = 0.8$ ), and negatively correlated with the damage caused by the necrotrophic fungus *Botrytis cinerea* ( $r = -0.7$ ) and caterpillar ( $r = -0.5$ ) to the *Arabidopsis* leaves (**Figure 1**). This suggests that the parasitic plant stress resembles these biotic stresses to some extent.

Plant hormones such as salicylic acid (SA) and jasmonic acid (JA) play essential roles in defense against these biotic stresses (De Moraes *et al.*, 2001, Moran & Thompson, 2001, Dos Santos *et al.*, 2003, Kusumoto *et al.*, 2007, Bar-Nun & Mayer, 2008, 2009, Pieterse *et al.*, 2009, Smith *et al.*, 2009, Torres-Vera *et al.*, 2016). For defense against *Orobanche* and *Phelipanche* spp., both SA and JA are involved according to previous reports (Dos Santos *et al.*, 2003; Bar-Nun and Mayer, 2008; 2009; Torres-Vera *et al.*, 2016). The SA pathway is generally associated with pathogen-elicited defenses and regulation of the initiation of a hypersensitive response (HR), whereas the JA pathway is generally activated in response to feeding by herbivores (especially chewing insects)(Smith *et al.*, 2009). The latter pathway controls the production of anti-feeding proteins and secondary metabolites as well as volatiles, which may attract natural enemies of the herbivores (De Moraes *et al.*, 2001, Chen *et al.*, 2005, Chen *et al.*, 2007). Aphids are phloem-feeding, non-chewing insects which usually cause less cell damage

than chewing insects, and the aphid-induced defense is similar to pathogen-induced defense (Smith *et al.*, 2009). In my GWA results for *Arabidopsis* susceptibility to the parasitic plant *P. ramosa* (**Chapter 2**), SNPs in the gene *LOX2* (*LIPOXYGENASE 2*, AT3G45140) were found to exhibit moderate associations with tubercle diameter ( $-\log_{10}(P) > 3$ , **Table S8** in **Chapter 2**). This *LOX2* gene is involved in wound-induced jasmonic acid biosynthesis and it is under SA-mediated suppression (Bell & Mullet, 1993, Bell *et al.*, 1995, Leon-Reyes *et al.*, 2010). Interestingly, expression of the *LOX2* gene is not only dramatically induced in *Arabidopsis* roots 2 weeks after infestation by *P. ramosa* (Dos Santos *et al.*, 2003), but also induced in *Arabidopsis* leaves by aphids (Moran & Thompson, 2001). This finding suggests that both parasitic plants and aphids trigger the JA pathway during infection. However, GWA mapping on aphid resistance using the same *Arabidopsis* population did not find strong or moderate associations between SNPs for this gene and resistance to aphids ( $-\log_{10}(P) < 3$ ) (Kloth *et al.*, 2016). Instead, SNPs for other *LOX* genes with even higher associations with aphid resistance were identified (data not published).

**Chapter 3** reveals a positive defense role of strigolactone during this specific stage of the host-parasite interaction. I found that strigolactone-deficient tomato lines (*SlCCD8* RNAi) showed a higher susceptibility to an infestation with *P. ramosa* during the post-germination process of the infection, compared to wild type tomato (Cheng *et al.*, 2017). One explanation for the high susceptibility of *SlCCD8* RNAi lines could be that because these lines have an altered hormonal balance so that the JA-dependent defense response is affected (Torres-Vera *et al.*, 2014). In addition to this, the MAX pathway negatively regulates polar auxin transport as was previously suggested in *Arabidopsis* (Bennett *et al.*, 2006). Once infected with parasitic plants, the vasculature of strigolactone-deficient tomato line might become a better auxin sink with enhanced polar auxin transport and increased local auxin level at the infection site, which facilitates the haustorium initiation and establishment of a vascular connection (Bar-Nun *et al.*, 2008, Ishida *et al.*, 2016). This hypothesis could be tested by application of the strigolactone analog GR24 and auxin transport inhibitors to see whether *SlCCD8* RNAi lines recover their resistance when these treatments are applied.

ABA may also play a role during the interaction between the host and parasitic plants. It has been proposed that ABA biosynthesis in the host root might be triggered by local water deficiency around the haustoria (Taylor *et al.*, 1996). An ABA gradient between host (with lower concentration of ABA) and attached parasite (with much higher concentration of ABA), especially

in the xylem, is formed after parasitic plants attach to the host as observed for holoparasite *Orobancha hederæ*, hemiparasite *Rhinanthus minor* and *Cuscuta reflexa* and their respective hosts (Ihl *et al.*, 1984, Ihl *et al.*, 1987, Jiang *et al.*, 2003, 2004). It is speculated that parasitic plants might stimulate their hosts to increase ABA synthesis which could be taken up by the parasite and influence stomata behavior (Lechowski, 1996). In my research work on the interaction between tomato and *P. ramosa* (**Chapter 3**), I indeed observed an increase in the accumulation of ABA and ABA metabolites in the leaves and roots of *P. ramosa*-infected wildtype and *SICCD8* RNAi lines, compared to non-infected plants (**Chapter 3**)(Cheng *et al.*, 2017). This is consistent with what other groups observed during the interaction between maize and sorghum and *S. hermonthica* (Taylor *et al.*, 1996, Frost *et al.*, 1997). In addition, the uninfected *SICCD8* RNAi lines have a higher level of ABA conjugate (ABA-glucose ester, ABA-GE) in the leaf than the wild type tomato, whereas *P. ramosa* infection induces a less extent of ABA-GE increase in the *SICCD8* RNAi lines (**Chapter 3**) (Cheng *et al.*, 2017). Previous research indicates that the cleavage of ABA-GE is a rapid route for ABA production in response to drought and osmotic stress (Lee *et al.*, 2006, Xu *et al.*, 2012, Liu *et al.*, 2015b). Future efforts are needed to unveil the complex mechanism of ABA (de)conjugation and prove whether the increased ABA conjugation is involved in the higher susceptibility of *SICCD8* RNAi lines to the parasitic plants. A more detailed study on the ABA flux between host and *Orobancha* / *Phelipanche* spp. is also highly recommended, as there is no such research in holoparasitic plants so far. One promising tool to study these questions might be the use of labeled ABA, which could facilitate dynamic tracking of the ABA. Dynamic measurement of gene expression of the ABA pathway in both host and parasite could also help us understand the regulation of ABA over host-parasite interaction.

In the GWA results for susceptibility to *P. ramosa* (**Chapter 2**), I also found several candidate genes that are involved in sugar metabolism/transport, such as sugar transporter *STP11* (*SUGAR TRANSPORTER 11*) and *SUC2* (*SUCROSE-PROTON SYMPORTER 2*). This is not surprising as sucrose is one of the major organic compounds transferred from host to the parasite (Abbes *et al.*, 2009a, Abbes *et al.*, 2009b) and sugar transport can mediate plant responses to stresses such as nutrient deprivation and biotic interactions (Juergensen *et al.*, 2003, Hammond & White, 2008, Lemoine *et al.*, 2013). One study on *P. ramosa* has shown that transcripts of a *P. ramosa* sucrose synthase gene *PrSUS1* (*SUCROSE SYNTHASES 1*) are extremely accumulated in the parasite tubercles (Péron *et al.*, 2012). The *PrSUS1* plays roles in utilization of host-derived sucrose and is also involved

in parasite xylem development under the regulation of host-derived auxin (Péron *et al.*, 2012). Host-parasite interaction is usually explained by sink-source relations (Hibberd *et al.*, 1998). *Orobanch*e infection (sink) significantly influence carbon partitioning by increasing the carbon flux moving downward from host shoot (source) and most of this carbon is intercepted by the parasite (Hibberd *et al.*, 1999). It would be interesting to further investigate the roles of above-mentioned sugar transporters in the sink-source relations of parasitism. In previous studies, *Orobanch*e *foetida*-tolerant faba bean lines show low osmotic potential in the infected roots and reduce the parasite capacity to utilize host-derived carbohydrates with low activities of soluble invertases in tubercles (Abbes *et al.*, 2009a, Abbes *et al.*, 2009b). This also points to a direction for future breeding goals, which aim to develop resistant or tolerant cultivars with optimal nutrient partitioning capacity in a way that parasitic plants cannot easily utilize host-derived nutrients. In addition, interestingly, expression of *SUC2* is induced in syncytia during nematode invasion (Juergensen *et al.*, 2003). Both a root parasitic plant and a root-knot nematode need to penetrate a host root and connect to the vasculature (Mitsumasu *et al.*, 2015). It will be interesting to see whether genes involved in host-nematode interactions also functions during the host-parasitic weed interactions, and vice versa.

Root parasitic plants need to break the cell wall barrier during infection of their host. Cell wall-degrading enzymes such as pectin methylesterase (PME) have been found to facilitate cyst nematode parasitism (Hewezi *et al.*, 2008), fungal infections (Bethke *et al.*, 2014), as well as broomrape parasitism (Losner-Goshen, 1998) (Mitsumasu *et al.*, 2015). PME proteins accumulate at the cell wall of intrusive cells of the *Orobanch*e haustorium and in the adjacent host apoplast (Losner-Goshen, 1998). In our GWA mapping results, one of the candidate genes for growth rate of tubercle diameter is the *PECTIN METHYLESTERASE INHIBITOR PROTEIN 1* (*PMEI1*) (De Caroli *et al.*, 2011), which inhibits PME activity from flowers and siliques in *Arabidopsis* (Wolf *et al.*, 2003, Raiola *et al.*, 2004). It is thus speculated that parasitic attachments, acting as sink organs, compete with host reproductive organs for assimilates from the sink (leaves), during which PME and PMEI enzymes might be involved. In addition, PMEIs have also been implicated for their role in plant immunity against fungal disease and drought tolerance (An *et al.*, 2008, An *et al.*, 2009, Lionetti *et al.*, 2015) (Lionetti *et al.*, 2017). Future investigation on the activity of PME and PMEI proteins at the infection site during haustorial attachment and tubercle growth (enlargement) will further our understanding of parasitism and comparisons between parasitic weed stress and other biotic stresses. In a recent study, focusing on the

plant response to an *O. foetida* infection, resistant chickpea mutants showed an enhanced root exudation level of metabolites that are possibly associated with cell-wall reinforcement and change of root oxidation status (Brahmi *et al.*, 2016). It would be interesting to further study these metabolites and to find out key enzymes/genes involved in the cell-wall strengthening and oxidation optimization.

Interestingly, I observed a negative correlation between tubercle size (diameter) and tubercle number at a population scale, implying that nutrient competition between tubercles exists (**Chapter 2**). This is consistent with a previous finding that the size (biomass) of individual parasites (*P. ramosa*, *O. cernua*, *O. crenata*,) was dependent (but not genetically controlled by) on the host species and resource availability as a result of resource competition between parasites, especially when the severity of the infection increases (Hibberd *et al.*, 1998, Moreau *et al.*, 2016), regardless of host growth rate (Moreau *et al.*, 2016).

### Perspectives

Strigolactones have not only been identified as signalling molecules in the rhizosphere for parasitic plants but also as a plant hormone that plays a role in various processes involved in plant development and plant defense. Currently, many components of the strigolactone biosynthetic and signalling pathways have been identified and characterized. But, still, new aspects are being revealed (Brewer *et al.*, 2016, Kameoka *et al.*, 2016, Lumba *et al.*, 2017, Wallner *et al.*, 2017, Wu *et al.*, 2017). In this thesis, I tried to validate the role of the MAX1 ortholog in tomato in strigolactone biosynthesis (**Chapter 5**). Besides, I have found diverse patterns of hypocotyl and root responses to GR24 treatment in an *Arabidopsis* population (**Chapter 6**). Candidate QTLs identified by GWA mapping might add to the collection of downstream signalling components (**Chapter 6**). In the future, the use of purified natural strigolactone analogs and stereoisomers could facilitate the investigation of the specific perception of a certain strigolactone during several biological processes.

With the expansion of our knowledge on strigolactone biosynthesis, signalling and transport, many aspects of strigolactones' biological functions have been revealed. Recently, more and more reports describe the positive role that strigolactones have in plant defense responses against various stresses (Ha *et al.*, 2014, Torres-Vera *et al.*, 2014, Liu *et al.*, 2015a, Pandey *et al.*, 2016), although other hormones seem to have a dominant role during



the defense (Wang *et al.*, 2013a). Our current finding that strigolactones also play a role in the host defense against parasitic plants is an addition to this knowledge. Future studies on the interaction between strigolactone and other hormones are needed to increase our understanding of strigolactones' role in plant defense responses even further.

Although in some aspects the plant response to an infection with parasitic plants might be similar to the defense response against other biotic stresses such as aphids and nematodes, parasitic plants have a very long lifecycle and the interaction between host and parasitic plant is a complex process which involves multiple stages. Indeed, as observed for other complex traits, the heritabilities of phenotypic traits in the genetic screening on resistance against *P. ramosa* were all very low and identified QTLs could only explain a small proportion of the phenotypic variation (**Chapter 2**). Considering the genetic complexity of the plant's response to parasitic plants, and the large influence of environmental factors, caution should be taken with the interpretation of the genetic analysis. Further confirmation is highly recommended either by repeating the genetic screening in different conditions and different years, or by validation of the current results using other approaches such as mutant analysis, genetic engineering and omics techniques etc. Besides, our current phenotyping tools for studying host responses against parasitic plants still have many limitations. An ideal high-throughput phenotyping platform would be easy to handle and maintain, less costly in both time and labor, and making use of automatic-imaging techniques. Our GWA study on *Arabidopsis* susceptibility to *P. ramosa* is the first case to use GWA techniques in a model plant population to identify QTLs associated with host susceptibility in a time series. The *a priori* candidate gene list offers a wealth of information which can be used in future studies on host-parasite interactions in crops such as tomato with the final aim to render crops that are more resistant to these devastating parasitic plants.



## Reference

- Abbes Z., Kharrat M., Delavault P., Chaïbi W., Simier P.** 2009a. Osmoregulation and nutritional relationships between *Orobancha foetida* and faba bean. *Plant Signal Behav* 4(4), 336-338.
- Abbes Z., Kharrat M., Delavault P., Chaïbi W., Simier P.** 2009b. Nitrogen and carbon relationships between the parasitic weed *Orobancha foetida* and susceptible and tolerant faba bean lines. *Plant Physiol Biochem* 47(2), 153-159.
- Abe S., Sado A., Tanaka K., et al.** 2014. Carlactone is converted to carlactonoic acid by MAX1 in *Arabidopsis* and its methyl ester can directly interact with AtD14 in vitro. *Proc Natl Acad Sci U S A* 111(50), 18084-18089.
- Akamatsu A., Shimamoto K., Kawano Y.** 2016. Crosstalk of signaling mechanisms involved in host defense and symbiosis against microorganisms in rice. *Curr Genomics* 17(4), 297-307.
- Aly R.** 2012. Advanced technologies for parasitic weed control. *Weed Sci* 60(2), 290-294.
- Aly R., Cholakh H., Joel D M., Leibman D., Steinitz B., Zelcer A., Naglis A., Yarden O., Gal-On A.** 2009. Gene silencing of mannose 6-phosphate reductase in the parasitic weed *Orobancha aegyptiaca* through the production of homologous dsRNA sequences in the host plant. *Plant Biotechnol J* 7(6), 487-498.
- Aly R., Dubey N. K., Yahyaa M., Abu-Nassar J., Ibdah M.** 2014. Gene silencing of *CCD7* and *CCD8* in *Phelipanche aegyptiaca* by tobacco rattle virus system retarded the parasite development on the host. *Plant Signal Behav* 9(8), e29376.
- An F., Zhao Q., Ji Y., et al.** 2010. Ethylene-induced stabilization of ETHYLENE INSENSITIVE3 and EIN3-LIKE1 is mediated by proteasomal degradation of EIN3 binding F-box 1 and 2 that requires EIN2 in *Arabidopsis*. *Plant Cell* 22(7), 2384-2401.
- An S. H., Choi H W., Hong J. K., Hwang B. K.** 2009. Regulation and function of the pepper pectin methylesterase inhibitor (*CaPMEI1*) gene promoter in defense and ethylene and methyl jasmonate signaling in plants. *Planta* 230(6), 1223-1237.
- An S. H., Sohn K. H., Choi H. W., Hwang I. S., Lee S. C., Hwang B. K.** 2008. Pepper pectin methylesterase inhibitor protein *CaPMEI1* is required for antifungal activity, basal disease resistance and abiotic stress tolerance. *Planta* 228(1), 61-78.
- Arite T., Umehara M., Ishikawa S., Hanada A., Maekawa M., Yamaguchi S., Kyoizuka J.** 2009. *d14*, a strigolactone-insensitive mutant of rice, shows an accelerated outgrowth of tillers. *Plant Cell Physiol* 50(8), 1416-1424.
- Aybeke M.** 2017. *Fusarium* infection causes genotoxic disorders and antioxidant-based damages in *Orobancha* spp. *Microbiol Res* 201, 46-51.
- Aybeke M., Sen B., Okten S.** 2014. *Aspergillus alliaceus*, a new potential biological control of the root parasitic weed *Orobancha*. *J Basic Microbiol* 54, S93-101.
- Baena-Gonzalez E.** 2010. Energy signaling in the regulation of gene expression during stress. *Mol Plant* 3(2), 300-313.
- Baena-Gonzalez E., Rolland F., Thevelein J. M., Sheen J.** 2007. A central integrator of

- transcription networks in plant stress and energy signalling. *Nature* 448(7156), 938-942.
- Baena-Gonzalez E., Sheen J.** 2008. Convergent energy and stress signaling. *Trends Plant Sci* 13(9), 474-482.
- Bandaranayake P. C. G., Filappova T., Tomilov A., Tomilova N. B., Jamison-Mcclung D., Ngo Q., Inoue K., Yoder J. I.** 2010. A single-electron reducing quinone oxidoreductase is necessary to induce haustorium development in the root parasitic plant *Triphysaria*. *Plant Cell* 22(4), 1404-1419.
- Bandaranayake P. C. G., Tomilov A., Tomilova N. B., Ngo Q. A., Wickett N., Depamphilis C. W., Yoder J. I.** 2012. The *TvPirin* gene is necessary for haustorium development in the parasitic plant *Triphysaria versicolor*. *Plant Physiol* 158(2), 1046-1053.
- Bar-Nun N., Mayer A. M.** 2008. Methyl jasmonate and methyl salicylate, but not cis-jasmone, evoke defenses against infection of *Arabidopsis thaliana* by *Orobanche aegyptiaca*. *Weed Biol Manage* 8(2), 91-96.
- Bar-Nun N., Mayer A. M.** 2009. Possible function of isoleucine in the methyl jasmonate response of *Arabidopsis* to *Phelipanche aegyptiaca*. *Phytoparasitica* 37(5), 485-488.
- Bar-Nun N., Sachs T., Mayer A. M.** 2008. A role for IAA in the infection of *Arabidopsis thaliana* by *Orobanche aegyptiaca*. *Ann Bot* 101(2), 261-265.
- Barbier F., Peron T., Lecerf M., et al.** 2015a. Sucrose is an early modulator of the key hormonal mechanisms controlling bud outgrowth in *Rosa hybrida*. *J Exp Bot* 66(9), 2569-2582.
- Barbier F. F., Lunn J. E., Beveridge C. A.** 2015b. Ready, steady, go! A sugar hit starts the race to shoot branching. *Curr Opin Plant Biol* 25, 39-45.
- Bell E., Creelman R. A., Mullet J. E.** 1995. A chloroplast lipoxygenase is required for wound-induced jasmonic acid accumulation in *Arabidopsis*. *Proc Natl Acad Sci U S A* 92(19), 8675-8679.
- Bell E., Mullet J. E.** 1993. Characterization of an *Arabidopsis* lipoxygenase gene responsive to methyl jasmonate and wounding. *Plant Physiol* 103(4), 1133-1137.
- Bennett T., Sieberer T., Willett B., Booker J., Luschnig C., Leyser O.** 2006. The *Arabidopsis* MAX pathway controls shoot branching by regulating auxin transport. *Curr Biol* 16(6), 553-563.
- Bethke G., Grundman R. E., Sreekanta S., Truman W., Katagiri F., Glazebrook J.** 2014. *Arabidopsis* PECTIN METHYLESTERASEs contribute to immunity against *Pseudomonas syringae*. *Plant Physiol* 164(2), 1093-1107.
- Boari A., Ciasca B., Pineda-Martos R., Lattanzio V. M., Yoneyama K., Vurro M.** 2016. Parasitic weed management by using strigolactone-degrading fungi. *Pest Manag Sci* 72(11), 2043-2047.
- Booker J., Sieberer T., Wright W., et al.** 2005. MAX1 encodes a cytochrome P450 family member that acts downstream of MAX3/4 to produce a carotenoid-derived branch-inhibiting hormone. *Dev Cell* 8(3), 443-449.
- Borghi L., Liu G-W., Emonet A., Kretschmar T., Martinoia E.** 2016. The importance

- of strigolactone transport regulation for symbiotic signaling and shoot branching. *Planta* 243(6), 1351-1360.
- Bouwmeester H. J., Matusova R., Zhongkui S., Beale M. H.** 2003. Secondary metabolite signalling in host–parasitic plant interactions. *Curr Opin Plant Biol* 6(4), 358-364.
- Brahmi I., Mabrouk Y., Brun G., Delavault P., Belhadj O., Simier P.** 2016. Phenotypical and biochemical characterisation of resistance for parasitic weed (*Orobancha foetida* Poir.) in radiation-mutagenised mutants of chickpea. *Pest Manag Sci* 72(12), 2330-2338.
- Brewer P. B., Yoneyama K., Filardo F., et al.** 2016. *LATERAL BRANCHING OXIDOREDUCTASE* acts in the final stages of strigolactone biosynthesis in *Arabidopsis*. *Proc Natl Acad Sci U S A* 113(22), 6301-6306.
- Bruno M., Al-Babili S.** 2016. On the substrate specificity of the rice strigolactone biosynthesis enzyme DWARF27. *Planta* 243(6), 1429-1440.
- Bu Q., Lv T., Shen H., et al.** 2014. Regulation of drought tolerance by the F-box protein MAX2 in *Arabidopsis*. *Plant Physiol* 164(1), 424-439.
- Cabrera J., Díaz-Manzano F. E., Barcala M., Arganda-Carreras I., De Almeida Engler J., Engler G., Fenoll C., Escobar C.** 2015. Phenotyping nematode feeding sites: three-dimensional reconstruction and volumetric measurements of giant cells induced by root-knot nematodes in *Arabidopsis*. *New Phytol* 206(2), 868-880.
- Cala A., Ghooray K., Fernández-Aparicio M., Molinillo J. M., Galindo J. C., Rubiales D., Macias F. A.** 2016. Phthalimide-derived strigolactone mimics as germinating agents for seeds of parasitic weeds. *Pest Manag Sci* 72(11), 2069-2081.
- Cardoso C., Zhang Y., Jamil M., et al.** 2014. Natural variation of rice strigolactone biosynthesis is associated with the deletion of two *MAX1* orthologs. *Proc Natl Acad Sci U S A* 111(6), 2379-2384.
- Castillejo M. Á., Fernández-Aparicio M., Rubiales D.** 2012. Proteomic analysis by two-dimensional differential in gel electrophoresis (2D DIGE) of the early response of *Pisum sativum* to *Orobancha crenata*. *J Exp Bot* 63(1), 107-119.
- Castillejo M. A., Maldonado A. M., Dumas-Gaudot E., Fernandez-Aparicio M., Susin R., Diego R., Jorin J. V.** 2009. Differential expression proteomics to investigate responses and resistance to *Orobancha crenata* in *Medicago truncatula*. *BMC Genomics* 10(1), 294.
- Chang M., Lynn D. G.** 1986. The haustorium and the chemistry of host recognition in parasitic angiosperms. *J Chem Ecol* 12(2), 561-579.
- Chang M., Netzly D. H., Butler L. G., Lynn D. G.** 1986. Chemical regulation of distance. Characterization of the first natural host germination stimulant for *Striga asiatica*. *J Am Chem Soc* 108(24), 7858-7860.
- Chao Q., Rothenberg M., Solano R., Roman G., Terzaghi W., Ecker J. R.** 1997. Activation of the ethylene gas response pathway in *Arabidopsis* by the nuclear protein ETHYLENE-INSENSITIVE3 and related proteins. *Cell* 89(7), 1133-1144.
- Chen H., Gonzales-Vigil E., Wilkerson C. G., Howe G. A.** 2007. Stability of plant defense proteins in the gut of insect herbivores. *Plant Physiol* 143(4), 1954-1967.

- Chen H., Wilkerson C. G., Kuchar J. A., Phinney B. S., Howe G. A.** 2005. Jasmonate-inducible plant enzymes degrade essential amino acids in the herbivore midgut. *Proc Natl Acad Sci U S A* 102(52), 19237-19242.
- Cheng X., Flokova K., Bouwmeester H., Ruyter-Spira C.** 2017. The role of endogenous strigolactones and their interaction with ABA during the infection process of the parasitic weed *Phelipanche ramosa* in tomato plants. *Front Plant Sci* 8, 392.
- Cheng X., Ruyter-Spira C., Bouwmeester H.** 2013. The interaction between strigolactones and other plant hormones in the regulation of plant development. *Front Plant Sci* 4, 199.
- Chevalier F., Nieminen K., Sanchez-Ferrero J. C., Rodriguez M. L., Chagoyen M., Hardtke C. S., Cubas P.** 2014. Strigolactone promotes degradation of DWARF14, an alpha/beta hydrolase essential for strigolactone signaling in *Arabidopsis*. *Plant Cell* 26(3), 1134-1150.
- Cimmino A., Fernández-Aparicio M., Andolfi A., Basso S., Rubiales D., Evidente A.** 2014. Effect of fungal and plant metabolites on broomrapes (*Orobanche* and *Phelipanche* spp.) seed germination and radicle growth. *J Agric Food Chem* 62(43), 10485-10492.
- Cissoko M., Boissard A., Rodenburg J., Press M. C., Scholes J. D.** 2011. New Rice for Africa (NERICA) cultivars exhibit different levels of post-attachment resistance against the parasitic weeds *Striga hermonthica* and *Striga asiatica*. *New Phytol* 192(4), 952-963.
- De Caroli M., Lenucci M. S., Di Sansebastiano G. P., Dalessandro G., De Lorenzo G., Piro G.** 2011. Dynamic protein trafficking to the cell wall. *Plant Signal Behav* 6(7), 1012-1015.
- De Moraes C. M., Mescher M. C., Tumlinson J. H.** 2001. Caterpillar-induced nocturnal plant volatiles repel conspecific females. *Nature* 410(6828), 577-580.
- Denev I., Deneva B., Batchvarova R., Westwood J.** 2014. Use of T-DNA activation tag *Arabidopsis* mutants in studying formation of germination stimulants for broomrapes (*Orobanche* spp.). *Biotechnol Biotechnol Equip* 21, 403-407.
- Díaz-Ruiz R., Torres A. M., Satovic Z., Gutierrez M. V., Cubero J. I., Román B.** 2010. Validation of QTLs for *Orobanche crenata* resistance in faba bean (*Vicia faba* L.) across environments and generations. *Theor Appl Genet* 120(5), 909-919.
- Die J. V., González Verdejo C. I., Dita M. A., Nadal S., Román B.** 2009. Gene expression analysis of molecular mechanisms of defense induced in *Medicago truncatula* parasitized by *Orobanche crenata*. *Plant Physiol Biochem* 47, 635-641.
- Dita M. A., Die J. V., Román B., Krajinski F., Küster H., Moreno M. T., Cubero J. I., Rubiales D.** 2009. Gene expression profiling of *Medicago truncatula* roots in response to the parasitic plant *Orobanche crenata*. *Weed Res* 49, 66-80.
- Dos Santos C. V., Letousey P., Delavault P., Thalouarn P.** 2003. Defense gene expression analysis of *Arabidopsis thaliana* parasitized by *Orobanche ramosa*. *Phytopathology* 93(4), 451-457.
- Echevarría-Zomeño S., Pérez-De-Luque A., Jorrín J., Maldonado A. M.** 2006. Pre-haustorial resistance to broomrape (*Orobanche cumana*) in sunflower (*Helianthus annuus*): cytochemical studies. *J Exp Bot* 57(15), 4189-4200.

- Ejeta G., Butler L. G.** 1993. Host-parasite interactions throughout the *Striga* life cycle, and their contributions to *Striga* resistance. *African Crop Sci J* 1(2), 75-80.
- El-Sayed A. F., Soliman S. S. A., Ismail T. A., Attia S. M.** 2012. Genetic nature and heritability of *Orobanche crenata* resistance in faba bean, *Vicia faba* L. *Zagazig J Agri Res.*
- Fernández-Aparicio M., Bernard A., Falchetto L., et al.** 2017. Investigation of amino acids as herbicides for control of *Orobanche minor* parasitism in red clover. *Front Plant Sci* 8, 842.
- Fernández-Aparicio M., Flores F., Rubiales D.** 2012a. Escape and true resistance to crenate broomrape (*Orobanche crenata* Forsk.) in grass pea (*Lathyrus sativus* L.) germplasm. *Field Crops Res* 125, 92-97.
- Fernández-Aparicio M., Kisugi T., Xie X., Rubiales D., Yoneyama K.** 2014. Low strigolactone root exudation: a novel mechanism of broomrape (*Orobanche* and *Phelipanche* spp.) resistance available for faba bean breeding. *J Agric Food Chem* 62(29), 7063-7071.
- Fernández-Aparicio M., Masi M., Maddau L., Cimmino A., Evidente M., Rubiales D., Evidente A.** 2016. Induction of haustorium development by sphaeropsidones in radicles of the parasitic weeds *Striga* and *Orobanche*. A structure-activity relationship study. *J Agric Food Chem* 64(25), 5188-5196.
- Fernández-Aparicio M., Moral A., Kharrat M., Rubiales D.** 2012b. Resistance against broomrapes (*Orobanche* and *Phelipanche* spp.) in faba bean (*Vicia faba*) based in low induction of broomrape seed germination. *Euphytica* 186(3), 897-905.
- Fernández-Aparicio M., Sillero J. C., Pérez-De-Luque A., Rubiales D.** 2008. Identification of sources of resistance to crenate broomrape (*Orobanche crenata*) in Spanish lentil (*Lens culinaris*) germplasm. *Weed Res* 48(1), 85-94.
- Fernández-Aparicio M., Sillero J. C., Rubiales D.** 2009. Resistance to broomrape species (*Orobanche* spp.) in common vetch (*Vicia sativa* L.). *Crop Protection* 28(1), 7-12.
- Fernández-Martínez J. M., Domínguez J., Pérez-Vich B.** 2008. Update on breeding for resistance to sunflower broomrape. *HELLA* 31(48), 73-84.
- Fondevilla S., Fernández-Aparicio M., Satovic Z., Emeran A. A., Torres A. M., Moreno M. T., Rubiales D.** 2009. Identification of quantitative trait loci for specific mechanisms of resistance to *Orobanche crenata* Forsk. in pea (*Pisum sativum* L.). *Mol Breeding* 25(2), 259-272.
- Foo E., Davies N. W.** 2011. Strigolactones promote nodulation in pea. *Planta* 234(5), 1073-1081.
- Foo E., Yoneyama K., Hugill C. J., Quittenden L. J., Reid J. B.** 2013. Strigolactones and the regulation of pea symbioses in response to nitrate and phosphate deficiency. *Mol Plant* 6(1), 76-87.
- Frost D. L., Gurney A. L., Press M. C., Scholes J. D.** 1997. *Striga hermonthica* reduces photosynthesis in sorghum: the importance of stomatal limitations and a potential role for ABA? *Plant Cell Environ* 20(4), 483-492.
- Gobena D., Shimels M., Rich P J., Ruyter-Spira C., Bouwmeester H., Kanuganti S.,**

- Mengiste T., Ejeta G.** 2017. Mutation in sorghum *LOW GERMINATION STIMULANT 1* alters strigolactones and causes *Striga* resistance. *Proc Natl Acad Sci U S A* 114(17), 4471-4476.
- Goh T., Kasahara H., Mimura T., Kamiya Y., Fukaki H.** 2012. Multiple AUX/IAA-ARF modules regulate lateral root formation: the role of *Arabidopsis* *SHY2/IAA3*-mediated auxin signalling. *Philos Trans R Soc Lond* 367(1595), 1461-1468.
- Goldwasser Y., Plakhine D., Yoder J. I.** 2000. *Arabidopsis thaliana* susceptibility to *Orobanche* spp. *Weed Sci* 48(3), 342-346.
- Goldwasser Y., Westwood J. H., Yoder J. I.** 2002. The use of *Arabidopsis* to study interactions between parasitic angiosperms and their plant hosts. *Arabidopsis Book* 1, e0035.
- Goldwasser Y., Yoder J. I.** 2001. Differential induction of *Orobanche* seed germination by *Arabidopsis thaliana*. *Plant Sci* 160(5), 951-959.
- Gomez-Roldan V., Fervas S., Brewer P. B., et al.** 2008. Strigolactone inhibition of shoot branching. *Nature* 455(7210), 189-194.
- González-Verdejo C. I., Barandiaran X., Moreno M. T., Cubero J. I., Di Pietro A.** 2005. An improved axenic system for studying pre-infection development of the parasitic plant *Orobanche ramosa*. *Ann Bot* 96(6), 1121-1127.
- Guillot B., Etemadi M., Audran C., Bouzayen M., Becard G., Combier J. P.** 2017. *SL-IAA27* regulates strigolactone biosynthesis and mycorrhization in tomato (var. Micro-Tom). *New Phytol* 213(3), 1124-1132.
- Guo S., Xu Y., Liu H., Mao Z., Zhang C., Ma Y., Zhang Q., Meng Z., Chong K.** 2013. The interaction between OsMADS57 and OsTB1 modulates rice tillering via DWARF14. *Nat Commun* 4, 1566.
- Gurney A. L., Slate J., Press M. C., Scholes J. D.** 2006. A novel form of resistance in rice to the angiosperm parasite *Striga hermonthica*. *New Phytol* 169(1), 199-208.
- Gutiérrez N., Palomino C., Satovic Z., et al.** 2013. QTLs for *Orobanche* spp. resistance in faba bean: identification and validation across different environments. *Mol Breeding* 32(4), 909-922.
- Ha C. V., Leyva-Gonzalez M. A., Osakabe Y., et al.** 2014. Positive regulatory role of strigolactone in plant responses to drought and salt stress. *Proc Natl Acad Sci U S A* 111(2), 851-856.
- Hacham Y., Hershenhorn J., Dor E., Amir R.** 2016. Primary metabolic profiling of Egyptian broomrape (*Phelipanche aegyptiaca*) compared to its host tomato roots. *J Plant Physiol* 205, 11-19.
- Hamiaux C., Drummond R. S., Janssen B. J., Ledger S. E., Cooney J. M., Newcomb R D., Snowden K. C.** 2012. DAD2 is an alpha/beta hydrolase likely to be involved in the perception of the plant branching hormone, strigolactone. *Curr Biol* 22(21), 2032-2036.
- Hammond J. P., White P. J.** 2008. Sucrose transport in the phloem: integrating root responses to phosphorus starvation. *J Exp Bot* 59(1), 93-109.
- Hepworth J. A.** 2012. Comparative analysis of the *MAX* pathway. PhD thesis. The University of York.



- Hibberd J. M., Quick W. P., Press M. C., Scholes J. D.** 1998. Can source–sink relations explain responses of tobacco to infection by the root holoparasitic angiosperm *Orobanche cernua*? *Plant Cell Environ* 21(3), 333-340.
- Hibberd J. M., Quick W. P., Press M. C., Scholes J.D., Jeschke W. D.** 1999. Solute fluxes from tobacco to the parasitic angiosperm *Orobanche cernua* and the influence of infection on host carbon and nitrogen relations. *Plant Cell Environ* 22(8), 937-947.
- Hu Z., Yamauchi T., Yang J., et al.** 2014. Strigolactone and cytokinin act antagonistically in regulating rice mesocotyl elongation in darkness. *Plant Cell Physiol* 55(1), 30-41.
- Ihl B., Jacob F., Meyer A., Sembdner G.** 1987. Investigations on the endogenous levels of abscisic acid in a range of parasitic phanerogams. *J Plant Growth Regul* 5, 191-205.
- Ihl B., Jacob F., Sembdner G.** 1984. Studies on *Cuscuta reflexa* ROXB. V. The level of endogenous hormones in the parasite, *Cuscuta reflexa*, and its host, *Vicia faba* L., and a suggested role in the transfer of nutrients from host to parasite. *Plant Growth Regul* 2, 77-90.
- Ishida J., Yoshida S., Shirasu K.** 2017. Haustorium induction assay of the parasitic plant *Phtheirospermum japonicum*. *Bio-Protocol* 7(9), e2260.
- Ishida J. K., Wakatake T., Yoshida S., Takebayashi Y., Kasahara H., Wafula E., Depamphilis C. W., Namba S., Shirasu K.** 2016. Local auxin biosynthesis mediated by a YUCCA flavin monooxygenase regulates haustorium development in the parasitic plant *Phtheirospermum japonicum*. *Plant Cell*, 28(8), 1795-1814.
- Jamil M., Charnikhova T., Houshyani B., Van Ast A., Bouwmeester H. J.** 2012a. Genetic variation in strigolactone production and tillering in rice and its effect on *Striga hermonthica* infection. *Planta* 235(3), 473-484.
- Jamil M., Charnikhova T., Verstappen F., Bouwmeester H.** 2010. Carotenoid inhibitors reduce strigolactone production and *Striga hermonthica* infection in rice. *Arch Biochem Biophys* 504, 123-131.
- Jamil M., Rodenburg J., Charnikhova T., Bouwmeester H. J.** 2011. Pre-attachment *Striga hermonthica* resistance of New Rice for Africa (NERICA) cultivars based on low strigolactone production. *New Phytol* 192(4), 964-975.
- Jamil M., Van Mourik T. A., Charnikhova T., Bouwmeester H. J.** 2012b. Effect of diammonium phosphate application on strigolactone production and *Striga hermonthica* infection in three sorghum cultivars. *Weed Res* 53(2), 121-130.
- Jia K. P., Luo Q., He S. B., Lu X. D., Yang H. Q.** 2014. Strigolactone-regulated hypocotyl elongation is dependent on cryptochrome and phytochrome signaling pathways in *Arabidopsis*. *Mol Plant* 7(3), 528-540.
- Jiang F., Jeschke W. D., Hartung W.** 2003. Water flows in the parasitic association *Rhinanthus minor*/*Hordeum vulgare*. *J Exp Bot* 54(389), 1985-1993.
- Jiang F., Jeschke W. D., Hartung W.** 2004. Absciscic acid (ABA) flows from *Hordeum vulgare* to the hemiparasite *Rhinanthus minor* and the influence of infection on host and parasite abscisic acid relations. *J Exp Bot* 55(406), 2323-2329.
- Jiang L., Liu X., Xiong G., et al.** 2013. DWARF53 acts as a repressor of strigolactone



signalling in rice. *Nature* 504, 401-405.

**Juergensen K., Scholz-Starke J., Sauer N., Hess P., Van Bel A. J. E., Grundler F. M. W.** 2003. The companion cell-specific *Arabidopsis* disaccharide carrier AtSUC2 is expressed in nematode-induced syncytia. *Plant Physiol* 131(1), 61-69.

**Kameoka H., Dun E. A., Lopez-Obando M., Brewer P. B., De Saint Germain A., Rameau C., Beveridge C. A., Kyozyuka J.** 2016. Phloem transport of the receptor DWARF14 protein is required for full function of strigolactones. *Plant Physiol* 172(3), 1844-1852.

**Kannan C., Aditi P., Zwanenburg B.** 2015. Quenching the action of germination stimulants using borax and thiourea, a new method for controlling parasitic weeds: A proof of concept. *Crop Prot* 70, 92-98.

**Kannan C., Zwanenburg B.** 2014. A novel concept for the control of parasitic weeds by decomposing germination stimulants prior to action. *Crop Prot* 61, 11-15.

**Kapulnik Y., Koltai H.** 2014. Strigolactone involvement in root development, response to abiotic stress, and interactions with the biotic soil environment. *Plant Physiol* 166(2), 560-569.

**Keyes W., Apos Malley R., Kim D., Lynn D.** 2000. Signaling organogenesis in parasitic angiosperms: xenognosin generation, perception, and response. *J Plant Growth Regul* 19(2), 217-231.

**Kgosi R. L., Zwanenburg B., Mwakaboko A. S., Murdoch A. J.** 2012. Strigolactone analogues induce suicidal seed germination of *Striga* spp. in soil. *Weed Res* 52(3), 197-203.

**Kloth K. J., Wieggers G. L., Busscher-Lange J., Van Haarst J. C., Kruijer W., Bouwmeester H. J., Dicke M., Jongsma M. A.** 2016. *AtWRKY22* promotes susceptibility to aphids and modulates salicylic acid and jasmonic acid signalling. *J Exp Bot* 67(11), 3383-396.

**Kohlen W., Charnikhova T., Lammers M., et al.** 2012. The tomato *CAROTENOID CLEAVAGE DIOXYGENASE 8 (SICCD8)* regulates rhizosphere signaling, plant architecture and affects reproductive development through strigolactone biosynthesis. *New Phytol* 196(2), 535-547.

**Kohlen W., Charnikhova T., Liu Q., et al.** 2011. Strigolactones are transported through the xylem and play a key role in shoot architectural response to phosphate deficiency in nonarbuscular mycorrhizal host *Arabidopsis*. *Plant Physiol* 155(2), 974-987.

**Kohlschmid E., Sauerborn J., Müller-Stöver D.** 2009. Impact of *Fusarium oxysporum* on the holoparasitic weed *Phelipanche ramosa*: biocontrol efficacy under field-grown conditions. *Weed Res* 49, 56-65.

**Koltai H., Lekkala S. P., Bhattacharya C., et al.** 2010. A tomato strigolactone-impaired mutant displays aberrant shoot morphology and plant interactions. *J Exp Bot* 61(6), 1739-1749.

**Kong X., Zhang M., Ding Z.** 2014. D53: the missing link in strigolactone signaling. *Mol Plant* 7(5), 761-763.

**Koren D., Resnick N., Mayzlish Gati E., Belausov E., Weininger S., Kapulnik Y., Koltai**

- H. 2013. Strigolactone signaling in the endodermis is sufficient to restore root responses and involves SHORT HYPOCOTYL 2 (SHY2) activity. *New Phytol* 198(3), 866-874.
- Kusumoto D., Goldwasser Y., Xie X., Yoneyama K., Takeuchi Y., Yoneyama K. 2007. Resistance of red clover (*Trifolium pratense*) to the root parasitic plant *Orobancha minor* is activated by salicylate but not by jasmonate. *Ann Bot* 100(3), 537-544.
- Labrousse P. 2001. Several mechanisms are involved in resistance of *Helianthus* to *Orobancha cumana* Wallr. *Ann Bot* 88(5), 859-868.
- Labrousse P., Arnaud M. C., Griveau Y., Fer A., Thalouarn P. 2004. Analysis of resistance criteria of sunflower recombined inbred lines against *Orobancha cumana* Wallr. *Crop Prot* 23(5), 407-413.
- Lechowski Z. 1996. Absciscic acid content in the root hemiparasite *Melampyrum arvense* L. before and after attachment to the host plant. *Biol Plant* 38(4), 489-494.
- Lee K. H., Piao H. L., Kim H. Y., et al. 2006. Activation of glucosidase via stress-induced polymerization rapidly increases active pools of abscisic acid. *Cell* 126(6), 1109-1120.
- Lemoine R., La Camera S., Atanassova R., et al. 2013. Source-to-sink transport of sugar and regulation by environmental factors. *Front Plant Sci* 4, 272.
- Leon-Reyes A., Van Der Does D., De Lange E. S., Delker C., Wasternack C., Van Wees S. C. M., Ritsema T., Pieterse C. M. J. 2010. Salicylate-mediated suppression of jasmonate-responsive gene expression in *Arabidopsis* is targeted downstream of the jasmonate biosynthesis pathway. *Planta* 232(6), 1423-1432.
- Lin H., Wang R., Qian Q., et al. 2009. DWARF27, an iron-containing protein required for the biosynthesis of strigolactones, regulates rice tiller bud outgrowth. *Plant Cell* 21(5), 1512-1525.
- Lionetti V., Fabri E., De Caroli M., Hansen A. R., Willats W. G., Piro G., Bellincampi D. 2017. Three pectin methylesterase inhibitors protect cell wall integrity for *Arabidopsis* immunity to *Botrytis*. *Plant Physiol* 173(3), 1844-1863.
- Lionetti V., Raiola A., Mattei B., Bellincampi D. 2015. The grapevine *VvPMEII* gene encodes a novel functional pectin methylesterase inhibitor associated to grape berry development. *PLoS ONE* 10(7), e0133810.
- Liu J., He H., Vitali M., et al. 2015a. Osmotic stress represses strigolactone biosynthesis in *Lotus japonicus* roots: exploring the interaction between strigolactones and ABA under abiotic stress. *Planta* 241(6), 1435-1451.
- Liu J., Novero M., Charnikhova T., et al. 2013. *CAROTENOID CLEAVAGE DIOXYGENASE 7* modulates plant growth, reproduction, senescence, and determinate nodulation in the model legume *Lotus japonicus*. *J Exp Bot* 64(7), 1967-1981.
- Liu Z., Yan J. P., Li D. K., et al. 2015b. UDP-glucosyltransferase71c5, a major glucosyltransferase, mediates abscisic acid homeostasis in *Arabidopsis*. *Plant Physiol* 167(4), 1659-1670.
- Löffler C., Czygan F. C., Proksch P. 1999. Role of indole-3-acetic acid in the interaction of the phanerogamic parasite *Cuscuta* and host plants. *Plant Biol* 1(6), 613-617.
- Losner-Goshen D. 1998. Pectolytic activity by the haustorium of the parasitic plant *Oro-*

- banche* L. (Orobanchaceae) in host roots. *Ann Bot* 81(2), 319-326.
- Louarn J., Boniface M-C, Pouilly N, Velasco L, Pérez-Vich B, Vincourt P, Muños S.** 2016. Sunflower resistance to broomrape (*Orobanche cumana*) is controlled by specific QTLs for different parasitism stages. *Front Plant Sci* 7, 590.
- Lozano-Baena M. D., Prats E., Moreno M. T., Rubiales D., Pérez-De-Luque A.** 2007. *Medicago truncatula* as a model for nonhost resistance in legume-parasitic plant interactions. *Plant Physiol* 145(2), 437-449.
- Lumba S., Holbrook-Smith D., Mccourt P.** 2017. The perception of strigolactones in vascular plants. *Nat Chem Biol* 13(6), 599-606.
- Mairhofer S., Zappala S., Tracy S. R., Sturrock C., Bennett M., Mooney S. J., Pridmore T.** 2012. RooTrak: automated recovery of three-dimensional plant root architecture in soil from x-ray microcomputed tomography images using visual tracking. *Plant Physiol* 158(2), 561-569.
- Mangnus E. M., Stommen P. L. A., Zwanenburg B.** 1992. A standardized bioassay for evaluation of potential germination stimulants for seeds of parasitic weeds. *J Plant Growth Regul* 11(2), 91-98.
- Mason M. G., Ross J. J., Babst B. A., Wienclaw B. N., Beveridge C. A.** 2014. Sugar demand, not auxin, is the initial regulator of apical dominance. *Proc Natl Acad Sci U S A* 111(16), 6092-6097.
- Mitsumasu K., Seto Y., Yoshida S.** 2015. Apoplastic interactions between plants and plant root intruders. *Front Plant Sci* 6, 617.
- Moran P. J., Thompson G. A.** 2001. Molecular responses to aphid feeding in *Arabidopsis* in relation to plant defense pathways. *Plant Physiol* 125(2), 1074-1085.
- Moreau D., Gibot-Leclerc S., Girardin A., Pointurier O., Reibel C., Strbik F., Fernández-Aparicio M., Colbach N.** 2016. Trophic relationships between the parasitic plant species *Phelipanche ramosa* (L.) and different hosts depending on host phenological stage and host growth rate. *Front Plant Sci* 7, 289-212.
- Mwakaboko A. S., Zwanenburg B.** 2011. Strigolactone analogs derived from ketones using a working model for germination stimulants as a blueprint. *Plant Cell Physiol* 52(4), 699-715.
- Nelson D. C., Scaffidi A., Dun E. A., Waters M. T., Flematti G. R., Dixon K. W., Beveridge C. A., Ghisalberti E. L., Smith S. M.** 2011. F-box protein MAX2 has dual roles in karrikin and strigolactone signaling in *Arabidopsis thaliana*. *Proc Natl Acad Sci U S A* 108(21), 8897-8902.
- Ortiz-Bustos C. M., Perez-Bueno M. L., Baron M., Molinero-Ruiz L.** 2017. Use of blue-green fluorescence and thermal imaging in the early detection of sunflower infection by the root parasitic weed *Orobanche cumana* Wallr. *Front Plant Sci* 8, 833.
- Otori K., Tamoi M., Tanabe N., Shigeoka S.** 2017. Enhancements in sucrose biosynthesis capacity affect shoot branching in *Arabidopsis*. *Biosci Biotechnol Biochem* 49, 1-8.
- Pandey A., Sharma M., Pandey G. K.** 2016. Emerging roles of strigolactones in plant responses to stress and development. *Front Plant Sci* 7, 18084-18017.

- Pavan S., Schiavulli A., Marcotrigiano A. R., et al.** 2016. Characterization of low-strigolactone germplasm in pea (*Pisum sativum* L.) resistant to crenate broomrape (*Orobancha crenata* Forsk.). *Mol Plant Microbe Interact* 29(10), 743-749.
- Pelaez-Vico M. A., Bernabeu-Roda L., Kohlen W., Soto M. J., Lopez-Raez J. A.** 2016. Strigolactones in the *Rhizobium*-legume symbiosis: Stimulatory effect on bacterial surface motility and down-regulation of their levels in nodulated plants. *Plant Sci* 245, 119-127.
- Pérez-De-Luque A., Jorrín J., Cubero J. I., Rubiales D.** 2005a. *Orobancha crenata* resistance and avoidance in pea (*Pisum* spp.) operate at different developmental stages of the parasite. *Weed Res* 45(5), 379-387.
- Pérez-De-Luque A., Lozano M. D., Cubero J. I., González-Melendi P., Risueño M. C., Rubiales D.** 2006. Mucilage production during the incompatible interaction between *Orobancha crenata* and *Vicia sativa*. *J Exp Bot* 57(4), 931-942.
- Pérez-De-Luque A., Rubiales D., Cubero J. I., Press M. C., Scholes J., Yoneyama K., Takeuchi Y., Plakhine D., Joel D. M.** 2005b. Interaction between *Orobancha crenata* and its host legumes: unsuccessful haustorial penetration and necrosis of the developing parasite. *Ann Bot* 95(6), 935-942.
- Pérez-Vich B., Akhtouch B., Knapp S. J., Leon A. J., Velasco L., Fernández-Martínez J. M., Berry S. T.** 2004. Quantitative trait loci for broomrape (*Orobancha cumana* Wallr.) resistance in sunflower. *Theor Appl Genet* 109(1), 92-102.
- Péron T., Véronési C., Mortreau E., Pouvreau J-B., Thoiron S., Leduc N., Delavault P., Simier P.** 2012. Role of the sucrose synthase encoding *PrSus1* gene in the development of the parasitic plant *Phelipanche ramosa* L. (Pomel). *Mol Plant Microbe Interact* 25(3), 402-411.
- Pieterse C. M. J., Leon-Reyes A., Van Der Ent S., Van Wees S. C. M.** 2009. Networking by small-molecule hormones in plant immunity. *Nat Chem Biol* 5(5), 308-316.
- Piisila M., Keceli M. A., Brader G., Jakobson L., Joesaar I., Sipari N., Kollist H., Palva E. T., Kariola T.** 2015. The F-box protein MAX2 contributes to resistance to bacterial phytopathogens in *Arabidopsis thaliana*. *BMC Plant Biol* 15(1), 53.
- Raiola A., Camardella L., Giovane A., Mattei B., De Lorenzo G., Cervone F., Bellincampi D.** 2004. Two *Arabidopsis thaliana* genes encode functional pectin methylesterase inhibitors. *FEBS Lett* 557(1-3), 199-203.
- Ranjan A., Ichihashi Y., Farhi M., Zumstein K., Townsley B., David-Schwartz R., Sinha N. R.** 2014. De novo assembly and characterization of the transcriptome of the parasitic weed dodder identifies genes associated with plant parasitism. *Plant Physiol* 166(3), 1186-1199.
- Rehker J., Lachnit M., Kaldenhoff R.** 2012. Molecular convergence of the parasitic plant species *Cuscuta reflexa* and *Phelipanche aegyptiaca*. *Planta* 236(2), 557-566.
- Rodenburg J., Cissoko M., Kayeke J., Dieng I., Khan Z. R., Midega C. O., Onyuka E. A., Scholes J. D.** 2015. Do NERICA rice cultivars express resistance to *Striga hermonthica* (Del.) Benth. and *Striga asiatica* (L.) Kuntze under field conditions? *Field Crops Res* 170, 83-94.

- Rolland F., Baena-Gonzalez E., Sheen J.** 2006. Sugar sensing and signaling in plants: conserved and novel mechanisms. *Annu Rev Plant Biol* 57, 675-709.
- Román B., Torres A. M., Rubiales D., Cubero J. I., Satovic Z.** 2002. Mapping of quantitative trait loci controlling broomrape (*Orobanche crenata* Forsk.) resistance in faba bean (*Vicia faba* L.). *Genome* 45(6), 1057-1063.
- Rubiales D., Fernández-Aparicio M., Wegmann K., Joel D. M.** 2009. Revisiting strategies for reducing the seedbank of *Orobanche* and *Phelipanche* spp. *Weed Res* 49(s1), 23-33.
- Rubiales D., Flores F., Emeran A. A., Kharrat M., Amri M., Rojas-Molina M. M., Sillero J. C.** 2014. Identification and multi-environment validation of resistance against broomrapes (*Orobanche crenata* and *Orobanche foetida*) in faba bean (*Vicia faba*). *Field Crops Res* 166, 58-65.
- Rubiales D., Pérez-De-Luque A., Fernández-Aparicio M., Sillero J. C., Román B., Kharrat M., Khalil S., Joel D. M., Riches C.** 2006. Screening techniques and sources of resistance against parasitic weeds in grain legumes. *Euphytica* 147(1-2), 187-199.
- Rubiales D., Pérez-De-Luque A., Joel D. M., Alcántara C., Sillero J. C.** 2003. Characterization of resistance in chickpea to crenate broomrape (*Orobanche crenata*). *Weed Sci* 51(5), 702-707.
- Rubiales D., Rojas-Molina M. M., Sillero J. C.** 2016. Characterization of resistance mechanisms in faba bean (*Vicia faba*) against broomrape species (*Orobanche* and *Phelipanche* spp.). *Front Plant Sci* 7, 1747.
- Ruiz-Lozano J. M., Aroca R., Zamarreno A. M., Molina S., Andreo-Jimenez B., Porcel R., Garcia-Mina J. M., Ruyter-Spira C., Lopez-Raez J. A.** 2016. Arbuscular mycorrhizal symbiosis induces strigolactone biosynthesis under drought and improves drought tolerance in lettuce and tomato. *Plant Cell Environ* 39(2), 441-452.
- Ruyter-Spira C., Al-Babili S., Van Der Krol S., Bouwmeester H.** 2013. The biology of strigolactones. *Trends Plant Sci* 18(2), 72-83.
- Samejima H., Babiker A. G., Takikawa H., Sasaki M., Sugimoto Y.** 2016. Practicality of the suicidal germination approach for controlling *Striga hermonthica*. *Pest Manag Sci* 72(11), 2035-2042.
- Seto Y., Sado A., Asami K., Hanada A., Umehara M., Akiyama K., Yamaguchi S.** 2014. Carlactone is an endogenous biosynthetic precursor for strigolactones. *Proc Natl Acad Sci USA* 111(4), 1640-1645.
- Shen H., Zhu L., Bu Q-Y., Huq E.** 2012. MAX2 affects multiple hormones to promote photomorphogenesis. *Mol Plant* 5(3), 750-762.
- Smith J. L., De Moraes C. M., Mescher M. C.** 2009. Jasmonate- and salicylate-mediated plant defense responses to insect herbivores, pathogens and parasitic plants. *Pest Manag Sci* 65(5), 497-503.
- Stanga J. P., Smith S. M., Briggs W. R., Nelson D. C.** 2013. SUPPRESSOR OF MORE AXILLARY GROWTH2 1 controls seed germination and seedling development in *Arabidopsis*. *Plant Physiol* 163(1), 318-330.

- Stirnberg P., Furner I. J., Ottoline Leyser H. M.** 2007. MAX2 participates in an SCF complex which acts locally at the node to suppress shoot branching. *Plant J* 50(1), 80-94.
- Stirnberg P., Van De Sande K., Leyser H. M. O.** 2002. MAX1 and MAX2 control shoot lateral branching in *Arabidopsis*. *Development* 129(5), 1131-1141.
- Sun H., Bi Y., Tao J., et al.** 2016. Strigolactones are required for nitric oxide to induce root elongation in response to nitrogen and phosphate deficiencies in rice. *Plant Cell Environ* 39(7), 1473-1484.
- Swarbrick P. J., Scholes J. D., Press M. C., Slate J.** 2009. A major QTL for resistance of rice to the parasitic plant *Striga hermonthica* is not dependent on genetic background. *Pest Manag Sci* 65(5), 528-532.
- Taylor A., Martin J., Seel W. E.** 1996. Physiology of the parasitic association between maize and witchweed (*Striga hermonthica*): is ABA involved? *J Exp Bot* 47(8), 1057-1065.
- Thoen M. P., Davila Olivas N. H., Kloth K. J., et al.** 2017. Genetic architecture of plant stress resistance: multi-trait genome-wide association mapping. *New Phytol* 213(3), 1346-1362.
- Torres-Vera R., Garcia J. M., Pozo M. J., Lopez-Raez J. A.** 2014. Do strigolactones contribute to plant defence? *Mol Plant Pathol* 15(2), 211-216.
- Torres-Vera R., García J. M., Pozo M. J., López-Ráez J. A.** 2016. Expression of molecular markers associated to defense signaling pathways and strigolactone biosynthesis during the early interaction tomato-*Phelipanche ramosa*. *Physiol Mol Plant Pathol* 94, 100-107.
- Trabelsi I., Yoneyama K., Abbes Z., Amri M., Xie X., Kisugi T., Kim H. I., Kharrat M., Yoneyama K.** 2017. Characterization of strigolactones produced by *Orobanche foetida* and *Orobanche crenata* resistant faba bean (*Vicia faba* L.) genotypes and effects of phosphorous, nitrogen, and potassium deficiencies on strigolactone production. *South African J Bot* 108, 15-22.
- Tracy S. R., Black C. R., Roberts J. A., et al.** 2011. Quantifying the effect of soil compaction on three varieties of wheat (*Triticum aestivum* L.) using X-ray Micro Computed Tomography (CT). *Plant Soil* 353(1-2), 195-208.
- Valderrama M. R., Román B., Satovic Z., Rubiales D., Cubero J. I., Torres A. M.** 2004. Locating quantitative trait loci associated with *Orobanche crenata* resistance in pea. *Weed Res* 44, 323-328.
- Van Zeijl A., Liu W., Xiao T. T., Kohlen W., Yang W-C., Bisseling T., Geurts R.** 2015. The strigolactone biosynthesis gene *DWARF27* is co-opted in rhizobium symbiosis. *BMC Plant Biol* 15(1), 260.
- Velasco L., Pérez-Vich B., Jan C. C., Fernández-Martínez J. M.** 2007. Inheritance of resistance to broomrape (*Orobanche cumana* Wallr.) race F in a sunflower line derived from wild sunflower species. *Plant Breeding* 126(1), 67-71.
- Vogel J. T., Walter M. H., Giavalisco P., et al.** 2010. *SlCCD7* controls strigolactone biosynthesis, shoot branching and mycorrhiza-induced apocarotenoid formation in tomato.



*Plant J* 61(2), 300-311.

- Vurro M., Boari A., Evidente A., Andolfi A., Zermane N.** 2009. Natural metabolites for parasitic weed management. *Pest Manag Sci* 65(5), 566-571.
- Wallner E S, Lopez-Salmeron V, Belevich I, et al.** 2017. Strigolactone- and karrikin-independent SMXL proteins are central regulators of phloem formation. *Curr Biol* 27(8), 1241-1247.
- Wang R. K., Wang C. E., Fei Y. Y., Gai J. Y., Zhao T. J.** 2013a. Genome-wide identification and transcription analysis of soybean carotenoid oxygenase genes during abiotic stress treatments. *Mol Biol Rep* 40, 4737-4745.
- Wang Y., Sun S., Zhu W., Jia K., Yang H., Wang X.** 2013b. Strigolactone/MAX2-induced degradation of brassinosteroid transcriptional effector BES1 regulates shoot branching. *Dev Cell* 27(6), 681-688.
- Waters M. T., Brewer P. B., Bussell J. D., Smith S. M., Beveridge C. A.** 2012. The *Arabidopsis* ortholog of rice *DWARF27* acts upstream of *MAX1* in the control of plant development by strigolactones. *Plant Physiol* 159(3), 1073-1085.
- Weijers D., Benková E., Jäger K. E., Schlereth A., Hamann T., Kientz M., Wilmoth J. C., Reed J. W., Jürgens G.** 2005. Developmental specificity of auxin response by pairs of ARF and Aux/IAA transcriptional regulators. *EMBO J* 24(10), 1874-1885.
- Westwood J. H.** 2000. Characterization of the *Orobanchae-Arabidopsis* system for studying parasite-host interactions *Weed Sci* 48(6), 742-748.
- Wolf S., Grsic-Rausch S., Rausch T., Greiner S.** 2003. Identification of pollen-expressed pectin methylesterase inhibitors in *Arabidopsis*. *FEBS Lett* 555, 551-555.
- Wu Y., Dor E., Hershenhorn J.** 2017. Strigolactones affect tomato hormone profile and somatic embryogenesis. *Planta* 245(3), 583-594.
- Xie X., Yoneyama K., Yoneyama K.** 2010. The strigolactone story. *Annu Rev Phytopathol* 48(1), 93-117.
- Xu Z. Y., Lee K. H., Dong T., et al.** 2012. A vacuolar beta-glucosidase homolog that possesses glucose-conjugated abscisic acid hydrolyzing activity plays an important role in osmotic stress responses in *Arabidopsis*. *Plant Cell* 24(5), 2184-2199.
- Yoshida S., Cui S., Ichihashi Y., Shirasu K.** 2016. The haustorium, a specialized invasive organ in parasitic plants. *Annu Rev Plant Biol* 67(1), 643-667.
- Yoshida S., Kameoka H., Tempo M., Akiyama K., Umehara M., Yamaguchi S., Hayashi H., Kyojuka J., Shirasu K.** 2012. The D3 F-box protein is a key component in host strigolactone responses essential for arbuscular mycorrhizal symbiosis. *New Phytol* 196(4), 1208-1216.
- Yoshida S., Shirasu K.** 2009. Multiple layers of incompatibility to the parasitic witchweed, *Striga hermonthica*. *New Phytol* 183(1), 180-189.
- Zhang X., Berkowitz O., Teixeira Da Silva J. A., Zhang M., Ma G., Whelan J., Duan J.** 2015. RNA-Seq analysis identifies key genes associated with haustorial development in the root hemiparasite *Santalum album*. *Front Plant Sci* 6, 661.
- Zhang Y, Van Dijk A. D., Scaffidi A., et al.** 2014. Rice cytochrome P450 MAX1 homologs



- catalyze distinct steps in strigolactone biosynthesis. *Nat Chem Biol* 10(12), 1028-1033.
- Zhou F., Lin Q., Zhu L., et al.** 2013. D14-SCF(D3)-dependent degradation of D53 regulates strigolactone signalling. *Nature* 504(7480), 406-410.
- Zhou W. J., Yoneyama K., Takeuchi Y., Iso S., Rungmekarat S., Chae S. H., Sato D., Joel D. M.** 2004. In vitro infection of host roots by differentiated calli of the parasitic plant *Orobanche*. *J Exp Bot* 55(398), 899-907.
- Zou J., Zhang S., Zhang W., et al.** 2006. The rice *HIGH TILLERING DWARF1* encoding an ortholog of *Arabidopsis MAX3* is required for negative regulation of the outgrowth of axillary buds. *Plant J* 48(5), 687-698.
- Zwanenburg B., Mwakaboko A. S., Kannan C.** 2016. Suicidal germination for parasitic weed control. *Pest Manag Sci* 72(11), 2016-2025.
- Zwanenburg B., Mwakaboko A. S., Reizelman A., Anilkumar G., Sethumadhavan D.** 2009. Structure and function of natural and synthetic signalling molecules in parasitic weed germination. *Pest Manag Sci* 65(5), 478-491.
- Zwanenburg B., Nayak S. K., Charnikhova T. V., Bouwmeester H. J.** 2013. New strigolactone mimics: structure-activity relationship and mode of action as germinating stimulants for parasitic weeds. *Bioorg Med Chem Lett* 23(18), 5182-5186.



## Summary

Root parasitic plant species such as broomrapes (*Orobanche* and *Phelipanche* spp.) and witchweeds (*Striga* spp.) are notorious agricultural weeds. They cause damage to crops by depriving them of water, nutrients and assimilates via a vascular connection. The difficulty in controlling root parasitic weeds is largely due to their intricate lifecycle and partially underground lifestyle. Their life cycle includes processes such as germination of the seed, the formation of the vascular connection with the host, the growth and development of the parasite after attachment and the emergence of shoots and flowers aboveground. The germination of many parasitic plants is induced by strigolactones that were recently shown to also be signalling compounds that stimulate mycorrhizal symbiosis. In addition, in the past few years, their role in plant development and plant defense has been established revealing them as a new class of plant hormones that exert their function likely in interaction with other hormones.

In **Chapter 1**, the root parasitic plants and their damage to crops are introduced. Moreover, current control methods and studies of host-parasitic plant interactions are addressed. In addition, the use of genome-wide association (GWA) mapping to explore host resistance mechanisms against parasitic plants is introduced. Furthermore, the biological functions of strigolactones and the strigolactone pathway are introduced.

In **Chapter 2**, I report of a genome-wide association mapping study on susceptibility of *Arabidopsis* to the root parasitic plant *Phelipanche ramosa*. This project was part of an STW-funded program “Learning from Nature (LFN)”, which aimed to explore resistance mechanisms against multiple biotic and abiotic stresses using one *Arabidopsis* GWA mapping population. In this chapter, the growth and development of the parasitic plants just after attachment on *Arabidopsis* roots was quantified. By performing GWA mapping, we identified multiple significant SNPs that are associated with tubercle development. A number of the QTLs identified were prioritized for further study. Most of the a priori candidate genes have not previously been reported as being involved in plant defense mechanisms against parasitic plants or parasitism in general. These genes need to be characterized and could then contribute to our knowledge reservoir for a better understanding of parasitism and resistance mechanisms against parasitic weeds. Hopefully, this knowledge in *Arabidopsis* can be translated to tomato and other crops in future breeding and research programs.

In **Chapter 3**, I show that strigolactones may play a positive role in plant defense against the parasitic plant *P. ramosa* during post-germination parasitism. In this study, I found that strigolactone-deficient tomato lines (*SICCD8* RNAi lines), infected with pre-germinated *P. ramosa* seeds, display an increased infection level and faster development of the parasite. Intrigu-

## Summary

---

ingly, strigolactone-deficient tomato plants lose their characteristic strigolactone-deficient phenotype during a *P. ramosa* infection through a reduction in the number and length of secondary branches and the number of internodes. *P. ramosa* infection also resulted in increased levels of abscisic acid (ABA) and conjugate ABA-glucose ester (ABA-GE) in both wild type and strigolactone-deficient lines. The potential roles of strigolactones and ABA in the host-parasite interaction is discussed.

In **Chapter 4**, I review the interaction of the strigolactones with other plant hormones in the regulation of plant development, such as shoot branching, root growth and secondary growth and in response to environmental stimuli. The coordinated action of these plant hormones helps plants to respond to environmental stimuli such as light and nutrient deprivation.

In **Chapter 5**, I studied the ortholog of the strigolactone biosynthetic gene *MORE AXILLARY GROWTH 1* in tomato (*SIMAX1*), by characterizing two lines containing an ethyl methanesulfonate (EMS) induced mutation in this gene. Compared to wild type tomato, the *Simax1* mutants produce significantly less strigolactones (solanachol, orobanchol and didehydro-orobanchol isomers), and display typical phenotypes as a strigolactone-deficient mutant, such as increased lateral branches. We show that *SIMAX1* oxidizes carlactone, the ubiquitous precursor of the strigolactones, to produce carlactonic acid. Presumably this carlactonic acid is a precursor for the formation of orobanchol, a mechanism that is different from the one described in rice. Orobanchol can subsequently be further oxidized, likely by additional cytochrome P450 enzymes or oxoglutarate dependent dioxygenases to produce solanachol and didehydro-orobanchol isomers.

In **Chapter 6**, I aimed to explore the underlying mechanisms of strigolactone signalling in hypocotyl and root growth using a GWA mapping approach. GWA mapping was used to find QTLs that are significantly associated with the hypocotyl and root elongation response to strigolactone treatment in the dark. This resulted in the identification of a number of significant genomic associations. *Arabidopsis* T-DNA lines were used to characterize the function of a number of candidate genes. This study is the first attempt to use GWA mapping to explore genetic mechanisms underlying strigolactone signalling.

In **Chapter 7**, I first give an update on the SL biosynthesis and signalling pathways. Then I discuss the current phenotyping tools for studying host-parasitic plant interaction during post-germination process and give my recommendations on improvement of these tools. Additionally, I discuss about parasitism and resistance mechanisms against parasitic plants, especially focusing on the post-germination stage. I discuss the similarities between parasitic weed

stress and other biotic/abiotic stresses based on the GWA results from **Chapter 2**. In addition, I emphasize the role of plant hormones during the interaction between host and parasitic weeds, including the results from **Chapter 3**. Finally, I discuss the perspectives for our understanding of the strigolactone biosynthetic pathway and the mechanisms underlying the host-parasitic plant interaction.



### Acknowledgements

Recalling the years since I chose to pursue research in plant science, I would like to sincerely say thank you to many people, including teachers/professors, lab mates, friends, my students and family members. Your accompany lighted up my PhD life and I have learned a lot from you.

About six years ago when I was a master student in the Huazhong Agricultural University in the Wuhan city of China, I was quite confused about myself, about the world and what kind of life I want. Thanks to the support of professor Zhibiao Ye, I was greatly encouraged to pursue my own research career abroad. Without his guidance and support, I would not be so determined to go outside of the city and country that I've lived for over 25 years.

In 2009, I met Harro, who was not a professor yet, in a horticultural conference held in the Huazhong Agricultural university. We had nice discussions about shade avoidance and plant-insect interactions. He was a very passionate researcher in my eyes and made me consider pursue PhD in the Netherlands. Thereafter, I joined his group in the Lab of Plant Physiology in Wageningen and chose to focus on plant-parasitic plant interaction. Harro, my promoter, I appreciate your constant encouragement, support and valuable suggestions throughout my PhD period. Thank you for giving valuable comments to my thesis. Your positive energy is also quite impressive and helpful especially when I'm depressed about negative experiment results or having no clear clues with problems.

Carolien, my co-promoter, you offered me tremendous help and guidance during my PhD. Your work is heavily-loaded but you are always stay positive and well-organized. We had appointments regularly to discuss about experiment design and results discussions. Your critical thinking and challenging questions inspired me a lot. I am also grateful for your support when I was writing at home in China. You and Harro kept well in touch with me and helped a lot with my thesis writing. I also thank you for our warm words and nice chats as a friend during these years.

I would also like to thank other staff members in the Lab of Plant Physiology: Sander, Dick, Henk, Wilco, Leonie and Richard for their encouragement and advice which are valuable for the realization of my thesis. I also appreciate professional advice on genetics and statistics from Willem, Fred and two Joost (Joost Keurentjes and Joost van Heerwaarden).



## Acknowledgements

---

Rina, special thanks to you for your kindly help with the office organization and document handling. I changed my seat position in the open office with your help several times. Thank you for listening to my concern and complaints.

I appreciate the friendship and assistance by all the lab mates. Carin, I still remember the moments you and Carolien help me with handling small parasitic plant seeds and *Arabidopsis* seedlings in the growth chamber. You helped me a lot get things prepared for the genetic screening. As a friend, you are always open and kind to share interesting stuffs and news for stamp collection and paper crafts for me. Diaan, Francel, Leo, Andrea, thank you for organizing the lab well and would always be glad to help when I had a request. Diaan, I enjoyed the moments with you and one of your dogs on the grassland on campus. Francel, a bit cold night when we had a lab dinner in your house is in my good memory. And thanks for your guidance in handling the LC-MS machine. Lidia, thanks for help with my chemical ordering and we had nice chats during coffee hours. Emilie, your passion and good work on drought inspired me, and thank you for nice suggestions for mutant analysis and data analysis. Kristýna and Tanya, your help with LC-MS measurement and result interpretation is very appreciated.

Yanxia, thank you for being a lab mate as well as a good friend of me. We shared lots of joy together. Your passion for science also impressed me. Yunmeng, Yuanyuan and Carin, thank you for helping with the arrangement of my thesis printing and defense preparation. Beatrix and Giovanni, thank you for teaching me to play with leaf imprinting and photosynthesis measurements. Nasr, Jamil, Imran, Maheder, I had nice time in the lab with you guys. You lab mates brought so much joy to my research life. I am also grateful to all my students such as Yonina, Mirjam, Marijke and Haicheng, who were willing to find solutions when they encountered problems. They helped a lot with my project.

Ralph, Jimmy, Wei, Julio, Bo, Esmer and Diaan, you are good neighbors in the open office. I enjoyed the nice chats with you. Ralph and Sander, thanks for teaching me luciferring stuff and letting me try stuffs in the dark room. Rik and Henri, thanks for letting me continue use LD tool for GWA analysis when I was not in Wageningen. Johanna, Emilie, Manus, Karen, Pingping, Nelson, Sonja, I enjoyed discussions with you on experiment setup and GWA mapping analysis. I always enjoyed being together with you guys within the same project Learning from Nature. Karen, thank you for inviting me to join the R Meetings and giving me a chance to present some

of my learnings of R programming. Hein, thanks for showing your nematode work and help me with microscopy.

I would also like to thank Karin and Frederic in the ENZA company. You helped with promoting the LFN project and also gave valuable and practical suggestions for my work.

Specially, many thanks to my Chinese friends. I enjoyed chats and dinner together with you. Your presence enriched my PhD life and brought a lot of joy. These include Yanxia, Yunmeng, Hui, Hanzhi, Junwei, Bo, Bing, Wei Song, Yuanyuan, Juan, Yu, Qin, Xianwen, Ting, Jun, Xiao, Chunxu, Wei Qin, Wei Liu, Tingting, Pingping, Jianhua, Yanli, Xu, Xuan, Guiling, Defeng, Hucheng, Zhen, Zhao, Feng, Kaile, Yiqian, Ningwen, Ke, Tao, Dong, Lemeng and many others.

I would also like to thank a Korean friend Sankseok, with whom I shared opinions between two different cultures. Beatrix and Cecilia, thank you both for teaching Spanish. Muchas gracias.

I would not also forget the great support from my parents. My father, who used to be an engineer, is the wisest man I've ever known. I can still remember what he told me before I left China for PhD, "Take these years as a journey. Just take it easy. You'll see a different world and be a different person. You'll have precious experiences which are the best rewards for yourself."

My big credits will give to my husband who is always supporting me. Although he can not really understand biology, he is always willing to listen to my complaints and worries and encouraging me in his way. Thank you very much for your constant love and care and also all your efforts for the whole family.

My sweet boy, you are a big surprise as well as a big gift for me. I did never image you would come to me before I graduate. I stay happy and feel warm when I see your smile.

All my colleagues, friends and family, who constantly remind me what is important, many thanks for your kind support during my PhD period.

### Curriculum Vitae

Xi Cheng was born on the 31<sup>st</sup> of 1984 in Wuhan, China. She studied Horticulture at Huazhong Agricultural University (the first major) and English Literature at Huazhong University of Science and Technology (the second major) during the year 2003 to 2007. Her BSc thesis for Horticulture was entitled “Exploration on the correlation between flower size and the age of microspore embryos in broccoli”.

After the completion of her BSc degree in 2007, she started a Master degree in Molecular Biology and Biotechnology for Vegetable Science at Huazhong Agricultural University. Her MSc thesis was entitled “Characterization of NBS-LRR genes and cloning of a resistance gene against root-knot nematode in a wild tomato”.

After her graduation from Huazhong Agricultural University in 2010, Xi joined the Laboratory of Plant Physiology for PhD in Wageningen University & Research Center under the supervision of Prof. Dr Bouwmeester and Dr Ruyter-Spira. The research focused on exploring resistance against root parasitic plant *Phelipanche ramosa*. The results of the PhD project are described in this thesis.

---

**Publications**

1. **Cheng X.**, Ruyter-Spira C., Bouwmeester H. 2013. The interaction between strigolactones and other plant hormones in the regulation of plant development. *Front Plant Sci* 4, 199. (IF=4.495)
2. Sasse J., Simon S., Gubeli C., Liu G. W., **Cheng X.**, Friml J., Bouwmeester H., Martinoia E. and Borghi L. 2015. Asymmetric localizations of the ABC transporter PaPDR1 trace paths of directional strigolactone transport. *Curr Biol* 25(5), 647-655. (IF=8.983)
3. Thoen M., Olivas N., Kloth K., Coolen S., Huang P., Aarts M., Johanna M., Bakker J., Bouwmeester H., Broekgaarden C., Bucher J., Busscher J., **Cheng X.**, Fradin E., Jongsma M., Julkowska M., Keurentjes J., Ligterink W., Pieterse C., Ruyter-Spira C., Smant G., Testerink C., Usadel B., van Loon J., van Pelt J., van Schaik C., Van Wees S C M., Visser R., Voorrips R., Vosman B., Vreugdenhil D., Warmerdam S., Wiegiers G., van Heerwaarden J., Kruijer W., van Eeuwijk F. 2016. Genetic architecture of plant stress resistance: multi-trait genome-wide association mapping. *New Phytol* 213 (3), 1346–1362. (IF=7.210)
4. **Cheng X.**, Flokova K., Bouwmeester H., Ruyter-Spira C. 2017. The role of endogenous strigolactones and their interaction with ABA during the infection process of the parasitic weed *Phelipanche ramosa* in tomato plants. *Front Plant Sci* 8 (294), 18084. (IF=4.495)



# Education Statement of the Graduate School

## Experimental Plant Sciences

Issued to: **Xi Cheng**  
Date: **19 October 2017**  
Group: **Laboratory of Plant Physiology**  
University: **Wageningen University & Research**

1) Start-up phase	<u>date</u>
► <b>First presentation of your project</b> Title: Natural Variation in Resistance against Parasitic Plants	12 Oct 2010
► <b>Writing or rewriting a project proposal</b> Title: Natural Variation in Resistance against Parasitic Plants	Jan 2011
► <b>Writing a review or book chapter</b> The interaction between strigolactones and other plant hormones in the regulation of plant development. Xi Cheng, Carolien Ruyter-Spira, and Harro Bouwmeester. Front Plant Sci. 2013; 4: 199. doi: 10.3389/fpls.2017.00392	24 Mar 2013
► <b>MSc courses</b>	
► <b>Laboratory use of isotopes</b>	

Subtotal Start-up Phase 13.5 credits\*

2) Scientific Exposure	<u>date</u>
► <b>EPS PhD student days</b> EPS PhD Student Day, Amsterdam, NL EPS PhD Student Day, Soest, NL	30 Nov 2012 29-30 Jan 2014
► <b>EPS theme symposia</b> EPS theme 4 'Genome Plasticity', Wageningen, NL EPS theme 3 'Metabolism and Adaptation', Wageningen, NL EPS theme 3 'Metabolism and Adaptation', Utrecht, NL EPS Theme 1 'Developmental Biology of Plants', Wageningen, NL	10 Dec 2010 07 Feb 2011 26 Apr 2012 24 Jan 2014
► <b>NWO Lunteren days and other National Platforms</b> Annual meeting 'Experimental Plant Sciences', Lunteren, NL Annual meeting 'Experimental Plant Sciences', Lunteren, NL Annual meeting 'Experimental Plant Sciences', Lunteren, NL Annual meeting 'Experimental Plant Sciences', Lunteren, NL	04-05 Apr 2011 02-03 Apr 2012 22-24 Apr 2013 14-15 Apr 2014
► <b>Seminars (series), workshops and symposia</b> CBSG Technology Symposium: 'Advances in life science technology' Plant Science Seminar: 'System Biology' Mini-symposium: 'How to write a world class paper' Symposium 'Improving yield prediction by combining statistics, genetics, physiology and phenotyping: the EU SPICY project in pepper' NCSB tutorial 'statistics with R'	25 Nov 2010 11 Jan 2011 19 Apr 2011 08-09 Mar 2012 20 Apr 2013
► <b>Seminar plus</b>	
► <b>International symposia and congresses</b> The 12th World Congress on Parasitic Plants, Sheffield, UK	15-20 Jul 2013
► <b>Presentations</b> Poster: Annual meeting 'Experimental Plant Sciences', Lunteren, NL Talk: World Congress on Parasitic Plants	02-03 Apr 2012 15-20 Jul 2013
► <b>IAB interview</b> Meeting with a member of the Interantional Advisory Board of EPS	15 Nov 2011
► <b>Excursions</b> Green Life Science Company Visit	23 Jun 2011

Subtotal Scientific Exposure 9.5 credits\*

3) In-Depth Studies	<u>date</u>
► <b>EPS courses or other PhD courses</b> PhD course 'Plant Metabolomics' PhD Summer School 'Environmental Signaling' PE&RC Post Graduate course 'Introduction to R for Statistical Analysis' LFN (Learning from Nature) project workshop 'Association mapping' Course 'Mixed model-based QTL mapping in GenStat' Course 'Microscopy and Spectroscopy in Food and Plant Science' iPlant workshop	26-28 Apr 2011 22-24 Aug 2011 25-25 Oct 2011 23 Feb 2012 14-16 May 2012 07-11 May 2012 03-04 Mar 2014
► <b>Journal club</b> Literature discussion in Plant Physiology group	2010-2014
► <b>Individual research training</b>	

Subtotal In-Depth Studies 8.7 credits\*

4) Personal development	<u>date</u>
► <b>Skill training courses</b> ExPeCtationS (EPS Career Day) PhD Competence Assessment Course 'Techniques for writing and presenting a scientific paper' Course 'Reviewing a Scientific Paper' Course 'Data Management' Course 'Imaging Science: Video and Audio content in Scientific Communication' Course 'Last Stretch of the PhD Programme'	19 Nov 2010 22 Mar & 19-20 Apr 2011 06-09 Sep 2011 08 Nov 2013 24 Feb 2014 16-27 Jun 2014 04 Jul 2014
► <b>Organisation of PhD students day, course or conference</b>	
► <b>Membership of Board, Committee or PhD council</b>	

Subtotal Personal Development 5.5 credits\*

TOTAL NUMBER OF CREDIT POINTS*	37.2
--------------------------------	------

Herewith the Graduate School declares that the PhD candidate has complied with the educational requirements set by the Educational Committee of EPS which comprises of a minimum total of 30 ECTS credits

\* A credit represents a normative study load of 28 hours of study.

The research described in this thesis was financially supported by the Dutch Technology Foundation STW (to Prof. Dr ir. H.J. Bouwmeester; grant number 10990), the Netherlands Organization for Scientific Research (NWO; VICI grant, 865.06.002 to Prof. Dr ir. H.J. Bouwmeester) and the Chinese Scholarship Council (CSC; to X. Cheng).

Financial support from Wageningen University for printing this thesis is gratefully acknowledged.

Cover design by Xi Cheng

Front cover image: a sketch of *Phelipanche ramosa* flowers (by Xi Cheng)

Back cover image: an illustration of research life (by Xi Cheng)

Printed by ProefschriftMaken





